The genus *Spongites* (Corallinales, Rhodophyta) in South Africa

Courtney Ann Puckree-Padua

Department of Biodiversity and Conservation Biology

University of the Western Cape

P. Bag X17, Bellville 7535

South Africa.

A thesis submitted in fulfillment of the requirements of the degree PhD in the Department of Biodiversity and Conservation Biology, University of the Western Cape.

Supervisor: Prof. Gavin W. Maneveldt

Co-supervisor: Dr. Paul W. Gabrielson

August 2019

I declare that

"The genus *Spongites* (Corallinales, Rhodophyta) in South Africa"

is my own work, that it has not been submitted for any degree or examination at any other university, and that all the sources I have used or quoted have been indicated and acknowledged by complete references.

CAPadua

…… 08 August 2019 ……

Courtney Ann Puckree-Padua Date

This thesis is dedicated to my family.

Thank you to my patient husband Yonnick, who has always supported my dreams, to my son Aaron, who has unknowingly given me the motivation I needed to persevere, to my sisters, Andrea and Nicole who have always kept me grounded and to my late mother, Loretta who had always believed in me.

To my friends who are my family, thank you for sharing this journey with me and never let me forget the importance of looking after oneself.

Thank you to the Holy Trinity for providing me with the strength to persevere especially when the path seemed impossible.

TABLE OF CONTENTS

Title page ……..... i

Declaration ……... ii

Dedication …… iii

Table of contents ……...…….. iv

Chapter 1 – General Introduction ……..…….. 2

1.1. Introduction ……... 2

1.1.1. Distribution and habitat ……. 2

1.1.2. Ecological importance …….. 3

1.2. Kinds of coralline……... 4

1.3. Habitus of non-geniculate coralline algae ……..……... 5

1.3.1. Attached vs. free-living forms ……..…….. 5

1.3.2. Growth forms …… 5

1.4. Taxon delineation …….. 6

1.5. High-level classification of coralline algae ……... 8

1.6. Monographic account of the genus *Spongites* …….. 9

1.6.1. History ……... 9

1.6.2. Characterisation …… 12

1.7. South African species ascribed to *Spongites* …… 13

1.8. Aims and objectives …….. 14

Chapter 2 – Materials and Methods …….. 16

2.1. Specimen collection and storage ……... 16

2.2. Molecular analysis …… 16

2.2.1. Specimen preparation …… 16

2.2.2. DNA extraction ……. 17

2.2.3. Amplification and sequencing protocols …….. 17

2.3. Phylogenetic analysis …… 18

2.4. Sequence divergence values ……. 20

2.5. Species delimitation …….. 20

2.5.1. Automatic Barcode Gap Discovery …….. 20

2.5.2. *BEAST (pronounced starBeast) analysis …… 20

2.6. Morpho-anatomical analysis ……. 22

2.6.1. Histological preparation …… 22

2.6.2. Microscopy and morpho-anatomical interpretations……. 23

Chapter 3 – Results……. 24

3.1. Molecular analyses …… 24

- Phylogenetic trees: Figs 1-5……... 29

- Pairwise Sequence Divergence: Tables 1-2 …….. 34

- *Beast analyses: Figs 6-8 …….. 36

3.2. Species descriptions……... 38

3.2.1. *Chamberlainium agulhense* (Maneveldt, E.van der Merwe & P.W.Gabrielson) Caragnano, Foetisch, Maneveldt & Payri ...…… 38

3.2.2. *Chamberlainium capense* Maneveldt, Puckree-Padua & P.W.Gabrielson *sp. nov*. …….. 40

3.2.3. *Chamberlainium cochleare* Maneveldt, Puckree-Padua & P.W.Gabrielson *sp. nov*. …….. 45

3.2.4. *Chamberlainium glebosum* Maneveldt, Puckree-Padua & P.W.Gabrielson *sp. nov*. ..…….. 50

3.2.5. *Chamberlainium impar* (Foslie) Maneveldt, Puckree-Padua & P.W.Gabrielson *comb. nov.* ….……... 55

3.2.6. *Chamberlainium natalense* (Foslie) Maneveldt, Puckree-Padua & P.W.Gabrielson, *comb. nov*. …….. 60
3.2.7. *Chamberlainium occidentale* Maneveldt, Puckree-Padua & P.W.Gabrielson *sp. nov.* …… 66
3.2.8. *Chamberlainium tenue* Maneveldt, Puckree-Padua & P.W.Gabrielson *sp. nov*. …… 72
3.2.9. *Pneophyllum neodiscoideum (*Foslie) Maneveldt, Puckree-Padua & Gabrielson *sp. nov.* …… 76

Chapter 4 – Discussion…… 82

4.1. Delineation in *Chamberlainium* …… 82
4.2. Assignment of species names ...…… 84
4.2.1. *Chamberlainium agulhense* ...……... 84
4.2.2. *Chamberlainium capense* …….. 85
4.2.3. *Chamberlainium cochleare* ……... 86
4.2.4. *Chamberlainium glebosum* ……... 88
4.2.5. *Chamberlainium impar* ……. 88
4.2.6. *Chamberlainium natalense* …… 89
4.2.7. *Chamberlainium occidentale* …...……. 90
4.2.8. *Chamberlainium tenue* …….. 91
4.2.9. *Pneophyllum neodiscoideum* ……...…. 92
4.3. Congruency between morpho-anatomical and DNA sequencing ...…….. 94
4.3.1. Tetrasporangial conceptacle roof development …...……. 94
4.3.2. Trichocyte arrangement …… 97
4.4. Keys to species previously ascribed to *Spongites* in South Africa ……... 99
4.4.1. Field key …… 99
4.4.2. Laboratory key …….. 101

4.5. Key to the genus *Pneophyllum* in South Africa …… 102

4.6. Cryptic diversity and biogeographic considerations…….. 103

4.7. Future research …….. 108

Acknowledgments ……. 109

Chapter 5 – References ……... 110

Morpho-anatomical tables ..……... 137

Figure captions …… 162

Morpho-anatomical plates …… 34 pp.

Supplementary Figure (Figure S1) ……... 1 pp.

Supplementary Table (Table S1) …….. 12 pp.

The genus Spongites (Corallinales, Rhodophyta) in South Africa

1. General introduction

1.1. Introduction

1.1.1. Distribution and habitat

Coralline red algae (Corallinales, Hapalidiales, Sporolithales: Corallinophycidae, Rhodophyta) are widespread and common in all the world's oceans (Adey & McIntyre 1973; Johansen 1981; Littler *et al.* 1985; Björk *et al.* 1995; Aguirre *et al*. 2007; Harvey & Woelkerling 2007; Littler & Littler 2013). They achieve their highest diversity in the tropics and subtropics (Björk *et al.* 1995; Littler & Littler 2013; Riosmena-Rodríguez *et al*. 2017), and within the photic zone of rocky shores (Lee 1967; Littler 1973; Adey 1978; Adey *et al*. 1982; Steneck 1986; Kendrick 1991; Kaehler & Williams 1996; Gattuso *et al*. 2006; van der Heijden & Kamenos 2015; Riosmena-Rodríguez *et al*. 2017) where they serve as important carbonate structures (Adey *et al*. 1982; Littler & Littler 1994, 1997; Vermeij *et al.* 2011) and habitats for a host of marine species (Foster 2001; Amado-Filho *et al*. 2010; Foster *et al*. 2013; Littler & Littler 2013; Riosmena-Rodríguez *et al*. 2017). Coralline algae are resilient, inhabiting extreme conditions that include: low temperatures (Adey 1970, 1973; Freiwald & Hendrich 1994; Barnes *et al*. 1996; Freiwald 1996; Aguirre *et al.* 2000; Roberts *et al*. 2002; Björk *et al*. 2005; Martone *et al*. 2010); limited light exposures (Adey 1970; Littler & Littler 1985; Littler *et al*. 1985; Liddell & Ohlhorst 1988; Dullo *et al.* 1990; Littler & Littler 1994; Iryu *et al*. 1995; Stellar and Foster 1995; Gattuso *et al*. 2006; Aguirre *et al.* 2007; Littler & Littler 2013); severe wave action (Steneck 1989; Littler & Littler 2013); intense grazing pressures (Steneck 1989; Steneck & Dethier 1994; Maneveldt & Keats 2008; Littler & Littler 2013), highly fluctuating salinities (Harlin *et al*. 1985; Barry & Woelkerling 1995; Barnes *et al*. 1996; Wilson *et al.* 2004); including occurring in freshwater (Žuljevic *et al.* 2016), and constant sand scouring (Littler & Littler 1984; D'Antonio 1986; Kendrick 1991; Chamberlain 1993; Dethier 1994).

Their ability to inhabit such harsh conditions allow them to colonise a host of substrates that include being: epilithic on stable, primary bedrock (Adey 1971; Adey & McIntyre 1973; Adey *et al.* 1976; Wray 1977; Steneck 1986; Bosence 1991) as well as on unstable boulders, cobbles and pebbles (Bosence 1991; Maneveldt & van der Merwe 2012); epizoic on molluscan shells (Adey 1971; Steneck 1986; Steneck & Paine 1986; Nelson 2009; Eager *et al*. 2015); epiphytic on other algae (Steneck 1986; Reyes & Afonso-Carrillo 1995; Kjøsterud 1997; Beavington-Penney *et al*. 2004; Morcom *et al*. 2005; Nelson 2009; Browne *et al*. 2013); and epigenous on various artificial substrates (Nelson 2009; Eager *et al*. 2015). Additionally, corallines may occur unattached in any and all of the environments they are encountered (Bosellini & Ginsburg 1971; Bosence 1983; Iryu 1985; Iryu *et al*. 1995; Foster *et al*. 2013; Riosmena-Rodríguez *et al*. 2017), as well as being parasitic or semi-endophytic in other corallines (Johansen 1976; Noble and Kraft 1983; Goff & Coleman 1985; Keats 1995; Broadwater *et al*. 2002; Zuccarello *et al*. 2004; Blouin & Lane 2012; Preuss *et al*. 2017).

1.1.2. Ecological importance

Coralline algae are important sources of sediments (Wray 1977; Johansen 1981; Littler & Littler 2013), of primary production (Hagen 1999; Chisholm 2003; Gattuso *et al*. 2006; Martin *et al.* 2013; Burdette *et al.* 2014) and of food for many herbivores (Branch 1971; Carpenter 1981; Steneck 1982, 1983, 1985; Littler *et al*. 1995; Maneveldt & Keats 2008; Maneveldt *et al*. 2008). They are regarded as one of the largest stores of carbon in the biosphere (Martin *et al*. 2007; Littler & Littler 2013), serving as important reef cementers by contributing to reef building and to the conservation of healthy reefs (Littler & Littler 1994, 1997; Vermeij *et al.* 2011). Coralline algae are critical for local biodiversity as their protuberant growth forms increase the surface area for the colonisation and settlement of a host of invertebrate species (Amado-Filho *et al*. 2010; Foster *et al.* 2013; Littler & Littler 2013). Most recently coralline

algae have even been identified as useful indicators of biomineral changes resulting from global climate change (Adey 1998; Nelson 2009; Basso 2012; Quaranta *et al*. 2012; Krayesky-Self *et al.* 2017) and ocean acidification (Nelson 2009; Quaranta *et al.* 2012), as well as serving as temporary microhabitats for several endolithic microalgal stages (Felder *et al*. 2014; Fredericq *et al*. 2014; Krayesky-Self *et al*. 2016, 2017), some of which are of public health concern (Krayesky-Self *et al*. 2017).

1.2. Kinds of coralline algae

Although having no taxonomic basis (Cabioch 1972, 1988; Bailey and Chapman 1998; Bailey 1999; Bittner *et al*. 2011; Kato *et al*. 2011; Janot & Martone 2018), coralline algae may be separated into either geniculate (articulated) or non-geniculate (encrusting, crustose) (Johansen 1981; Woelkerling 1988) forms. Geniculate corallines are flexible and branched, consisting of alternating shorter uncalcified (genicula or joints) segments and longer calcified (intergenicula) segments (Johansen 1981; Woelkerling 1988). Non-geniculate corallines lack the uncalcified genicula and thus are completely calcified, except for their outermost meristematic and reproductive cells (Johansen 1981; Woelkerling 1988).

Taxonomic relationships based on the presence or absence of genicula was initially proposed by Kützing (1843) and much later supported by Desikachary *et al.* (1998) who placed the geniculate taxa and the non-geniculate taxa into the families Corallinaceae and Spongitaceae (this latter name proposed by Kützing [1843]) respectively. This argument, however, never gained general acceptance and even before Desikachary *et al.* (1998), several studies (e.g. Cabioch 1972, 1988; Woelkerling 1988) already showed these characters to have no taxonomic basis for separating taxa. Molecular evidence (e.g. Bailey and Chapman 1998; Bailey 1999; Bittner *et al*. 2011; Kato *et al*. 2011; Janot & Martone 2018) has subsequently confirmed our

current understanding. Even so, the presence or absence of genicula is the most easily recognisable feature.

1.3. Habitus of non-geniculate coralline algae

1.3.1. Attached vs. free-living forms

Like most other seaweeds, non-geniculate coralline algae are largely epilithic, occurring as encrustations on primary bedrock and other hard substrates (Johansen 1981; Woelkerling 1988; Andrew 1993; Connell 2005). Under exposed conditions and/or in the absence of hard substrates, they may also occur as free-living rhodoliths (nodules, rhodolites, maërl, red algal balls, algaliths) (Adey & MacIntyre 1973; Wray 1977; Bosence 1991; Foster 2001; Aguirre *et al*. 2007; Foster *et al*. 2013; Riosmena-Rodríguez *et al*. 2017). Rhodoliths are a result of attached non-geniculate coralline algae breaking off and continuing as roughly spherical growth forms due to wave action and bioturbation (Stellar & Foster 1995; Harrington *et al.* 2004; Littler & Littler 2013).

1.3.2. Growth forms

Non-geniculate coralline algae display a range of morphologies, from fast growing thin, sheet-like crusts to slow growing thick pavers. They have a high level of phenotypic plasticity – a single species may have numerous morphologies and alternatively many species may display the same morphology (Steneck & Adey 1976; Wilks & Woelkerling 1991; Woelkerling & Harvey 1993; Womersley 1996; Harvey & Woelkerling 2007; Maneveldt & Keats 2008; Bittner *et al.* 2011). Despite their phenotypic plasticity, consistent applications of growth forms terminologies (unconsolidated, encrusting, warty, lumpy, fruticose, discoid, layered, foliose, ribbon-like, arborescent; see Woelkerling *et al*. 1993) are now encouraged to promote a universal understanding of observed coralline morphologies.

1.4. Taxon delineation

Mikael Foslie and Franz Heydrich were the pioneers of coralline algal taxonomy, describing some 470 specific and 84 intraspecific taxa between 1895 and 1911. The delineations and descriptions of taxa in their early works were based solely on external morphological differences between species, with little emphasis on reproductive features (Bailey & Chapman 1996). Subsequent to these authors, greater emphasis was placed on the vegetative anatomy and on development, and more importantly on the reproductive features (e.g. Lemoine 1911; Setchell 1943; Adey 1970; Cabioch 1971, 1972, 1988; Johansen 1976, 1981; Lebednick 1977; Turner & Woelkerling 1982; Chamberlain 1993, 1994a, b). During this intermediate phase in coralline taxonomy there was a progressive shift from placing greater emphasis on external morphology (e.g. growth form, trichocyte arrangement, etc.) and vegetative features (e.g. absence/presence of cell fusions vs. that of secondary pit connections) (e.g. Adey 1970; Cabioch 1972), to placing greater emphasis on reproductive features (e.g. Johansen 1981; Woelkerling 1988; Penrose & Woelkerling 1988; Harvey & Woelkerling 2007; Farr *et al*. 2009).

The most recent phase in coralline taxonomy, initially pioneered by Bailey & Chapman (1996, 1998), saw DNA sequence comparisons used to resolve phylogenies. A great advance, beginning in the late 2000s was using DNA sequences generated from type specimens (Gabrielson *et al.* 2011; Hind *et al.* 2014a, b; van der Merwe *et al.* 2015, Maneveldt *et al*. 2017; Caragnano *et al.* 2018), to apply species names to specimens, rather than morphological and anatomical similarity. The use of comparative sequences from type (preferably) or 'topotype' and recently collected material to assign names soon became the expected norm. For phylogenetic analyses, initially only one (e.g. Bailey & Chapman 1996, 1998, Bailey 1999; Harvey *et al*. 2003; Bailey *et al*. 2004; Martone *et al*. 2012) or two (e.g. Kim *et al.* 2007; Broom

et al. 2008; Kato *et al*. 2011; Hind *et al.* 2014b, Peña *et al.* 2014, 2015; van der Merwe *et al.* 2015; Maneveldt *et al*. 2017) genes were sequenced, but it quickly became apparent that a multi-gene approach (e.g. Bittner *et al*. 2011; Hind *et al*. 2014a; Rösler *et al*. 2016; Caragnano *et al.* 2018) was necessary to resolve phylogenies, especially at the higher taxonomic levels. It is interesting to note that some of the recent molecular findings (e.g. Bailey & Chapman 1996; 1998; Bailey 1999; Harvey *et al*. 2003; Bittner *et al*. 2011; Kato *et al*. 2011; Hind *et al.* 2016; Janot & Martone 2018) have indeed supported some of the historic conclusions (e.g. Cabioch [1972] hypothesized that it was possible for geniculate and non-geniculate species to belong to the same subfamily, arguing that genicula arose independently, several times, over time).

Until recently, most approaches to taxonomy still relied heavily on first identifying species based on traditional morpho-anatomical characteristics and then supported that with genetic data, an approach otherwise known as Molecular Assisted Alpha Taxonomy or MAAT (Saunders 2005, 2008, Hind *et al.* 2014a, b). However, this method is flawed in that much of the assigning of names amounts to making educated guesses (Maneveldt *et al*. 2017). This type of analysis is compounded by the fact that often type material had not been properly annotated (often a type 'specimen' bears more than one individual crust or even more than one species) or catalogued or even fully described (e.g. lack of reproductive information) (Bailey & Chapman 1996). The only unequivocal way to assign a name is through DNA sequencing of unambiguous type (preferably) or 'topotype' material. This is best achieved using an Integrated Taxonomic Approach (ITA) (e.g. Gabrielson *et al*. 2011; Maneveldt *et al*. 2017; Maneveldt *et al*. in prep.) that firstly utilizes DNA sequences from both type and field-collected specimens and then attempts to determine the morpho-anatomical features/differences.

1.5. High-level classification of coralline algae

The coralline red algae are placed within the Class Florideophyceae Cronquist, subclass Corallinophycidae L.Le Gall & G.W.Saunders (Guiry & Guiry 2018). The Corallinophycidae is characterised by the following combination of features (Le Gall & Saunders 2007): 1) pit plugs with two cap layers at cytoplasmic faces, the outer cap an enlarged dome-like layer that lacks a membrane; 2) carpogonial branches two-celled; 3) tetrasporangia zonate or cruciately divided; and 4) calcification in the form of calcite. The subclass currently comprises three orders, namely Corallinales P.C.Silva & H.W.Johansen *emend*. W.A.Nelson, J.E.Sutherland, T.J.Farr & H.S.Yoon, Hapalidiales W.A.Nelson, J.E.Sutherland, T.J.Farr & H.S.Yoon and Sporolithales L.Le Gall & G.W.Saunders *emend*. Bahia, Amado-Filho, Maneveldt & Yoneshigue-Valentin. Within Corallinophycidae, the Corallinales are characterised by the following combination of features (Nelson *et al*. 2015): 1) tetrasporangia in uniporate conceptacles; 2) tetrasporangia zonately divided; 3) tetrasporangial conceptacles lacking apical pore plugs; and 4) cell fusions or secondary pit connections present between adjacent filaments. Within Corallinophycidae, the Hapalidiales is characterised by the following combination of features (Nelson *et al*. 2015): 1) multiple tetra/bisporangia in multiporate conceptacles; 2) tetrasporangia zonately divided; 3) tetra/bisporangial conceptacles bearing apical pore plugs; 4) thallus non-geniculate; and 5) secondary pit-connections absent between adjacent filaments. Within Corallinophycidae the Sporolithales is characterised by the following combination of features (Le Gall *et al*. 2010, Bahia *et al*. 2015): 1) individual tetrasporangia in calcified compartments; 2) tetrasporangia cruciately divided; 3) tetrasporangial compartments bearing apical pore plugs; 4) short (one to two cells) gonimoblast filaments, with oblong terminal carposporangia, distributed across the floor in conceptacles that lack a central fusion cell; and 5) cell fusions and secondary pit connections present between adjacent filaments.

1.6. Monographic account of the genus *Spongites*

1.6.1. History

The genus *Spongites* was originally established by Kützing (1841) to accommodate six species in the Corallinaceae J.V.Lamouroux (Corallinales) he considered distinct from *Lithothamnium* Philippi (Philippi 1837, earlier homonym of the conserved name *Lithothamnion* Heydrich [Heydrich 1897] and thus unavailable for use according to Art. 14.10 of the *International Code of Botanical Nomenclature*) and *Lithophyllum* Philippi (Philippi 1837). Between 1842 and 1866 the genus went through a series of taxonomic changes with varying degrees of support (Woelkerling 1985). *Spongites* was initially subsumed in *Melobesia* J.V.Lamouroux (Decaisne 1842, see also Lindley 1846; Harvey 1847) and became one of three subgenera. Kützing (1843), however, maintained *Spongites* as a distinct genus but went on to subsume both *Lithothamnium* and *Lithophyllum* into *Spongites* along with all other non-geniculate corallines to a new family Spongitaceae (as 'Spongiteae'). Over the next several years, some species of *Spongites* were placed in *Melobesia* (Areschoug 1852, see also Ardissone 1883), some in *Lithothamnium* (Areschoug 1852, see also Harvey 1860; Rosanoff 1866; Farlow 1881; Ardissone 1883; Schmitz 1889; Hauptflesch 1897) and still others in *Lithophyllum* (Rosanoff 1866; see also De Toni 1905; Mazza 1916; Kylin 1956). All of these proposals, however, were made in the absence of examining Kützing's original collections or without any consideration of the generitypes of *Melobesia*, *Lithophyllum* and *Lithothamnion* (Woelkerling 1985). Incidentally, Kützing (1841) had not assigned a generitype to *Spongites* and additionally had used superficial morphological features to characterise the genus (Woelkerling 1985).

Woelkerling (1985) was the first to re-asses *Spongites* in a modern context and in reference to the original Kützing collections. Using Johansen's (1981: 10) classification system, Woelkerling (1985) resurrected *Spongites* (prior to this *Spongites* had not been recognised as a

distinct genus since 1880) and placed it under the subfamily Mastophoroideae Setchell with the characteristics of Corallinaceae (Johansen 1981): 1) genicula absent; 2) cell fusions present; and 3) uniporate tetra/bisporangial conceptacles. Woelkerling (1985) proposed that three species (*Spongites fruticulosus* Kützing, *Spongites racemosus* Kützing and *Spongites stalactiticus* Kützing), the best preserved of the original six species described by Kützing (1841), were all conspecific. *Spongites fruticulosus*, the only species that bore tetrasporangial material, was subsequently lectotypified and assigned as the generitype. Under this revised system Woelkerling (1985) additionally characterised *Spongites* as having: 1) a plumose (non-coaxial) medulla; and 2) trichocytes present that are either solitary or in vertical rows.

Shortly after Woelkerling (1985), Penrose and Woelkerling (1988) subsumed *Hydrolithon* (Foslie) Foslie, *Porolithon* Foslie, and *Pseudolithophyllum* Me.Lemoine in *Spongites* (the oldest name), creating a '*Spongites*-complex', arguing that their types could not be separated based on the anatomical (trichocyte occurrence and arrangement, and thallus construction) features proposed to separate them. However, upon examination of representative material Penrose and Woelkerling (1992) were subsequently able to demonstrate that *Spongites* and *Hydrolithon* (incl. *Porolithon* – *Hydrolithon* having nomenclatural priority) could be separated by their tetrasporangial conceptacle roof development (from peripheral roof filaments in *Spongites vs.* from both peripheral and interspersed filaments in *Hydrolithon*), and by the shape and orientation of the pore canal cells (papillate and oriented more or less parallel or at a sharp angle to the roof in *Spongites vs.* enlarged and orientated more or less perpendicular to the roof in *Hydrolithon*).

The taxonomy of the coralline algae remained largely stable for the next decade. With the introduction of molecular techniques, however, the genus *Spongites* underwent further

taxonomic changes. Using 18S rRNA gene, Bailey *et al*. (2004) showed that the Mastophoroideae was polyphyletic. Bailey *et al*. (2004), however, did not include specimens from the type genus *Mastophora* Decaisne in their analyses, leaving their conclusions unresolved and preventing them from proposing a revision of the subfamily. It was much later that analyses using several genes amended the Mastophoroideae to be limited to the genera *Mastophora* and *Metamastophora* Setchell (Kato *et al*. 2011, see also Bittner *et al*. 2011), comprising specimens with: 1) a thin thallus and a basal layer of palisade cells; 2) tetrasporangial conceptacle roofs formed by filaments peripheral to the fertile area; and 3) spermatangial systems restricted to the floor of male conceptacles. Even in these latter studies, however, the precise phylogenetic placement of *Spongites* was not possible because neither Bittner *et al*. (2011) nor Kato *et al*. (2011) included the generitype of the genus in their respective studies. Several years later Rösler *et al*. (2016) epitypified a specimen of *S. fruticulosus* (generitype of *Spongites*) and subsequently placed the species in the subfamily Neogoniolithoideae (A.Kato & M.Baba) *emend*. A.Rösler, Perfectti, V.Peña & J.C.Braga, the latter taxon characterised by specimens with: 1) non-geniculate, monomerous or thin dimerous thalli; 2) basal filaments composed of non-palisade cells; 3) trichocytes present; 4) uniporate tetra/bisporangial conceptacles with roofs formed by filaments peripheral to the fertile area; and 5) filaments lining the tetra/bisporangial conceptacle pore canal orientated parallel to oblique (more or less parallel) to the roof surface and may protrude into the pore. Throughout these latter studies (Bittner *et al*. 2011; Kato *et al*. 2011; Rösler *et al*. 2016), *Spongites* was polyphyletic, with some species remaining unresolved and placed in a "Southern Hemisphere group" (Rösler *et al*. 2016). Shortly thereafter Caragnano *et al*. (2018), using a multi-gene approach, demonstrated that many species previously ascribed to *Spongites*, including taxa that correspond to the "Southern Hemisphere group", belonged in a new genus and subfamily, proposing *Chamberlainium* Caragnano, Foetisch, Maneveldt & Payri (Chamberlainoideae

Caragnano, Foetisch, Maneveldt & Payri) to accommodate them. Anatomically, *Chamberlainium* and *Spongites* may be separated from each other by their tetra/bisporangial conceptacle diameters (< 300 μm in *Chamberlainium vs.* > 300 μm in *Spongites*) and the thickness of their tetra/bisporangial conceptacle roofs (< 8 cells in *Chamberlainium vs.* > 8 cells in *Spongites*). Under this latest classification system, *Spongites* remains in the subfamily Neogoniolithoideae.

1.6.2. Characterisation

Until recently *Spongites*, a largely temperate genus, was characterised by: 1) being non-geniculate; 2) possessing cell fusions between adjacent filaments with secondary pit connections absent; 3) absence of a basal layer of palisade cells; 4) absence of trichocytes in large tightly packed horizontal fields (without vegetative cells between individual trichocytes); 5) uniporate tetrasporangial conceptacles in which the roof development occurs only from filaments peripheral to the fertile area; and 6) spermatangial systems confined to the floor of male conceptacles (Kato *et al.* 2011). The latest classification system, proposed by Caragnano *et al*. (2018), has *Chamberlainium* characterised by: 1) thalli non-geniculate and non-endophytic, epilithic or epizoic; 2) thalli thin (up to 1 mm), encrusting to warty to lumpy; 3) thallus construction primarily dimerous or monomerous, but not both; in dimerous thalli, the single basal layer comprises non-palisade cells in radial view (along the filament), whereas in tangential section (across the filaments) they may appear palisade-like; 4) epithallus single to multilayered; 5) trichocytes absent or single/paired with complete obliteration of the trichocytes in the final step of development leading to their absence deeper in the perithallus (cortex); 6) tetra/bisporangial conceptacles uniporate with roofs formed from filaments peripheral to the developing sporangial initials; 7) tetra/bisporangial conceptacle chambers generally < 300 μm in diameter with chamber roofs < 8 cells thick; 8) tetra/bisporangial

conceptacle pore canal lined by cells orientated more or less parallel or at a sharp angle to the roof surface, protruding into the pore canal as papillae; and 9) male conceptacles with simple (unbranched) spermatangial systems confined to the chamber floor.

1.7. South African species ascribed to the genus *Spongites*

The South African rocky intertidal and shallow subtidal zones have a high diversity of non-geniculate coralline algae (Stephenson & Stephenson 1972; Maneveldt *et al*. 2008, 2017) with members of *Spongites* being particularly widespread (Chamberlain 1993; Maneveldt *et al.* 2008, 2016). Until recently, only four species ascribed to *Spongites* have been recorded for South Africa: *Spongites agulhensis* Maneveldt, E.van der Merwe & P.W.Gabrielson (now *Chamberlainium agulhense* (Maneveldt, E.van der Merwe & P.W.Gabrielson) Caragnano, Foetisch, Maneveldt & Payri, see Caragnano *et al*. 2018), *Spongites discoideus* (Foslie) D.Penrose & Woelkerling, *Spongites impar* (Foslie) Y.M.Chamberlain and *Spongites yendoi* (Foslie) Y.M.Chamberlain. Two of these species (*C. agulhense* [L'Agulhas, Cape Agulhas, Western Cape Province], *S. impar* [Cape of Good Hope, Western Cape Province]) have South African type localities (Chamberlain 1994b; van der Merwe *et al*. 2015). The type locality of *S. discoideus* is Tierra del Fuego (mouth of the Rio Grande), Argentina, while that of *S. yendoi*, which is reported to be cosmopolitan (see Guiry & Guiry [2018] for a detailed reported distribution), is Shimoda Harbour, Shizuoka Prefecture, Japan (Chamberlain 1993; Guiry & Guiry 2018).

Of all species attributed to the genus in South Africa, *S. yendoi* is reported to be the most abundant intertidally, occurring along the entire South African coast (Chamberlain 1993; Maneveldt *et al*. 2008). *Spongites yendoi* is reported to be a relatively thin species that is distributed along the mid- to lower intertidal zones on rocky shores (Chamberlain 1993;

Maneveldt & Keats 2008). The species' thin morphology has been considered to result from either grazing or sand scour (Chamberlain 1993; Maneveldt & Keats 2008). The species is ecologically important, especially within the Cochlear zone (low intertidal zone) of the west and south west coasts where it forms the basal crust as well as being an essential food source for the territorial gardening limpet, *Scutellastra cochlear* (Branch & Branch 1981; Maneveldt & Keats 2008). In the absence of grazing, the species was reported to become variably thick and protuberant (Maneveldt & Keats 2008) and consequently has been reported to achieve a range of morphologies (Chamberlain 1993; Maneveldt & Keats 2008).

Chamberlain (1993) reported and described *S. yendoi* from South Africa, and throughout its geographic range ascribed specimens of variable morphologies to the species, including the type of *Lithophyllum natalense* Foslie (type locality: KwaZulu-Natal Province, South Africa). Recent DNA sequence data, however, have demonstrated that several cryptic species, across different ocean basins, including here in South Africa, are classified under *S. yendoi* (Broom *et al*. 2008; Bittner *et al*. 2011; Nelson *et al*. 2015; Rösler *et al*. 2016; van der Merwe *et al*. 2015, Caragnano *et al*. 2018).

1.8. Aims and Objectives

Recent molecular-assisted alpha taxonomy has suggested that several cryptic species are posing under the name *S. yendoi* in South Africa, all of which are unique compared with all other named *Spongites* specimens sequenced to date, including those from New Zealand (van der Merwe *et al*. 2015; Caragnano *et al*. 2018). These South African species appear to be strongly geographically distributed and gross morphology does indeed appear to be a useful character for their local separation (G.W. Maneveldt *pers. com*.). Rösler *et al*. (2016) had suggested that the species currently attributed to *Spongites* will have to be assigned to more than one genus,

notably because the southern hemisphere taxa ascribed to the genus, do not align with the generitype. To accommodate these and other northern hemisphere taxa, as well as some South African specimens, Caragnano *et al*. (2018) proposed the genus *Chamberlainium* in honour of the British phycologist Dr Yvonne M. Chamberlain (whose research focused extensively on taxa belonging to this genus).

Using an integrated taxonomic approach (Gabrielson *et al*. 2011; Maneveldt *et al*. 2017), that firstly utilizes DNA sequencing of type (most importantly) and field-collected specimens, along with traditional histological examination of morpho-anatomical characters, the aim of this study was to understand the biodiversity of the non-geniculate coralline algae that historically would have been ascribed to *Spongites*.

2. Materials and Methods

2.1. Specimen collection and storage

Fresh specimens were collected during spring low tides from the rocky intertidal and shallow subtidal zones at various locations between Port Nolloth (Northern Cape Province) and Ballito Bay (KwaZulu-Natal Province), South Africa. Additional specimens from Namibia (southern West Africa), housed in the UWC herbarium, were also examined. Specimens on the bedrock were removed using a geological hammer and chisel. Where specimens occurred on pebbles or gastropod shells, the entire pebble or gastropod shell along with the coralline was sampled. Specimens were sorted in the field. For each specimen, a fragment was air dried, a fragment was placed in silica gel and a further fragment was fixed in 10 % formalin. Voucher specimens were deposited in UWC and type specimens sent to L (Naturalis, Netherlands, Leiden). Herbarium acronyms followed Thiers (2018, continuously updated).

2.2. Molecular analysis

2.2.1. Specimen preparation

Silica dried, field collected specimens or type specimens borrowed from TRH were used for DNA extraction. Type specimens, specifically sequenced for this study, included *Lithophyllum impar*, *Lithophyllum discoideum* and *Lithophyllum natalense*. The type specimen, *Goniolithon yendoi* (basionym of *Spongites yendoi*: type locality, Shimoda, Shizuoka Prefecture, Japan), however, is a rock fragment that has multiple epilithic, individual thalli on it, with the *G. yendoi* crust identified by the number 66 (Fig. S1). The crust identified as *G. yendoi* is thin and has overgrown another crust (Fig. S1), resulting in DNA sequencing of this type specimen being extremely difficult; the type specimen has thus not been successfully sequenced. Sequenced specimens were initially examined under a dissecting microscope and any observable epiphytes

were removed. A three mm^3 total volume of each sample was placed in separate paper packets and ground to a fine coralline powder using the heavy end of a crescent wrench.

2.2.2. DNA extraction

Under a hood, 700 µL of extraction buffer (Dellaporta *et al*. 1983) was added to a 1.7-mL microcentrifuge tube. The buffer contained 100 mM Tris (pH 8.0), 50 mM EDTA, 500 mM NaCl, and 10 mM (1 µL) 2-mercaptoethanol. The tube was capped and placed in a heat block at 65 ºC. To this was added 50 µL of 20% SDS, 4 mg of lyophilized Proteinase K (Invitrogen, Carlbad, California, USA), and the finely ground coralline powder sample, all of which were incubated for 1 h at 65 ºC. Polysaccharides were removed by incubating the samples on ice for 30 min with an added 250 µL of potassium acetate (5 M), then centrifuged for 25 min at 12,000 g (Dellaporta *et al.* 1983). The supernatant (750 L) was extracted with chloroform (equal volume) in a sterile tube and centrifuged for 15 min at 12,000 g. 600 µL of the aqueous layer was removed and the DNA was precipitated with the addition of two-thirds volume isopropanol overnight at -20 ºC, spun for 30 min at 12,000 g, washed with 450 µL of 70 % ethanol, spun for a further 5 min and the ethanol decanted. The precipitated DNA was rotoevaporated for 45 min and resuspended in 100 L of distilled water. A working solution of 10:1 (water: DNA) was prepared for PCR in a separate tube. A negative control was performed with each set of extractions.

2.2.3. Amplification and sequencing protocols

One µL of diluted DNA was added to each 25 µL reaction containing 5 µL of 10 × reaction buffer (containing 15 mM magnesium chloride), 10 µL of Q-solution (for amplification of GC-rich templates), 7 µL from each 10 µL primer, 200 µM of each dNTP, and 2.5-5.0 units of Taq DNA Polymerase (Qiagen, Valencia, California, USA). The primer pairs used for *rbc*L were

F57 (forward)—R1150 (reverse) and F753 (forward),—*rbc*S (reverse) (Freshwater & Rueness 1994). The primer pair combination used for *psb*A was *psb*A-F and *psb*A-R2 (Yoon *et al.* 2002). Due to DNA fragmenting in 19th and early 20th Century type specimens, only shorter sequences could be generated of either *rbc*L or *psb*A using the following primer combinations. For *rbc*L, forward primer F1150Cor (Adey *et al*. 2015) was combined with either reverse primer R1308 (Gabrielson *et al*. 2011) or R1460Cor (Hernández-Kantún *et al*. 2016). For *psb*A, a newly designed forward primer (TAGGTATATCTGGTACATTCAA) was combined with *psb*A-R2. Reactions were cycled in a PTC-100 PCR Thermocycler (Applied Biosystems, Foster City, California, USA) at 94 °C for 3 min, followed by 40 cycles of 95 °C for 30 s, 50 °C for 90 s, and 72 °C for 90 s, and finally at 72 °C for 5 min. PCR products were electrophoresed on 1.5 % agarose gels which contained EtBr (0.5 µg· mL^{-1}) and purified using the QIAquick PCR Purification Kit following the manufacturers' instructions (Qiagen, Valencia, California, USA). A negative control was performed with each set of reactions.

Sequences were obtained from an ABI 3100 Genetic Analyzer (DNA Analysis Core Facility, Centre for Marine Sciences, University of North Carolina, Wilmington, North Carolina, USA) and were manually aligned and compiled using Sequencher (Gene Codes Corp., Ann Arbor, Michigan, USA), and Sequence Alignment Editor available at http://tree.bio.ed.ac.uk/software/seal/.

2.3. Phylogenetic analysis

A total of 80 *psb*A (including *Lithophyllum natalense*) and 60 *rbc*L (included *L. impar* and *L. discoideum*) sequences from specimens previously ascribed to *Spongites* from South Africa, six (*psb*A and *rbc*L) sequences from unknown species within Chamberlainoideae from Chile and Antarctica, 16 (*psb*A only) sequences from specimens assigned to *S. yendoi* and 1 (*psb*A)

sequence from a specimen assigned to *P. fragile* from New Zealand, two (*psb*A only) and four (*psb*A and *rbc*L) sequences from established species within *Pneophyllum* and *Chamberlainium* respectively and the generitype (*psb*A), *S. fruticulosus*, were used for the phylogenetic analyses (Table S1). Both *rbc*L and *psb*A sequences from the orders Gelidiales (one), Sporolithales (three), Hapalidiales (five) and Corallinales (two) were used as the outgroup in order to provide phylogenetic placement of Chamberlainoideae. Sequences from New Zealand specimens, sequences from the already established species in Chamberlainoideae and sequences used as the outgroup, were obtained from GenBank (Clark *et al.* 2016). For the *psb*A gene, the type sequence from *L. natalense* and sequences from *S. yendoi* from New Zealand had shorter base pair lengths, 420 bp and 467 bp respectively. For the *rbc*L gene, the type sequences from *L. discoideum* and *L. impar* were 269 bp long while the outgroup sequence lengths ranged between 293 bp and 1364 bp. The rest of the *psb*A and *rbc*L sequences were 851 bp and 1387 bp long respectively. The sequences for each gene were aligned using MUSCLE (Edgar 2004) alignment with a maximum of eight iterations.

Geneious v11.1.5 (https://www.geneious.com, Kearse *et al.* 2012) was used for all phylogenetic analyses. Separate Neighbour-joining trees were constructed for *psb*A (Total: 121) and *rbc*L (Total: 81) sequences. The default parameters for Neighbour-joining trees were used namely HKY (genetic distance model), bootstrap model (resampling method) with a support threshold of 50 %. This was merely to display all the sequences used in this study for each gene. Identical sequences were removed from the respective datasets before Maximum likelihood (RaxML) analyses were performed on *psb*A (Total: 70 after removing identical sequences) and *rbc*L (Total: 60 after removing identical sequences) separately, applying the Rapid-hill climbing and then the Rapid Bootstrapping and search for best-scoring ML tree algorithm, using the GTR CAT model of evolution with 500 bootstrap replicates. The same

RaxML protocols were applied to the concatenated dataset (Total: 37) where the two loci were combined.

2.4. Sequence divergence values

Interspecific pairwise distances were calculated separately for the *psb*A and *rbc*L genes based on the RaxML analysis using % Identity: Percentage of bases/residues that are identical. The outgroup sequences and short sequences were removed as not to over or underestimate the divergence % between species. Intraspecific pairwise distances were similarly calculated for species that had more than one sequence.

2.5. Species delimitation

2.5.1. Automatic Barcode Gap Discovery

The Automatic Barcode Gap Discovery (ABGD, Puillandre *et al*. 2012) method was applied separately to the *psb*A (Total: 70 after removing identical sequences), *rbc*L (Total: 60 after removing identical sequences) and concatenated (37 sequences) RaxML datasets (Table S1) for further species delimitation support. For this study, the ABGD method was used as secondary support for species delimitated by molecular analyses. The analyses were performed at http://wwwabi.snv.jussieu.fr/public/abgd/abgdweb.html. All parameters were set to default (Pmin = 0.001, Pmax = 0.100, Steps = 10, Number of bins = 20) apart from the minimum gap width (set at: X = 1.0) and the distance (Simple Distance).

2.5.2. *BEAST (pronounced starBeast) analysis

Based on the sequence analysis of the *psb*A gene, specimens assigned to *C. capens*e shared six single nucleotide polymorphisms (SNPs) with specimens assigned to *C. occidentale*, and seven SNPs with specimens assigned to *C. glebosum*. Furthermore, the *rbc*L sequence of a single

specimen (UWC 16/05) assigned to *C. capense* was identical to the *rbc*L sequences of all specimens assigned to *C. occidentale*. The *rbc*L sequence of a single specimen (UWC 16/27) assigned to *C. capense* was similarly identical to the *rbc*L sequences of all specimens assigned to *C. glebosum*. In order to establish the conspecificity of these three species, both independent gene sequence alignments (*psb*A, *rbc*L) as well as the concatenated gene alignment were analysed using *BEAST (Bayesian Evolutionary Analysis by Sampling Trees, Drummond *et al*. 2012), a cross-platform programme for Bayesian analysis of molecular sequences that is orientated towards rooted, time-measured phylogenies inferred using molecular clock models. Using multiple genes sampled from multiple individuals across a set of closely related species, this analysis provides gene trees based on a combined inference of species tree topology, divergence times and population sizes. All sequences in each alignment were assigned to either *C. capense*, *C. glebosum* or *C. occidentale* so that they may be associated with a species *a-priori* to enable inference of species tree implemented in *BEAST (Drummond *et al.* 2012). The analysis was performed under an uncorrelated relaxed Molecular clock model (which allows for the rate of evolution to vary along tree branch and be informed by the sequence data) and was run using the best fitting (HKY+G+I) and a linear with constant root models. The population sizes were assigned gamma priors and default settings were used as priors for species tree estimation. Markov chain Monte Carlo (MCMC) chains were run for 100 million generations, sampling tress every 10,000 generations. Effective Sample Sizes (ESS) (values > 200) and trace plots estimated with Tracer v1.7 (10 % burn-in) (Rambaut *et al*. 2018) were used as convergence diagnostics.

The final maximum clade credibility tree was obtained by summarising trees generated after discarding the first 1,000 trees (10 %) as burn-in from the 100 million generations in TreeAnnotator v1.8.4 (Rambaut & Drummond 2017). The divergence among species was

annotated from median heights of the clades within the Maximum Clade Credibility (MCC) tree. The species tree obtained was visualized in FigTree v.1.4.3 (Rambaut 2016) and population dynamics was assessed by visualising the tree in DensiTree v.2.2.6 (Bouckaert & Heled 2014).

2.6. Morpho-anatomical analysis

2.6.1. Histological preparation

Specimens were prepared following Maneveldt & van der Merwe (2012). Formalin preserved specimens were used for light microscopy. Specimens were first decalcified in 10 % nitric acid. Thereafter they were immersed in 70 %, 90 % and 100 % ethanol solutions respectively for a minimum of 60 min each in order to displace any water and acid in the specimens. Specimens were removed from the 100 % ethanol solution and allowed to air dry for a few seconds. Leica HistoResin filtration medium (Leica Biosystems, Nussloch GmbH, Heidelberg, Germany) was used to infiltrate (12-48 hrs depending on the crust thickness) submerged specimens. Once specimens were completely infiltrated (sinking to the bottom of infiltration vials), a hardening solution was added to the filtration medium and the specimens were orientated in this final solution. Hardening took approximately 30-50 min at room temperature; for more rapid hardening, specimens were placed in an oven (with an extractor fan) at 60 °C for approximately 10-20 min.

Using a Bright 5030 microtome (Bright Industrial Company LTD, Huntingdon, England) specimens were sectioned at 6-8 μm thickness. A fine sable hair brush was used to transfer sections to a slide covered with distilled water and allowed to air dry for 24 hrs so that sections could stick. The slides were then stained with toluidine blue (0.25 g borax 100 ml^{-1} distilled water, combined with 0.06 g toluidine blue 100 ml^{-1} distilled water), and once air dried were

covered with cover slips using DPX Mountant (BDH Laboratory Supplies, The Birches, Willard Way, Imberhorne Industrial Estate, East Grinstead, West Sussex RH19 1XZ, UK) for microscopy.

2.6.2. Microscopy and morpho-anatomical interpretations

In cell measurements, length donates the distance between primary pit connections, and diameter the maximum width of the cell lumen at right angles to this. Conceptacle measurements followed Adey & Adey (1973). Following Maneveldt *et al*. (2017), there was no uniform number of cells and chambers measured (thus we provided ranges and not averages with means). For these ranges, measurements from hundreds of individual sections were taken, looking at all fragments (fragments were 5-7 mm in length X thickness of specimen) from all sections (18 sections per slide) on all slides (4-6 slides per specimen number). For chambers, only those perfectly through the pore were measured, these ranging from tens to less than 100 measurements. Here we established the minimum and maximum value, looking at a nearly exhaustible number of cells/conceptacles and only stopped measuring when we no longer found any measurements smaller or larger than what had already been observed. Thallus anatomical terminology followed Chamberlain (1990) and morphological (growth forms) terminology followed Woelkerling *et al*. (1993).

3. Results

3.1. Molecular analysis

A total of 121 (80 generated specifically for this study, 41 from GenBank) *psb*A and 81 (60 generated specifically for this study, 21 from GenBank) *rbc*L sequences were used in the phylogenetic analyses (Figs 1-2, Table S1). For RaxML analyses of each gene individually (*psb*A, 70 sequences and *rbc*L, 60 sequences) and a concatenation of both genes, there is full bootstrap support (BS = 100 %) for the subfamily Chamberlainoideae as a monophyletic clade (Figs 3-5). Within Chamberlainoideae, the analysis also provided full bootstrap support (BS = 100%) for *Pneophyllum* and *Chamberlainium* as monophyletic genera. The topologies of the Maximum Likelihood trees were congruent in all phylograms with the species previously ascribed to *Spongites* from South Africa forming well-supported, monophyletic clades within Chamberlainoideae. Interspecific sequence divergences for the *psb*A gene ranged from 2.4-11.5 % for *Chamberlainium* species and 5.5-8.1 % for *Pneophyllum* species while intraspecific sequence divergences ranged from 1.3-2.0 % and 1.2 % respectively (Table 1). The *rbc*L interspecific and intraspecific sequence divergences for *Chamberlainium* species ranged from 4.6-16.0 % and 1.0-4.0 % respectively, while an intraspecific sequence divergence of 0.8 % was attained for *P. neodiscoideum* (Table 2).

Chamberlainoideae contains two genera, *Pneophyllum*, well-supported in *psb*A (BS = 90 %) and with full support in *rbc*L and concatenated trees and *Chamberlainium* moderately supported in *psb*A (BS = 75 %) and strongly supported in *rbc*L (BS = 97 %) and concatenated (BS = 100 %) trees. The species (clade C and *C. agulhense*) previously ascribed to *Spongites* from South Africa are fully supported within *Chamberlainium* in all three trees, while the species (clades B, D-H) previously ascribed to *Spongites yendoi* from South Africa, similarly are well to fully supported within this genus (*psb*A BS = 94-100 %, *rbc*L BS = 96-100 %,

concatenated BS = 100 %). For both the *psb*A and *rbc*L genes as well as the concatenated dataset, *Chamberlainium decipiens* and *C. tumidum* have strong support as sister to the South African *Chamberlainium* species, with clade B being a well-supported sister taxon to the fully supported clade of *C. decipiens* and *C. tumidum*. The ML analysis of the *psb*A gene shows '*Spongites yendoi*' specimens from New Zealand in a clade with *Chamberlainium* species from Chile, but without support (Fig. 3). Clade A comprised of a single species (previously ascribed to *Spongites*), *Chamberlainium* species from Chile and Antarctica and *P. fragile* from New Zealand form a well-supported (*psb*A BS = 90 %, *rbc*L BS = 100 %, concatenated BS = 100 %) clade within *Pneophyllum*, aligning with the generitype species, *P. fragile* (Fig. 3). In the absence of the established *Pneophyllum* sequences and those from New Zealand, clade A, *Pneophyllum* species from Chile and *L. discoideum* (Type locality, Mouth of Río Grande, Tierra del Fuego Argentina) formed a well-supported clade (*rbc*L = 100 %, concatenated = 100 %), with a species of *Chamberlainium* from Antarctica as a sister taxon to this clade (Figs 4-5).

Based on the *psb*A and *rbc*L results herein, Chamberlainoideae has nine species in South Africa in both *Chamberlainium* and *Pneophyllum*. There are eight species in *Chamberlainium* (Figs 3-5; clades B-H), where clades B and D-H were all previously ascribed to *Spongites yendoi* and all (excluding clade D) are newly described herein. Clade D, includes specimens that were previously ascribed, based on morpho-anatomy, as *Lithophyllum natalense* (Type locality: South Africa, KwaZulu-Natal [as Natal]). This species was subsumed into *Spongites yendoi* by Chamberlain (1994b), but based on the phylogenetic results herein, is resurrected as a distinct species in *Chamberlainium*. Also included in *Chamberlainium* is clade C, previously described as *Spongites impar* (Type locality: South Africa, Natal or between Natal and the Cape of Good Hope) and herein transferred to *Chamberlainium*. The results also re-affirm the

placement of the already established and transferred species, *Chamberlainium agulhense* (Type locality: South Africa, Western Cape Province, Cape Agulhas: L'Agulhas, Stinkbaai). South Africa has one, clade A, confirmed by both genetics and morpho-anatomy, species of *Pneophyllum*. Clade A was previously described as *S. discoideus* (Type locality: Tierra del Fuego [mouth of the Rio Grande], Argentina).

Also included in *Chamberlainium* are seven specimens that were ascribed, based on morpho-anatomy, to *S. yendoi* from New Zealand, two specimens collected from Chile, and two already established species from the genus *Chamberlainium* (*C. decipiens*), including the generitype species (*C. tumidum*). Except for two instances (the specimens genetically and morpho-anatomically identical to the type of *Lithophyllum natalense* [type locality, Durban? KwaZulu-Natal, South Africa] and the relationship between *Spongites* sp. (C40.2xii08) and *Chamberlainium* sp. (C174.2xii08), the ABGD results were consistent between the two genes. The ABGD delineation for the *psb*A and *rbc*L genes was inconsistent for specimens genetically and morpho-anatomically identical to the type of *L. natalense*. According to the ABGD results, *Spongites* sp. (C40.2xii08) and *Chamberlainium* sp. (C174.2xii08) are separate species based on the *psb*A phylogeny (intraspecific sequence divergence of 1.7 %). However, there is greater support, based on the *rbc*L gene (intraspecific sequence divergence of 4.9 %) and the concatenated dataset that the two species are conspecific.

Specimens assigned to three of the cryptic species (clades F, G, H) previously ascribed to *S. yendoi* produced some very interesting findings. Based on the sequence analysis of the *psb*A gene, specimens in clade G share seven unique SNPs with the specimens from clade F and six SNPs with the specimens from clade H (Fig. 3). Furthermore, the *rbc*L sequence of specimen UWC 16/05 (clade G) is identical to all of the specimen sequences in clade F. Additionally,

the *rbc*L sequence of specimen UWC 16/27 (clade G) is identical to all of the specimen sequences in clade H. The three clades were delineated as separate species based on ABGD results for *psb*A and *rbc*L (Figs 3-4) genes while clades F and G are conspecific in the ML analysis of the concatenated dataset (Fig. 5). Based on the *BEAST analysis, however, the three clades were resolved as distinct species (Figs 6, 7). The three gene tree topologies (Fig. 6) were congruent with one another with maximum posterior values obtained for all nodes. The DensiTree representation supported this finding (Fig. 8) and suggested that clade H had speciated to give rise to both clades F and G that are more closely related to one another as their divergence occurred much more recently (Figs 7, 8).

South African specimens (clade A) previously ascribed to *S. discoideus* (basionym *Lithophyllum discoideum*; type locality, Tierra del Fuego, Argentina) and the type of *Lithophyllum discoideum* are not conspecific, both resolving in the genus *Pneophyllum* along with *P. fragile*, the generitype species (Figs 3, 4). The South African species (clade A) and *S. discoideus* therefore do not belong in *Spongites* and need to be transferred to *Pneophyllum*. Also included in *Pneophyllum* are one specimen from Antarctica (*Chamberlainium* sp. [ANT2-16.15viii16]), three specimens from Chile (*Chamberlainium* sp. [C18.17ii09], *Chamberlainium* sp. [AMC17.2x17], *Chamberlainium* sp. [AMC13.9x17]) that were assigned to *Chamberlainium*, four specimens ascribed to *S. yendoi* from New Zealand, and one specimen ascribed to *P. fragile* from New Zealand. While the ABGD results delineated each of these as distinct species across both genes, the *psb*A and concatenated dataset has delineated *Chamberlainium* sp. (AMC13.9x17) as belonging to *P. neodiscoideum* (sequence divergence: *psb*A 2.0 %, *rbc*L 4.1 %) (Tables 1, 2, Fig. 5).

Clade B, which appears to be a South African endemic, formed a well-supported (*psb*A, 98 %; *rbc*L, 93 %; concatenated dataset, 99 %) sister clade to two species (*C. decipiens* and *C. tumidum*) from the Northeast Pacific, rather than to the other species of *Chamberlainium* from South Africa. Similarly, although without any support, several other South African *Chamberlainium* species (clades E, F, G, H) aligned closer to several New Zealand specimens identified as *S. yendoi* than they did to other South African *Chamberlainium* species

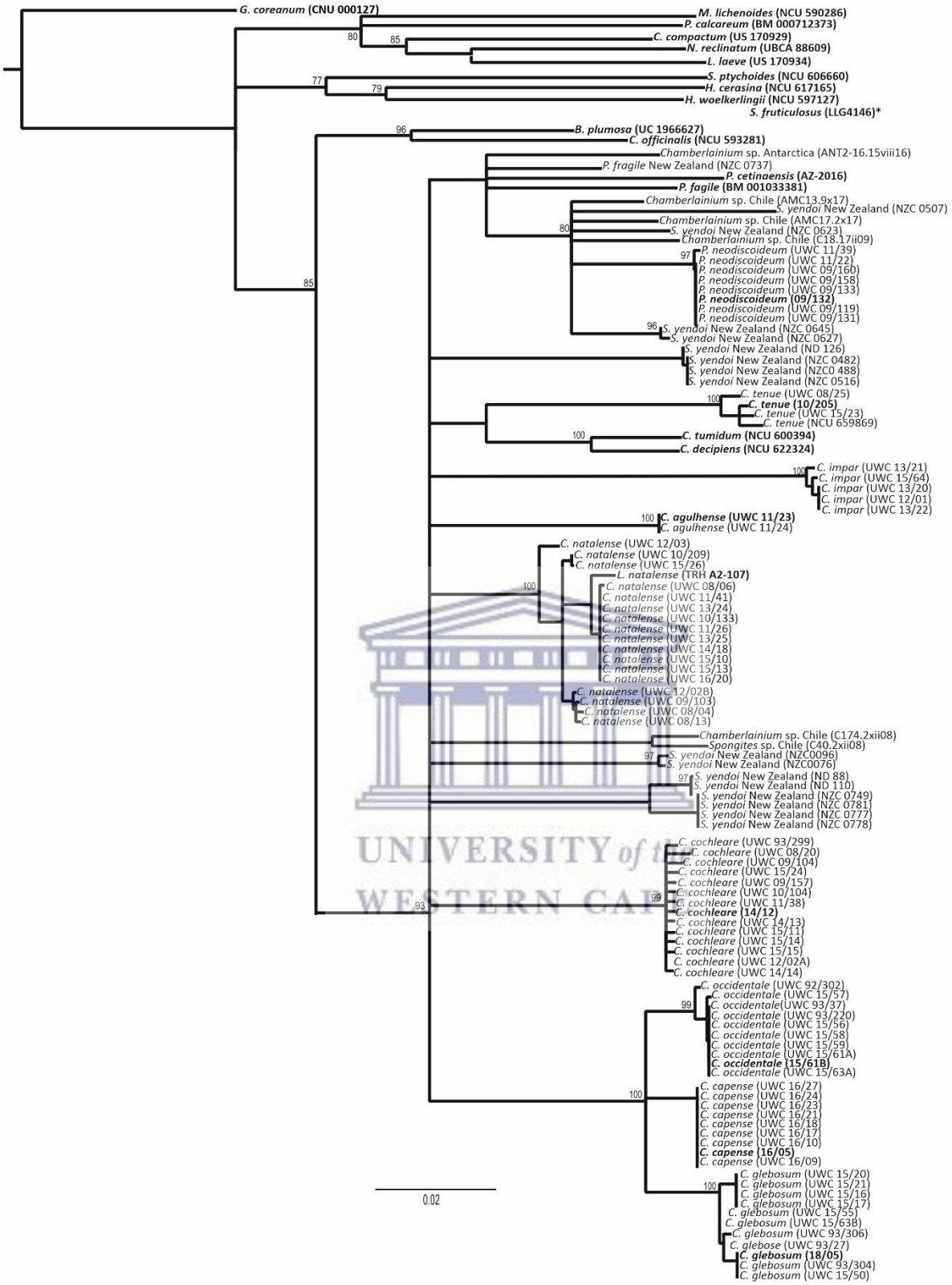

Fig. 1. Neighbour-Joining tree based on *psb*A sequences. Species with sequenced type/'topotype' material are highlighted in bold. Species names are followed (in brackets) by their specimen herbarium voucher number. Newly established South African species names are followed (in brackets) by their collection number as they are yet to be assigned official herbarium (L = Naturalis, Netherlands, Leiden) numbers. Bootstrap support (BS) values are provided at branch nodes; BS values < 75 % are not shown. The asterisk (*) indicates the molecular reference for the generitype of *Spongites*, *Spongites fruticulosus*.

Fig. 2. Neighbour-Joining tree based on *rbc*L sequences. Species with sequenced type/'topotype' material are highlighted in bold. Species names are followed (in brackets) by their specimen herbarium voucher number. Newly established South African species names are followed (in brackets) by their collection number as they are yet to be assigned official herbarium (L = Naturalis, Netherlands, Leiden) numbers. Bootstrap support (BS) values are provided at branch nodes; BS values < 75 % are not shown.

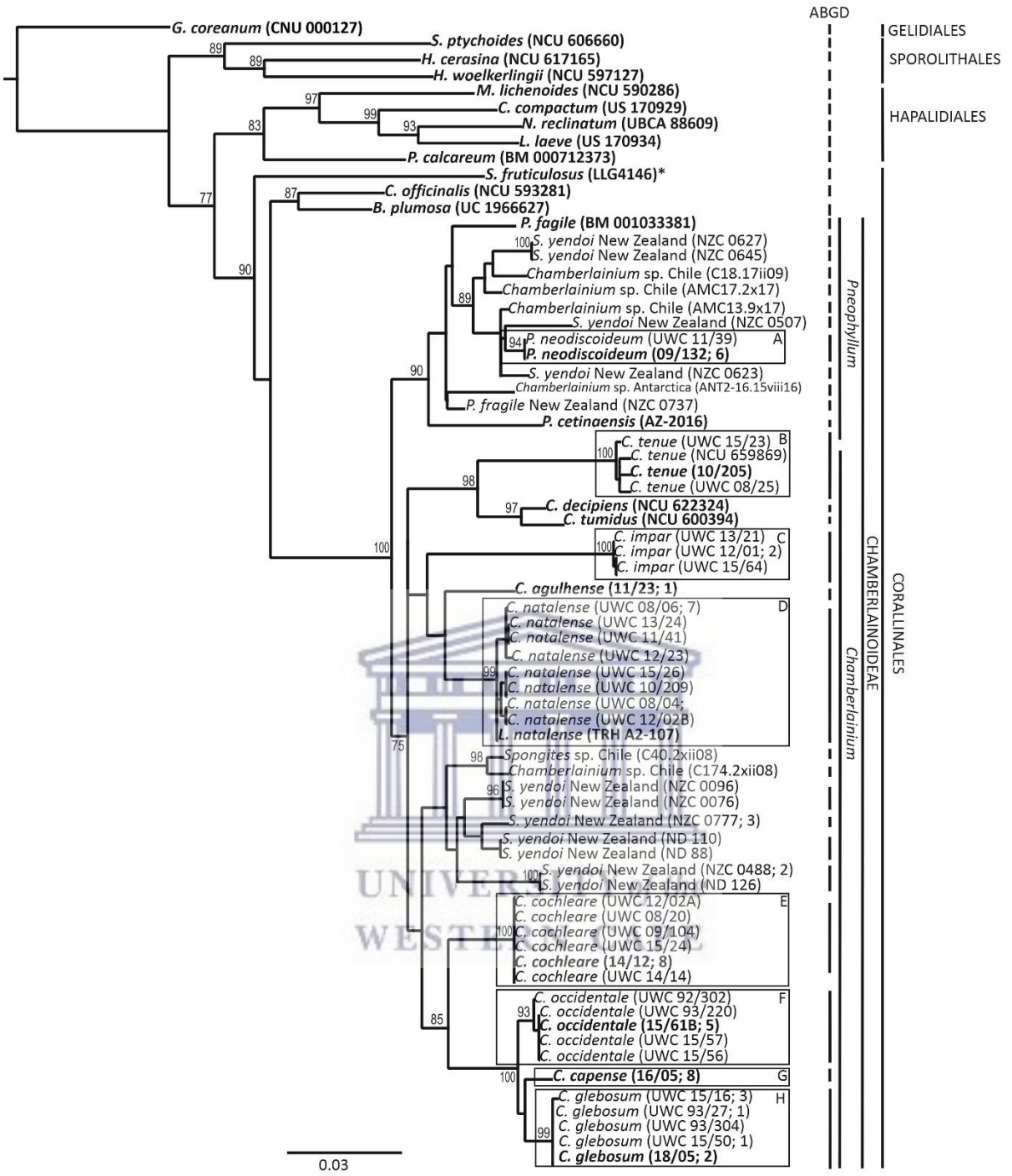

Fig. 3. Maximum likelihood tree based on *psb*A sequences. Species with sequenced type/'topotype' material are highlighted in bold. The first set of vertical lines indicates the Primary Species Hypothesis as determined by ABGD and identify individual species. Species names are followed (in brackets) by their specimen herbarium voucher number. Newly established South African species (identified as boxed clades A-H) names are followed (in brackets) by their collection number as they are yet to be assigned official herbarium (L = Naturalis, Netherlands, Leiden) numbers. Bootstrap support (BS) values are provided at branch nodes; BS values < 75 % are not shown. The asterisk (*) indicates the molecular reference for the generitype of *Spongites*, *Spongites fruticulosus*.

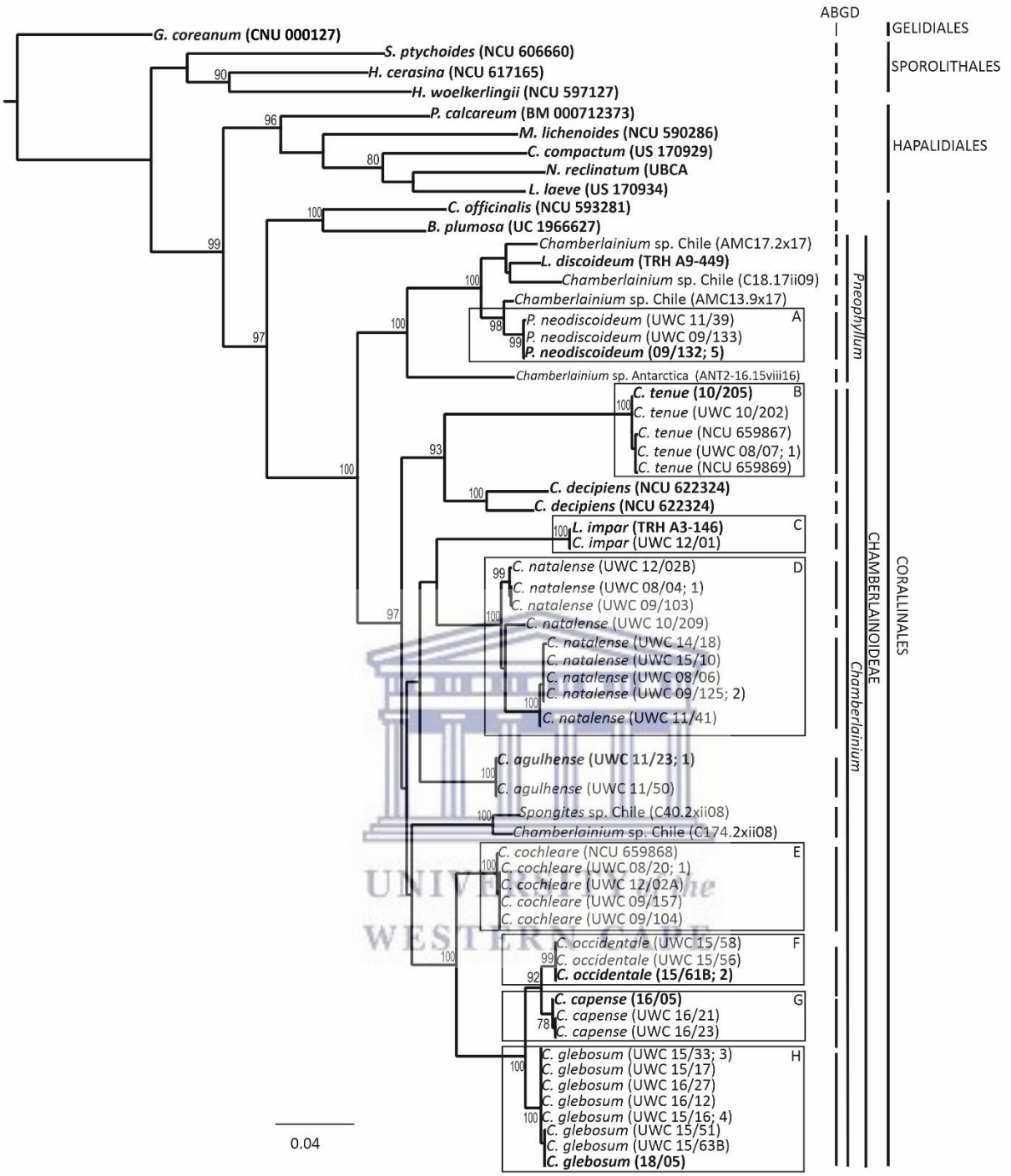

Fig. 4. Maximum likelihood tree based on *rbc*L sequences. Species with sequenced type/'topotype' material are highlighted in bold. The first set of vertical lines indicate the Primary Species Hypothesis as determined by ABGD and identify individual species. Species names are followed (in brackets) by their specimen herbarium voucher number. Newly established South African species (identified as boxed clades A-H) names are followed (in brackets) by their collection number as they are yet to be assigned official herbarium (L = Naturalis, Netherlands, Leiden) numbers. Bootstrap support (BS) values are provided at branch nodes; BS values < 75 % are not shown.

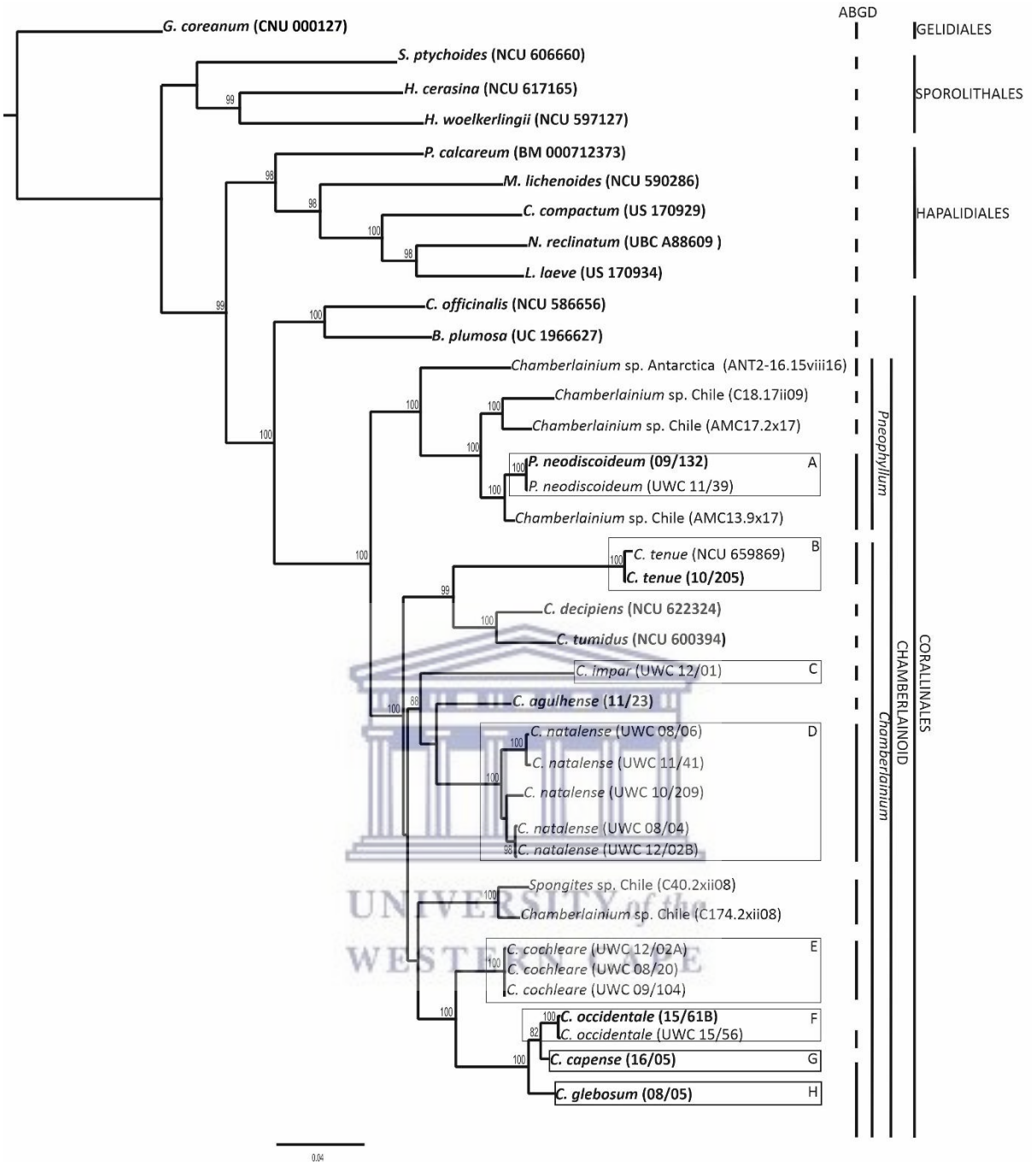

Fig. 5. Maximum likelihood tree based on concatenated *psb*A and *rbc*L sequences. Species with sequenced type/'topotype' material are highlighted in bold. The first set of vertical lines indicate the Primary Species Hypothesis as determined by ABGD and identify individual species. Species names are followed (in brackets) by their specimen herbarium voucher number. Newly established South African species (identified as boxed clades A-H) names are followed (in brackets) by their collection number as they are yet to be assigned official herbarium (L = Naturalis, Netherlands, Leiden) numbers. Bootstrap support (BS) values are provided at branch nodes; BS values < 75 % are not shown.

Table 1. Pairwise sequence divergences (%) for *psb*A sequences (851 bp) reported for specimens aligning to Chamberlainoideae and to *S. fruticulosus* in this study. Only sequences of comparable length have been included. Species highlighted in bold are sequences from type/'topotype' material. Values in grey-shaded cells represent the intraspecific pairwise sequence divergences for the newly established South African species (which include the type specimen for each of those species) with more than one sequenced specimen. Specimen details can be found in Table S1.

	Taxa	1	2	3	4	5	6	7	8	9	10	11	12	13	14	15	16	17	18	19	20	21
1	*Chamberlainium* sp. Antarctica (ANT2-16.15viii16)																					
2	*Chamberlainium* sp. Chile (C174.2xii08)	6.9																				
3	*Chamberlainium* sp. Chile (AMC17.2x17)	4.8	7.8																			
4	*Chamberlainium* sp. Chile (C18.17ii09)	5.2	8.1	2.4																		
5	*Chamberlainium* sp. Chile (AMC13.9x17)	4.5	6.9	2.5	3.6																	
6	***C. agulhense***	7.5	6.8	8.4	8.3	8.0																
7	***C. capense***	8.9	7.2	8.6	9.0	8.5	7.2															
8	*C. cochleare*	8.0	7.3	8.2	8.7	7.6	6.2	6.5	1.3													
9	***C. decipiens***	8.9	9.2	8.7	8.3	8.4	7.7	9.0	8.7													
10	*C. glebosum*	9.1	7.5	9.1	9.5	9.0	7.7	3.0	6.8	9.0	1.4											
11	*C. impar*	10.3	10.3	10.6	11.0	10.6	8.1	11.4	9.7	11.1	11.3	1.2										
12	*C. natalense*	7.8	7.8	8.3	8.4	8.5	5.1	8.3	6.8	7.6	8.5	9.8	1.9									
13	*C. occidentale*	8.9	7.5	8.7	8.8	8.3	7.6	2.8	6.8	8.5	3.3	11.4	8.4	1.4								
14	*C. tenue*	10.4	10.0	11.0	11.1	9.7	9.6	9.9	9.9	8.2	10.0	11.5	9.1	9.7	2.0							
15	***C. tumidum***	10.0	9.5	9.7	9.8	9.8	7.6	8.6	8.5	3.9	8.7	11.1	7.8	8.7	8.9							
16	***P. cetinaensis***	7.7	9.2	7.0	7.7	7.5	8.5	9.5	9.1	10.5	9.7	11.5	9.8	9.6	11.0	10.6						
17	***P. fragile***	5.8	7.1	4.7	5.5	5.1	8.4	7.7	7.3	9.3	8.4	9.9	7.5	8.0	9.9	9.3	5.8					
18	*P. fragile* (New Zealand)	4.9	7.9	4.4	5.2	4.8	7.4	8.5	7.2	8.6	8.8	10.3	7.3	8.9	10.4	9.6	6.6	3.3				
19	*P. neodiscoideum*	6.2	8.7	4.0	4.5	2.0	8.7	9.8	8.2	8.8	10.0	10.4	8.9	9.6	10.5	9.9	8.1	5.5	5.4	1.2		
20	***S. fruticulosus***	12.2	12.8	12.0	12.0	11.7	12.8	13.5	12.7	12.2	13.5	14.1	12.2	12.4	14.0	12.5	12.0	12.8	11.8	12.5		
21	*Spongites* sp. (C40.2xii08)	6.9	1.7	7.8	8.3	7.1	6.7	7.1	7.1	9.2	7.4	10.2	7.6	7.4	9.6	9.5	9.3	6.6	7.9	8.9	13.2	

Table 2. Pairwise sequence divergences (%) for *rbc*L sequences (1387 bp) reported for specimens aligning to Chamberlainoideae in this study. Only sequences of comparable length have been included. Species highlighted in bold are sequences from type/'topotype' material. Values in grey-shaded cells represent the intraspecific pairwise sequence divergences for the newly established South African species (which include the type specimen for each of those species) with more than one sequenced specimen. Specimen details can be found in Table S1.

	Taxa	1	2	3	4	5	6	7	8	9	10	11	12	13	14	15	16	17
1	*Chamberlainium* sp. Antarctica (ANT2-16.15viii16)																	
2	*Chamberlainium* sp. Chile (C174.2xii08)	13.5																
3	*Chamberlainium* sp. Chile (AMC17.2x17)	12.3	13.8															
4	*Chamberlainium* sp. Chile (C18.17ii09)	13.0	14.3	6.7														
5	*Chamberlainium* sp. Chile (AMC13.9x17)	11.6	13.4	6.9	7.8													
6	***C. agulhense***	13.5	10.5	14.5	14.8	13.5	1.0											
7	***C. capense***	13.8	11.9	14.5	15.5	13.7	11.6											
8	*C. cochleare*	13.8	10.5	14.8	15.6	13.4	9.1	8.6	2.1									
9	***C. decipiens***	13.8	11.5	14.8	15.3	14.0	9.8	12.0	10.5									
10	*C. glebosum*	14.0	12.0	14.7	15.6	13.8	11.4	4.6	8.7	12.2	2.8							
11	*C. impar*	14.4	11.7	15.5	16.0	15.0	10.8	12.7	10.8	12.2	12.9							
12	*C. natalense*	13.6	11.6	14.6	15.1	13.7	8.6	11.5	9.3	10.4	11.6	10.1	2.7					
13	*C. occidentale*	15.8	13.6	16.6	17.5	15.6	13.0	5.1	10.1	14.0	6.5	14.3	13.2	4.0				
14	*C. tenue*	16.4	14.9	16.3	16.8	15.8	13.1	14.8	12.9	12.0	14.8	14.1	13.6	16.0	1.6			
15	***C. tumidum***	14.5	13.1	15.1	15.6	14.4	10.5	11.8	10.7	6.2	11.8	12.8	10.3	13.6	12.8			
16	*P. neodiscoideum*	11.8	13.3	7.5	8.4	4.1	12.6	14.4	12.7	13.2	14.3	14.0	12.7	16.0	15.1	13.7	0.8	
17	*Spongites* sp. (C40.2xii08)	14.1	4.9	14.3	14.6	13.8	10.8	12.2	10.9	12.2	12.3	12.4	11.9	14.1	15.4	13.6	14.1	

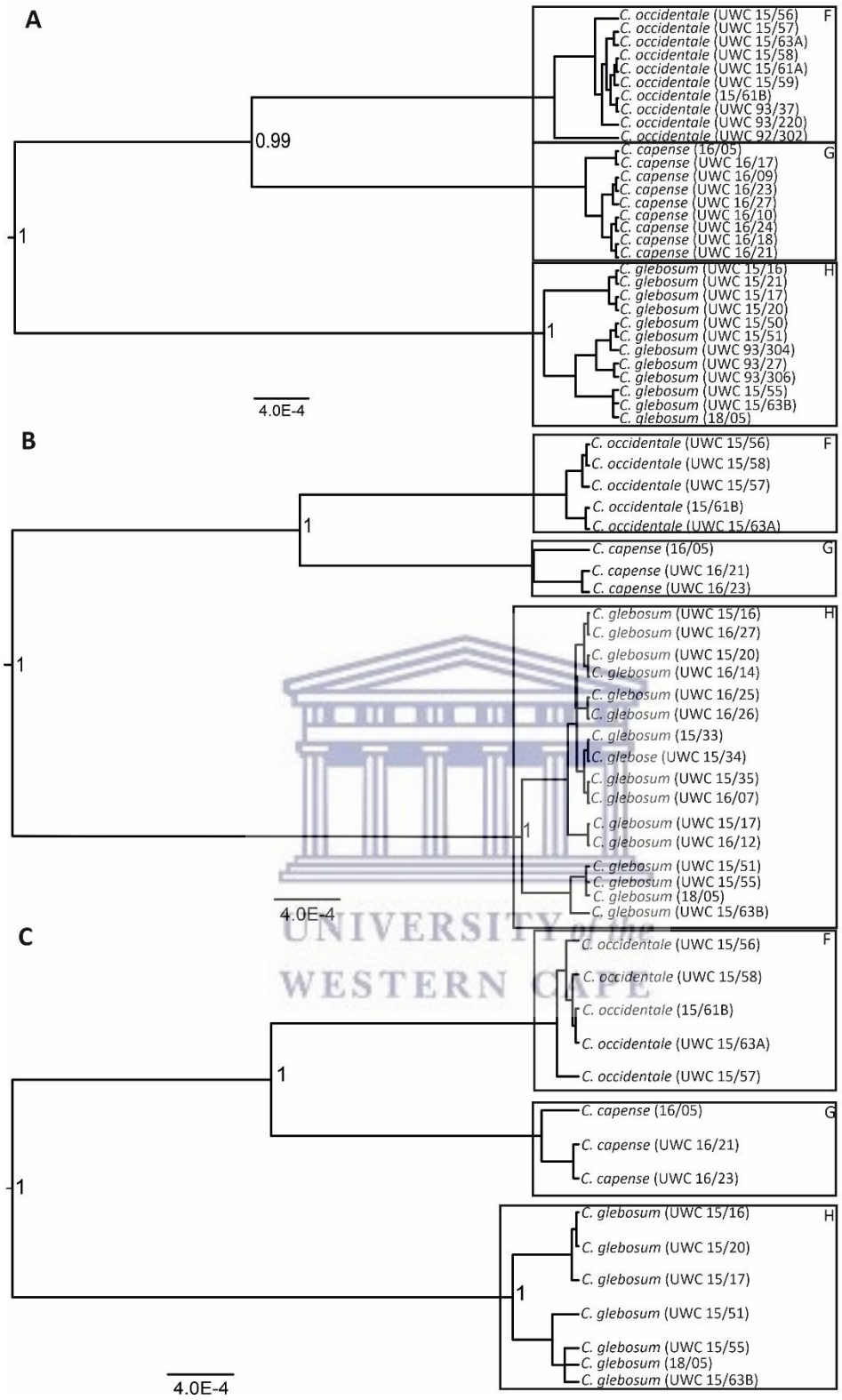

Fig. 6. Gene tree topologies estimated in *BEAST for *C. occidentale* (clade F), *C. capense* (clade G) and *C. glebosum* (clade H) based on *psb*A (A) and *rbc*L (B) gene sequences (*psb*A, 851 bp; *rbc*L, 1365 bp), and the concatenated dataset (C). Posterior probabilities from the *BEAST analysis are provided at the branch nodes. Scale bar indicates estimated mean evolutionary rate (0.0004 substitutions per site per year).

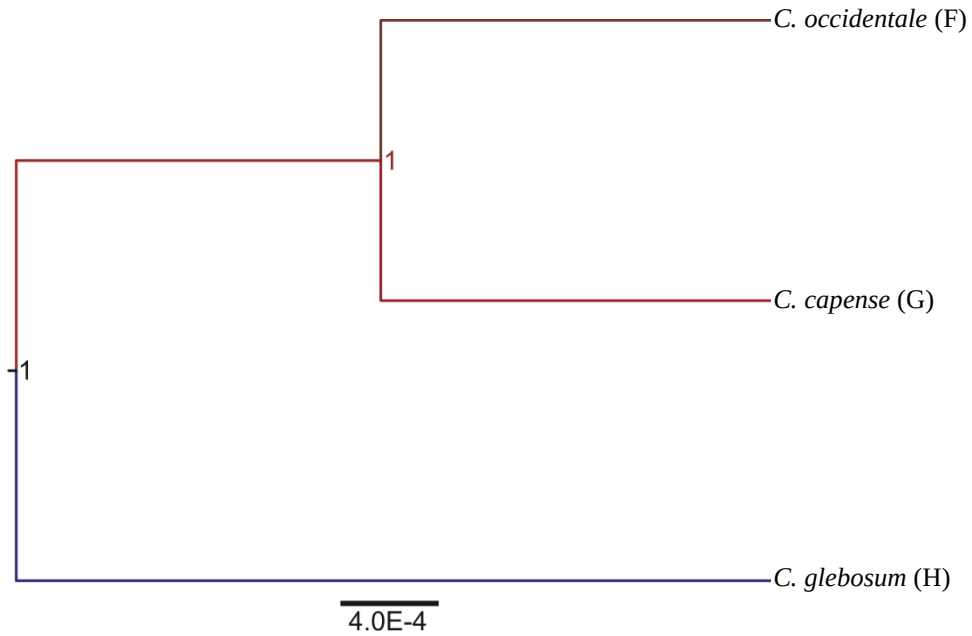

Fig. 7. Species tree topology estimated in *BEAST for *C. occidentale* (clade F), *C. capense* (clade G) and *C. glebosum* (clade H) based on the *psb*A and *rbc*L gene sequences, and the concatenated dataset. Posterior probabilities from the *BEAST analysis are provided at the branch nodes. Scale bar indicates estimated mean evolutionary rate (0.0004 substitutions per site per year).

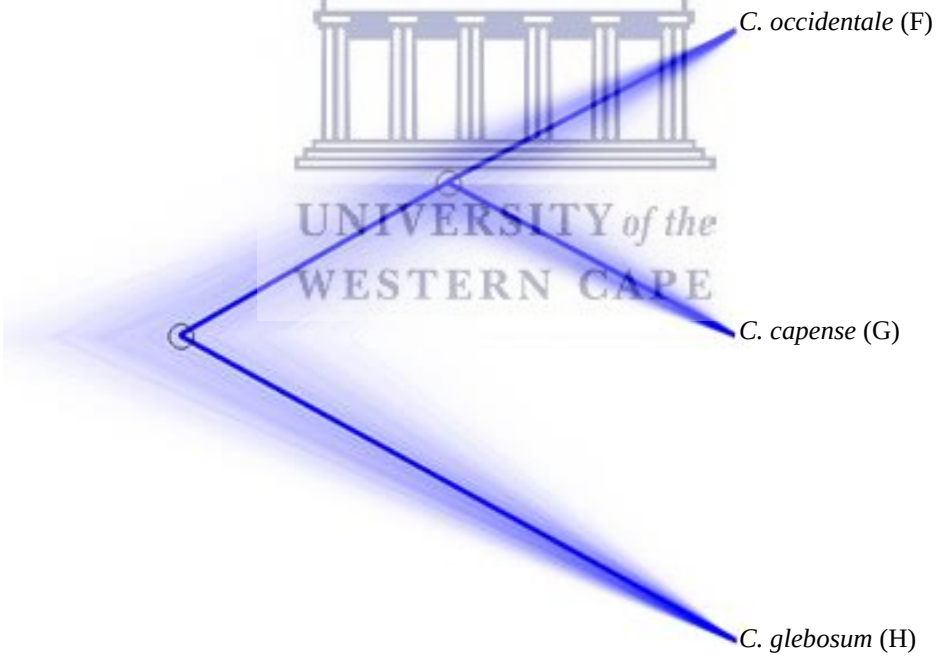

Fig. 8. DensiTree representation of the consensus tree for *C. occidentale* (clade F), *C. capense* (clade G) and *C. glebosum* (clade H) with population sizes indicated as variably shaded (each shade representing a single sequence) line widths.

3.2. Species descriptions

3.2.1. *Chamberlainium agulhense* (Maneveldt, E.van der Merwe & P.W.Gabrielson) Caragnano, Foetisch, Maneveldt & Payri

(Fig. 9; Tables 3-5)

BASIONYM: *Spongites agulhensis* Maneveldt, E.van der Merwe & P.W.Gabrielson, 2015: 475.

HOLOTYPE: L 0820786, 21.x.2011, *leg. G.W. Maneveldt*, collection number 11/53, epilithic on shale platform in the high intertidal zone. See van der Merwe *et al*. (2015).

ISOTYPE: UWC 11/53.

TYPE LOCALITY: South Africa, Western Cape Province, Cape Agulhas: L'Agulhas, Stinkbaai (34°49'26.26"S, 20°01'0.69"E).

ETYMOLOGY: '*agulhense*' from '*agulhensis*', making reference to the type locality at L'Agulhas, Cape Agulhas.

DNA SEQUENCES: *psb*A (851 bp) and *rbc*L (1467 bp) gene sequences, obtained from two specimens (one a 'topotype', the other a paratype) (Table S1), were all identical to each other. DNA sequences showed that *Chamberlainium agulhense* was different from all other named species sequenced to date (Figs 3-5; Table S1).

DISTRIBUTION: Confirmed by DNA sequence data to have a very restricted distribution (± 10 km) along the southern west coast, occurring from L'Agulhas (Cape Agulhas) to Struisbaai (Western Cape Province), South Africa (van der Merwe *et al*. 2015).

HABIT AND MORPHOLOGY: Plants non-geniculate, thalli thin, encrusting (smooth) (Fig. 9), firmly adherent, brownish-pink when freshly collected. Individual crusts not coalescing (do

not fuse together) and easily discernible (Fig. 9). Thalli epilithic on primary bedrock (shale and quartzitic sandstone) in high and mid-intertidal zones (Fig. 9).

ANATOMY AND REPRODUCTION: See van der Merwe *et al.* (2015) for a detailed description.

3.2.2. *Chamberlainium capense* Maneveldt, Puckree-Padua & P.W.Gabrielson *sp. nov*.

(Figs 10-19; Tables 3-5)

HOLOTYPE: L ???????, 09.x.2016, *leg. G.W. Maneveldt*, collection number 16/05 (Fig.11), epilithic on primary bedrock in mid-intertidal, sand inundated rock pool. Fragments of the holotype are retained in UWC and NCU.

TYPE LOCALITY: South Africa, Western Cape Province, Mouille Point (33°53'56.64"S, 18°24'31.71"E).

ETYMOLOGY: '*capense*' in reference to the species' restricted distribution along the Cape Peninsula historically known as the 'Cape of Good Hope, South Africa' (*Caput Bonae Spei*).

DIAGNOSIS: Thalli thick, encrusting to variably lumpy and slightly protuberant, not becoming secondarily thick and discoid with orbicular protrusions, nor wrinkled; individual crusts not coalescing (not fusing together) and easily discernible; colour of living thalli bright to dusky pink in well-lit conditions to rosy or purple-pink in dim light; thallus construction monomerous; epithallus single layered; central columella present in tetrasporangial conceptacles, disintegrating to form a low mound with maturity; pore opening in mature tetrasporangial conceptacles occluded by a corona of filaments that project above the pore opening; *psb*A (GenBank??????) and *rbc*L (GenBank ??????) sequences collectively[1] unique.

DNA SEQUENCES: *psb*A (851 bp) and *rbc*L (1467 bp) gene sequences, obtained from nine specimens (including the holotype) (Table S1), were all identical to each other. DNA sequences collectively showed that *Chamberlainium capense* was different from all other named species sequenced to date (Figs 3-8; Table S1).

[1] *Chamberlainium capense* shares seven single nucleotide polymorphisms (SNPs) with *C. occidentale*, with the *rbc*L sequence of the holotype of *C. capense* being identical to all *C. occidentale* specimens sequenced. *Chamberlainium capense* also shares six SNPs with *C. glebosum*, with the *rbc*L sequence of UWC 16/27 (*C. capense*) being identical to all *C. glebosum* specimens sequenced.

SPECIMENS EXAMINED: Nine samples (including the holotype), all confirmed by DNA sequencing, represent our entire collection for this taxon. Data below are presented geographically from north to south (along the southern west coast) followed chronologically by the collection numbers.

South Africa – Western Cape Province: Mouille Point. L ???????, 09.x.2016, *leg. G.W. Maneveldt, C.A. Puckree-Padua, A. Haywood,* collection number 16/05 (33°53'56.64"S, 18°24'31.71"E) (holotype), epilithic on primary bedrock in mid-intertidal rock pool.

Western Cape Province: Sea Point. UWC 16/09, 09.v.2016, *leg. G.W. Maneveldt & C.A. Puckree-Padua*, collection number 16/09 (33º55'20.77"S, 18º22'35.97"E), epizoic on *Scutellastra cochlear* (limpet) shell in the Cochlear zone (low intertidal zone); UWC 16/10, 09.v.2016, *leg. G.W. Maneveldt & C.A. Puckree-Padua,* collection number 16/10 (33º55'20.77"S, 18º22'35.97"E,), epizoic on *S. cochlear* shell (limpet) in the Cochlear zone (low intertidal zone).

Western Cape Province: Kommetjie. UWC 16/17, 10.v.2016, *leg. G.W. Maneveldt, C.A. Puckree-Padua, A. Haywood*, collection number 16/17 (34º08'22.99"S, 18º19'13.71"E), epilithic on primary bedrock in mid-shore; UWC 16/18, 10.v.2016, *leg. G.W. Maneveldt, C.A. Puckree-Padua, A. Haywood*, collection number 16/18 (34º08'22.99"S, 18º19'13.71"E), epilithic on primary bedrock in low shore; UWC 16/21, 10.v.2016, *leg. G.W. Maneveldt, C.A. Puckree-Padua, A. Haywood*, collection number 16/21 (34º08'22.99"S, 18º19'13.71"E), epilithic on primary bedrock and boulders in mid-shore rock pool.

Western Cape Province: Slangkop. UWC 16/23, 10.v.2016, *leg. G.W. Maneveldt, C.A. Puckree-Padua, A. Haywood*, collection number 16/23 (34º8'51.07"S, 18º19'6.10"E), epizoic on *S. cochlear* shell (limpet) in the Cochlear zone; UWC 16/24, 10.v.2016, *leg. G.W. Maneveldt, C.A. Puckree-Padua, A. Haywood*, collection number 16/24 (34º8'51.07"S, 18º19'6.10"E), epilithic on primary bedrock, among *S. cochlear* (limpet) territories in the

Cochlear zone (low intertidal zone); UWC 16/27, 10.v.2016, *leg. G.W. Maneveldt, C.A. Puckree-Padua, A. Haywood*, collection number 16/27 (34º8'51.07"S, 18º19'6.10"E), epilithic on primary bedrock in mid-intertidal zone.

DISTRIBUTION: Confirmed by DNA sequence data to have a comparatively restricted distribution (± 43 km) along the southern west coast, occurring from Mouille Point to Slangkop (Western Cape Province) along the Cape Peninsula, South Africa.

HABIT AND MORPHOLOGY: Plants non-geniculate, thalli thick, encrusting and variably lumpy and slightly protuberant (protuberances up to 4 mm in height), firmly adherent, dusky pink to mauve (in well-lit conditions) to rosy or purple-pink (in dim light) when freshly collected (Fig. 10). Individual crusts not coalescing (do not fuse together) and easily discernible (Figs 10-12). Thalli epilithic on primary bedrock and on large boulders in rock pools and on exposed platforms in mid-intertidal zone. Thalli also epilithic on primary bedrock between *S. cochlear* (limpet) territories and epizoic on *S. cochlear* shells in low intertidal zone (Figs 11-12).

ANATOMY: Thalli dorsiventrally organised, monomerous and haustoria absent. Medulla thin and plumose (non-coaxial) (Figs 13-14). Medullary filaments comprise rectangular cells and give rise to cortical filaments that comprise mainly square to rectangular cells (Fig. 14). Contiguous medullary and cortical filaments joined by cell fusions; secondary pit connections absent (Fig. 14). Subepithallial initials square to rectangular (Fig. 15). Epithallus single layered with oval to rounded cells (Fig. 15). Trichocytes common at thallus surface, occurring singularly (mostly) to paired (Fig. 15); always terminal and never intercalary in the cortex/perithallus; buried trichocytes not observed. Data on morphological and measured vegetative characters are summarised in Table 3.

REPRODUCTION: Gametangial thalli appear to be dioecious, although female plants were not observed.

Spermatangial (male) conceptacles uniporate, low-domed, raised above surrounding thallus surface (Figs 16-18). Chambers transversely elliptical to flattened; roof nearly twice as thick along pore canal (Figs 17-18). Roof formed from filaments peripheral to the fertile area (Fig. 16). Throughout early development, a protective layer of epithallial cells surrounds conceptacle primordium (Fig. 16). This protective layer is shed once the pore canal is near fully developed; the pore opening occluded by a mucilage plug (Figs 17-18). In mature conceptacles terminal initials along pore canal are enlarged and papillate, they project into pore canal and are orientated more or less parallel to the conceptacle roof surface (Fig. 18). Unbranched (simple) spermatangial systems confined to floor of mature conceptacle (Figs 16-18). Senescent male conceptacles appear to be shed as no buried conceptacles were observed.

Tetrasporangial thalli are morphologically similar to spermatangial thalli. Conceptacles uniporate, low domed and raised above surrounding thallus surface (Figs 19-21). Chambers transversely elliptical to bean-shaped; roof nearly twice as thick along the pore canal and 5-7 cells (incl. an epithallial cell) thick. Pore canal tapered towards surface and arching (Fig. 20), lined by elongated papillate cells that project into pore canal and are orientated more or less parallel or at a sharp angle to the conceptacle roof surface (Fig. 20). Roof formed from filaments peripheral to the fertile area (Fig. 19); terminal initials more elongate than their inward derivatives (Fig. 19). Throughout early development a protective layer of epithallial cells surrounds conceptacle primordium (Fig. 19). This protective layer is shed once pore canal is near fully developed; pore opening occluded by a corona of filaments that project above the pore opening (Figs 20, 22). Corona appears to form from filaments near the upper half of roof, directly adjacent to pore canal (Figs 20, 22). Throughout development of immature tetrasporangial conceptacle, a prominent columella of sterile filaments forms at the centre of conceptacle chamber and extends into the pore canal (Figs 19-20); central columella appears weakly calcified as with maturity it disintegrates to form a low mound (Fig. 21). Base of pore

canal sunken into chamber and terminal initials near the base point downward (Fig. 22). Mature conceptacle floors sunken 11-17 cells (including the epithallial cell) below surrounding thallus surface. Zonately divided tetrasporangia arranged at the extreme periphery of conceptacle chamber, attached via a stalk cell (Figs 20-21); where central columella has disintegrated or diminished, tetrasporangia fill the chamber and appear to be distributed across the chamber floor (Fig. 21). Senescent tetrasporangial conceptacles appear to be shed as no buried conceptacles were observed. Data on reproductive characters summarised in Table 4.

3.2.3. *Chamberlainium cochleare* Maneveldt, Puckree-Padua & P.W.Gabrielson *sp. nov*.

(Figs 23-37; Tables 3-7)

HOLOTYPE: L ???????, 18.xii.2014, *leg. G.W. Maneveldt*, collection number 14/12, epilithic on primary bedrock in *Oxystele tigrina* (winkle) and *Cymbula oculus* (limpet) dominated mid-shore rock pool (Fig. 24). Fragments of the holotype were retained in UWC and NCU.

ISOTYPES: UWC 14/13, UWC 14/14.

TYPE LOCALITY: South Africa, Western Cape Province, Cape Agulhas: L'Agulhas, Stinkbaai (34°49'26.37"S, 20°01'0.71"E).

ETYMOLOGY: '*cochleare*' in reference to the species' strong ecological association in the 'Cochlear zone' along the southern west and south coasts with the territorial, gardening limpet *S. cochlear* (Fig. 23).

DIAGNOSIS: Thalli thin, uniformly encrusting (smooth), lacking protuberances and not becoming secondarily thick and discoid with orbicular protrusions, nor warty, nor wrinkled; individual crusts coalescing (fusing) and not easily discernible; colour of living thalli greyish in well-lit conditions to blueish mauve in dim light; thallus construction monomerous; epithallus single layered; spermatangial and tetrasporangial conceptacles produced successively in cortex directly above, and in the same area as the modified cortex of an earlier generation; central columella present in tetrasporangial conceptacles, disintegrating to form a low mound with maturity; pore opening in mature tetrasporangial conceptacles occluded by a mucilage plug; *psb*A (GenBank ??????) and *rbc*L (GenBank ??????) sequences unique.

DNA SEQUENCES: *psb*A (851 bp) and *rbc*L (1467 bp) gene sequences, obtained from 15 specimens (including the holotype and isotypes) (Table S1), were all identical to each other. DNA sequences showed that *Chamberlainium cochleare* was different from all other named species sequenced to date (Figs 3-5; Table S1).

SPECIMENS EXAMINED: Fifteen samples (including the holotype and isotypes), all confirmed by DNA sequencing, represent our entire collection for this taxon. Data below are presented geographically from west to east followed chronologically by collection numbers.

South Africa – Western Cape Province: Kalk Bay. UWC 09/157, 21.ix.2009, *leg*. *G.W. Maneveldt & E. van der Merwe*, collection number 09/157 (34°7'52.39"S, 18°26'54.55"E), epilithic on primary bedrock in mid-intertidal zone; UWC 11/38, 11.iv.2011, *leg*. *G.W. Maneveldt*, collection number 11/38 (34°7'52.95"S, 18°26'53.58"E), epilithic on primary bedrock among *S. cochlear* (limpet) territories in the Cochlear zone (low intertidal zone); UWC 12/02A, 23.ii.2012, *leg*. *G.W. Maneveldt*, collection number 12/02A (34°7'53.28"S, 18°26'53.38"E), epilithic on primary bedrock in mid-intertidal rock pool.

Western Cape Province: Pringle Bay, Holbaaipunt. UWC 93/299, 14.xi.1993, *leg*. *G.W. Maneveldt*, collection number 93/299 (34°22'45.24"S, 18°50'46.04"E), epilithic on primary bedrock among *S. cochlear* (limpet) territories and epizoic on *S. cochlear* shells in the Cochlear zone (low intertidal zone).

Western Cape Province: Cape Agulhas, Stinkbaai. L ???????, 18.xii.2014, *leg*. *G.W. Maneveldt*, collection number 14/12 (34°49'26.37"S, 20°01'0.71"E) (holotype), epilithic on primary bedrock in *O. tigrina* (winkle) and *C. oculus* (limpet) dominated mid-intertidal rock pool; UWC 14/13, 18.xii.2014, *leg*. *G.W. Maneveldt*, collection number 14/13 (34°49'26.37"S, 20°01'0.71"E) (isotype), epilithic on primary bedrock in *Scutellastra longicosta* (limpet) dominated mid-intertidal zone; UWC 14/14, 18.xii.2014, *leg*. *G.W. Maneveldt*, collection number 14/14 (34°49'26.37"S, 20°01'0.71"E) (isotype), epilithic on primary bedrock among *S. cochlear* (limpet) territories in the Cochlear zone (low intertidal zone).

Western Cape Province: Struisbaai. UWC 09/104, 06.vii.2009, *leg*. *G.W. Maneveldt & E. van der Merwe*, collection number 09/104 (34°48'48.36"S, 20°03'14.99"E), epilithic on

primary bedrock in mid-intertidal zone; UWC 15/11, 01.v.2015, *leg. G.W. Maneveldt*, collection number 15/11 (34°48'51.74"S, 20°01'49.34"E), epilithic on primary bedrock, amongst *S. longicosta* (limpet) and *C. oculus* (limpet) in mid-intertidal zone; UWC 15/14, 01.v.2015, *leg. G.W. Maneveldt*, collection number 15/14 (34°48'50.65"S, 20°01'50.90"E), epilithic on primary bedrock (shale platforms) edges in the mid-intertidal zone; UWC 15/15, 01.v.2015, *leg. G.W. Maneveldt*, collection number 15/15 (34°48'50.49"S, 20°01"50.91"E), epilithic on primary bedrock (shale platforms) flats in the mid-intertidal zone.

Western Cape Province: Stilbaai. UWC 10/104, 12.vi.2010, *leg. G.W. Maneveldt & E. van der Merwe*, collection number 10/104 (34°23'35.70"S, 21°25'45.54"E), epilithic on primary bedrock in low shore rock pool.

Western Cape Province: Tsitsikamma, Nature's Valley. UWC 08/20, 06.iv.2008, *leg. G.W. Maneveldt & U. van Bloemstein*, collection number 08/20 (33°59'27.21"S, 23°32'20.79"E), epizoic on *S. cochlear* (limpet) shell in Cochlear zone (low intertidal zone).

Eastern Cape Province: Kidds Beach. NCU 659868, 19.xii.2009, *leg. T. Klenk*, collection number 926 (33°09'28.32"S, 27°41'15.15"E), epilithic on primary bedrock in mid-intertidal zone.

KwaZulu-Natal Province: Durban, Ballito Bay. UWC 15/24, 22.vi.2015, *leg. G.W. Maneveldt & C.A. Puckree-Padua*, collection number 15/24 (29°32'42.49"S, 31°12'56.95"E), epilithic on primary bedrock in high shore rock pool above oyster belt.

DISTRIBUTION: Confirmed by DNA sequence data to be widely distributed (± 1,700 km) along the southern and eastern coasts, occurring from Kalk Bay (False Bay, Western Cape Province) to Ballito Bay (KwaZulu-Natal Province), South Africa; possibly more widespread up the east coast.

HABIT AND MORPHOLOGY: Plants non-geniculate, thalli thin, encrusting (smooth), firmly adherent, greyish (in well-lit conditions) (Fig. 23) to blueish mauve (in dim light) when freshly

collected. Individual crusts coalescing (fusing together) and not easily discernible (Figs 23-25). Thalli epilithic on primary bedrock in mid- and low intertidal zones; also epizoic on mollusc shells from these zones. The species has a very common ecological association with the territorial, gardening limpet *S. cochlear* (Fig. 23).

ANATOMY: Thalli dorsiventrally organised, monomerous and haustoria absent. Medulla thin and plumose (non-coaxial) (Fig. 26). Medullary filaments comprise rectangular to elongate cells and give rise to cortical filaments that comprise square to rectangular cells (Figs 26-27). Contiguous medullary and cortical filaments joined by cell fusions; secondary pit connections absent (Figs 27-28). Subepithallial initials square to rectangular (Fig. 28). Epithallus single layered with elliptical to domed cells (Fig. 28). Trichocytes common at thallus surface, occurring singularly (mostly), but also in small clusters of up to 6 cells, all separated by normal vegetative filaments (Fig. 28); always terminal and never intercalary in the cortex/perithallus; buried trichocytes not observed. Data on morphological and measured vegetative characters are summarised in Table 3 and Table 6.

REPRODUCTION: Gametangial thalli appear to be dioecious, although female plants were not observed.

Spermatangial (male) conceptacles uniporate, low-domed, raised above or only occasionally flush with surrounding thallus surface (Figs 29-31). Chambers transversely elliptical to flattened; roof nearly twice as thick along pore canal (Figs 30-31). Spermatangial conceptacles appear to be produced successively in the cortex directly above, and in the same area as the modified cortex of an earlier generation (Fig. 29). Roof formed from filaments peripheral to the fertile area (Fig. 29). Throughout early development, a protective layer of epithallial cells surrounds conceptacle primordium (Fig. 29). This protective layer is shed once the pore canal is near fully developed; the pore opening occluded by a mucilage plug (Figs 30-31). In mature conceptacles terminal initials along pore canal are enlarged and papillate, they project into pore

canal and are orientated more or less parallel to the conceptacle roof surface (Fig. 31). Unbranched (simple) spermatangial systems confined to floor of mature conceptacle (Figs 29-31). Senescent male conceptacles appear to be shed as no buried conceptacles were observed.

Tetrasporangial thalli are morphologically similar to spermatangial thalli. Conceptacles uniporate, low domed and raised to flush to slightly sunken below surrounding thallus surface (Figs 32-36). Chambers transversely elliptical to markedly bean-shaped; roof nearly twice as thick along the pore canal and 6-8 cells (incl. an epithallial cell) thick (Figs 32, 36-37). Pore canal tapered towards surface, lined by elongated papillate and enlarged cells that project into pore canal and are orientated more or less parallel or at a sharp angle to the conceptacle roof surface (Figs. 36-37). Similar to spermatangial conceptacles, tetrasporangial conceptacles appear to be produced successively in the cortex directly above, and in the same area as the modified cortex of an earlier generation (Fig. 32). Roof formed from filaments peripheral to the fertile area (Figs 33-35); terminal initials more elongate than their inward derivatives (Figs 36-37). Throughout early development a protective layer of epithallial cells surrounds conceptacle primordium (Figs 33-35). This protective layer is shed once pore canal is near fully developed; pore opening occluded by a mucilage plug (Figs 36-37). Throughout development of immature tetrasporangial conceptacle, a prominent columella of sterile filaments forms at centre of conceptacle chamber (Figs 34-35); central columella appears weakly calcified as with maturity it disintegrates to form a low mound (Figs 32, 36). Base of pore canal sunken into chamber and terminal initials near the base point downward (Figs 36-37). Mature conceptacle floors sunken 12-22 cells (including the epithallial cell) below surrounding thallus surface. Zonately divided tetrasporangia at maturity arranged at the extreme periphery of conceptacle chamber and attached via a stalk cell (Fig. 36). Senescent tetrasporangial conceptacles appear to be shed as no buried conceptacles were observed. Data on reproductive characters are summarised in Table 4 and Table 7.

3.2.4. *Chamberlainium glebosum* Maneveldt, Puckree-Padua & P.W.Gabrielson *sp. nov*.

(Figs 38-50; Tables 3-5)

HOLOTYPE: L ???????, 17vii.2015, *leg. G.W. Maneveldt*, collection number 18/05, epilithic on primary bedrock in the mid-intertidal rock pool (Fig. 39).

TYPE LOCALITY: South Africa, Western Cape Province, Melkbosstrand (33°44'15.11"S, 18°26'8.06"E).

ETYMOLOGY: '*glebosum*' from '*glebosus*', making reference to the species' lumpy and highly protuberant growth form.

DIAGNOSIS: Thalli thick, lumpy becoming highly protuberant, not becoming secondarily thick and discoid with orbicular protrusions, nor wrinkled; individual crusts not coalescing (not fusing together) and easily discernible; colour of living thalli brownish pink to grey in well-lit conditions and blue-grey in dim light; thallus construction monomerous; epithallus single layered; central columella present in tetrasporangial conceptacles, disintegrating to form a low mound with maturity; pore opening in mature tetrasporangial conceptacles unoccluded; *psb*A (GenBank??????) and *rbc*L (GenBank ??????) sequences collectively[2] unique.

DNA SEQUENCES: *psb*A (851 bp) and *rbc*L (1467 bp) gene sequences, obtained from 21 specimens (including the holotype and isotypes) (Table S1), were all identical to each other. DNA sequences collectively showed that *Chamberlainium glebosum* was different from all other named species sequenced to date (Figs 3-8; Table S1).

SPECIMENS EXAMINED: Twenty-one samples (including the holotype and isotypes), all confirmed by DNA sequencing, represent our entire collection for this taxon. Data below are

[2] *Chamberlainium glebosum* shares six single nucleotide polymorphisms (SNPs) with *C. capense*, with the *rbc*L sequence of UWC 16/27 (*C. capense*) being identical to all *C. glebosum* specimens sequenced.

presented geographically from north to south followed chronologically by the collection numbers.

South Africa – Northern Cape Province: Port Nolloth. UWC 93/27, 05.vii.1993, *leg. G.W. Maneveldt*, collection number 93/27 (29°14’22.77”S, 16°51’13.32”E), epilithic on primary bedrock in mid-intertidal zone; UWC 93/304, 14.xii.1993, *leg. G.W. Maneveldt*, collection number 93/304 (29°14’22.77”S, 16°51’13.32”E), epilithic on primary bedrock in mid-intertidal zone; UWC 93/306, 14.xii.1993, *leg. G.W. Maneveldt*, collection number 93/306 (29°14’22.77”S, 16°51’13.32”E), epilithic on primary bedrock in mid-intertidal zone; UWC 15/50, 29.ix.2015, *leg. G.W. Maneveldt & C.A. Puckree-Padua*, collection number 15/50 (29°14’51.74”S, 16°52’3.48”E), epilithic on primary bedrock in mid-intertidal rock pool; UWC 15/51, 29.ix.2015, *leg. G.W. Maneveldt & C.A. Puckree-Padua*, collection number 15/51 (29°14’51.74”S, 16°52’3.48”E), epilithic on primary bedrock in low intertidal rock pool.

Northern Cape Province: Groenriviermond. UWC 15/55, 30.ix.2015, *leg. G.W. Maneveldt & C.A. Puckree-Padua*, collection number 15/55 (30°51’53”S, 17°34’40.68”E), epilithic on primary bedrock in mid-intertidal rock pool.

Western Cape Province: Cape St. Martin. UWC 15/63B, 02.x.2015, *leg. G.W. Maneveldt & C.A. Puckree-Padua*, collection number 15/63B (32°44’9.86”S, 17°54’25.93”E), epilithic on primary bedrock among *S. cochlear* (limpet) territories in the Cochlear zone (low intertidal zone).

Western Cape Province: Jacobsbaai. UWC 15/16, 14.v.2015, *leg. G.W. Maneveldt*, collection number 15/16 (32°57’55.92”S, 17°52’53.04”E), epilithic on primary bedrock in mid-intertidal rock pool; UWC 15/17, 14.v.2015, *leg. G.W. Maneveldt*, collection number 15/17 (32°57’55.92”S, 17°52’53.04”E), epilithic on primary bedrock in mid-intertidal rock pool; UWC 15/20, 14.v.2015, *leg. G.W. Maneveldt*, collection number 15/20 (32°57’55.92”S, 17°52’53.04”E), epilithic on primary bedrock in mid-intertidal rock pool; UWC 15/21,

14.v.2015, *leg. G.W. Maneveldt,* collection number 15/21 (32°57’55.92”S, 17°52’53.04”E), epilithic on primary bedrock in mid-intertidal rock pool.

Western Cape Province: Grotto Bay. UWC 15/33, 17.vii.2015, *leg. G.W. Maneveldt*, collection number 15/33 (33°30’22.23”S, 18°18’50.42”E), epilithic on primary bedrock in *Scutellastra granularis* (limpet) dominated mid-intertidal zone; UWC 15/34, 17.vii.2015, *leg. G.W. Maneveldt,* collection number 15/34 (33°30’22.23”S, 18°18’50.42”E), epilithic on primary bedrock in mid-intertidal rock pool; UWC 15/35, 17.vii.2015, *leg. G.W. Maneveldt*, collection number 15/34 (33°30’22.23”S, 18°18’50.42”E), epilithic on primary bedrock in high intertidal rock pool.

Western Cape Province: Melkbosstrand. L ??????? 18/05, 12.ix.2018, *leg. G.W. Maneveldt,* collection number 18/05 (33°44’15.11”S, 18°26’8.06”E) (holotype), epilithic on primary bedrock in the mid-intertidal rock pool.

Western Cape Province: Mouille Point. UWC 16/07, 09.v.2016, *leg. G.W. Maneveldt, C.A. Puckree-Padua & A. Haywood*, collection number 16/07 (33°53’56.64”S, 18°24’31.71”E), epilithic on primary bedrock among *Siphonaria capensis* (false limpet) in high intertidal zone, UWC 16/12, 09.v.2016, *leg. G.W. Maneveldt, C.A. Puckree-Padua & A. Haywood*, collection number 16/12 (33°53’56.64”S, 18°24’31.71”E), epilithic on primary bedrock in high intertidal rock pool.

Western Cape Province: Sea Point. UWC 16/14, 09.v.2016, *leg. G.W. Maneveldt & C.A. Puckree-Padua*, collection number 16/14 (33º55’20.77”S, 18º22’35.97”E), epilithic on primary bedrock in high intertidal rock pool.

Western Cape Province: Slangkop. UWC 16/25, 10.v.2016, *leg. G.W. Maneveldt, C.A. Puckree-Padua & A. Haywood*, collection number 16/25 (34º8’51.07”S, 18º19’6.10”E), epilithic on primary bedrock in mid-intertidal rock pool; UWC 16/26, 10.v.2016, *leg. G.W. Maneveldt, C.A. Puckree-Padua & A. Haywood*, collection number 16/26 (34º8’51.07”S,

18º19’6.10”E), epilithic on primary bedrock in mid-intertidal rock pool; UWC 16/27, 10.v.2016, *leg. G.W. Maneveldt, C.A. Puckree-Padua & A. Haywood*, collection number 16/27 (34º8’51.07”S, 18º19’6.10”E), epilithic on primary bedrock in high intertidal rock pool.

DISTRIBUTION: Confirmed by DNA sequence data to have a wide, but disjunct distribution along the west coast, occurring from Port Nolloth (Northern Cape Province) to Groenriviermond (Northern Cape Province) (± 220 km) and then from Cape St. Martin (Western Cape Province) to Slangkop (Western Cape Province) (± 200 km), South Africa.

HABIT AND MORPHOLOGY: Plants non-geniculate, thalli thick, lumpy becoming highly protuberant (protuberances up to 6 mm in height) (Figs 38-40), firmly adherent, mostly brownish pink to greyish when freshly collected (Fig. 38). Individual crusts not coalescing (not fusing together) and easily discernible (Figs 38-39). Thalli epilithic on the primary bedrock in the high and mid-intertidal zones and only occasionally on the low shore (Fig. 38).

ANATOMY: Thalli dorsiventrally organised, monomerous and haustoria absent. Medulla thin and plumose (non-coaxial) (Fig. 41). Medullary filaments comprise rectangular to elongate cells and give rise to cortical filaments that comprise square to rectangular cells (Figs 42-43). Contiguous medullary and cortical filaments joined by cell fusions; secondary pit connections absent (Figs 42-43). Subepithallial initials square to rectangular (Fig. 43). Epithallus single layered with rounded to elliptical cells (Fig. 43). Trichocytes not observed. Data on morphological and measured vegetative characters are summarised in Table 3.

REPRODUCTION: Gametangial thalli appear to be dioecious, although female plants were not observed.

Spermatangial (male) conceptacles uniporate, low-domed, raised above surrounding thallus surface (Fig. 44-45). Chambers transversely elliptical to flattened; roof nearly twice as thick along pore canal (Fig. 45). Roof formed from filaments peripheral to the fertile area (Fig. 44). Throughout early development, a protective layer of epithallial cells surrounds conceptacle

primordium (Fig. 44). This protective layer is shed once the pore canal is near fully developed; the pore opening occluded by a mucilage plug (Fig.45). In mature conceptacles terminal initials along pore canal are enlarged and papillate, they project into pore canal and are orientated more or less parallel to the conceptacle roof surface (Fig. 45). Unbranched (simple) spermatangial systems confined to floor of mature conceptacle (Figs 44-45). Senescent male conceptacles appear to be shed as no buried conceptacles were observed.

Tetrasporangial thalli are morphologically similar to spermatangial thalli. Conceptacles uniporate, low domed and raised above surrounding thallus surface (Figs 46-49). Chambers transversely elliptical to bean-shaped; roof nearly twice as thick along the pore canal and 4-8 (9) cells (incl. an epithallial cell) thick (Fig. 49). Pore canal tapered towards surface, lined by elongated papillate cells that project into pore canal and are orientated more or less parallel or at a sharp angle to the conceptacle roof surface (Fig. 50). Roof formed from filaments peripheral to the fertile area (Figs 46-48); terminal initials more elongate than their inward derivatives (Fig. 47). Throughout early development a protective layer of epithallial cells surrounds conceptacle primordium (Figs 46-48). This protective layer is shed once pore canal is near fully developed; the pore opening in mature conceptacles unoccluded (Figs 49-50). Throughout development of immature tetrasporangial conceptacle, a prominent columella of sterile filaments forms at centre of conceptacle chamber and extends into the pore canal (Figs 47-49); central columella appears weakly calcified as with maturity it disintegrates to form a low mound. Base of pore canal sunken into chamber and terminal initials near the base point downward (Figs 49-50). Mature conceptacle floors sunken 11-24 cells (including the epithallial cell) below surrounding thallus surface. Zonately divided tetrasporangia at maturity arranged at the extreme periphery of conceptacle chamber and attached via a stalk cell (Fig. 49). Senescent tetrasporangial conceptacles appear to be shed as no buried conceptacles were observed. Data on reproductive characters are summarised in Table 4.

3.2.5. *Chamberlainium impar* (Foslie) Maneveldt, Puckree-Padua & P.W.Gabrielson *comb. nov.*

(Figs 51-71; Tables 3-5, 8-9)

BASIONYM: *Lithophyllum impar* Foslie, 1909: 13.

HOLOTYPE: TRH! (A3-146), collector A. Weber van Bosse, 1893, no other collection data. See Printz 1929 (Pl. LIV, figs 18-21).

TYPE LOCALITY: Likely Cape of Good Hope, South Africa. There is doubt as to whether Mme Weber van Bosse collected the type material in KwaZulu-Natal (as Natal) or somewhere between that location and the Western Cape Province (as Cape Province). The species has never been observed in KwaZulu-Natal and it is more likely to have been the Western Cape Province (see Chamberlain 1994b).

SYNONYMS: *Lithophyllum marlothii f. subplicata* Foslie, 1902:19; *Pseudolithophyllum impar* (Foslie) Adey, 1970: 13.

ETYMOLOGY: '*impar'* means unequal (Stearn 1973), presumably making reference to the variable (and unequal) size of individual crusts (Figs 51-53).

DNA SEQUENCES: *psb*A (851 bp) and *rbc*L (1467 bp) gene sequences, obtained from six specimens (including the holotype) (Table S1), were all identical to each other. DNA sequences showed that *Chamberlainium impar* was different from all other named species sequenced to date (Figs 3-5; Table S1).

SPECIMENS EXAMINED: Five samples (in addition to the holotype specimen), all confirmed by DNA sequencing, represent our entire collection for this taxon. Data below are presented geographically from north to south followed chronologically by collection numbers.

South Africa – Western Cape Province: Cape St. Martin. UWC 15/64, 02.x.2015, *leg*. *G. W. Maneveldt & C.A. Puckree-Padua*, collection number 15/64 (32°44'9.86"S, 17°54'25.93"E), epilithic on primary bedrock in mid-intertidal zone.

Western Cape Province: Sea Point. UWC 12/01, 23.ii.2012, *leg*. *G.W. Maneveldt*, collection number 12/01 (33º55'20.77"S, 18º22'35.97"E), epilithic on primary bedrock in mid-intertidal zone; UWC 13/20, 05.xi.2013, *leg*. *G.W. Maneveldt*, collection number 13/20 (33º55'20.77"S, 18º22'35.97"E), epilithic on primary bedrock in low intertidal zone; UWC 13/21, 05.xi.2013, *leg*. *G.W. Maneveldt*, collection number 13/21 (33º55'20.77"S, 18º22'35.97"E), epilithic on primary bedrock in low intertidal zone; UWC 13/22, 05.xi.2013, *leg*. *G.W. Maneveldt*, collection number 13/22 (33º55'20.77"S, 18º22'35.97"E), epilithic on primary bedrock in low intertidal zone.

DISTRIBUTION: Confirmed by DNA sequence data to be distributed (± 170 km) along the southern west coast, occurring from Cape St. Martin (Western Cape Province) to Sea Point (Western Cape Province), South Africa; probably more widespread down the southern west coast (see Chamberlain 1994b).

HABIT AND MORPHOLOGY: Plants non-geniculate, thalli thick, encrusting (smooth) and orbicular becoming confluent, may remain flat in heavily grazed conditions (Figs 51-53), firmly adherent, yellowish to yellow-brown (in well-lit conditions) to purple-brown (in dim light) when freshly collected (Fig. 51). Surface roughly ridged to strongly pachydermatous like an elephant's skin (Figs 51-53). Individual crusts not coalescing (not fusing together) and discernible (Figs 51-53); adjacent crusts producing characteristic marginal up growths when they meet (Fig. 53). Thalli epilithic on primary bedrock in mid- to low intertidal zones, forming a distinctive band above the Cochlear zone (low intertidal zone) (Fig 51).

ANATOMY: Thalli dorsiventrally organised, monomerous and haustoria absent. Medulla plumose (non-coaxial) (Fig. 54). Medullary filaments comprise rectangular to elongate cells

and give rise to cortical filaments that comprise squarish to beaded cells (Figs 55-56). Contiguous medullary and cortical filaments joined by cell fusions; secondary pit connections absent (Figs 55-57). Subepithallial initials square to rectangular (mostly) (Fig. 56-57). Epithallus multilayered, comprising up to nine (mostly 4-6) elliptical to rounded epithallial cells (Figs 56-57). Trichocytes rare at thallus surface, occurring singularly or paired (Figs 56-57); always terminal and never intercalary in the cortex/perithallus; buried trichocytes not observed. Data on morphological and measured vegetative characters are summarised in Table 3 and Table 8.

REPRODUCTION: Gametangial thalli dioecious.

Spermatangial (male) conceptacles uniporate, low-domed, initially raised above surrounding thallus surface, becoming flush with surrounding thallus surface at maturity (Figs 58-61). Chambers transversely elliptical to flattened; roof nearly twice as thick along pore canal (Figs 60-61). Roof formed from filaments peripheral to the fertile area (Figs 58-59). Throughout early development, a protective layer of epithallial cells surrounds conceptacle primordium (Fig. 58). This protective layer is shed once the pore canal is near fully developed; the pore opening in mature conceptacles occluded by a mucilage plug or more commonly a mucilage spout (Figs 60-61). In mature conceptacles terminal initials along pore canal are enlarged and papillate, project into pore canal and are orientated more or less parallel to the conceptacle roof surface (Fig. 61). Unbranched (simple) spermatangial systems confined to floor of mature conceptacle (Figs 59-61). Senescent male conceptacles appear to be shed as no buried conceptacles were observed.

Carpogonial (female) conceptacles similar in size and shape to spermatangial conceptacles; flush with to sunken below surrounding thallus surface (Fig. 62-63). In mature conceptacles terminal initials along pore canal are enlarged and papillate, they project into pore canal and are orientated more or less parallel to the conceptacle roof surface (Fig. 63). Carpogonial

branches develop across the floor of conceptacle chamber, comprising a single support cell, a hypogynous cell and a carpogonium extended into a trichogyne (Fig. 63). Sterile cells also present on some hypogynous cells.

After presumed karyogamy, carposporophytes develop within female conceptacles and form carposporangial conceptacles (Figs 64-66). Carposporangial conceptacles comparatively large, low-domed, slightly raised to flush with to sunken below surrounding thallus surface (Fig. 64). Chambers transversely elliptical, with flattened bottoms presumably caused by growth of gonimoblast filaments. Pore canal tapered towards surface, lined by enlarged and papillate cells that project into pore canal and are orientated more or less parallel to the conceptacle roof surface (Fig. 64-65). In mature conceptacles, cells lining the pore canal were more elongate than their inward derivatives; base of pore canal sunken into the chamber and terminal initials near the base characteristically point downward (Figs 64-65). Discontinuous fusion cell present and 5-7 celled gonimoblast filaments (incl. a terminal carposporangium) develop along the periphery of conceptacle chamber (Fig. 66). The remains of unfertilized carpogonia persist across the dorsal surface of the fusion cell (Figs 64, 66). Senescent carposporangial conceptacles appear to be shed as no buried conceptacles were observed.

Tetrasporangial thalli are morphologically similar to gametangial thalli. Conceptacles uniporate, low domed and raised, becoming flush (at maturity) with the surrounding thallus surface (Figs 67-70). Chambers transversely elliptical to bean-shaped; roof nearly twice as thick along the pore canal and 6-7 cells (incl. an epithallial cell) thick (Figs 70-71). Pore canal tapered towards the surface, lined by elongate papillate cells that project into the pore canal and are orientated more or less parallel or at a sharp angle to the conceptacle roof surface (Figs 69, 71). Roof formed from filaments peripheral to the fertile area (Figs 67-69); terminal initials more elongate than their inward derivatives (Fig. 69). Throughout early development a thick protective layer of epithallial cells surrounds conceptacle primordium (Figs 67-69). This

protective layer is shed once pore canal is near fully developed; pore opening occluded by a mucilage plug (Figs 70-71). A prominent columella of sterile filaments forms early in tetrasporangial conceptacle development, extending into the pore canal (Figs 69-70) and persists to maturity (Fig. 70). Base of pore canal sunken into chamber and terminal initials near the base point downward (Fig. 71). Mature conceptacle floors sunken 15-21 cells (including the epithallial cell) below surrounding thallus surface. Zonately divided tetrasporangia at maturity arranged at the extreme periphery of conceptacle chamber and attached via a stalk cell (Fig. 70). Senescent tetrasporangial conceptacles appear to be shed as no buried conceptacles were observed. Data on reproductive characters are summarised in Table 4 and Table 9.

3.2.6. *Chamberlainium natalense* (Foslie) Maneveldt, Puckree-Padua & P.W.Gabrielson, *comb. nov.*

(Figs 72-88; Tables 3-7)

BASIONYM: *Lithophyllum natalense* Foslie, 1907: 24.

LECTOTYPE: TRH! (A2-107), collector A. Weber-van Bosse, 1894, no other collection data. Designated by Adey in Adey & Lebednik (1967: 16), Foslie slide 703, lectotype depicted in Printz (1929, Pl. LIII, fig. 6) and Chamberlain (1993, fig. 28). A previous reference to the typification was by Adey 1970: 13 (as *Pseudolithophyllum*).

TYPE LOCALITY: Likely KwaZulu-Natal (as Natal), South Africa, as suggested by the epithet. Incidentally, all other specimens (TRH A2-105, TRH A2-106) ascribed to this epithet were sampled from KwaZulu-Natal (as Natal), with a reference made to Durban (Woelkerling *et al*. 2005: 35). See Chamberlain (1993: 111) for comments on the confusion around the labelling of the specimens.

SYNONYMS: *Pseudolithophyllum natalense* (Foslie) W.H.Adey, 1970: 13.

ETYMOLOGY: '*natalense*', making reference to the type locality in the province of KwaZulu-Natal (as Natal) (Foslie 1907: 24).

DNA SEQUENCES: *psb*A (851 bp) and *rbc*L (1467 bp) gene sequences, obtained from 19 specimens (including the lectotype) (Table S1), were all identical to each other. DNA sequences showed that *Chamberlainium natalense* was different from all other named species sequenced to date (Figs 3-51; Table S1).

SPECIMENS EXAMINED: Eighteen samples (in addition to the lectotype specimen), all confirmed by DNA sequencing, represent our entire collection for this taxon. Data below are presented geographically from west to east followed chronologically by the collection numbers.

South Africa - Western Cape Province: Kommetjie. UWC 16/20, 10.v.2016, *leg. G.W. Maneveldt, C.A. Puckree-Padua & A. Haywood*, collection number 16/20 (34°8'21.96"S, 18°19'12.62"E), epilithic on boulder in mid-intertidal rock pool.

Western Cape Province: Kalk Bay. UWC 11/41, 20.iv.2011, *leg. G.W. Maneveldt*, collection number 11/41 (34°7'52.39"S, 18°26'54.55"E), epilithic on small boulder in mid-intertidal rock pool; UWC 12/02B, 23.ii.2012, *leg. G.W. Maneveldt*, collection number 12/02B (34°7'53.28"S, 18°26'53.38"E), epilithic on boulder in mid-intertidal rock pool; UWC 12/03, 23.ii.2012, *leg. G.W. Maneveldt*, collection number 12/03 (34°7'53.28"S, 18°26'53.38"E), epilithic on boulder in mid-intertidal rock pool; UWC 13/24, 05.xi.2013, *leg. G.W. Maneveldt*, collection number 13/24 (34°7'52.39"S, 18°26'54.55"E), epilithic on boulder in mid-intertidal rock pool; UWC 13/25, 05.xi.2013, *leg. G.W. Maneveldt*, collection number 13/25 (34°7'52.39"S, 18°26'54.55"E), epilithic on boulder in mid-intertidal rock pool.

Western Cape Province: Cape Agulhas, Stinkbaai. UWC 10/133, 15.vi.2010, *leg. G.W. Maneveldt & E. van der Merwe*, collection number 10/133 (34°49'27.58"S 20°01'5.30"E), epilithic on small boulder in low intertidal rock pool.

Western Cape Province: Shark Bay. UWC 14/18, 18.xii.2014, *leg. G.W. Maneveldt*, collection number 14/18 (34°48'51.69"S, 20°1'48.33"E), epilithic on boulder in mid-intertidal rock pool; UWC 15/10, 01.v.2015, *leg. G.W. Maneveldt*, collection number 15/10 (34°48'51.69"S, 20°1'48.33"E), epilithic on boulder in mid-intertidal rock pool; UWC 15/13, 01.v.2015, *leg. G.W. Maneveldt*, collection number 15/13 (34°48'51.69"S, 20°1'48.33"E), epilithic on primary bedrock (shale) in high intertidal rock pool.

Western Cape Province: Struisbaai. UWC 09/103, 06.vii.2009, *leg. G.W. Maneveldt & E. van der Merwe*, collection number 09/103 (34°48'48.36"S, 20°03'14.99"E), epizoic on *Oxystele sinensis* (winkle) shell in low intertidal rock pool; UWC 09/125, 07.vii.2009, *leg. G.W. Maneveldt & E. van der Merwe*, collection number 09/125 (34°48'48.36"S,

20°03’14.99”E), epilithic on boulder in mid-intertidal rock pool; UWC 11/26, 03.xi.2011, *leg. G.W. Maneveldt,* collection number 11/26 (34°48’48.36”S, 20°03’14.99”E), epilithic on boulder in sandy gully in low intertidal zone.

Western Cape Province: Tsitsikamma, Natures Valley. UWC 08/04, 04.iv.2008, *leg. G.W. Maneveldt & U. van Bloemstein*, collection number 08/04 (33°59’22.34”S 23°32’39.62”E), epilithic on primary bedrock in low intertidal rock pool; UWC 08/06, 04.iv.2008, *leg. G.W. Maneveldt & U. van Bloemstein*, collection number 08/06 (33°59’22.34”S 23°32’39.62”E), epilithic on primary bedrock in low intertidal rock pool; UWC 08/13, 04.iv.2008, *leg. G.W. Maneveldt & U. van Bloemstein*, collection number 08/13 (33°59’22.34”S 23°32’39.62”E), epilithic on pebbles in high intertidal rock pool.

Eastern Cape Province: Kei Mouth. UWC 10/209, 11.vii.2010, *leg. G.W. Maneveldt & E. van der Merwe*, collection number 10/209 (32°41’19.32”S, 28°22’31.15”E), epilithic on primary bedrock amongst *S. cochlear* (limpet) territories in low intertidal zone.

KwaZulu-Natal Province: Durban, Ballito Bay. UWC 15/26, 22.vi.2015, *leg. G.W. Maneveldt* & *C.A. Puckree-Padua*, collection number 15/26 (29°32’42.49”S, 31°12’56.22”E), epilithic on boulder in shallow high shore rock pool above oyster belt.

DISTRIBUTION: Confirmed by DNA sequence data to be widely distributed (± 1,720 km) along the southern west and eastern coasts, occurring from Kommetjie (Western Cape Province) to Ballito Bay (KwaZulu Natal), South Africa; possibly more widespread up the east coast.

HABIT AND MORPHOLOGY: Plants non-geniculate, thalli thin, encrusting (smooth) (Figs 72-73), firmly adherent, blue-grey (in well-lit conditions) to brown (in dim light) when freshly collected (Fig. 72). Individual crusts not coalescing (not fusing together) and easily discernible (Figs 72-73). Thalli epilithic mostly on boulders and pebbles, but also occasionally on primary

bedrock in mid- and low intertidal rock pools and gullies; occasionally also epizoic on winkle shells (Figs 72-73).

ANATOMY: Thalli dorsiventrally organised, monomerous and haustoria absent (Fig. 74). Medulla thin and plumose (non-coaxial) (Figs 74). Medullary filaments comprise rectangular to elongate cells and give rise to cortical filaments that comprise square to rectangular cells (Figs 75). Contiguous medullary and cortical filaments joined by cell fusions; secondary pit connections absent (Fig 75-76). Subepithallial initials square to rectangular (Fig. 76). Epithallus single layered with flattened to elliptical cells (Fig. 76). Trichocytes rare at the thallus surface, occurring singularly (mostly), but also in small clusters of up to 6 cells, all separated by normal vegetative filaments (Fig. 76); always terminal and never intercalary in the cortex/perithallus; buried trichocytes not observed. Data on morphological and measured vegetative characters are summarised in Table 3 and Table 6.

REPRODUCTION: Gametangial thalli are both dioecious (mostly) and monoecious.

Spermatangial (male) conceptacles uniporate, low-domed, raised above surrounding thallus surface (Figs 77-78). Chambers transversely elliptical to flattened; roof nearly twice as thick along the pore canal (Fig. 78). Roof formed from filaments peripheral to the fertile area (Fig. 77). Throughout early development, a protective layer of epithallial cells surrounds conceptacle primordium (Fig. 77). This protective layer is shed once the pore canal is near fully developed; the pore opening occluded by a mucilage plug (Fig. 78). In mature conceptacles terminal initials along pore canal are enlarged and papillate, they project into pore canal and are orientated more or less parallel to the conceptacle roof surface. Unbranched (simple) spermatangial systems confined to floor of mature conceptacles (Figs 77-78). Senescent male conceptacles appear mostly shed, but occasionally buried ones were observed.

Carpogonial (female) conceptacles similar in size and shape to spermatangial conceptacles; raised above surrounding thallus surface (Fig. 79). In mature conceptacles terminal initials

along pore canal are enlarged and papillate, they project into pore canal and are orientated more or less parallel to the conceptacle roof surface. Carpogonial branches develop across the floor of conceptacle chamber, comprising a single support cell, a hypogynous cell and a carpogonium extended into a trichogyne (Fig. 79). Sterile cells also present on some hypogynous cells. Trichogynes often project through the pore opening (Fig. 79).

After presumed karyogamy, carposporophytes develop within female conceptacles and form carposporangial conceptacles (Fig. 80-82). Carposporangial conceptacles comparatively large, low-domed, and slightly raised above surrounding thallus surface (Fig. 80). Chambers transversely elliptical, with flattened bottoms presumably caused by growth of gonimoblast filaments. Pore canal slightly tapered towards surface, lined by elongated papillate that project into pore canal and are orientated more or less parallel to the conceptacle roof surface. In mature conceptacles, cells lining the pore canal more elongate than their inward derivatives; base of pore canal sunken into the chamber and terminal initials near the base characteristically point downward (Figs 80-81). A corona of filaments often occludes the pore opening and projects above it (80-81). Corona appears to form from filaments near the upper half of roof, directly adjacent to pore canal (Figs 81); fully mature or senescent carposporangial conceptacles often lack the corona of filaments. Discontinuous central fusion cell present and 5-7 celled gonimoblast filaments (incl. a terminal carposporangium) develop along the periphery of conceptacle chamber (Figs 80, 82). The remains of unfertilized carpogonia persist across the dorsal surface of the fusion cell. Senescent carposporangial conceptacles appear to be shed as no buried conceptacles were observed.

Tetrasporangial thalli are morphologically similar to gametangial thalli. Conceptacles uniporate, low domed and raised above to flush with surrounding thallus surface (Figs 83-86). Chambers transversely elliptical to markedly bean-shaped; roof nearly twice as thick along the pore canal and 6-8 cells (incl. an epithallial cell) thick. Pore canal tapered towards the surface,

lined by elongate papillate cells that project into pore canal and are orientated more or less parallel or at a sharp angle to the conceptacle roof surface. Roof formed from filaments peripheral to the fertile area (Figs 83-85); terminal initials more elongate than their inward derivatives (Fig. 85). Throughout early development a protective layer of epithallial cells surrounds conceptacle primordium (Figs 83-85). This protective layer is shed once pore canal is near fully developed; pore opening occluded by a large corona of filaments that project well above the pore opening (Fig. 86-88). Corona appears to form from filaments near the upper half of roof, directly adjacent to pore canal (Fig. 87). In fully mature or senescent tetrasporangial conceptacles the pore canal is often straight sided and lack the corona of filaments. Throughout development of immature tetrasporangial conceptacles, a prominent columella of sterile filaments forms at centre of conceptacle chamber (Figs 84-86, 88); central columella appears weakly calcified as with maturity it disintegrates to form a low mound that is often also absent (Fig. 88). Base of pore canal sunken into chamber and terminal initials point downward (Figs 86-87). Mature conceptacle floors sunken 12-21 cells (including the epithallial cell) below surrounding thallus surface. Zonately arranged tetrasporangia initially arranged at the extreme periphery of the conceptacle chamber (Fig. 86), attached via a stalk cell; where central columella has disintegrated or diminished, tetrasporangia fill the chamber and appear to be distributed across the chamber floor (Fig. 88). Senescent tetrasporangial conceptacles mostly shed but occasionally buried ones were observed. Data on reproductive characters summarised in Table 4 and Table 7.

3.2.7. *Chamberlainium occidentale* Maneveldt, Puckree-Padua & P.W.Gabrielson *sp. nov.*

(Figs 89-105; Tables 3-5)

HOLOTYPE: L ???????, 01.x.2015, *leg. G.W. Maneveldt & C.A. Puckree-Padua*, collection number 15/61B (90), epilithic on primary bedrock among *S. cochlear* (limpet) territories in the Cochlear zone (low intertidal zone).

ISOTYPES: UWC 15/58, UWC 15/59, UWC 15/61A

Type Locality: South Africa, Western Cape Province, Lamberts Bay (32°6'34.37"S, 18°18'7.62"E).

ETYMOLOGY: '*occidentale*' from '*occidentalis*', meaning western, making reference to the species' widespread distribution along the west coast of Southern Africa.

DIAGNOSIS: Thalli variably thick, encrusting (smooth) to warty (mostly) to lumpy, becoming only slightly protuberant, not becoming secondarily thick and discoid with orbicular protrusions, nor wrinkled; individual crusts not coalescing (not fusing together) and easily discernible; colour of living thalli brownish beige in well-lit conditions and blue-grey to rosy pink in dim light; thallus construction monomerous; epithallus single layered; central columella present in tetrasporangial conceptacles, persisting to maturity; pore opening in mature tetrasporangial conceptacles unoccluded and slightly sunken below surrounding pore opening; *psb*A (GenBank ??????) and *rbc*L (GenBank ??????) sequences collectively[3] unique.

DNA SEQUENCES: *psb*A (851 bp) and *rbc*L (1434 bp) gene sequences, obtained from 10 specimens (including the holotype and isotypes) (Table S1), were all identical to each other. DNA sequences collectively showed that *Chamberlainium occidentale* was different from all other named species sequenced to date (Figs 3-8; Table S1).

[3] *Chamberlainium occidentale* shares seven single nucleotide polymorphisms (SNPs) with *C. capense*, with the *rbc*L sequence of the holotype of *C. capense* being identical to all *C. occidentale* specimens sequenced.

SPECIMENS EXAMINED: Ten samples (including the holotype and isotypes), all confirmed by DNA sequencing, represented our entire collection for this taxon. Data below are presented geographically from north to south (along the west coast and southern west coast) followed chronologically by the collection numbers.

Namibia – Lüderitz: Grosse Bucht. UWC 92/302, 13.vii.1992, *leg*. *D.W. Keats & A. Groener*, collection number 92/302 (26°44'28.98"S, 15°6'7.20"E), epilithic on primary bedrock in mid-intertidal zone.

South Africa – Northern Cape Province: Groenriviermond. UWC 93/37, 05.viii.1993, *leg*. *G.W. Maneveldt*, collection number 93/37 (30º51'53"S, 17°34'40.68"E), epilithic on primary bedrock among *S. cochlear* (limpet) territories in the Cochlear zone (low intertidal zone); UWC 15/56, 30.ix.2015, *leg*. *G.W. Maneveldt & C.A. Puckree-Padua*, collection number 15/56 (30º51'53"S, 17°34'40.68"E), epilithic on primary bedrock in mid-intertidal rock pool; UWC 15/57, 30.ix.2015, *leg*. *G.W. Maneveldt & C.A. Puckree-Padua*, collection number 15/57 (30º51'53"S, 17°34'40.68"E), epizoic on *S. cochlear* (limpet) shell in the Cochlear zone (low intertidal zone).

Western Cape Province: Lamberts Bay. UWC 15/58, 01.x.2015, *leg*. *G.W. Maneveldt, & C.A. Puckree-Padua*, collection number 15/58 (32°6'34.37"S, 18°18'7.62"E) (isotype), epilithic on primary bedrock in *S. granularis* (limpet) dominated high shore rock pool; UWC 15/59, 01.x.2015, *leg*. *G.W. Maneveldt, & C.A. Puckree-Padua*, collection number 15/59 (32°6'34.37"S, 18°18'7.62"E) (isotype), epilithic on primary bedrock in *Cymbula granatina* (limpet) dominated mid-shore rock pool; UWC 15/61A, 01.x.2015, *leg*. *G.W. Maneveldt, & C.A. Puckree-Padua*, collection number 15/61A (32°6'34.37"S, 18°18'7.62"E) (isotype), epilithic on primary bedrock in *C. granatina* (limpet) dominated mid-shore rock pool; L ???????, 01.x.2015, *leg*. *G.W. Maneveldt, & C.A. Puckree-Padua*, collection number 15/61B

(32°6’34.37”S, 18°18’7.62”E) (holotype), epilithic on primary bedrock among *S. cochlear* (limpet) territories in the Cochlear zone (low intertidal zone).

Western Cape Province: Cape St. Martin. UWC 15/63A, 02.x.2015, *leg. G.W. Maneveldt & C.A. Puckree-Padua*, collection number 15/63A (32°44’9.86”S, 17°54’25.93”E), epizoic on *S. cochlear* shell (limpet) in the Cochlear zone (low intertidal zone).

Western Cape Province: Holbaaipunt. UWC 93/220, 01.xi.1993, *leg. G.W. Maneveldt*, collection number 93/220 (34°22’45.24”S, 18°50’46.04”E), epilithic on primary bedrock among *S. cochlear* (limpet) territories in the Cochlear zone (low intertidal zone).

DISTRIBUTION: Confirmed by DNA sequence data to be widely distributed (± 1,200 km) along the west and southern west coasts, occurring from Lüderitz (Namibia) to Holbaaipunt (Western Cape Province), South Africa.

HABIT AND MORPHOLOGY: Plants non-geniculate, thalli variably thick, encrusting (smooth) to warty (mostly) to lumpy, becoming only slightly protuberant (protuberances 4 mm in height) (Figs 89-90), firmly adherent, brownish beige (in well-lit conditions) to blue-grey to rosy pink (in dim light) when freshly collected (Fig. 89). Individual crusts not coalescing (not fusing together) and easily discernible (Figs 89-90). Thalli epilithic on primary bedrock in low, mid- and low intertidal exposed platforms and in rock pools; epizoic on *S. cochlear* (limpet) shells in the Cochlear zone (low intertidal zone) (Figs 89).

ANATOMY: Thalli dorsiventrally organised, monomerous and haustoria absent. Medulla thin and plumose (non-coaxial) (Fig. 91). Medullary filaments comprise square to rectangular to elongate cells and give rise to cortical filaments that comprise square to rectangular cells (Figs 92-93). Contiguous medullary and cortical filaments joined by cell fusions; secondary pit connections absent (Figs 92-93). Subepithallial initials square to rectangular (Fig. 94). Epithallus single layered with elliptical to round to elongate cells (Fig. 94). Trichocytes common, mostly singularly, but also in clusters of up to 6 cells, separated by normal vegetative

filaments (Fig. 94); always terminal and never intercalary in the cortex/perithallus; buried trichocytes not observed. Data on morphological and measured vegetative characters are summarised in Table 3.

REPRODUCTION: Gametangial thalli dioecious.

Spermatangial (male) conceptacles uniporate, low-domed, raised above surrounding thallus surface (Figs 95-96). Chambers transversely elliptical to flattened; roof nearly twice as thick along pore canal (Figs 96-97). Roof formed from filaments peripheral to the fertile area (Fig. 95). Throughout early development, a protective layer of epithallial cells surrounds conceptacle primordium (Fig. 95). This protective layer is shed once the pore canal is near fully developed; the pore opening occluded by a mucilage plug (Figs 96). In mature conceptacles terminal initials along pore canal are enlarged and papillate, they project into pore canal and are orientated more or less parallel to the conceptacle roof surface (Fig. 97). Unbranched (simple) spermatangial systems confined to floor of mature conceptacle (Figs 95-96). Senescent male conceptacles appear to be shed as no buried conceptacles were observed.

Carpogonial (female) conceptacles similar in size and shape to spermatangial conceptacles; raised above surrounding thallus surface (Fig. 98). In mature conceptacles terminal initials along pore canal are enlarged and papillate, they project into pore canal and are orientated more or less parallel or at a sharp angle to the conceptacle roof surface (Fig. 98). Carpogonial branches develop across the floor of conceptacle chamber, comprising a single support cell, a hypogynous cell and a carpogonium extended into a trichogyne (Fig. 98). Sterile cells also present on some hypogynous cells (Fig. 98).

After presumed karyogamy, carposporophytes develop within female conceptacles and form carposporangial conceptacles (Fig. 99). Carposporangial conceptacles comparatively large, low-domed, and raised above surrounding thallus surface. Chambers transversely elliptical, with flattened bottoms presumably caused by growth of gonimoblast filaments. Pore canal

tapered towards surface, lined by enlarged papillate cells that project into pore canal and are orientated more or less parallel to the conceptacle roof surface (Fig. 99). In mature conceptacles, cells lining the pore canal more elongate than their inward derivatives; base of pore canal sunken into the chamber and terminal initials near the base characteristically point downward (Figs 99). Discontinuous central fusion cell present and 5-7 celled gonimoblast filaments (incl. a terminal carposporangium) developed along the periphery of conceptacle chamber (Figs 99-100). The remains of unfertilized carpogonia persist across the dorsal surface of the fusion cell. Senescent carposporangial conceptacles appear to be shed as no buried conceptacles were observed.

Tetrasporangial thalli are morphologically similar to gametangial thalli. Conceptacles uniporate, low domed and raised above surrounding thallus surface (Figs 101-104). Chambers transversely elliptical to bean-shaped; roof nearly twice as thick along the pore canal and 5-7 cells (incl. an epithallial cell) thick. Pore canal tapered towards surface and arching, lined by elongated papillate cells that project into pore canal and are orientated more or less parallel or at a sharp angle to the conceptacle roof surface (Fig. 105). Roof formed from filaments peripheral to the fertile area (Figs 101-103); terminal initials more elongate than their inward derivatives. Throughout early development a protective layer of epithallial cells surrounds conceptacle primordium (Figs 101-103). This protective layer is shed once pore canal is near fully developed; pore opening unoccluded and becomes slightly sunken below surrounding roof surface (Figs 104-105). Throughout development of immature tetrasporangial conceptacle a prominent columella of sterile filaments forms at the centre of conceptacle chamber (Figs 102-104); central columella appears weakly calcified as with maturity it disintegrates to form a low mound. Base of pore canal sunken into chamber and terminal initials near the base point downward (Fig.105). Mature conceptacle floors sunken 14-19 cells (including the epithallial cell) below surrounding thallus surface. Zonately divided

tetrasporangia at maturity arranged at the extreme periphery of conceptacle chamber, attached via a stalk cell (Fig. 104); where central columella has disintegrated, tetrasporangia fill the chamber and appear to be distributed across the chamber floor. Senescent tetrasporangial conceptacles appear to be shed as no buried conceptacles were observed. Data on reproductive characters summarised in Table 4.

3.2.8. *Chamberlainium tenue* Maneveldt, Puckree-Padua & P.W.Gabrielson *sp. nov*.

(Figs 106-117, Tables 3-5)

HOLOTYPE: L ???????, 11.vii.2010, *leg. G.W. Maneveldt & E. van der Merwe*, collection number 10/205 (107), epilithic on primary bedrock in mid-intertidal rock pool.

ISOTYPE: UWC 10/202

TYPE LOCALITY: South Africa, Eastern Cape Province, Kei Mouth (32°41'19.32"S, 28°22'31.15"E).

ETYMOLOGY: '*tenue'* from '*tenuis*', making reference to the species' thin thallus.

DIAGNOSIS: Thalli thin, uniformly encrusting (smooth), not becoming secondarily thick and discoid with orbicular protrusions, nor warty, nor wrinkled; individual crusts not coalescing (not fusing together) and easily discernible; colour of living thalli yellowish (on shale platforms) to bright pink in well-lit conditions to blue-grey or brownish in dim light; thallus construction monomerous; epithallus single layered; central columella present in tetrasporangial conceptacles, disintegrating to form a low mound with maturity; pore opening occluded by a mucilage plug and sunken below the surrounding roof; *psb*A (GenBank ??????) and *rbc*L (GenBank ??????) sequences unique.

DNA SEQUENCES: *psb*A (851 bp) and *rbc*L (1464 bp) gene sequences, obtained from seven specimens (including the holotype and isotype) (Table S1), were all identical to each other. DNA sequences showed that *Chamberlainium tenue* was different from all other named species sequenced to date (Figs 3-5; Table S1).

SPECIMENS EXAMINED: Seven samples (including the holotype and isotype), all confirmed by DNA sequencing, represent our entire collection for this taxon. Data below are presented geographically from west to east followed chronologically by the collection numbers.

South Africa – Western Cape Province: Knysna Heads. UWC 08/25, 07iii.2008, *leg. G.W. Maneveldt & U. van Bloemstein*, collection number 08/25 (34°4'36.3"S, 23°3'37.57"E), epilithic on primary bedrock in high shore zone.

Western Cape Province: Tsitsikamma, Nature's Valley. UWC 08/07, 04.iii.2008, *leg. G.W. Maneveldt & U. van Bloemstein*, collection number 08/07 (33°59'22"S, 23°32'36"E), epilithic on primary bedrock in high shore zone.

Eastern Cape Province: Kidds Beach. NCU 659869, 19.xii.2009, *leg. T. Klenk*, collection number 929 (33°09'28.32"S, 27°41'15.15"E), epilithic on primary bedrock in mid-intertidal zone; NCU 659867, 19.xii.2009, *leg. T. Klenk*, collection number 925 (33°09'28.32"S, 27°41'15.15"E), epilithic on primary bedrock in mid-intertidal zone.

Eastern Cape Province: Kei Mouth. UWC 10/202, 11.vii.2010, *leg. G.W. Maneveldt & E. van der Merwe*, collection number 10/202 (32°41'19.32"S, 28°22'31.15"E) (isotype), epilithic on primary bedrock in high shore zone; L ???????, 11.vii.2010, *leg. G.W. Maneveldt & E. van der Merwe*, collection number 10/205 (32°41'19.32"S, 28°22'31.15"E) (holotype), epilithic on primary bedrock in mid--intertidal rock pool.

KwaZulu-Natal Province: Durban, Ballito Bay. UWC 15/23, 22.vi.2015, *leg. G.W. Maneveldt & C.A. Puckree-Padua*, collection number 15/23 (29°32'42.49"S, 31°12'56.95"E), epilithic on primary bedrock in high shore rock pool above oyster belt.

DISTRIBUTION: Confirmed by DNA sequence data to be widely distributed (± 1,220 km) along the south and east coasts, occurring from Knysna Heads (Western Cape Province) to Ballito Bay (KwaZulu-Natal Province), South Africa; possibly more widespread up the east coast.

HABIT AND MORPHOLOGY: Plants non-geniculate, thalli thin, encrusting (smooth) (Figs 106-107), firmly adherent, yellowish (on shale platforms) to bright pink (in well-lit conditions) (Fig. 106) to blue-grey or brownish (in dim light) when freshly collected. Individual crusts not

coalescing (not fusing together) and easily discernible (Figs 106-107). Thalli epilithic on primary bedrock in high intertidal and midshore rock pools (Fig. 106).

ANATOMY: Thalli dorsiventrally organised, monomerous and haustoria absent. Medulla thin and plumose (non-coaxial) (Fig. 108). Medullary filaments comprise square to rectangular to elongate cells and give rise to cortical filaments that comprise squat to square to rectangular cells (Figs 109-110). Contiguous medullary and cortical filaments joined by cell fusions; secondary pit connections absent (Figs 109-110). Subepithallial initials square to rectangular to elongate (Fig. 110). Epithallus single layered with squat to elliptical to domed cells (Fig. 8). Trichocytes common at thallus surface, occurring singularly (Fig. 110); always terminal and never intercalary in the cortex/perithallus; buried trichocytes not observed. Data on morphological and measured vegetative characters are summarised in Table 3.

REPRODUCTION: Gametangial thalli appear to be dioecious, although female plants were not observed.

Spermatangial (male) conceptacles uniporate, low-domed, raised above the surrounding thallus surface (Figs. 111-112). Chambers transversely elliptical to flattened; roof nearly twice as thick along pore canal (Fig. 111-112); the pore opening occluded by a mucilage plug (Fig. 112). Spermatangial conceptacle primordia not observed. In mature conceptacles terminal initials along pore canal are enlarged and papillate, they project into pore canal and are orientated more or less parallel to the conceptacle roof surface (Fig. 112). Unbranched (simple) spermatangial systems confined to floor of mature conceptacle (Fig. 111). Senescent male conceptacles appear to be shed as no buried conceptacles were observed.

Tetrasporangial thalli are morphologically similar to spermatangial thalli. Conceptacles uniporate, low domed and raised to slightly sunken below surrounding thallus surface (Figs 113-116). Chambers transversely elliptical to bean-shaped; roof nearly twice as thick along the pore canal and 5-7 cells (incl. an epithallial cell) thick. Pore canal tapered towards surface

and arching, lined by elongated papillate cells that project into pore canal and are orientated more or less parallel or at a sharp angle to the conceptacle roof surface (Figs 115-117). Roof formed from filaments peripheral to the fertile area (Figs 113-114); terminal initials more elongate than their inward derivatives (Fig. 114). Throughout early development a protective layer of epithallial cells surrounds conceptacle primordium (Figs 113-114). This protective layer is shed once pore canal is near fully developed; pore opening occluded by a mucilage plug (Figs 115-117) and becomes sunken below the surrounding roof surface (Fig. 117). Throughout early development of tetrasporangial conceptacle, a prominent columella of sterile filaments forms at centre of conceptacle chamber (Figs 115-116); central columella appears weakly calcified as with maturity it disintegrates to form a low mound. Base of pore canal sunken into chamber and terminal initials near the base point downward (Fig.117). Mature conceptacle floors sunken 12-16 cells (including the epithallial cell) below surrounding thallus surface. Zonately divided tetrasporangia at maturity arranged at the extreme periphery of conceptacle chamber and attached via a stalk cell (Fig. 116); where the central columella has disintegrated, tetrasporangia fill the chamber and appear to be distributed across the chamber floor. Senescent tetrasporangial conceptacles appear to be shed as no buried conceptacles were observed. Data on reproductive characters are summarised in Table 4.

3.2.9. *Pneophyllum neodiscoideum (*Foslie) Maneveldt, Puckree-Padua & P.W.Gabrielson *sp. nov.*

(Figs 118-136; Tables 3-5, 10-11)

HOLOTYPE: L ???????, 08.vii.2009, leg. *G.W. Maneveldt & E. van der Merwe*, collection number 09/132, epilithic on small boulder in low shore rock pool (Fig. 120).

ISOTYPE: UWC 09/131, UWC 09/133

TYPE LOCALITY: South Africa, Western Cape Province, Cape Agulhas, L'Agulhas (34°49'26.37"S, 20°01'0.71"E).

ETYMOLOGY: '*neodiscoideum*' from '*neo*' meaning new and '*discoideum*', making reference to the species' close resemblance to *Spongites discoideus* (Foslie) D.Penrose & Woelkerling, for which the species has till now been misidentified.

DIAGNOSIS: Thalli encrusting (smooth), initially (primary crusts) very thin becoming secondarily thick and discoid with orbicular protrusions that often produce crowded, contiguous, swollen protuberances; individual primary crusts coalescing (fusing) and not easily discernible, secondary crusts not coalescing (not fusing), easily discernible; colour of living thalli pink to light purple to yellowish brown in well-lit conditions to reddish brown in dim light; primary thallus construction dimerous, secondarily monomerous in orbicular protrusions, plumose (non-coaxial); central columella present in tetrasporangial conceptacles; terminal initials in mature conceptacles pore canal straight-sided, lined by cells that project into pore canal as papillae; pore canal cells near the base orientated more or less parallel or at a sharp angle to the conceptacle roof surface but the distal ends of those near the pore opening are orientated nearly perpendicular to the roof; base of tetrasporangial conceptacle pore canal sunken into chamber and terminal initials near the base point downward; pore opening occluded by a prominent mucilage plug that may fill the entire pore canal and that appears to

form from cells lining the pore canal; *psb*A (GenBank ??????) and *rbc*L (GenBank ??????) sequences unique.

DNA SEQUENCES: The *psb*A (851 bp) and *rbc*L (1387 bp) gene sequences obtained from eight specimens (including the holotype and isotypes) (Table S1) were all identical to each other. These DNA sequences showed that *Pneophyllum neodiscoideum* was different from all other named species sequenced to date (Figs 3-5; Table S1).

SPECIMENS EXAMINED: Eight samples (including the holotype and isotypes), all confirmed by DNA sequencing, represent our entire collection for this taxon. Data below are presented geographically from west to east followed chronologically by the collection numbers.

South Africa - Western Cape Province: Kalk Bay. UWC 09/158, 21.ix.2009, *leg. G.W. Maneveldt & E. van der Merwe*, collection number 09/158 (34°7’52.39”S, 18°26’54.55”E), epilithic on primary bedrock in mid-shore rock pool; UWC 09/160, 21.ix.2009, *leg. G.W. Maneveldt & E. van der Merwe*, collection number 09/160 (34°7’52.39”S, 18°26’54.55”E), epizoic on *O. sinensis* (winkle) shell in low shore zone; UWC 11/39, 20.iiii.2011, *leg. G.W. Maneveldt*, collection number 11/39 (34°7’52.39”S, 18°26’54.55”E), epilithic on boulder in mid-shore rock pool.

Western Cape Province: Cape Agulhas, L’Agulhas, Stinkbaai. UWC 09/131, 08.vii.2009, *leg. G.W. Maneveldt & E. van der Merwe*, collection number 09/131 (34°49’26.37”S, 20°01’0.71”E) (isotype), epizoic on *O. sinensis* (winkle) shell in low shore rock pool; L ???????, 08.vii.2009, *leg. G.W. Maneveldt & E. van der Merwe*, collection number 09/132 (34°49’26.37”S, 20°01’0.71”E) (holotype), epilithic on small boulder in low shore rock pool; UWC 09/133, 08.vii.2009, *leg. G.W. Maneveldt & E. van der Merwe*, collection number 09/131 (34°49’26.37”S, 20°01’0.71”E) (isotype), epilithic on small boulder in low shore rock pool; UWC 11/22, 19.iii.2011, *leg. G.W. Maneveldt*, collection number 11/22 (34°49’26.37”S, 20°01’0.71”E), epilithic on primary bedrock in low shore sandy gully.

Western Cape Province: Struisbaai. UWC 09/119, 07.vii.2009, *leg. G.W. Maneveldt & E. van der Merwe*, collection number 09/119 (34°48'48.36"S, 20°03'14.99"E), epilithic on pebble in mid-shore rock pool.

DISTRIBUTION: Confirmed by DNA sequence data to be distributed (± 220 km) along the southern west coast from Kalk Bay (False Bay) to Cape Agulhas (Western Cape Province), South Africa; possibly more widespread up the west coast (see Chamberlain 1994b).

HABIT AND MORPHOLOGY: Plants non-geniculate, encrusting (smooth), primary thalli initially very thin becoming secondarily thick and discoid with orbicular protrusions (Figs 118-119) that often produce crowded, contiguous, swollen protuberances (Fig. 119) up to 10 mm in height. Thalli firmly adherent, pink to light purple to yellowish brown (in well-lit conditions) to reddish brown (in dim light) when freshly collected (Fig. 118). Individual primary crusts coalescing (fusing) and not easily discernible; secondary crusts not coalescing (not fusing), easily discernible; (Figs 118, 120). Thalli epilithic on primary bedrock, boulders and pebbles in mid- and low intertidal rock pools and in sandy gullies; also epizoic on winkle shells from these zones (Figs 118, 120).

ANATOMY: Primary thallus dimerous becoming secondarily monomerous, haustoria absent. The single basal layer in primary thalli comprising cells that were irregularly square and had the appearance of an upright book (Figs 121-122). In radial section ('cover view' i.e. along the filament) basal cells non-palisade (Fig. 121-122); in tangential section ('spine view' i.e. across the filaments) basal cells rectangular to palisade like (Fig. 123). In tangential view fusions between cells of contiguous basal filaments abundant and frequently occupied most of the adjoining cell wall (Fig. 123). Basal cells gave rise to erect filaments that comprised the bulk of the primary thallus (Figs. 121-123). Erect filaments comprise square to rectangular to elongate cells with rounded corners (Figs 121-123). Fusions between cells of contiguous erect filaments abundant and frequently also occupied most of the adjoining cell wall (Figs 121-

123). Secondarily monomerous thalli result from overgrowing orbicular protrusions that produce disc-like thalli (Figs 121, 124). In these secondarily monomerous thalli medulla thin and plumose (non-coaxial) (Fig. 124). Medullary filaments comprise rectangular to elongate cells and give rise to cortical filaments that comprise square to rectangular to elongate cells (Figs 124-125). Contiguous medullary and cortical filaments joined by cell fusions; secondary pit connections absent (Figs 124-125). Subepithallial initials square to elongate (Fig. 125). Epithallus up to four cell layers with elliptical to rounded cells (Fig. 125). Trichocytes not observed. Data on morphological and measured vegetative characters summarised in Table 3 and Table 10.

REPRODUCTION: Gametangial thalli dioecious.

Spermatangial (male) conceptacles uniporate, low-domed, raised slightly above or only occasionally flush with surrounding thallus surface at maturity (Fig. 126). Chambers transversely elliptical to flattened; roof nearly twice as thick along pore canal (Fig. 126). Spermatangial conceptacle primordia not observed. Pore opening occluded by a mucilage plug (Fig. 126). In mature conceptacles terminal initials along pore canal are enlarged and papillate, they project into pore canal and are orientated more or less parallel to the conceptacle roof surface (Fig. 126). Unbranched (simple) spermatangial systems confined to floor of mature conceptacle (Fig. 126). Senescent male conceptacles buried.

Carpogonial (female) conceptacles similar in size and shape to spermatangial conceptacles. Roof formed from filaments peripheral to the fertile area (Fig. 127). In mature conceptacles terminal initials along pore canal are enlarged and papillate, they project into pore canal and are orientated more or less parallel to the conceptacle roof surface (Fig. 128). Carpogonial branches develop across floor of conceptacle chamber, comprising a single support cell, a hypogynous cell and a carpogonium extended into a trichogyne (Fig. 128). Sterile cells also

present on some hypogynous cells (Fig 128). Only buried carpogonial conceptacles observed (Fig. 128).

After presumed karyogamy, carposporophytes develop within female conceptacles and form carposporangial conceptacles (Figs 129-130). Carposporangial conceptacles comparatively large, low-domed, flush with to slightly raised above surrounding thallus surface (Fig.129). Chambers transversely elliptical to bean-shaped, with mostly flattened bottoms presumably caused by growth of gonimoblast filaments. Pore canal more or less straight-sided, lined by enlarged papillate cells that project into pore canal and are orientated more or less parallel to the conceptacle roof surface. In mature conceptacles, cells lining the pore canal more elongate than their inward derivatives; base of pore canal sunken into the chamber and terminal initials near the base point downward (Figs 130-131). Pore opening occluded by a prominent mucilage plug that may fill the entire pore canal and that appears to form from cells lining the pore canal (Figs 129, 131). Discontinuous fusion cell present and 6-7 celled gonimoblast filaments (incl. a terminal carposporangium) developed along the periphery of conceptacle chamber (Fig. 130). The remains of unfertilized carpogonia persist across the dorsal surface of the fusion cell (Fig.129). Senescent carposporangial conceptacles buried.

Tetrasporangial thalli morphologically similar to carposporangial thalli. Conceptacles uniporate, low domed, flush with, to sunken, to raised above surrounding thallus surface (Figs 133, 135). Chambers transversely elliptical to markedly bean-shaped; roof 6-22 cells (incl. an epithallial cell) thick. Pore canal straight-sided, lined by elongated papillate cells that project into pore canal; pore canal cells near the base orientated more or less parallel or at a sharp angle to the conceptacle roof surface but the distal ends of those near the pore opening are orientated nearly perpendicular to the roof (Figs 135-136). Roof formed by filaments both peripheral to and interspersed amongst sporangial initials (Figs 132-133); filaments rarely persist to maturity (Fig. 134). Throughout early development a protective layer of epithallial cells surrounds

conceptacle primordium (Figs 132-133). This protective layer is shed once pore canal is near fully developed; pore opening occluded by a prominent mucilage plug that may fill the entire pore canal and that appears to form from cells lining the pore canal (Figs 135-136). Throughout development of immature tetrasporangial conceptacle, a prominent columella of sterile filaments forms at centre of conceptacle chamber (Figs 132-133); central columella appears weakly calcified as with maturity it disintegrates to form a low mound (Fig. 135). Base of pore canal sunken into chamber and terminal initials near the base point downward (Fig. 136). Mature conceptacle floors sunken 15-30 cells (including the epithallial cell) below surrounding thallus surface. Zonately divided tetrasporangia at maturity arranged at the extreme periphery of conceptacle chamber and attached via a stalk cell (Fig. 135). Senescent tetrasporangial conceptacles buried. Data on reproductive characters summarised in Table 4 and Table 11.

4. Discussion

4.1. Delineation in *Chamberlainium*

Caragnano *et al.* (2018) established the subfamily Chamberlainoideae (Corallinales, Rhodophyta), for their new genus *Chamberlainium* and for the established genus *Pneophyllum*, including several species previously assigned to *Spongites* (Neogoniolithoideae, Corallinales, Rhodophyta - Rösler *et al*. 2016). *Chamberlainium* currently contains all taxa possessing: 1) thalli non-geniculate and non-endophytic, epilithic or epizoic; 2) thalli thin (up to 1 mm), encrusting to warty to lumpy; 3) thallus construction primarily dimerous or monomerous, but not both; 4) epithallus single to multilayered; 5) trichocytes absent or occurring singly/paired; 6) tetra/bisporangial conceptacles uniporate with roofs formed from filaments peripheral to the developing sporangial initials; 7) tetra/bisporangial conceptacle chambers < 300 µm in diameter with chamber roofs < 8 cells thick; 8) tetra/bisporangial conceptacle pore canal lined by cells orientated more or less parallel or at a sharp angle to the roof surface, protruding into the pore canal as papillae; and 9) male conceptacles with simple (unbranched) spermatangial systems confined to the chamber floor. *Pneophyllum* currently contains all taxa possessing: 1) thalli non-geniculate, epizoic or epiphytic lacking haustoria; 2) thalli thin (< 200 µm); 3) thallus construction primarily dimerous with a basal layer comprised of non-palisade cells; 4) epithallus single layered; 5) trichocytes absent or occurring singly/paired; 6) tetra/bisporangial conceptacles uniporate with roofs formed from filaments both peripheral to as well as interspersed amongst the developing sporangial initials; 7) tetra/bisporangial conceptacle chambers < 350 µm in diameter with chamber roofs < 8 cells thick; 8) tetra/bisporangial conceptacle pore canal lined by cells orientated more or less parallel or at a sharp angle to the roof surface, protruding into the pore canal as papillae, that sometimes also form a distinct corona that projects above the pore opening; and 9) male conceptacles with simple (unbranched) spermatangial systems confined to the chamber floor. To separate these *Chamberlainium* and

Pneophyllum the following characters are considered useful; 1) thallus construction (primarily dimerous or monomerous in *Chamberlainium vs.* only dimerous in *Pneophyllum*); 2) number of epithallial cell layers (may be more than one in *Chamberlainium vs.* only one in *Pneophyllum*); 3) tetrasporangial roof development (Type 1 in *Chamberlainium* vs. Type 2 in *Pneophyllum*); 4) diameter of tetrasporangial conceptacle chambers (< 300 μm in *Chamberlainium vs.* < 350 μm in *Pneophyllum*); and 5) distribution of tetrasporangia in tetrasporangial conceptacles (peripheral or across the chamber floor in *Chamberlainium vs.* peripheral only in *Pneophyllum*) (Caragnano *et al.* 2018).

Based on an integrated taxonomic approach (ITA) that utilizes DNA sequencing of field-collected specimens and, most importantly, DNA sequencing of type/'topotype' specimens, along with traditional morpho-anatomical characters (Gabrielson *et al*. 2011; Maneveldt *et al*. 2017), we were able to show that all of the species previously assigned to *Spongites* in South Africa (in addition to *C. agulhense* – see Caragnano *et al*. 2018) belong in the newly established Chamberlainoideae and not in *Spongites* (Neogoniolithoideae), these species variously possessing (with minor differences) the morpho-anatomical characters that define *Chamberlainium* and *Pneophyllum*. Notably *S. yendoi* reported for South Africa is not that species and currently comprises at least six different cryptic species, all of which appear to be southern African endemics and mostly South African endemics. Due to the crust identified as *G. yendoi* being thin and overgrowing another crust (Fig. S1), DNA sequencing of this type specimen is extremely difficult. As such, *G. yendoi* has not been successfully sequenced and no direct comparison can be made between *S. yendoi* and the cryptic *Chamberlainium* species that were previously assigned to *S. yendoi*. However, based on the genetic evidence multiple species were passing as *S. yendoi* in South Africa, as well as in New Zealand. Our data show that none of the sequences of species passing as *S. yendoi* from South Africa match those from

New Zealand passing under the same name, and consequently, South African *S. yendo*i and New Zealand *S. yendoi*, are not conspecific. Temperate, non-geniculate coralline species (confirmed by sequencing) are yet to be reported to be distributed across ocean basins, and it is highly unlikely that a temperate species with a type locality in Japan would be the same temperate species in South Africa (or New Zealand) (P.W. Gabrielson *pers. com*.). Similarly, *S. discoideus* reported for South Africa is not that species and belongs in *Pneophyllum* as it is currently circumscribed. For South Africa, as a result of this study eight species are now recognised to occur in *Chamberlainium* compared to four previously and five in *Pneophyllum* compared to four previously.

4.2. Assignment of species names

Sequences from type (preferable) or 'topotype' specimens are the only reliable way to unequivocally apply a name for morphologically variable taxa or taxa with few characters (and that includes nearly all coralline algae (Gabrielson 2008a; Lindstrom *et al*. 2011; Hind & Saunders 2013; Hernández-Kantún *et al*. 2015; Hind *et al*. 2015; Rösler *et al*. 2016; Peña *et al*. 2018; Richards *et al*. 2018). Our data supports this view and we consequently argue against the placing into synonymy, coralline algal species, based solely on morpho-anatomical similarity, particularly if such species are geographically widely separated. With this in mind, we have recognised the following species within the subfamily Chamberlainoideae from South Africa.

4.2.1. *Chamberlainium agulhense*

Chamberlainium agulhense is characterised by the following combination of features: 1) thalli up to 650 µm thick, encrusting (smooth); 2) individual crusts not coalescing (not fusing together) and easily discernible; 3) colour of living thalli brownish pink in well-lit conditions;

4) thallus construction dimerous and plumose; 5) epithallus 1-3 cells thick; 6) tetrasporangial conceptacle chambers raised, with floors 10-15 cells below the surrounding thallus surface; 7) tetrasporangial conceptacle chambers 66-108 µm in height and 137-196 µm in diameter with roofs 4-8 cells thick; 8) central columella present in tetrasporangial conceptacles, disintegrating to form a low mound with maturity; 9) pore opening in mature tetrasporangial conceptacles appears to be unoccluded (van der Merwe *et al*. 2015); and 10) *psb*A and *rbc*L sequences unique.

Chamberlainium agulhense is a range-restricted endemic (± 10 km) along the southern west coast of South Africa occurring in the high to mid-intertidal zones. Additionally, the dimerous thallus construction is a useful character for distinguishing it anatomically from all other South African species of *Chamberlainium*.

4.2.2. *Chamberlainium capense*

Chamberlainium capense is characterised by the following combination of features: 1) thalli up to 1000 µm thick , encrusting to variably lumpy and slightly protuberant (up to 4 mm in height), not becoming secondarily thick and discoid with orbicular protrusions, nor wrinkled; 2) individual crusts not coalescing (not fusing together) and easily discernible; 3) colour of living thalli bright to dusky pink in well-lit conditions to rosy or purple-pink in dim light; 4) thallus construction monomerous and plumose; 5) epithallus single layered; 6) tetrasporangial conceptacle chambers raised, with floors 11-17 cells below the surrounding thallus surface; 7) tetrasporangial conceptacle chambers 74-125 µm in height and 157-299 µm in diameter with roofs 5-7 cells thick; 8) central columella present in tetrasporangial conceptacles, disintegrating to form a low mound with maturity; 9) pore opening in mature tetrasporangial conceptacles

occluded by a corona of filaments that project above the pore opening; and 10) *psb*A and *rbc*L sequences collectively unique.

Chamberlainium capense is also a range-restricted endemic (± 43 km) along the southern west coast of South Africa occurring in the mid- to low intertidal zones. Additionally, the projecting corona in tetrasporangial conceptacles is a useful character for distinguishing this species anatomically from all other South African species of *Chamberlainium* species (except *C. natalense* that has thin thalli (up to 800 µm) and lacks protuberances, being featureless and smooth. The corona in *C. capense* appears to develop from the filaments near the upper half of the tetrasporangial conceptacle roof, directly adjacent to the pore canal.

4.2.3. *Chamberlainium cochleare*

Chamberlainium cochleare is characterised by the following combination of features: 1) thalli up to 370 µm thick, uniformly encrusting (smooth), lacking protuberances and not becoming secondarily thick and discoid with orbicular protrusions, nor warty, nor wrinkled; 2) individual crusts coalescing (fusing) and not easily discernible; 3) colour of living thalli greyish in well-lit conditions to bluish mauve in dim light; 4) thallus construction monomerous and plumose; 5) epithallus single layered; 6) spermatangial and tetrasporangial conceptacles produced successively in the cortex directly above and in the same area as the modified cortex of an earlier generation; 7) tetrasporangial conceptacle chambers raised to flush to slightly sunken, with floors 12-22 cells below the surrounding thallus surface; 8) tetrasporangial conceptacle chambers 59-110 µm in height and 179-294 µm in diameter with roofs 6-8 cells thick; 9) central columella present in tetrasporangial conceptacles, disintegrating to form a low mound with maturity; 10) pore opening in mature tetrasporangial conceptacles occluded by a mucilage plug; and 11) *psb*A and *rbc*L sequences unique.

Chamberlainium cochleare is widely distributed along the southern and eastern coasts of south Africa occurring in the mid- and low intertidal zones. The species has a strong ecological association in the low intertidal zone with the territorial, gardening limpet *Scutellastra cochlear*. The apparent successive production of spermatangial and tetrasporangial conceptacles in the cortex directly above and in the same area as the modified cortex of an earlier generation, as seen in *C. cochleare*, has not been reported for any other species in the Corallinales, although it has been reported for female plants of *Heydrichia cerasina* Maneveldt & E.van der Merwe (Sporolithales) from South Africa (Maneveldt & van der Merwe 2012) and for tetra/bisporangial plants of *Phymatolithon repandum* (Foslie) Wilks & Woelkerling (Hapalidiales) from Australia (Wilks & Woelkerling 1994). This may well be a useful character for distinguishing *C. cochleare* anatomically from all other South African species of *Chamberlainium*, as the scars left by the earlier generation are very noticeable in the thallus cross sections.

Chamberlainium cochleare appears to be the species that Chamberlain (1993) largely considered synonymous with the type of *S. yendoi* (type locality: Shimoda, Shizuoka Prefecture, Japan). The variable morphologies exhibited by South African *S. yendoi* were attributed largely to wave action and to the presence/absence of grazing pressure (Chamberlain 1993; Maneveldt & Keats 2008). It is only now, through DNA sequencing that we have demonstrated that morphology (along with geographical and intertidal distribution) is useful for separating species previously ascribed to *S. yendoi* and that the comparatively thin plants, in association with the limpet *S. cochlear*, are *C. cochleare*.

4.2.4. *Chamberlainium glebosum*

Chamberlainium glebosum is characterised by the following combination of features: 1) thalli up to 2000 µm thick, lumpy becoming highly protuberant (up to 6 mm in height), not becoming secondarily thick and discoid with orbicular protrusions, nor wrinkled; 2) individual crusts not coalescing (not fusing together) and easily discernible; 3) colour of living thalli brownish pink to grey in well-lit conditions and blue-grey in dim light; 4) thallus construction monomerous and plumose; 5) epithallus single layered; 6) tetrasporangial conceptacle chambers raised with floors 11-24 cells below the surrounding thallus surface; 7) tetrasporangial conceptacle chambers 44-110 µm in height and 135-265 µm in diameter with roofs 4-8 (9) cells thick; 8) central columella present in tetrasporangial conceptacles, disintegrating to form a low mound with maturity; 9) pore opening in mature tetrasporangial conceptacles unoccluded; and 10) *psb*A and *rbc*L sequences collectively unique.

Chamberlainium glebosum has a wide, but disjunct distribution along the west coast of South Africa, occurring mostly in the high and mid-intertidal zones. Of all the species reported here, *C. glebosum* is the most protuberant. Chamberlain (1993) and Maneveldt & Keats (2008) documented protuberance heights of up to 3 mm for South African *S. yendoi*. These authors attributed the morphological variation in *S. yendoi* to wave action and the presence/absence of grazing pressure. However, based on DNA sequence data we have showed that highly protuberant specimens, in the absence of the limpet *S. cochlear* and/or under low grazing pressure, are a unique species.

4.2.5. *Chamberlainium impar*

Chamberlainium impar is characterised by the following combination of features: 1) thalli up to 1800 µm thick, encrusting (smooth) and orbicular becoming confluent; 2) individual crusts

not coalescing (not fusing together) and easily discernible, adjacent crusts producing characteristic marginal upgrowths/crests (up to 10 mm in height, see Chamberlain 1994) where they meet; 3) colour of living thalli yellowish to yellow-brown in well-lit conditions to purple-brown in dim light; 4) thallus construction monomerous and plumose; 5) epithallus 4-6 (9) cells thick; 6) tetrasporangial conceptacle chambers slightly raised becoming flush with maturity, with floors 15-21 cells below the surrounding thallus surface; 7) tetrasporangial conceptacle chambers 98-103 µm in height and 270-352 µm in diameter with roofs 6-7 cells thick; 8) central columella present in tetrasporangial conceptacles, persisting to maturity; 9) pore opening in mature tetrasporangial conceptacles occluded by a mucilage plug; and 10) *psb*A and *rbc*L sequences unique.

Chamberlainium impar also has a somewhat restricted distribution (± 170 km) along the southern west coast of South Africa, occurring in the mid- to low intertidal zones. The species' gross morphology (yellowish to yellow-brown in colour with a surface roughly ridged to strongly pachydermatous like an elephant's skin) is very distinct. Additionally, the mucilage spout above male conceptacle pore is a useful anatomical character for distinguishing this species anatomically from all other South African species of *Chamberlainium*. The spout appears to originate from mucilage secreted by the filaments lining the pore canal near the pore opening.

4.2.6. *Chamberlainium natalense*

Chamberlainium natalense is characterised by the following combination of features: 1) thalli up to 800 µm thick, encrusting (smooth); 2) individual crusts not coalescing (not fusing together) and easily discernible; 3) colour of living thalli blue-grey in well-lit conditions to brown in dim light; 4) thallus construction monomerous and plumose; 5) epithallus single

layered; 6) tetrasporangial conceptacle chambers raised to flush, with floors 12-21 cells below the surrounding thallus surface; 7) tetrasporangial conceptacle chambers 44-96 µm in height and 147-196 µm in diameter with roofs 6-8 cells thick; 8) central columella present in tetrasporangial conceptacles, disintegrating to form a low mound with maturity; 9) pore opening in mature tetrasporangial conceptacles occluded by a corona of filaments that project above the pore opening; and 10) *psb*A and *rbc*L sequences unique.

Chamberlain (1993) attributed the variable morphologies of *S. yendoi* to external environmental conditions (e.g. wave action and grazing). Based on this observation, and on similarities in measured vegetative and reproductive characters, she synonymised *Lithophyllum natalense* with *S. yendoi*. However, DNA sequencing has demonstrated that the type of *L. natalense,* and specimens aligning with this type, are a distinct species.

Chamberlainium natalense is widely distributed along the southern west to eastern coasts of South Africa and is epilithic mostly on boulders and pebbles, and only occasionally on the primary bedrock in the mid- and low intertidal zones. Additionally, the corona in tetrasporangial conceptacles is a useful anatomical character for distinguishing this species from all other South African species of *Chamberlainium*, except for *C. capense* that is thick (up to 1000 µm) and somewhat protuberant (up to 4 mm in height). Similar to *C. capense*, the corona appears to develop from the filaments near the upper half of the conceptacle roof, directly adjacent to the pore canal.

4.2.7. *Chamberlainium occidentale*

Chamberlainium occidentale is characterised by the following combination of features: 1) thalli up to 1000 µm thick, encrusting (smooth) to warty (mostly) to lumpy, becoming only

slightly protuberant (up to 4 mm in height); 2) individual crusts not coalescing (not fusing together) and easily discernible; 3) colour of living thalli brownish beige in well-lit conditions and blue-grey to rosy pink in dim light; 4) thallus construction monomerous and plumose; 5) epithallus single layered; 6) tetrasporangial conceptacle chambers raised, with floors 16-19 cells below the surrounding thallus surface; 7) tetrasporangial conceptacle chambers 110-147 µm in height and 206-365 µm in diameter with roofs 5-7 cells thick; 8) central columella present in tetrasporangial conceptacles, persisting to maturity; 9) pore opening in mature tetrasporangial conceptacles not occluded and slightly sunken below the surrounding pore opening; and 10) *psb*A and *rbc*L sequences collectively unique.

Chamberlainium occidentale is widely distributed along the west and southern west coasts of South Africa, occurring throughout the intertidal zone. The species is similarly protuberant (up to 4 mm in height) to *C. capense*. However, the sunken pore in tetrasporangial conceptacles is a useful character for distinguishing this species anatomically from all other South African species of *Chamberlainium*, except from *C. tenue*, which is very thin (no more than 250 µm thick) and featureless (smooth). *Chamberlainium occidentale* is the only non-endemic South African species of *Chamberlainium*, also occurring in Namibia.

4.2.8. *Chamberlainium tenue*

Chamberlainium tenue is characterised by the following combination of features: 1) thalli very thin, up to only 250 µm thick, encrusting (smooth); 2) individual crusts not coalescing (not fusing together) and easily discernible; 3) colour of living thalli yellowish (on shale platforms) to bright pink in well-lit conditions to blue-grey or brownish in dim light; 4) thallus construction monomerous and plumose; 5) epithallus single layered; 6) tetrasporangial conceptacle chambers raised to slightly sunken, with floors 12-16 cells below the surrounding

thallus surface; 7) tetrasporangial conceptacle chambers 76-118 µm in height and 196-208 µm in diameter with roofs 5-7 cells thick; 8) central columella present in tetrasporangial conceptacles, disintegrating to form a low mound with maturity; 9) pore opening occluded by a mucilage plug and sunken below the surrounding roof; and 10) *psb*A and *rbc*L sequences unique.

Chamberlainium tenue is widely distributed along the south and east coasts of South Africa, occurring in high and mid-intertidal rock pools. The species has a characteristically thin (no more than 250 µm thick) thallus. Additionally, the sunken pore in tetrasporangial conceptacles is a useful character for distinguishing this species anatomically from all other South African species of *Chamberlainium*, except from *C. occidentale* that is thicker (up to 1000 µm) and somewhat protuberant (up to 4 mm in height).

4.2.9. *Pneophyllum neodiscoideum*

Pneophyllum neodiscoideum is characterised by the following combination of features: 1) thalli encrusting (smooth), initially (primary crusts) very thin (up to 310 µm thick), becoming secondarily thick (up to 3000 µm) and discoid with orbicular protrusions that often produce crowded, contiguous, swollen protuberances (up to 10 mm in height); 2) individual primary crusts coalescing (fusing) and not easily discernible, secondary crusts not coalescing (not fusing) and easily discernible; 3) colour of living thalli pink to light purple to yellowish brown in well-lit conditions to reddish brown in dim light; 4) thallus construction primarily dimerous, becoming secondarily monomerous (and plumose) in orbicular protrusions due to overgrowth; 5) epithallus 2-4; 6) tetrasporangial conceptacle chambers flush to sunken to raised, with floors 12-16 cells below the surrounding thallus surface; 7) tetrasporangial conceptacle chambers 44-74 µm in height and 172-225 µm in diameter with roofs 6-22 cells thick; 8) central columella

present in tetrasporangial conceptacles, disintegrating to form a low mound with maturity; 9) pore opening occluded by a prominent mucilage plug that may fill the entire pore canal; and 10) *psb*A and *rbc*L sequences unique.

Pneophyllum neodiscoideum has a somewhat restricted distribution along the southern west coast of South Africa, occurring in mid- to low intertidal rock pools. The species' gross morphology, thin (no more than 310 µm thick), encrusting (smooth) primary thallus that becomes secondarily very thick (up to 3000 µm) and discoid with orbicular protrusions, which often produce crowded, contiguous, swollen protuberances (up to 10 mm in height), is very distinct. In addition to *P. neodiscoideum* there are four other species in South Africa ascribed to *Pneophyllum*. These include: *Pneophyllum amplexifrons* (Harvey) Y.M.Chamberlain & R.E.Norris (Chamberlain & Norris 1994), *Pneophyllum coronatum* (Rosanoff) Penrose (Chamberlain 1994b), *Pneophyllum keatsii* Y.M.Chamberlain (Chamberlain 1994b) and *P. fragile*, all ascribed solely on morpho-anatomical data. Of the four species, *P. amplexifrons* (Durban, KwaZulu-Natal Province) and *P. keatsii* (Oudekraal, Western Cape Province) have type localities in South Africa, while *P. coronatum* and *P. fragile* have type localities in Port Phillip Bay, Victoria, Australia and the Mediterranean Sea (exact location unknown) respectively. Based on accumulating DNA sequence data, specimens assigned to the latter two species in South Africa are likely not those species. Furthermore, these latter four species are all epiphytic in South Africa, occurring on either seagrasses (*P. amplexifrons* and *P. fragile*, Chamberlain & Norris 1994, Maneveldt *et al*. 2008, 2016), on the stipes and holdfasts of the kelp *Ecklonia maxima* (Osbeck) Papenfuss (*P. coronatum*, *P. fragile* and *P. keatsii*, Chamberlain 1994b; Maneveldt *et al*. 2008, 2016) and on other red seaweeds, (*P. fragile*, Maneveldt *et al*. 2008, 2016). *Pneophyllum neodiscoideum* has not been found to be epiphytic and occurs mostly epilithically, but also epizoically. The four species are also reported to

remain encrusting (smooth) while *P. neodiscoideum* becomes characteristically secondarily thick and discoid with orbicular protrusions.

4.3. Congruency between morpho-anatomical and DNA sequencing data

According to Caragnano *et al.* (2018) *Chamberlainium*, *Pneophyllum* and *Spongites* may be morpho-anatomically separated by a combination of characters (Table 12) that include (but are not limited to): 1) the thallus construction (primarily dimerous or monomerous in *Chamberlainium* and *Spongites vs.* only dimerous in *Pneophyllum*); 2) the presence/absence of a coaxial medulla/hypothallus (may be present in *Spongites vs.* absent in *Chamberlainium* and *Pneophyllum*); 3) the number of epithallial cell layers (may be more than one in *Chamberlainium* and *Spongites vs.* only one in *Pneophyllum*); 4) the trichocyte arrangement (may be in horizontal rows or fields in *Spongites vs.* never in horizontal rows or fields in *Chamberlainium* and *Pneophyllum*); 5) the diameters of tetrasporangial conceptacle chambers (< 300 μm in *Chamberlainium vs.* < 350 μm in *Pneophyllum vs.* > 300 μm in *Spongites*); 6) number of tetrasporangial conceptacle roof cells (< 8 in *Chamberlainium* and *Pneophyllum vs.* > 8 in *Spongites*); and 7) distribution of tetrasporangia in tetrasporangial conceptacles (peripheral or across the chamber floor in *Chamberlainium vs.* peripheral only in *Pneophyllum* and *Spongites*).

4.3.1. Tetrasporangial conceptacle roof development

Caragnano *et al.* (2018) concluded that, except for the development of the tetrasporangial conceptacle roof (Type 1 in *Chamberlainium*, Type 2 in *Pneophyllum*, Johansen 1981) (in which primordia are not always evident), *Chamberlainium* and *Pneophyllum* currently have no diagnostic morpho-anatomical characters that enable one to assign a specimen to them without DNA sequence data. The placements, initially through DNA sequencing, of the specimens

examined in the current study are in complete agreement in this regard. The specimens identified molecularly as belonging to *Chamberlainium* all possessed the Type 1 (development from filaments peripheral to the sporangial initials) tetrasporangial conceptacle roof development. Similarly, the specimens identified molecularly as belonging to *Pneophyllum* all possessed the Type 2 (development from filaments both peripheral to, as well as from filaments interspersed amongst the sporangial initials) tetrasporangial conceptacle roof development. Until now, specimens assigned to *P. neodiscoideum* would have been ascribed to *Spongites* (as *S. discoideus*, Chamberlain 1994b), largely because of gross morphology, but also because of the previously reported Type 1 tetrasporangial conceptacle roof development (Penrose 1991; Penrose & Woelkerling 1992; Chamberlain 1993, 1994b; Keats *et al*. 1993). Chamberlain (1994b) described the tetrasporangial conceptacle roof development as occurring from filaments surrounding (peripheral to) the sporangia (i.e. Type 1). Through DNA sequencing and with reciprocal morpho-anatomical support, we have shown that *P. neodiscoideum* belongs in *Pneophyllum* and has the Type 2 tetrasporangial conceptacle roof development in which the roof is formed from filaments both peripheral to, as well as from filaments interspersed amongst the sporangial initials. We suspect that Chamberlain (1994b) and others may not have observed a sufficient number of early stage specimens to accurately identify the Type 2 tetrasporangial conceptacle roof development in *P. neodiscoideum*, making instead the assumption of a Type 1 tetrasporangial conceptacle roof development, which beyond a certain stage of development results in similar looking tetrasporangial conceptacles (see Harvey *et al*. 2006a).

In the absence of well-defined tetrasporangial conceptacle primordia that showed unequivocally the type of tetrasporangial conceptacle roof development, previous authors used (amongst other characters) the substratum type to assign specimens to a genus. Within the then

Mastophoroideae, epilithic and epizoic crusts were assigned to *Spongites* and *Neogoniolithon*, while epiphytic crusts were assigned to *Pneophyllum* (e.g. Chamberlain 1978, 1983; Woelkerling 1996; Kjøsterud 1997; Farr *et al*. 2009). However, while there have been several reports of *Pneophyllum* species occurring epiphytically (e.g. Chamberlain 1994a, b; Chamberlain & Norris 1994; Penrose & Woelkerling 1991; Penrose 1996; Harvey *et al*. 2005), there have also been several other reports of *Pneophyllum* species occurring epizoically (Chamberlain 1994a, b; Penrose 1996; Keats *et al.* 1997; Harvey *et al.* 2005), epilithically (Chamberlain 1994a; Penrose & Woelkerling 1991; Penrose 1996; Harvey *et al.* 2005), as well as displaying no settlement preference (Keats *et al*. 1997). All of these reports are based solely on morpho-anatomical data; here we present unequivocal data, using both DNA sequencing and morpho-anatomical data, of a *Pneophyllum* species that can occur epilithically and epizoically. Substratum type should thus be used with caution in assigning names to a species in the absence of congruent molecular data.

Additionally, *P. neodiscoideum* is inconsistent in a number of other morpho-anatomical characters reported for the genus (Table 12). Caragnano *et al*. (2018) considered *Chamberlainium* and *Pneophyllum* to be similar in their tetrasporangial conceptacle features, including the number of roof cells (< 8). However, the number of tetrasporangial conceptacle roof cells in *P. neodiscoideum* is significantly more than eight (up to 22), contrary to what had been considered by Caragnano *et al*. (2018) to be a character useful for separating *Chamberlainium* and *Pneophyllum* from *Spongites*. Furthermore, the thallus thickness (up to 3000 µm) and the number of epithallial cells (2-4) are also inconsistent with that reported for *Pneophyllum* by Caragnano *et al.* (2018). These examples reinforce the notion that without DNA sequence data, very few useful anatomical characters (expect perhaps for the gross

morphology and the mode of tetrasporangial conceptacle roof development, which might not always be available) exist to assign a specimen to either *Chamberlainium* or *Pneophyllum*.

4.3.2. Trichocyte arrangement

In keeping with previous studies, we report here on trichocyte arrangement and on our hypotheses about trichocyte development. For Chamberlainoideae, Caragnano *et al*. (2018) report trichocytes to be solitary or paired when present, always terminal and never intercalary in the cortex/perithallus. Our findings are mostly consistent with those of Caragnano *et al*. (2018), except that we did observe trichocytes to occasionally occur (in *C. cochleare*, *C. natalense* and *C. occidentale*) in small horizontal clusters (fields) of up to six trichocytes, although they were all separated by one or more vegetative filaments (i.e. not in tightly packed horizontal fields). Caragnano *et al*. (2018) also suggested that trichocyte development in *Chamberlainium* (the authors were not able to comment on the type of development in *Pneophyllum*) seems to be of the *Jania rubens* type (see Cabioch 1971; Johansen 1981), in which complete obliteration of trichocytes and their initials occurs in the final step, leading to their absence deeper in the cortex/perithallus. However, our specimens suggest that trichocyte development in *Chamberlainium* is rather of the *Fosliella* type, in which there is first a loss of the overlying epithallial cell, then trichome (hair) elongation, and finally degeneration of the trichome and protoplast, leaving an empty trichocyte wall that persists unaltered even after the trichomes have been shed (Figure 138, Johansen 1981: 34, fig. 18). For all intents and purposes the development types look similar with the main difference being the trichome projecting through the epithallial cell in the *Jania rubens* type, whereas the epithallial cell is shed prior to the elongation of the trichome in the *Fosliella* type. In all of our observations the epithallial cell was not evident, suggesting it had been shed prior to the trichome formation. Caragnano *et al*. (2018) used *Chamberlainium decipiens* as the example (see van der Merwe *et al*. 2015:

474, fig. 8) to substantiate their *J. rubens* type of trichocyte development. However, in that species the epithallial cell is also absent, suggesting that instead it is of the *Fosliella* type. This suggests that trichocyte development (notably because of interpretational issues) is not a useful character to delimit taxa although trichocyte arrangement might still be useful (see e.g. Kato *et al*. 2011; Bittner *et al*. 2011). All of these contradictory examples suggest that the descriptions of *Chamberlainium* and *Pneophyllum* will need emending. However, this can only be successfully achieved once more species are assigned (firstly through DNA sequencing) to these genera to provide a more comprehensive morpho-anatomical view of the taxa.

Figure 138: Adopted from Johansen (1981). Diagram showing two types of trichocyte development. *Fosliella* type (A-D): Note the cell division, loss of overlying epithallial cell, hair elongation and degeneration of hair and protoplast leaving an empty trichocyte wall. *Jania rubens* type (E-H): Note the hair grows through the overlying epithallial cell, and cell degeneration and renewed meristematic activity obliterates evidence of the trichocyte.

4.4. Keys to species previously ascribed to *Spongites* in South Africa

These keys are designed for southern African species identification only. The characters/concepts used in the keys are not necessarily diagnostic of the species to which they pertain. The following two keys include all species currently recognised under *Chamberlainium*.

4.4.1. Field key

1. Plants restricted to the cold temperate west and southern west coasts ……..... 2

   Plants distributed largely from the warm temperate south coast to the subtropical east coast …..……..…….. 6

2. Plants restricted to the southern west coast ……..……..……..... 3

   Plants more common along the west coast ……,……..... 5

3. Thalli producing initially thin (no more than 310 µm thick) crusts that become secondarily thick (up to 3000 µm) and discoid with orbicular protrusions that often produce crowded, contiguous, swollen protuberances (up to 10 mm in height) (Fig. 118) ...…….. *Pneophyllum neodiscoideum*

   Thalli producing only primary crusts, that may be featureless (smooth), orbicular becoming confluent or becoming variably lumpy, protuberant and or warty …..……..... 4

4. Thalli producing thick (up to 1800 µm) crusts that are orbicular, becoming confluent; characteristically yellowish to yellow-brown (in well-lit conditions); surface roughly ridged to strongly pachydermatous like an elephant's skin (Fig. 51) ……
   …….. *Chamberlainium impar*

Thalli producing thick (up to 1000 µm) crusts that are variably lumpy and slightly protuberant (up to 4 mm in height); dusky pink to mauve (in well-lit conditions) (Fig. 10) ……... *Chamberlainium capense*

5. Plants with disjunct distribution; occurring in high to mid-intertidal zone; thalli producing thick crusts (up to 2000 µm) that are lumpy becoming highly protuberant (up to 6 mm in height); brownish pink to greyish (in well-lit conditions) (Fig. 38) …… ……..…….. *Chamberlainium glebosum*

   Plants widely distributed; occurring mostly in mid-to low intertidal zone; thalli producing variably thick (up to 1000 µm) crusts that are warty (mostly) to lumpy, becoming only slightly protuberant (up to 4 mm); brownish beige (in well-lit conditions) (Fig. 89) ..……..…….. *Chamberlainium occidentale*

6. Plants restricted to the Cape Agulhas region; occurring in high (mostly) to mid-intertidal zone; thalli producing thin (up to 650 µm) crusts that are characteristically brownish-pink (Fig. 9) ...……..…… *Chamberlainium agulhense*

   Plants widely distributed; occurring throughout the intertidal zone; thalli producing variably thin crusts that are greyish to blue-grey to yellowing to bright pink (in well-lit conditions ...…….……...…. 7

7. Individual thalli not discernible, coalescing (fusing) to form large expanses; thalli greyish (in well-lit conditions); commonly associated with the territorial, gardening limpet *Scutellastra cochlear* (Fig. 25) ……..... *Chamberlainium cochleare*

   Individual thalli discernible, not coalescing (fusing), remaining as separate individual crusts; blue-grey to yellowing to bright pink (in well-lit conditions); is not commonly associated with the territorial, gardening limpet *Scutellastra cochlear* ….…….. 8

8. Plants occurring mostly on boulders or pebbles in mid- to low intertidal rock pools; blue-grey (in well-lit conditions) (Fig. 72) ……...……... *Chamberlainium natalense*

Plants occurring mostly on exposed rocky platforms in high to mid-intertidal zone; yellowish (high intertidal) to bright pink (mid-intertidal) (Fig. 106) ……... *Chamberlainium tenue*

4.4.2. Laboratory key

1. Tetrasporangial conceptacle roof development from filaments both peripheral to, as well as interspersed amongst the sporangial initials (Figs 132-142); tetrasporangial conceptacle roof mostly > 8 cells thick (Figs 135-136) ….. *Pneophyllum neodiscoideum*
   Tetrasporangial conceptacle roof development only from filaments peripheral to the sporangial initials (see e.g. Figs 34-35); tetrasporangial conceptacle roof ≤ 8 cells thick (see e.g. Figs 36-37) ..…….....……. 2
2. Thallus construction dimerous ……..……... *Chamberlainium agulhense*
   Thallus construction monomerous (see e.g. Fig. 26) ……..……..…… 3
3. Thalli producing thick (up to 1800 µm) crusts that are orbicular, becoming confluent, roughly ridged to strongly pachydermatous like an elephant's skin (Fig. 51); epithallus multi-layered, commonly up to 6 cells thick (Figs 56-57) ...…..... *Chamberlainium impar*
   Thalli producing variably thin to thick crusts that are encrusting to variably warty to lumpy to protuberant; epithallus single layered (see e.g. Fig. 28) ……..…...…...….. 4
4. Thalli entirely encrusting (smooth) and featureless (see e.g. Fig. 25) ……..…….. 5
   Thalli mostly warty to lumpy to protuberant (see e.g. Fig. 10) ...……...…..…….. 7
5. Tetrasporangial conceptacle pore opening occluded by a prominent corona of filaments that projects well above the pore opening (Figs 86-88) ….... *Chamberlainium natalense*
   Tetrasporangial conceptacle pore opening occluded by a mucilage plug (see e.g. Figs 36-37) ..……..……..…….. 6

6. Tetrasporangial conceptacles produced successively in the cortex directly above, and in the same area as the modified cortex of an earlier generation (Fig. 32); tetrasporangial conceptacle pore canal not arching (Fig. 37) ….....……..... *Chamberlainium cochleare*

   Tetrasporangial conceptacles not produced successively in the cortex directly above, and in the same area as the modified cortex of an earlier generation; tetrasporangial conceptacle pore canal arching (Fig. 117) ……..……..…… *Chamberlainium tenue*

7. Tetrasporangial conceptacle pore opening occluded by a corona of filaments that projects above the pore opening (Fig. 20) ……..… *Chamberlainium capense*

   Tetrasporangial conceptacle pore opening not occluded (see e.g. Fig. 104) …..... 8

8. Tetrasporangial conceptacle pore canal arching (Fig. 105) ……...
   ……. *Chamberlainium occidentale*

   Tetrasporangial conceptacle pore canal tapering towards the surface (Fig. 50) ……
   ……..… *Chamberlainium glebosum*

4.5. Key to the genus *Pneophyllum* in South Africa

This key, modified from Maneveldt *et al*. (2008, 2016), is designed for South African species only. The characters/concepts used in the key are not necessarily diagnostic of the species to which they pertain.

1. Thalli epilithic and/or epizoic, initially encrusting (smooth) and thin (no more than 310 µm thick), becoming secondarily thick (up to 3000 µm) and discoid with orbicular protrusions that often produce crowded, contiguous, swollen protuberances (up to 10 mm in height) (Fig. 118) ...…….. *Pneophyllum neodiscoideum*

   Thalli entirely epiphytic, remaining encrusting (smooth) and not becoming secondarily discoid with orbicular protrusions ……..…… 2

2. Plants forming successive, trumpet-shaped adjoining thalli encircling seagrass and green algal stalks ……... *Pneophyllum amplexifrons*

   Plants encrusting (smooth) on *Ecklonia maxima* stipes and/or holdfasts and various red algae ……..……..……... 3

3. Plants epiphytic only on *Ecklonia maxima*; thalli with very prominent raised conceptacles ..……..……... *Pneophyllum coronatum*

   Plants epiphytic on *Ecklonia maxima* and red algal host; thalli with flush conceptacles ...……...…….…….. 4

4. Plants epiphytic on *Ecklonia maxima* and red algal hosts; thalli with a single layer of epithallial cells ...…….…….…. *Pneophyllum fragile*

   Plants epiphytic only on *Ecklonia maxima*; thalli with up to 4 layers of epithallial cells ……... *Pneophyllum keatsii*

4.6. Cryptic diversity and biogeographic considerations

Until recently, coralline algal taxonomy and identification relied exclusively on the use of morpho-anatomical characteristics (Adey 1970; Cabioch 1972; Johansen 1981; Penrose and Woelkerling 1988; Woelkerling 1988; Harvey & Woelkerling 2007; Farr *et al*. 2009). However, these features became increasingly difficult to use as non-geniculate coralline algae displays simple but highly convergent morphologies (Johansen 1981; Steneck 1986; Bittner *et al*. 2011; Kato *et al*. 2011; Hind *et al.* 2016; Janot & Martone 2016, 2018) and a high degree of phenotypic plasticity, which is further influenced by environmental conditions (Steneck & Adey 1976; Wilks & Wolkerling 1991; Woelkerling & Harvey 1993; Womersely 1996; Harvey & Woelkerling 2007; Maneveldt & Keats 2008). Convergent morphologies and phenotypic plasticity within coralline algae has sometimes led to incorrect ecological conclusions (see e.g.

Maneveldt & Keats 2014 and corresponding comments from Gabrielson *et al*. 2018) and misrepresentations of the true species diversity of the corallines (Robba *et al.* 2006; Walker *et al*. 2009; Nelson *et al.* 2015; Melbourne *et al*. 2017; Gabrielson *et al*. 2018). Studies are increasingly showing that distinct species may have variable morphologies (e.g. Gabrielson *et al*. 2011; Hind *et al*. 2014b). Still other genetically distinct species may display almost identical morphologies (e.g. Basso *et al*. 2014; Hind *et al*. 2015; van der Merwe *et al*. 2015; Gabrielson *et al*. 2018).

The high degree of morpho-anatomical similarity seen in the non-geniculate coralline algae is likely due to either convergent evolution and/or to speciation that has yet to reflect as morpho-anatomical change (van der Merwe *et al*. 2015; Richards *et al*. 2017; Maneveldt *et al*. 2017; Gabrielson *et al*. 2018). Species originally reported to belong to the genus *Spongites* from South Africa, not only belong in two different genera, but are significantly more speciose than previously reported based solely on morpho-anatomy. Needless to say, despite their high degree of cryptic diversity, South African Chamberlainoideae may be variably separated in the field by their: 1) geographic distribution; 2) intertidal zonation; 3) substrate type; and 4) external appearance (Table 5, Key 4.4.1). Anatomically the following characters are useful for separating the South African Chamberlainoideae: 1) thallus construction; 2) number of epithallial cell layers; 3) type of tetrasporangial conceptacle roof development; 4) tetrasporangial conceptacle pore characteristics; and 5) location of conceptacle production in the cortex (Table 5, Key 4.4.2). It is important to note that in the absence of some very diagnostic morphological features, which exist for only a few species, and more importantly DNA sequence data, it will be impossible to unequivocally assign a name to any of the South African Chamberlainoideae.

Maneveldt *et al.* (2008, 2016) concluded that the true diversity of the South African non-geniculate coralline flora could not be decisively stated, suggesting that one of the reasons was that many species were very cryptic. The current research has affirmed this comment, and it is now evident that we have highly underestimated the true diversity of the South African non-geniculate coralline flora. Several other studies have similarly demonstrated a high degree of cryptic diversity among the coralline algae (Harvey *et al*. 2003; Le Gall & Saunders 2007; Nelson *et al*. 2015; Adey *et al*. 2015; Rösler *et al.* 2016; Caragnano *et al*. 2018; Gabrielson *et al*. 2018). While research on the coralline algae have lagged behind somewhat, high degrees of cryptic diversity have already been demonstrated for fleshy red (Hughey *et al*. 2001, 2002; Neefus *et al*. 2002; Gabrielson 2008a, b; Payo *et al*. 2013; Lindstrom *et al*. 2015; Freshwater *et al*. 2017; Yang & Kim 2018), brown (Stache-Crain *et al.* 1997; Montecinos *et al*. 2016; Viera *et al*. 2016, 2017; Neiva *et al.* 2017) and green (Kooistra *et al.* 1999, 2002, Fama *et al*. 2002; van der Strate *et al.* 2002; Verbruggen *et al*. 2009; Hofmann *et al*. 2010; Boedeker *et al*. 2018) macroalgae, with genetic differentiation amongst some of these algae occurring in less than 10 km (Faugeron *et al*. 2001; Engel *et al*. 2004; Andreakis *et al*. 2009; Montecinos *et al*. 2012).

Genetic differentiation over short distances may result in what is known as range-restricted endemics. There are now multiple examples of coralline algae with restricted geographical ranges (see e.g. Wilson *et al*. 2004; Maneveldt & van der Merwe 2012; Pardo *et al.* 2014; Peña *et al*. 2014, 2015; van der Merwe *et al*. 2015; Hind *et al*. 2016; this study). The underlying mechanisms of diversification that result in these coralline range-restricted endemics remain unknown (Hind *et al.* 2016). For most other marine species, such range-restrictions are affiliated with phylogenetic breaks associated with biogeographic boundaries or transition zones (Anderson *et al*. 2009; Montecinos *et al*. 2012). Until now, *Heydrichia cerasina* (Maneveldt & van der Merwe 2012) and *C. agulhense* (van der Merwe *et al*. 2015) were the

only known South African range-restricted endemic corallines, restricted to a 10 km stretch within the Cape Agulhas transition zone (Anderson *et al*. 2009). Based on the results from this study, *C. capense* (43 km; southern west coast), *C. impar* (170 km; southern west coast) and *P. neodiscoideum* (220 km; southern west coast) are also recorded as being range-restricted, although not nearly as restricted as the former two species. The geographical distributions of *C. capense* and *P. neodiscoideum* also fall within the Cape Agulhas transition zone, suggesting a possible biogeographic affinity. These observations support the concept that diversifications may largely be associated with phylogenetic breaks associated with biogeographic boundaries. Maneveldt *et al.* (2016) hypothesised that with an increase in ITA studies, the number of range-restricted endemic coralline algal species would likely increase.

Several authors (e.g. Sissini *et al.* 2014; Hind *et al.* 2015; Lindstrom *et al*. 2015; van der Merwe *et al.* 2015; Maneveldt *et al*. 2016; Richards *et al.* 2017) have questioned whether the many reports of widely distributed non-geniculate coralline algae across different ocean basins and biogeographic provinces were correct. While this has been demonstrated using DNA sequencing for some tropical (e.g. Hernández-Kantún *et al*. 2016; Rösler *et al*. 2016; Maneveldt *et al*. 2017), and some arctic (e.g. Adey *et al.* 2015; Gabrielson *et al. in press*) species, until now no temperate species has been reported to be widely distributed across ocean basins (although they have been reported to be widely distributed within an ocean basin – see e.g. Richards *et al*. 2018). While most of the South African *Chamberlainoideae* are seemingly endemic and thus not distributed across an ocean basin, at least one is. Our data have shown that a specimen from Chile is conspecific with the South African specimens assigned to *P. neodiscoideum*, confirming (through DNA sequencing) that it is possible for a temperate species to be widely distributed across an ocean basin.

The phylogenetic results have provided some very interesting biogeographic trends, which are contradictory to previous findings (see van der Merwe *et al*. 2015). While most South African *Chamberlainium* species align with each other, *C. tenue* aligns closer to two species (*C. decipiens* and *C. tumidum*) from the Northeast Pacific, rather than to the other species of *Chamberlainium* from South Africa. These results suggest that sequence divergence values may not necessarily align with biogeographic patterns, but that for some species they may indeed align with morpho-anatomical similarities.

The intraspecific *psb*A sequence divergence values obtained for Chamberlainoideae in this study are consistent with what has previously been reported for South African specimens (see van der Merwe *et al*. 2015). However, the unusually high intraspecific *rbc*L sequence divergence values seen in *C. occidentale* and *P. neodiscoideum* (including *Chamberlainium* sp. [AMC13.9x17]) may reflect the wide geographic range of these two species (McIvor *et al.* 2001; Mamoozadeh & Freshwater 2012). As DNA sequencing of specimens is still a comparatively recent phenomenon, fully understanding biogeographic trends remains an ongoing challenge.

Based on the findings from this study it is doubtful that South Africa has any representative species from *Spongites* as it is currently circumscribed. We suspect that this may be true for several other regions within the southern temperate latitudes and notably so for New Zealand, although Caragnano *et al*. (2018) did align several unidentified tropical specimens with the generitype of *Spongites*. It is possible that true *Spongites* species are largely restricted to the northern temperate and tropical/subtropical latitudes (Rösler *et al*. 2016; Caragnano *et al*. 2018). The results of this study support the comment by Maneveldt *et al*. (2016) that … "all South African names for non-geniculate corallines based on type localities of species from

other continents and ocean basins need to be reassessed based on DNA sequence data". This seems not only to be true for South Africa, but also for the rest of the world.

4.7. Future research

Based on the results from this study it is clear that the diversity of the South African non-geniculate coralline algae has been underestimated. Similar results will more than likely be encountered for other genera, should they be given the same level of scrutiny. To fully resolve the Chamberlainoideae in South Africa, a full account of the genus *Pneophyllum* should also be considered, along with other specimens and taxa seemingly closely related. This same Integrated Taxonomic Approach should be used with particular attention paid to those species/specimens that do not have type localities in South Africa. It will be interesting to know, by including all available sequences of *Pneophyllum*, if previously established species within this genera are really as widely distributed as has been previously reported. The results of this study and so many others (e.g. Maneveldt & van der Merwe 2012; Pardo *et al*. 2014; Peña *et al*. 2014, 2015; van der Merwe *et al*. 2015; Hind *et al*. 2016) suggest that likely this will not be the case.

Acknowledgments

I thank the Department of Biodiversity and Conservation Biology (BCB) at the University of the Western Cape (UWC) and the Herbarium and Biology Department at the University of North Carolina, Chapel Hill for providing funding and research equipment. The South African National Research Foundation (NRF), the South African National Botanical Institute (SANBI) through their Foundational Biodiversity Information Programme (FBIP) and the Department of Science and Technology (DST) through the African Coelacanth Ecosystem Programme (ACEP) Phuhlisa Programme are thanked for research funding, bursaries and travel awards to GWM and CAP-P. Thank you to the undergraduate students from the BCB Department who assisted with the laboratory preparation of histological slides, which was a tireless endeavour. A special thank you to my supervisors, Prof. Gavin W. Maneveldt and Dr. Paul W. Gabrielson for their continued guidance, support and patience.

5. References

ADEY W.H. 1970. The effects of light and temperature on growth rates in boreal-subarctic crustose corallines. *Journal of Phycology* 6: 269–276.

ADEY W.H. 1971. The sublittoral distribution of crustose corallines on the Norwegian coast. *Sarsia* 46: 41–58.

ADEY W.H. 1973. Temperature control of reproduction and productivity in a subarctic coralline alga. *Phycologia* 12: 111–118.

ADEY W.H. 1978. Algal ridges of the Caribbean Sea and West Indies. *Phycologia* 17: 361–367

ADEY W.H. 1998. Coral reefs: algal structured and mediated ecosystems in shallow, turbulent, and alkaline waters. *Journal of Phycology* 34:393–406.

ADEY W.H. & ADEY P.J. 1973. Studies on the biosystematics and ecology of the epilithic crustose Corallinaceae of the British Isles. *British Phycological Journal* 8: 343–407.

ADEY W.H., HERNÁNDEZ-KANTÚN J.J., JOHNSON G. & GABRIELSON P.W. 2015. DNA sequencing, anatomy and calcification patterns support a monophyletic, subarctic, carbonate reef-forming *Clathromorphum* (Hapalidiaceae, Corallinales, Rhodophyta). *Journal of Phycology* 51: 189–203.

ADEY W.H. & MACINTYRE I.G. 1973. Crustose coralline algae: A re-evaluation in the geological sciences. *Geological Society of America Bulletin* 84: 883–904.

ADEY W.H. MASAKI T. & AKIOKA H. 1976. The distribution of crustose corallines in Eastern Hokkaido and the biogeographic relationships of the Flora. *Bulletin of the Faculty of Fisheries* 26: 303–313.

ADEY W.H., TOWNSEND R.A. & BOYKINS W.T. 1982. The crustose coralline algae (Rhodophyta: Corallinaceae) of the Hawaiian Islands. *Smithsonian Contributions to Marine Science* 15: 1–74.

AGUIRRE J., BACETA J.I. & BRAGA J.C. 2007. Recovery of marine primary producers after the Cretaceous-Tertiary mass extinction: Paleocene calcareous red algae from the Iberian Peninsula. *Palaeogeography, Palaeoclimatology, Palaeoecology* 249: 393–411.

AGUIRRE J., RIDING R. & BRAGA J.C. 2000. Diversity of Coralline Red Algae: Origination and extinction patterns from the early Cretaceous to the Pleistocene. *Paleobiology* 26: 651–667.

AMADO-FILHO G.M., MANEVELDT G.W., PEREIRA-FILHO G.H., MANSO R.C.C., BAHIA R.G., BARROS-BARRETO M.B. & GUIMARÃES S.M.P.B. 2010. Seaweed diversity associated with a Brazilian tropical rhodolith bed. *Ciencias Marinas* 36: 371–391.

ANDERSON R.J., BOLTON J. J. & STEGENGA H. 2009. Using the biogeographic distribution and diversity of seaweed species to test the efficacy of marine protected areas in the warm temperate Agulhas Marine Province, South Africa. *Diversity and Distributions* 15: 1017–1027.

ANDREW N.L. 1993. Spatial heterogeneity, sea urchin grazing, and habitat structure on reefs in temperate Australia. *Ecology* 74: 292–302.

ANDREAKIS N. KOOISTRA W.H.C.F. & PROCACCINI G. 2009. High genetic diversity and connectivity in the polyploid invasive seaweed *Asparagopsis taxiformis* (Bonnemaisoniales) in the Mediterranean, explored with microsatellite alleles and multilocus genotypes. *Molecular Ecology* 18: 212–226.

ARDISSONE F. 1883. *Phycologia mediterranea, Part 1.* Varesse, Maj e Malnati. 516 pp.

ARESCHOUG J.E. 1852. Ordo XII. Corallinaceae. In: *Species, Genera, et Ordines Algarum.* (Ed. By J. Agardh), vol. 2/2. C. W. K. Gleerum, Lundae. 382 pp.

BAHIA R.G., AMADO-FILHO G.M., MANEVELD G.W., ADEY W.H., JOHNSON G., JESIONEK M.B. & LONGO L.L. 2015. *Sporolithon yoneshigueae* sp. nov. (Sporolithales, Corallinophycidae, Rhodophyta), a new rhodolith-forming coralline alga from the southwest Atlantic. *Phytotaxa* 224: 140–158.

BAILEY C.J. 1999. Phylogenetic positions of *Lithophyllum incrustans* and *Titanoderma pustulatum* (Corallinaceae, Rhodophyta) based on 18S rRNA gene sequence analyses, with a revised classification of the Lithophylloideae. *Phycoiogia* 38: 208–216

BAILEY J.C. & CHAPMAN R.L. 1996. Evolutionary relationships among coralline red algae (Corallinaceae, Rhodophyta) inferred from 18S rRNA gene sequence analysis. In: *Cytology, Genetics and Molecular Biology of Algae* (Ed. by B.R. Chaudhary & S.B. Agrawal), pp 363–376. SPB Academic Publishing, Amsterdam.

BAILEY J.C. & CHAPMAN L.R. 1998. A phylogenetic study of the Corallinales (Rhodophyta) based on nuclear small-subunit rRNA gene sequences. *Journal of Phycology* 34: 692–705.

BAILEY J.C., GABEL J.E. & FRESHWATER D.W. 2004. Nuclear 18S rRNA gene sequence analyses indicate that the Mastophoroideae (Corallinaceae, Rhodophyta) is a polyphyletic taxon. *Phycologia* 4: 3–12

BARNES K.A., ROTHERY P. & CLARKE A. 1996. Colonisation and development in encrusting communities from the Antarctic intertidal and sublittoral. *Journal of Experimental Marine Biologv and Ecologv* 196: 251–265.

BARRY G.C. & WOELKERLING W.M.J. 1995. Non-geniculate species of Corallinaceae (Corallinales, Rhodophyta) in Shark Bay, Western Australia: biodiversity, salinity tolerances and biogeographic affinities. *Botanica Marina* 38: 135–150.

BASSO D. 2012. Carbonate production by calcareous red algae and global change. *Geodiversitas* 34: 13–33.

BASSO D., CARAGNANO A., RODONDI G. 2014. Trichocytes in *Lithophyllum kotschyanum* and *Lithophyllum* spp. (Corallinales, Rhodophyta) from the NW Indian Ocean. *Journal of Phycology* 50: 711–717.

BOUCKAERT R. R. & HELED J. 2014. DensiTree 2: seeing trees through the forest. *BioRxiv*.

BEAVINGTON-PENNEY S.J., WRIGHT V.P. & WOELKERLING W.M.J. 2004. Recognizing macrophyte-vegetated environments in the rock record: a new criterion using 'hooked' forms of crustose coralline red algae. *Sedimental Geology* 166: 1–9.

BITTNER L., PAYRI C.E, MANEVELDT G.W., COULOUX A., CRUAUD C., DE REVIERS B. & LE GALL L. 2011. Evolutionary history of the Corallinales (Corallinophycidae, Rhodophyta) inferred from nuclear, plastidial and mitochondrial genomes. *Molecular Phylogenetics and Evolution* 61: 697–713.

BJÖRK M., MOHAMMED S.M., BJÖRKLUND M. & SEMESI A. 1995. Coralline algae. Important coral-reef builders threatened by pollution. *Ambio A Journal of the Human Environment* 24: 502–505.

BLOUIN N.A. & LANE C.E. 2012. Red algal parasites: Models for a life history evolution that leaves photosynthesis behind again and again. *BioEssays* 34: 226–235.

BOEDECKER C., LELIAERT F., TIMOSHKIN O.A., VISHNYAKOV V.S., DÍAZ-MARTÍNEZ S. & ZUCCARELLO G.C. 2018. The endemic Cladophorales (Ulvophyceae) of ancient Lake Baikal represent a monophyletic group of very closely related but morphologically diverse species. *Journal of Phycology* 54: 616–629.

BOSELLINI A. & GINSBURG R.N. 1971. Form and internal structures of recent algal nodules (rhodolites) from Bermuda. *Journal of Geology* 79: 669–682.

BOSENCE D.W.J. 1983. Coralline algal reef frameworks. *Journal of the Geological Society* 140: 365–367.

BOSENCE D.W.J. 1991. Coralline algae: mineralization, taxonomy, and palaeoecology. In: *Calcareous Algae and Stromatolites* (Ed. by R. Riding), pp. 98–113. Springer, Berlin.

BRANCH G.M. 1971. The ecology of *Patella* Linnaeus from the Cape Peninsula, South Africa. I. Zonation, movements and feeding. *Zoologica Africana* 6: 1–38.

BRANCH G. & BRANCH M. 1981. *The living shores of Southern Africa*. Struik Publishers, Cape Town. 272 pp.

BROADWATER S.T., HARVEY A.S. & WOELKERLING W.M.J. 2002. Conceptacle structure of the parasitic coralline red alga *Choreonema thuretii* (Corallinales) and its taxonomic implications. *Journal of Phycology* 38: 1157–1168.

BROOM J.E.S., HART D.R., FARR T.J., NELSON W.A., NEILL K.F., HARVEY A.S. & WOELKERLING W.M.J. 2008. Utility of *psb*A and nSSU for phylogenetic reconstruction in the Corallinales based on New Zealand taxa. *Molecular Phylogenetics and Evolution* 46: 958–973.

BROWNE C.M., MANEVELDT G.W., BOLTON J.J. & ANDERSON R.J. 2013. Abundance and species composition of non-geniculate coralline red algae epiphytic on the South African populations of the rocky shore seagrass *Thalassodendron leptocaule* M.C.Duarte, Bandeira & Romeiras. *South African Journal of Botany* 86: 101–110.

BURDETT H.L., KEDDIE V., MACARTHUR N., MCDOWALL L., MCLEISH J., SPIELVOGEL E., HATTON A.D. & KAMENOS N.A. 2014. Dynamic photoinhibition exhibited by red coralline algae in the red sea. *BMC Plant Biology* 14: 139–149.

CABIOCH J. 1971 Essai d'une nouvelle classification des Corallinacées actuelles. *Comptes Rendus de l'Académie des Sciences* 2721: 1916–1919.

CABIOCH J. 1972. Etude sur les Corallinacées II. La morphogenèse, conséquences systématiques et phylogénétiques. *Cahiers de Biologie Marine* 13: 137–287.

CABIOCH J. 1988. Morphogenesis and generic: concepts in coralline algae - a reappraisal. *Helgoland Marine Research* 42: 493–509.

CARAGNANO A., FOETISCH A., MANEVELDT G.W., MILLET L., LIU L.C., LIN S.M., RODONDI G. & PAYRI C.E. 2018. Revision of Corallinaceae (Corallinales, Rhodophyta): recognizing *Dawsoniolithon* gen. nov., *Parvicellularium* gen. nov. and Chamberlainoideae

subfam. nov. containing *Chamberlainium* gen. nov. and *Pneophyllum*. *Journal of Phycology* 54: 391–409.

CHAMBERLAIN Y.M.C. 1978. Investigation of taxonomic relationships amongst epiphytic crustose Corallinaceae. In: *Modern approaches to the taxonomy of red and brown algae* (Ed. by D.E.G. Irvine & J.H. Price), pp. 223–246. Academic Press, London.

CHAMBERLAIN Y.M.C. 1983. Studies in the Corallinaceae with special reference to *Fosliella* and *Pneophyllum* in the British Isles. *Bulletin of the British Museum (Natural History) Botany* 11: 291–463.

CHAMBERLAIN Y.M.C. 1990. The genus *Leptophytum* (Rhodophyta, Corallinales) in the British Isles with descriptions of *Leptophytum bornetii*, *L. elatum* sp. nov. and *L. laevae*. *British Phycological Journal* 25: 179–199.

CHAMBERLAIN Y.M.C. 1993. Observations on the crustose coralline red alga *Spongites yendoi* (Foslie) comb. nov. in South Africa and its relationship to *S. decipiens* (Foslie) comb. nov. and *Lithophyllum natalense* Foslie. *Phycologia* 32: 100–115.

CHAMBERLAIN Y.M.C. 1994a. Mastophoroideae. In: *Seaweeds of the British Isles*. (Ed. L.M. Irvine, & Y.M. Chamberlain), vol1. HMSO, London. 276 pp.

CHAMBERLAIN Y.M.C. 1994b. *Pneophyllum coronatum* (Rosanoft) D. Penrose comb. nov., *P. keatsii* sp. nov., *Spongites discoideus* (Foslie) D. Penrose et Woelkerling and *S. impar* (Foslie) Y. Chamberlain comb. nov. (Rhodophyta, Corallinaceae) from South Africa. *Phycologia* 33: 141–157.

CHAMBERLAIN Y.M.C & KEATS D.W. 1994. Three melobesioid crustose coralline red algae from South Africa: *Leptophytum acervatum* (Foslie) comb. nov., *L. foveatum* sp. nov. and *L. ferox* (Foslie) comb. nov. *Phycologia* 33: 111–133.

CHAMBERLAIN Y.M.C. & NORRIS R.E. 1994. *Pneophyllum amplexifrons* (Harvey) comb. nov., a Mastophoroid crustose coralline red algal epiphyte from Natal, South Africa. *Phycologia* 33: 8–18.

CARPENTER R.C. 1981. Grazing by *Diudema antillurum* Philippi and its effects on the benthic algal community. *Journal of Marine Research* 39: 149–765.

CHISHOLM J.R.M. 2003. Primary productivity of reef-building crustose coralline algae. *Limnology and Oceanography* 48: 1376–1387.

CLARK K., KARSCH-MIZRACHI I., LIPMAN DJ., OSTELL J. & SAYERS EW. 2016. GenBank. *Nucleic Acids Research* 44: 67–D72.

CONNELL S.D. 2005. Assembly and maintenance of subtidal habitat heterogeneity: synergistic effects of light penetration and sedimentation. *Marine Ecology Progress Series* 289: 53–61.

D'ANTONIO C.M. 1986. Role of sand in the domination of hard substrata by the intertidal alga, *Rhodomela larixi. Marine Ecology Progress Series* 27: 263–275.

DECAISNE M. J. 1842. Versuch einer Klassifikation der Algen und der kalkfiihrenden Polypen des Lamouroux. *Flora* 26: 85–104.

DELLAPORTA S.L., WOOD J. & HICKS J.B. 1983. A plant DNA mini preparation: Version II. *Plant Molecular Biology Reporter* 1: 19–21.

DESIKACHARY T.V., KRISHNAMURTHY V., BALAKRISHNAN M.S. 1998. *Rhodophyta Vol. II-Part-IIB.* Madras Science Foundation, Chennai. 359 pp.

DETHIER M.N. 1994. The ecology of intertidal algal crusts: variation within a functional group. *Journal of Experimental Biology and Ecology* 177: 37–71.

DE TONI G.B. 1905. *Sylloge Algarum Omnium Hucusque Cognitarum, Vol. 4. Sylloge Floridearum*. Privately published, Padova. 476 pp.

DRUMMOND A.J., SUCHARD M.A., XIE D & RAMBAUT A. 2012. Bayesian phylogenetics with beauti and the beast 1.7. *Molecular Biology Evolution* 29: 1969–73.

DULLO W.C., MOUSSAVIAN E. & BRACHERT T.C. 1990. The foralgal crust facies of the deeper fore reefs in the Red Sea: a deep diving survey by submersible. *Geobios* 23: 261–273.

EAGER R., PUCKREE-PADUA C. & MANEVELDT G.W. 2015. Understanding the association between the non-geniculate coralline red alga *Spongites discoidea* and the mollusc *Oxystele sinensis*. *African Journal of Marine Science* 37: 335–344.

EDGAR R.C. 2004. MUSCLE: multiple sequence alignment with high accuracy and high throughput. *Nucleic Acids Research* 32: 1792–97.

ENGEL C. R., DESTOMBE C. & VALERO M. 2004. Mating system and gene flow in the red seaweed *Gracilaria gracilis*: effect of haploid–diploid life history and intertidal rocky shore landscape on fine-scale genetic structure. *Heredity* 92:289–98.

FAMÁ P., WYSOR B., KOOISTRA W.H.C.F. & ZUCCARELLO G.C. 2002. Molecular phylogeny of the genus *Caulerpa* (Caulerpales, Chlorophyta) inferred from chloroplast *tuf*A gene. *Journal of Phycology* 38: 1040–1050.

FARLOW W.G. 1881. The marine algae of New England. *Rep. U.S. Commissioner of Fish and Fisheries* l: 1–210.

FARR T., BROOM J., HART D., NEILL K. & NELSON W. 2009. *Common coralline algae of northern New Zealand: an identification guide.* NIWA, Wellington. 125 pp.

FAUGERON S., VALERO M., DESTOMBE C., MARTÍNEZ E.A. & CORREA J.A. 2001. Hierarchical spatial structure and discriminant analysis of genetic diversity in the red alga *Mazzaella laminarioides* (Gigartinales, Rhodophyta). *Journal of Phycology* 37: 705–716.

FELDER D.L., THOMA B.P., SCHIMDT W.E., SAUVAGE T., SELF-KRAYESY S.L., CHRISTOSERDOV A. & BRACKEN-GRISSOM H.D., FREDERICQ S., 2014. Seaweeds and decapod crustaceans on Gulf Deep Banks after the Macondo Oil Spill. *BioScience* 64: 808–819.

FOSTER M.S. 2001. Rhodoliths: Between rocks and soft places. *Journal of Phycology* 37: 659–667.

FOSTER M.S., AMADO FILHO G.M., KAMENOS N.A., RISOMENA-RODRÍGUEZ R. & STELLER D. L. 2013. Rhodoliths and rhodolith beds. *Smithsonian Contribution to the Marine Sciences* 39:143–55.

FREDERICQ S., ARAKAKI N., CAMACHO O., GABRIEL D., KRAYESKY D., SELF-KRAYESKY S., REES G., RICHARDS J., SAUVAGE T., VENERA-PONTON D. & SCHMIDT W.E. 2014. A Dynamic Approach to the Study of Rhodoliths: A Case Study for the Northwestern Gulf of Mexico. *Cryptogamie Algologie* 35: 77–98.

FREIWALD A. 1996. Sedimentological and biological aspects in the formation of branched rhodoliths in northern Norway. *Beiträge zur Paläontologie Österreich-Ungarns und des Orients* 20: 7–19.

FREIWALD A. & HENRICH R. 1994. Reefal coralline algal build-ups within the Arctic Circle: morphology and sedimentary dynamics under extreme environmental seasonality. *Sedimentology* 41: 963–984.

FRESHWATER D.W., IDOL J.N., PARHAM S.L., FERNÁNDEZ-GARCÍA C., LEÓN N., GABRIELSON P.W. & WYSOR B. 2017. Molecular assisted identification reveals hidden red algae diversity from the Burica Peninsula, Pacific Panama. *Diversity* 9: 1–38.

FRESHWATER D.W. & RUENESS J. 1994. Phylogenetic relationships of some European *Gelidium* (Gelidiales, Rhodophyta) species, based on *rbc*L nucleotide sequence analysis. *Phycologia* 33:187–194.

GABRIELSON P.W. 2008a. Molecular sequencing of Northeast Pacific type material reveals two earlier names for *Prionitis lyallii*, *Prionitis jubata* and *Prionitis sternbergii*, with brief comments on *Grateloupia versicolor* (Halymeniaceae, Rhodophyta). *Phycologia* 47: 89–97.

GABRIELSON P.W. 2008b. On the absence of previously reported Japanese and Peruvian species of *Prionitis* (Halymeniaceae, Rhodophyta) in the northeast Pacific. *Phycological Research* 56: 105–114.

GABRIELSON P.W., HUGHEY J.R. & DIAZ-PULIDO G. 2018. Genomics reveals abundant speciation in the coral reef building alga *Porolithon onkodes* (Corallinales, Rhodophyta). *Journal of Phycology* 54: 429–434.

GABRIELSON P.W., MILLER K.A. & MARTONE P.T. 2011. Morphometric and molecular analyses confirm two distinct species of *Calliarthron* (Corallinales, Rhodophyta), a genus endemic to the northeast Pacific. *Phycologia* 50: 298–316.

GABRIELSON P.W., LINDSTROM S.C. & HUGHEY J.R. *Neopolyporolithon loculusum* is a junior synonym of *N. arcticum comb.nov.* (Hapalidiales, Rhodophyta), based on sequencing type material. *Phycologia in press*.

GATTUSO J.P., GENTILI B., DUARTE C.M., KLEYPAS J.A., MIDDELBURG J.J. & ANTOINE D. 2006. Light availability in the coastal ocean: impact on the distribution of benthic photosynthetic organisms and their contribution to primary production. *Biogeosciences* 3: 489–513.

GOFF L.J. & COLEMAN A.W. 1985. The role of secondary pit connections in red algal parasitism. *Journal of Phycology* 21: 483–508.

GUIRY M.D. & GUIRY G.M. 2018. *AlgaeBase*. World-wide electronic publication, National University of Ireland, Galway. http://www.algaebase.org; last accessed 6 November 2018.

HAGEN N.T. 1999. Survival and growth of juvenile green sea urchins on different macroalgal settlement substrates. *Journal of Shellfish Research* 18: 303.

HAUPTFLEISCH P. 1897. Die als Fossile Algen (undBacterien) beschrieben Pflanzenreste oder Abrficke. In *Die Naturlichen Pflanzenfamilien* (Ed. by A. Engler & K. Prantl), Vol. 1/2. W. Englemann, Leipzig. 570 pp.

HARLIN M.M., WOELKERLING W.M.J. & WALKER D.I. 1985. Effects of a hypersalinity gradient on epiphytic Corallinaceae (Rhodophyta) in Shark Bay Western Australia. *Phycologia* 24: 389–402.

HARRINGTON L., FABRICIUS K., DE'ATH G. & NEGRI A. 2004. Recognition and selection of settlement substrata determine post-settlement survival in corals. *Ecology* 85: 3428–3437

HARVEY W.H. 1847. *Phycologia Britannica, Vol. 1.* Reeve & Benham, London. 512 pp.

HARVEY W. 1860. *Index Generum Algarum.* van Voorst, London. 58 pp.

HARVEY A.S., BROADWATER S., WOELKERLING W.M.J. & MITROVSKI P.J. 2003 *Choreonema* (Corallinales, Rhodophyta): 18S rRNA phylogeny and resurrection of the Hapalidiaceae for the subfamilies Choreonematoideae, Austrolithoideae and Melobesioideae. *Journal of Phycology* 39: 988–998.

HARVEY A.S., PHILLIPS L.E., WOELKERLING W.M.J. & MILLER A.J.K. 2006. The Corallinaceae, subfamily Mastophoroideae (Corallinales, Rhodophyta) in south-eastern Australia. *Australian Systematic Botany* 19: 387–429.

HARVEY A.S. & WOELKERLING W.M.J. 2007. A guide to nongeniculate coralline red algal (Corallinales, Rhodophyta) rhodolith identification. *Ciencas Marinas* 33: 411–426.

HARVEY A.S, WOELKERLING W.M.J., FARR T., NEILL K., NELSON W. 2005. Coralline algae of central New Zealand: an identification guide to common 'crustose' species. National Institute of Water & Atmospheric Research Information series No. 57. Wellington.

HERNÁNDEZ-KANTÚN J.J., RINDI F., ADEY W.H., HEESCH S., PEÑA V., LE GALL L. & GABRIELSON P.W. 2015. Sequencing type material resolves the identity and distribution of the generitype *Lithophyllum incrustans*, and related European species *L. hibernicum* and *L. bathyporum* (Corallinales, Rhodophyta). *Journal of Phycology* 51: 791–807.

HERNÁNDEZ-KANTÚN J.J., GABRIELSON P., HUGHEY, J.R., PEZZOLESI L., RINDI F., ROBINSON N.M., PEÑA V., RIOSMENA-RODRÍGUEZ R., LE GALL L. & ADEY W. 2016. Reassessment of

the branched *Lithophyllum* spp. (Corallinales, Rhodophyta) in the Caribbean Sea with global implications. *Phycologia* 55: 619–639.

HEYDRICH F. 1897. Melobesieae. *Berichte der deutsche botanischen Gesellschaft* 15: 403–420.

HIND K.R. & SAUNDERS G.W. 2013. A molecular phylogenetic study of the tribe Corallineae (Corallinales, Rhodophyta) with an assessment of genus-level taxonomic features and descriptions of novel genera. *Journal of Phycology* 49: 103–114.

HIND K.R., GABRIELSON P.W. & SAUNDERS G.W. 2014a. Molecular-assisted alpha taxonomy reveals pseudocryptic diversity among species of *Bossiella* (Corallinales, Rhodophyta) in the eastern Pacific Ocean. *Phycologia* 3: 443–456.

HIND K.R., GABRIELSON P.W., LINDSTROM S.C. & MARTONE P.T. 2014b. Misleading morphologies and the importance of sequencing type specimens for resolving coralline taxonomy (Corallinales, Rhodophyta): *Pachyarthron cretaceum* is *Corallina officinalis*. *Journal of Phycology* 50: 760–764.

HIND K.R., GABRIELSON P.W., JENSEN C.P. & MARTONE P.T. 2016. *Crusticorallina* gen. nov., a non-geniculate genus in the sub family Corallinoideae (Corallinales, Rhodophyta). *Journal of Phycology* 52: 929–941.

HIND K.R., MILLER K.A., YOUNG M., JENSEN C., GABRIELSON P.W. & MARTONE P.T. 2015. Resolving cryptic species of *Bossiella* (Corallinales, Rhodophyta) using contemporary and historical DNA. *American Journal of Botany* 102: 1–19.

HOFMANN L.C., NETTLETON J.C., NEEFUS C.D. & MATHIESON A.C. 2010. Cryptic diversity of *Ulva* (Ulvales, Chlorophyta) in the Great Bay Estuarine System (Atlantic USA): introduced and indigenous distromatic species. *European journal of phycology* 45: 230–239.

HUGHEY J.R., SILVA P.C. & HOMMERSAND M.H. 2001. Solving taxonomic and nomenclatural problems in Pacific Gigartinaceae (Rhodophyta) using DNA from type material. *Journal of Phycology* 37: 1091–1109.

HUGHEY J.R., SILVA P.C. & HOMMERSAND M.H. 2002. ITS1 sequences of type specimens of *Gigartina* and *Sarcothalia* and their significance for the classification of South African Gigartinaceae (Gigartinales, Rhodophyta). *European Journal of Phycology* 37: 209–216.

IRYU Y. 1985. Study on the recent rhodoliths around the Ryukyu Islands. In: *Prompt Reports of the Comprehensive and Scientific Survey in the Ryukyu Archipelago* (Ed. by T. Takeishi), pp 123–133. Tohoko University, Japan.

IRYU Y., NAKAMORI T., MATSUDA S. & ABE O. 1995. Distribution of marine organisms and its geological significance in the modern reef complex of the Ryukyu Islands. *Sedimentary Geology* 99: 243–258.

JOHANSEN H.W. 1976. Current status of generic concepts in coralline algae (Rhodophyta). *Phycologia* 15: 221–244.

JOHANSEN H.W. 1981. *Coralline algae, a first synthesis*. CRC Press, Boca Raton, Florida. 239 pp.

JANOT K.G. & MARTON P.T. 2016. Convergence of joint mechanics in independently evolving, articulated coralline algae. *Journal of Experimental Biology* 219: 383–391.

JANOT K.G. & MARTON P.T. 2018. Bending strategies of convergently evolved, articulated coralline algae. *Journal of Phycology* 54: 305–316.

KAEHLER S. & WILLIAMS G.A. 1996. Distribution of algae on tropical rocky shores: spatial and temporal patterns of non-coralline encrusting algae in Hong Kong. *Marine Biology* 125: 177–187.

KATO A., BABA M. & SUDA S. 2011. Revision of the Mastophoroideae (Corallinales, Rhodophyta) and polyphyly in nongeniculate species widely distributed on Pacific coral reefs. *Journal of Phycology* 47: 662–72.

KEARSE M., MOIR R., WILSON A., STONES-HAVAS S., CHEUNG M., STURROCK S., BUXTON S., COOPER A., MARKOWITZ S., DURAN C., THIERER T., ASHTON B., MEINTJES P. & DRUMMOND A. 2012. Geneious Basic: an integrated and extendable desktop software platform for the organization and analysis of sequence data. *Bioinformatics* 28: 1647–1649.

KEATS D.W. 1995. *Lithophyllum cuneatum* sp. nov. (Corallinaceae, Rhodophyta), a new species of non-geniculate coralline alga semi-endophytic in *Hydrolithon onkodes* and *Neogoniolithon* sp. from Fiji, South Pacific. *Phycological Research* 43: 151–160.

KEATS D.W., GROENER A., & CHAMBERLAIN Y.M.C. 1993. Cell sloughing in the littoral zone coralline alga, *Spongites yendoi* (Foslie) Chamberlain (Corallinales, Rhodophyta). *Phycologia*: 32: 143–150.

KEATS D.W., CHAMBERLAIN Y.M.C, BABA M. 1997. *Pneophyllum conicum* (Dawson) comb. nov. (Rhodophyta, Corallinaceae) a widespread Indo-Pacific non-geniculate coralline alga that overgrows and kills live coral. *Botanica Marina* 40: 263–279.

KENDRICK G.A. 1991. Recruitment of coralline crusts and filamentous turf algae in the Galapagos archipelago: effect of simulated scour, erosion and accretion. *Journal of Experimental Marine Biology and Ecology* 147: 47–63.

KIM J.H., GUIRY M.D., OAK J.H., CHOI D.S., KANG S.H. & CHOI H.G. 2007. Phylogenetic relationships within the tribe *Janieae* (Corallinales, Rhodophyta) based on molecular and morphological data: a reappraisal of *Jania*. *Journal of Phycology* 43: 1310–1319.

KJØSTERUD A.B. 1997. Epiphytic coralline crusts (Corallinales, Rhodophyta) from South Norway. *Sarsia* 82: 23–37.

KOOISTRA W.H.C.F., CALDERÓN M. & HILLIS L.W. 1999. Development of the extant diversity in *Halimeda* is linked to vicariant events. *Hydrobiologia*: 398/399: 39–45.

KOOISTRA W.H.C.F., COPPEJANS E.G.G. & PAYRI C. 2002. Molecular systematics, historical ecology, and phylogeography of *Halimeda*. (Bryopsidales). *Molecular Phylogenetics and Evolution* 24: 121–138.

KRAYESKY-SELF S., RICHARDS J.L., RAHMATIAN M. & FREDERICQ S. 2016. Aragonite infill in overgrown conceptacles of coralline *Lithothamnion* spp. (Hapalidiaceae, Hapalidiales, Rhodophyta): new insights in biomineralization and phylomineralogy. *Journal of Phycology* 52: 161–173.

KRAYESKY-SELF S., SCHMIDT W.F., PHUNG D., HENRY C., SAUVAGE T., CAMACHO O., FELGENHAUER B.E. & FREDERICQ S. 2017. Eukaryotic life inhabits rhodolith-forming coralline algae (Hapalidiales, Rhodophyta), remarkable marine benthic microhabitats. *Scientific Reports* 7: 1–12.

KÜTZING F.T. 1841. Ü*eber die "Polypières calcifères" des Lamouroux*. Thiele, Nordhausen. 34 pp.

KÜTZING F.T. 1843. *Phycologia generalis oder Anatomie, Physiologie und Systemkunde der Tange.* Brockhaus, Leipzig. 458 pp.

KYLIN H. 1956. *Die Gattungen der Rhodophyceen.* C.W.K. Gleerups, Lurid. 673 pp.

LE GALL L. & SAUNDERS G.W. 2007. A nuclear phylogeny of the Florideophyceae (Rhodophyta) inferred from combined EF2, small subunit and large subunit ribosomal DNA: Establishing the new red algal subclass Corallinophycidae. *Molecular Phylogenetics and Evolution* 43: 1118–1130.

LE GALL L., PAYRI C.E., BITTNER L. & SAUNDERS G.W. 2010. Multigene phylogenetic analyses support recognition of the Sporolithales ord. nov. *Molecular Phylogenetics and Evolution* 54: 302–305.

LEBEDNIK P.A. 1977. Postfertilization development in *Clathromorphum*, *Melobesia*, and *Mesophyllum* with comments on the evolution of the Corallinaceae and Cryptonemiales (Rhodophyta). *Phycologia* 16: 389–406.

LEE R. 1967. Taxonomy and distribution of the melobesioid algae on Rongelap atoll, Marshall Islands. *Canadian Journal of Botany* 45: 985–1001.

LIDDELL W.D. & OHLHORST S.L. 1988. Hard substrata community patterns, 1–120 M, North Jamaica. *Palaios* 3: 413–423.

LEMOINE MME. P. 1911. Structure anatomique des Mélobésiées. Application à la classification. *Annales de l'Institut Océanographique.* 2: 1–213.

LINDLEY J. 1846. *The Vegetable Kingdom.* Bradbury & Evans, London. 908 pp.

LINDSTROM S.C., GABRIELSON P.W., HUGHEY J.R., MACAYA E.C. & NELSON W.A. 2015 Sequencing of historic and modern specimens reveals cryptic diversity in *Nothogenia* (Scinaiaceae, Rhodophyta). *Phycologia* 54: 97–108.

LINDSTROM S.C., HUGHEY J.R. & MARTONE P.T. 2011. New, resurrected and redefined species of *Mastocarpus* (Phyllophoraceae, Rhodophyta) from the northeast Pacific. *Phycologia* 50: 661–683.

LITTLER M.M. 1973. The distribution, abundance, and communities of deepwater Hawaiian crustose Corallinaceae (Rhodophyta, Cryptonemiales). *Pacific Science* 27: 281–289.

LITTLER M.M. & LITTLER D.S. 1984. Models of tropical reef biogenesis: The contribution of algae. In: *Progress in phycological research* (Ed. by F.E. Round & D.J. Chapman), pp. 323–364. Biopress, UK.

LITTLER M.M. & LITTLER D.S. 1994. Essay: tropical reefs as complex habitats for diverse macroalgae. In: *Seaweed Ecology and Physiology* (Ed. by C.S. Lobban & P.J. Harrison), pp. 72–75. Cambridge University Press, New York.

LITTLER M.M. & LITTLER D.S. 1997. Disease-induced mass mortality of crustose coralline algae on coral reefs provides rationale for the conservation of herbivorous fish stocks. *Proceedings of the 8th International Coral Reef Symposium* 1: 719–724.

LITTLER M.M. & LITTLER D.S. 2013. The Nature of crustose coralline algae and their interactions on reefs. *Smithsonian Contributions to the Marine Sciences* 39: 199–212.

LITTLER M.M., LITTLER D.S., BLAIR S.M. & NORRIS N. 1985. Deepest known plant life discovered on an uncharted seamount. *Science* 227: 57–59.

LITTLER M.M., LITTLER D.S. & TAYLOR P.R. 1995. Selective herbivore increases biomass of its prey: A chiton-coralline reef-building association. *Ecology* 76: 1666–1681.

MAMOOZADEH N.R. & FRESHWATER D.W. 2012. *Polysiphonia* sensu lato (Ceramiales, Florideophyceae) species of Caribbean Panama including *Polysiphinia lobophoralis* sp. nov. and *Polysiphonia nuda* sp. nov. *Botanica Marina* 55: 317–347.

MANEVELDT G.W., CHAMBERLAIN Y.M.C. & KEATS D.W. 2008. A catalogue with keys to the non-geniculate coralline algae (Corallinales, Rhodophyta) of South Africa. *South African Journal of Botany* 74: 555–566.

MANEVELDT G.W., GABRIELSON P.W. & KANGWE J. 2017. *Sporolithon indopacificum* sp. nov. (Sporolithales, Rhodophyta) from tropical western Indian and western Pacific oceans: First report, confirmed by DNA sequence data, of a widely distributed species of *Sporolithon. Phytotaxa* 326: 115–128.

MANEVELDT G.W. & KEATS D.W. 2008. Effects of herbivore grazing on the physiognomy of the coralline alga *Spongites yendoi* and on associated competitive interactions. *African Journal of Marine Science* 30: 581–593.

MANEVELDT G.W. & KEATS D.W. 2014. Taxonomic review based on new data of the reef building alga *Porolithon onkodes* (Corallinaceae, Corallinales, Rhodophyta) along with other taxa found to be conspecific. *Phytotaxa* 190: 216–249.

MANEVELDT G.W. & VAN DER MERWE E. 2012. *Heydrichia cerasina* sp. nov. (Sporolithales, Corallinophycidae, Rhodophyta) from the southern-most tip of Africa. *Phycologia* 51: 11–21.

MANEVELDT G.W., VAN DER MERWE E. & KEATS D.W. 2016. Updated keys to the non-geniculate coralline red algae (Corallinophycidae, Rhodophyta) of South Africa. *South African Journal of Botany* 106: 158–164.

MARTIN S., CHARNOZ A. & GATTUSO J. 2013. Photosynthesis, respiration and calcification in the Mediterranean crustose coralline alga *Lithophyllum cabiochae* (Corallinales, Rhodophyta). *European Journal of Phycology* 48: 163–172.

MARTIN S., CLAVIER J., CHAUVAUD L. & THOUZEAU G. 2007. Community metabolism in temperate maërl beds. I. Carbon and carbonate fluxes. *Marine Ecology Series* 335: 19–29.

MARTONE P.T., ALYONO M. & STITES S. 2010. Bleaching of an intertidal coralline alga: untangling the effects of light, temperature, and desiccation. *Marine Ecology Progress Series* 416: 57–67.

MARTONE P.T., LINDSTROM S.C., MILLER K.A. & GABRIELSON P.W. 2012. *Chiharaea* and *Yamadaia* (Corallinales, Rhodophyta) represent reduced and recently derived articulated coralline morphologies. *Journal of Phycology* 47: 1–10.

MAZZA A. (1916-1922). *Saggio di Algologia Oceanica,* Vol. 3. Seminario, Padova, Italy. 1057–1584 pp.

MCIVOR L., MAGGS C.A., PROVAN J. & STANHOPE M.J. 2001. *rbc*L sequences reveal multiple cryptic introductions of the Japanese red alga *Polysiphonia harveyi. Molecular Ecology* 10: 911–919.

MELBOURNE L.A., HERNÁNDEZ-KANTÚN J.J., RUSSELL S. & BRODIE J. 2017. There is more to maërl than meets the eye: DNA barcoding reveals a new species in Britain, *Lithothamnion*

erinaceum sp. nov. (Hapalidiales, Rhodophyta). *European Journal of Phycology* 52: 166–178.

MONTECINOS A., BROITMAN B.R., FAUGERON S., HAYE P.A., TELLIER F. & GUILLEMIN M. 2012. Species replacement along a linear coastal habitat: phylogeography and speciation in the red alga *Mazzaella laminarioides* along the south east pacific. *BMC Evolutionary Biology* 12:97.

MONTECINOS A.E., COUCEIRO L., PETERS A.F., DESRUT A., VALERO M. & GUILLEMIN M.L. 2016. Species delimitation and phylogeographic analyses in the *Ectocarpus* subgroup *siliculosi* (Ectocarpales, Phaeophyceae). *Journal of Phycology* 53: 17–31.

MORCOM N.F., WOELKERLING W.M.J. & WARD S.A. 2005. Epiphytic nongeniculate corallines found on *Laurencia filiformis f. heteroclada* (Rhodomelaceae, Ceramiales). *Phycologia* 44: 202–211.

NEEFUS C.D., MATHIESON A.C., KLEIN A.S., TEASDALE B., BRAY T. & YARISH C. 2002. *Porphyra birdiae* sp. nov. (Bangiales, Rhodophyta): A New Species from the Northwest Atlantic. *Algae* 17: 203–216.

NEIVA J., SERRAO E. A., ANDERSON L., RAIMONDI P.T., MARTINS N., GOUVEIA L., PAULINO C., COELHO N.C., MILLER K.A., REED D., LADAH L.B. & PEARSON G.A. 2017. Cryptic diversity, geographical endemism and allopolyploidy in NE Pacific seaweeds. *BMC Evolutionary Biology* 17: 1–12.

NELSON W.A. 2009. Calcified macroalgae – critical to coastal ecosystems and vulnerable to change: a review. *Marine and Freshwater Research* 60: 787–801.

NELSON W.A., SUTHERLAND J.E., FARR T.J., HART D.R., NEILL K.T., KIM H.J. & YOON H.S. 2015. Multi-gene phylogenetic analyses of New Zealand coralline algae: *Corallinapetra novaezelandiae* gen. et sp. nov. and recognition of the Hapalidiales ord. nov. *Journal of Phycology* 51: 454–468.

NOBLE J.M. & KRAFT G.T. 1983. Three new species of parasitic red algae (Rhodophyta) from Australia: *Holmsella australis* sp. nov., *Meridiocolax bracteata* sp. nov. and *Trichidium pedicellatum* gen. et sp. nov. *British Phycological Society* 18:391–413.

PARDO C., LÓPEZ L., PEÑA V., HERNÁNDEZ-KANTÚN J., LE GALL L., BÁRBARA I. & BARREIRO R. 2014. A multilocus species delimitation reveals a striking number of species of coralline algae forming maërl in the OSPAR maritime area. *PLoS One* 9: 1–9.

PAYO D.A., LELIAERT F., VERBRUGGEN H., D'HONDT S., CALUMPONG H.P. & DE CLERCK O. 2013. Extensive cryptic species diversity and fine-scale endemism in the marine red alga *Portieria* in the Philippines. *Proceedings of the Royal Society B: Biological Sciences* 280: 1–8.

PEÑA V., DE CLERCK O., AFONSO-CARRILLO J., BALLESTEROS E., BÁRBARA I., BARREIRO R. & LE GALL L. 2015. An integrative systematic approach to species diversity and distribution in the genus *Mesophyllum* (Corallinales, Rhodophyta) in Atlantic and Mediterranean Europe. *European Journal of Phycology* 50: 1–15.

PEÑA V., HERNÁNDEZ-KANTÚN J.J., ADEY W.H. & LE GALL L. 2018. Assessment of coralline species diversity in the European coasts supported by sequencing of type material: The case study of *Lithophyllum nitorum* (Corallinales, Rhodophyta). *Cryptogamie, Algologie* 39: 123–137.

PEÑA V., ROUSSEAU F., DE REVIERS B. & LE GALL L. 2014. First assessment of the diversity of coralline species forming maërl and rhodoliths in Guadeloupe, Caribbean using an integrative systematic approach. *Phytotaxa* 190: 190–215.

PENROSE D.L. 1991. *Spongites fruticulosus* (Corallinaceae, Rhodophyta), the type species of *Spongites*, in southern Australia. *Phycologia* 30: 438–448.

PENROSE D.L. 1996. Genus *Pneophyllum*. In: *The Marine Benthic Flora Of Southern Australia-Gracilariales, Rhodymeniales, Corallinales And Bonnemaisoniales*. (Ed. by H.B.S Womersley), Australian Biological Resources Study: Canberra pp. 266–272.

PENROSE D.L. & WOELKERLING W.M.J. 1988. A taxonomic reassessment of *Hydrolithon* Foslie, *Porolithon* Foslie and *Pseudolithophyllum* Lemoine emend. Adey (Corallinaceae, Rhodophyta) and their relationships to *Spongites* Kützing. *Phycologia* 27: 159–176.

PENROSE D.L. & WOELKERLING W.M.J. 1991. *Pneophyllum fragile* in southern Australia: implications for generic concepts in the Mastophoroideae (Corallinaceae, Rhodophyta). *Phycologia* 30: 495–506.

PENROSE D.L. & WOELKERLING W.M.J. 1992. A reappraisal of *Hydrolithon* and its relationship to *Spongites* (Corallinaceae, Rhodophyta). *Phycologia* 3: 81–88.

PHILIPPI R.A. 1837. Beweis dafs die Nulliporen Pflanzen sind. *Archiv für Naturgeschichte.* 3: 387–392.

PREUSS M; NELSON W.A. & ZUCCARELLO G.C. 2017. Red algal parasites: a synopsis of described species, their hosts, distinguishing characters and areas for continued research. *Botanica Marina* 60: 13–25.

PUILLANDRE N., LAMBERT A., BROUILLET S. & ACHAZ G. 2012. ABGD, Automatic Barcode Gap Discovery for primary species delimitation. *Molecular Ecology* 21: 1864–1877.

QUARANTA F., TOMASSETTI L., VANNUCCI G. & BRANDANO M. 2012. Coralline algae as environmental indicators: a case study from the Attard member (Chattian, Malta). *Geodiversitas* 34: 151–166.

RAMBAUT A. 2016. FigTree version 1.3.1 [computer program] http://tree.bio.ed.ac.uk.

RAMBAUT A. & DRUMMOND AJ., 2017. TreeAnnotator version 1.6.1 [computer program] http://beast.bio.ed.ac.uk.

RAMBAUT A., DRUMMOND A.J., XIE D., BAELE G. & SUCHARD M.A. 2018 Posterior summarisation in Bayesian phylogenetics using Tracer 1.7. *Systematic Biology* 67: 901–904.

REYES J. & AFONSO-CARRILLO J. 1995. Morphology and distribution of nongeniculate coralline alga (Corallinaceae, Rhodophyta) on the leaves of the seagrass *Cymodocea nodosa* (Cymodoceaceae). *Phycologia* 34: 179–190.

RICHARDS J.L., GABRIELSON P.W. HUGHEY J.R. & FRESHWATER D.W. 2018. A re-evaluation of subtidal *Lithophyllum* species (Corallinales, Rhodophyta) from North Carolina, USA, and the proposal of *L. searlesii* sp. nov. *Phycologia* 57: 318–330.

RICHARDS J.L., SAUVAGE T., SCHMIDT W.E., FREDERICQ S., HUGHEY J.R. & GABRIELSON P.W. 2017. The coralline genera *Sporolithon* and *Heydrichia* (Sporolithales, Rhodophyta) clarified by sequencing type material of their generitypes and other species. *Journal of Phycology* 53:1044–1059.

RIOSMENA-RODRÍGUEZ R., NELSON W. & AGUIRRE J. 2017. *Rhodolith/ maërl beds: a global perspective*. Springer International Publishing, Basel. 362 pp.

ROBBA L., RUSSELL S.J., BARKER G.L. & BRODIE J. 2006. Assessing the use of the Mitochondrial Cox1 marker for use in DNA Barcoding of red algae (Rhodophyta). *American Journal of Botany* 93: 1101–1108.

ROBERTS R.D., KÜHL M., GLUD R.N. & RYSGAARD S. 2002. Primary production of crustose coralline red algae in a high arctic fjord. *Journal of Phycology* 38: 273–283.

Rosanoff S. 1866. Recherches anatomiques sur les Mélobésiées (*Hapalidium, Melobesia, Lithophyllum* et *Lithothamnion*). *Mémoires de la Société Impériale des Sciences Naturelles de Cherbourg* 12: 112 pp.

RÖSLER A., PERFECTTI F., PEÑA V. & BRAGA J.C. 2016. Phylogenetic relationships of Corallinaceae (Corallinales, Rhodophyta): taxonomic implications for reef-building corallines. *Journal of Phycology* 52: 412–431.

SALOMAKI E.D., NICKLES K.R. & LANE C.E. 2015. The ghost plastid of *Choreocolax polysiphoniae*. *Journal of Phycology* 51: 217–221.

SAUNDERS G.W. 2005. Applying DNA barcoding to red macroalgae: a preliminary appraisal holds promise for future applications. *Philosophical Transactions of the Royal Society Biological Sciences* 360: 1879–1888.

SAUNDERS G.W. 2008. A DNA barcode examination of the red algal family *Dumontiaceae* in Canadian waters reveals substantial cryptic species diversity. 1. The foliose *Dilsea–Neodilsea* complex and *Weeksia*. *Botany* 86: 773–789.

SCHMITZ F. 1889. Systematische übersicht der bisher bekannten Gattungen der Florideen. *Flora* 72: 435–456.

SETCHELL W.A. 1943. *Mastophora* and the Mastophoreae: Genus and subfamily of Corallinaceae. *Proceedings of the National Academy of Science of the United States of America* 29: 127–135.

SISSINI M.N., OLIVEIRA M.C., GABRIELSON P.W., ROBINSON N.M., OKOLODKOV Y.B., RIOSMENA-RODRÍGUEZ R. & HORTA P.A. 2014. *Mesophyllum erubescens* (Corallinales, Rhodophyta): so many species in one epithet. *Phytotaxa* 190:299–319.

STELLER D.L. & FOSTER M.S. 1995. Environmental factors influencing distribution and morphology of rhodoliths in Bahia Concepcion, B.C.S., Mexico. *Journal of Experimental Marine Biology and Ecology* 194: 201–212.

STACHIE-CRAIN B., MÜLLER D.G. & GOFF L.J. 1997. Molecular systematics of *Ectocarpus* and *Kuckuckia* (Ectocarpales, Phaeophyceae) inferred from phylogenetic analysis of nuclear and plastid-encoded sequences. *Journal of Phycology* 33: 152–168.

STENECK R.S. 1982. A limpet-coralline alga association: adaptations and defences between a selective herbivore and its prey. *Ecology* 63: 507–522.

STENECK R.S. 1983. Escalating herbivory and resulting adaptive trends in calcareous algal crusts. *Paleobiology* 9: 44–61.

STENECK R.S. 1985. Adaptations of crustose coralline algae to herbivory: patterns in space and time. In: *Paleoalgology contemporary research and applications* (Ed. by D.F. Toomey & M.H. Nitecki), pp. 352–3660. Springer-Verlag, Berlin.

STENECK R.S. 1986. The ecology of coralline algal crusts: Convergent patterns and adaptive strategies. *Annual Review of Ecology and Systematics* 17: 273–303.

STENECK R.S. 1989. Herbivory on coral reefs: A synthesis. *Proceedings of the sixth International Coral Reef Symposium* 1: 37–49.

STENECK R.S. & ADEY W.H. 1976. The role of environment in control of morphology in *Lithophyllum congestum*, a Caribbean algal ridge builder. *Botanica Marina* 19: 197–215.

STENECK R. S. & DETHIER M. N. 1994. A functional group approach to the structure of algal dominated communities. *Oikos* 69 (3), 476–498

STENECK R.S. & PAINE R.T. 1986. Ecological and taxonomic studies of shallow-water encrusting Corallinaceae (Rhodophyta) of the boreal northeastern Pacific. *Phycologia* 25: 221–240.

STEPHENSON T.A. & STEPHENSON A. 1972. Life between Tidemarks on Rocky Shores. Freeman, San Francisco. 425 pp.

THIERS B.M. 2018 [Continuously updated electronic resource]. *Index herbariorum: A global directory of public herbaria and associated staff.* New York Botanical Garden's Virtual Herbarium, New York. http://sweetgum.nybg.org/ih/.

TURNER J.A. & WOELKERLING W.M.J. 1982. Studies on the *Mastophora* - *Lithoporella* complex (Corallinaceae, Rhodophyta). II. Reproduction and generic concepts. *Phycologia* 21: 218–235.

VAN DER HEIJDEN L.H. & KAMENOS N.A., 2015. Calculating the global contribution of coralline algae. *Biogeosciences* 12: 6429–6441.

VAN DER MERWE E., MIKLASZ K., CHANNING A., MANEVELDT G. W. & GABRIELSON P. W. 2015. DNA sequencing resolves species of Spongites (Corallinales, Rhodophyta) in the Northeast Pacific and South Africa, including *S. agulhensis* sp. nov. *Phycologia* 54:471–90.

VAN DER STRATE H.J., BOELE-BOS S.A., OLSEN J.L., VAN DE ZANDE L. & STAM W.T. 2002. Phylogeographic studies in the tropical seaweed *Cladophoropsis membranacea* (Chlorophyta, Ulvophyceae) reveal a cryptic species complex. *Journal of Phycology* 38: 572–582.

VERMEIJ M.J.A., DAILER M.L. & SMITH C.M. (2011) Crustose coralline algae can suppress macroalgal growth and recruitment on Hawaiian coral reefs. *Marine Ecology Progress Series* 422: 1–7.

VERBRUGGEN H., VLAEMINCK C., SAUVAGE T., SHERWOOD A.R., LELIAERT F. & DE CLERCK O. 2009. Phylogenetic analysis of *Pseudochlorodesmis* strains reveals cryptic diversity above the family level in the siphonous green algae (Bryopsidales, Chlorophyta). *Journal of Phycology* 45: 726–731.

VIEIRA C., CAMACHO O., WYNNE M.J., MATTIO L., ANDERSON R.J., BOLTON J.J., SANSÓN M., D'HONDT S., LELIAERT F., FREDERICQ S. & PAYRI C. 2016. Shedding new light on old algae: Matching names and sequences in the brown algal genus *Lobophora* (Dictyotales, Phaeophyceae). *Taxon* 65: 689–707.

VIEIRA C., CAMACHO O., SUN Z., FREDERICQ S., LELIAERT F. & PAYRI C. 2017. Historical biogeography of the highly diverse brown seaweed *Lobophora* (Dictyotales, Phaeophyceae). *Molecular Phylogenetics and Evolution* 110: 81–92.

WALKER R.H., BRODIE J., RUSSELL S. & IRVINE L.M. 2009. Biodiversity of coralline algae in the northeastern Atlantic including *Corallina caespitosa* sp. nov. (Corallinoideae, Rhodophyta). *Journal of Phycology* 45: 287–297.

WILKS K.M. & WOELKERLING W.M.J. 1991. Southern Australian species of *Melobesia* (Corallinaceae, Rhodophyta). *Phycologia* 30: 507–533.

WILKS K.M. & WOELKERLING W.M.J. 1994. An account of southern Australian species of *Phymatolithon* (Corallinaceae, Rhodophyta) with comments on *Leptophytum*. *Australian Systematic Botany* 7: 183–223.

WILSON S. BLAKE C., BERGES J.A. & MAGGS C.A. 2004. Environmental tolerances of free-living coralline algae (maërl): implications for European marine conservation. *Biological Conservation* 120: 279–289.

WOELKERLING W.M.J. 1985. A taxonomic reassessment of *Spongites* (Corallinaceae, Rhodophyta) based on studies of Kützing's original collections. *British Phycological Journal* 20: 123–153.

WOELKERLING W.M.J. 1996. Genus *Pneophyllum*. In: *The Marine Benthic Flora of Southern Australia-Gracilariales, Rhodymeniales, Corallinales and Bonnemaisoniales*. (Ed. by H.B.S Womersley), pp. 153–265. Australian Biological Resources Study, Canberra.

WOELKERLING W.M.J. 1988. *The coralline Red Algae: An Analysis of the Genera and Subfamilies of Nongeniculate Corallinaceae*. British Museum (Natural History) and Oxford University Press, London and Oxford. 268 pp.

WOELKERLING W.M.J. & HARVEY A. 1993. An Account of Southern Australian Species of *Mesophyllum* (Corallinaceae. Rhodophyta). *Australian Systematic Botany* 6: 571–637.

WOELKERLING W.M.J., IRVINE L.M. & HARVEY A.S. 1993. Growth-forms in non-geniculate coralline red algae (Corallinales, Rhodophyta). *Australian Systematic Botany* 6: 277–293.

WOMERSLEY H.B.S. 1996. *The Marine Benthic Flora of Southern Australia, Part IIIB. Gracilariales, Rhodymeniales, Corallinales and Bonnemaisoniales*. Australian Biological Resources Study, Canberra. 386 pp.

WRAY J.L. 1977. *Calcareous algae. Developments in Palaeontology and Stratigraphy*. Elsevier, Amsterdam. 185 pp.

YANG M.Y. & KIM M.S. 2018. Cryptic species diversity of ochtodenes-producing *Portieria* species (Gigartinales, Rhodophyta) from the northwest Pacific. *Algae. An International Journal of Algal Research* 33: 205–214.

YOON H.S., HACKETT J.D. & BHATTACHARYA D. 2002. A single origin of the peridinin- and fucoxanthin-containing plastids in dinoflagellates through tertiary endosymbiosis. *Proceedings of the Natural Academy of Sciences of the United States of America* 99: 11724–11729.

ZUCCARELLO G., MOON D. & GOFF L.J. 2004. A phylogenetic study of parasitic genera placed in the family Choreocolacaceae (Rhodophyta). *Journal of Phycology* 40: 937–945.

ŽULJEVIC A., KALEB S., PEÑA V., DESPALATOVIĆ M., CVITKOVIĆ I., DE CLERCK O., LE GALL L., FALACE A., VITA F., BRAGA J.C. & ANTOLIĆ B. 2016. First freshwater coralline alga and the role of local features in a major biome transition. *Scientific Reports* 6: 1–12.

TABLE 3. Comparison of the appearance and vegetative structure of South African species that would previously have been assigned to *Spongites*. Unless otherwise stated, all measurements are in micrometres. L, H and D = length, height and diameter respectively. ND = No data provided.

Character	*Chamberlainium agulhense*[1]	*Chamberlainium capense*	*Chamberlainium cochleare*	*Chamberlainium glebosum*	*Chamberlainium impar*	*Chamberlainium natalense*	*Chamberlainium occidentale*	*Chamberlainium tenue*	*Pneophyllum neodiscoidium*
Growth form	Encrusting (smooth)	Encrusting (smooth), becoming variably lumpy and slightly protuberant	Encrusting (smooth)	Lumpy, becoming highly protuberant	Encrusting (smooth), orbicular becoming confluent	Encrusting (smooth)	Encrusting (smooth) to warty (mostly) to lumpy, becoming slightly protuberant	Encrusting (smooth)	Primary thallus encrusting (smooth). Secondary thallus, discoid with orbicular protrusions that often produce crowded, contiguous, swollen protuberances
Maximum protuberance height	-	4 mm	-	6 mm	-	-	4 mm	-	10 mm
Thallus construction	Dimerous	Monomerous	Monomerous	Monomerous	Monomerous	Monomerous	Monomerous	Monomerous	Primary thallus dimerous, becoming secondarily monomerous
Maximum thallus thickness	650	1000	370	2000	1800	800	1000	250	Primary thallus 310; Secondary thallus 3000
Habit	Individual thalli discernible, not fusing	Individual thalli discernible, not fusing	Individual thalli not discernible, fusing to form large expanses	Individual thalli discernible, not fusing	Individual thalli discernible, not fusing	Individual thalli discernible, not fusing	Individual thalli discernible, not fusing	Individual thalli discernible, not fusing	Individual primary thalli not discernible, fusing. Secondary discoid protrusions discernible, not fusing
Trichocytes	None observed	Common, solitary (mostly) to paired	Common, solitary (mostly) to clustered, up to 6 (separated by	None observed	Rare, solitary to paired	Rare, solitary (mostly) to clustered, up to 6 (separated by	Common, solitary (mostly) to clustered, up to 6 (separated by	Common, solitary (mostly) to paired	None observed

			normal vegetative filaments)			normal vegetative filaments)	normal vegetative filaments)		
Trichocyte dimensions	-	L = 22-29; D = 5-7	L = 15-27; D = 7-12	-	L = 22-39; D = 10-12	L = 12-29; D = 7-10	L = 22-37; D = 7-10	L = 22-25; D = 10-12	-
No. of epithallial cell layers	1-3 (mostly 1-2)	1	1	1	4-6 (9)	1	1	1	2-4
Epithallial cell shape	Rounded to domed	Oval to round	Elliptical to domed	Rounded to elliptical	Elliptical to rounded	Flattened to elliptical	Elliptical to rounded to elongate	Squat to elliptical to domed	Rounded
Epithallial cell dimensions	ND	L = 5-7; D = 5-7	L = 2-7; D = 5-7	L = 5-7; D = 2-7	L = 5-7; D = 5-7	L = 5-7; D = 5-7	L = 5-8; D = 2-7	L = 2-5; D = 2-5	L = 5-7; D = 5-7
Subepithallial cell shape	Square to rectangular	Square to rectangular	Square to rectangular	Rectangular	Square to rectangular	Square to rectangular	Rectangular	Square to elongate	Elongate
Subepithallial cell dimensions	ND	L = 5-15; D = 5-10	L = 3-10; D = 4-7	L = 5-12; D = 2-7	L = 5-12; D = 5-7	L = 7-10; D = 5-7	L = 10-12; D = 5-7	L = 3-7; D = 5-7	L = 5-10; D = 5-7
Cortical cell shape	ND	Square to rectangular	Square to rectangular	Square to rectangular	Square to beaded	Square to rectangular	Square to rectangular	Squat to square to rectangular	Square to rectangular
Cortical cell dimensions	ND	L = 7-10; D = 7-10	L = 5-12; D = 4-12	L = 5-15; D = 5-10	L = 7-10; D = 2-5	L = 7-25; D = 5-7	L = 7-10; D = 7-12	L = 5-15; D = 5-10	L = 5; D = 3-5
Medullary cell shape	ND	Rectangular	Rectangular to elongate	Rectangular to elongate	Rectangular to elongate	Rectangular to elongate	Square to rectangular	Square to rectangular	Rectangular to elongate
Medullary cell dimensions	ND	L = 22-44; D = 15-25	L = 10-30; D = 3-16	L = 12-25; D = 7-12	L = 5-25; D = 7-14	L = 15-20 D = 5-7	L = 15-17; D = 7-10	L = 20-22; D = 7-12	L = 12-20; D = 5-7
Erect filament cell shape	Square to rectangular with rounded corners	-	-	-	-	-	-	-	Square to rectangular to elongate with rounded corners
Erect filament cell dimensions	ND	-	-	-	-	-	-	-	L = 4-17; H = 2-12
Basal filament cell shape (in radial view)	Non-palisade, irregularly square	-	-	-	-	-	-	-	Non-palisade, irregularly square

Basal filament cell dimensions (in radial view)	L = 10-29; H = 10-22	-	-	-	-	-	-	-	L = 17-22; H = 10-15
Basal filament cell shape (in tangential view)	Rectangular to palisade-like	-	-	-	-	-	-	-	Rectangular to palisade-like
Basal filament cell dimensions (in tangential view)	L = 10-22; H = 5-10	-	-	-	-	-	-	-	L = 12 – 15; H = 5-7

[1]Data for *C. agulhense* have been taken from the description and Table S2 from van der Merwe *et al.* (2015).

TABLE 4. Comparison of the reproductive structures of South African species that would previously have been assigned to *Spongites*. Unless otherwise stated, all measurements are in micrometres. L and D = length and diameter respectively. ND = No data provided.

Character	*Chamberlainium agulhense*[1]	*Chamberlainium capense*	*Chamberlainium cochleare*	*Chamberlainium glebosum*	*Chamberlainium impar*	*Chamberlainium natalense*	*Chamberlainium occidentale*	*Chamberlainium tenue*	*Pneophyllum neodiscoideum*
Spermatangial conceptacle elevation	Raised to occasionally flush	Raised	Raised to occasionally flush	Raised	Slightly raised becoming flush with maturity	Raised	Raised	Raised	Slightly raised to flush
Mature spermatangial conceptacle external diameter	150-260 (340)	233-392	123-306	235-345	160-221	110-130	245-333	108-120	81-103
Mature spermatangial conceptacle chamber diameter	98-160	123-201	103-162	132-157	170-213	64-120	110-147	110-120	83-98
Mature spermatangial conceptacle chamber height	25-40	39-66	20-49	46-49	39-73	25-69	27-51	34-39	34-39
Mature spermatangial pore characteristics	Pore opening initially occluded by a mucilage plug, later by extruding filaments that project out and above the pore opening	Pore opening occluded by a mucilage plug	Pore opening occluded by a mucilage plug	Pore opening occluded by a mucilage plug	Pore opening occluded by either a mucilage plug or more commonly a mucilage spout	Pore opening occluded a by mucilage plug	Pore opening occluded by a mucilage plug	Pore opening occluded by a mucilage plug	Pore opening occluded by a mucilage plug
Carpogonial conceptacle elevation	None observed	None observed	None observed	None observed	Flush to sunken	Raised	Raised	None observed	Only buried carpogonial conceptacles observed
Mature carpogonial conceptacle external diameter	-	-	-	-	196-294	113-208	172-196	-	-

Mature carpogonial conceptacle chamber diameter	-	-	-	-	110-135	56-76	91-125	-	-
Mature carpogonial conceptacle chamber height	-	-	-	-	29-54	17-22	27-34	-	-
Carposporangial conceptacle elevation	Raised[2]	None observed	None observed	None observed	Raised to flush to sunken	Slightly raised	Raised	None observed	Flushed to slightly raised
Mature carposporangial conceptacle external diameter	200-460	-	-	-	420-550	301-502	294-319	-	345-588
Mature carposporangial conceptacle chamber diameter	118-220	-	-	-	225-233	137-169	149-194	-	127-157
Mature carposporangial conceptacle chamber height	56-64	-	-	-	91-96	34-74	88-110	-	29-71
Mature carposporangial pore characteristics	Pore opening appears to be occluded by a small corona of filaments; canal tapered towards surface[3]	-	-	-	Pore opening occluded by mucilage plug; canal tapered towards surface	Pore opening occluded by corona; canal tapered towards surface	Occlusion of pore opening unknown; canal tapered towards surface	-	Pore opening and canal occluded by a prominent mucilage plug; canal straight-sided
No. of cells in gonimoblast filament	4-7	-	-	-	5-7	5-7	5-7	-	6-7
Fusion cell shape	Discontinuous	-	-	-	Discontinuous	Discontinuous	Discontinuous	-	Discontinuous
Tetrasporangial development	Type 1	Type 1	Type 1	Type 1	Type 1	Type 1	Type 1	Type 1	Type 2
Tetrasporangial conceptacle elevation	Raised	Raised	Raised to flush to slightly sunken	Raised	Slightly raised becoming flush with maturity	Raised to flush	Raised	Raised to slightly sunken	Flush to sunken to raised

Mature tetrasporangial conceptacle external diameter	220-450	355-466	191-466	294-627	294-490	221-343	404-625	343-441	490-660
Mature tetrasporangial conceptacle chamber diameter	137-196	157-299	179-294	135-265	270-352	147-196	206-365	196-208	172-225
Mature tetrasporangial conceptacle chamber height	66-108	74-125	59-110	44-110	98-103	44-96	110-147	76-118	44-74
Mature tetrasporangial pore characteristics	ND	Pore opening occluded by a corona of filaments	Pore opening occluded by a mucilage plug	Pore opening unoccluded	Pore opening occluded by a mucilage plug	Pore opening occluded by a large corona	Pore opening unoccluded; pore slightly sunken below the surrounding roof	Pore opening occluded by a mucilage plug; pore slightly sunken below the surrounding roof	Pore opening and canal occluded by a prominent mucilage plug
Thickness of mature tetrasporangial conceptacle roof	29-47	47-96	29-76	27-115	47-61	27-66	42-83	15	39-44
No. of cells (incl. epithallial cells) in mature tetrasporangial conceptacle roof	4-8	5-7	6-8	4-8 (9)	6-7	6-8	5-7	5-7	6-22
Depth (no. of cells) of mature tetrasporangial conceptacle floor	10-15	11-17	12-22	11-24	15-21	12-21	16-19	12-16	15-30
Shape of pore canal	Pore canal not arching, tapered towards surface[4]	Pore canal arching, tapered towards surface	Pore canal not arching, tapered towards the surface or straight in very mature conceptacles	Pore canal not arching, tapered towards surface	Pore canal not arching, tapered towards surface	Pore canal not arching, tapered towards the surface or straight in very mature conceptacles	Pore canal arching, tapered towards surface	Pore canal arching, tapered towards surface	Pore canal not arching, remains straight sided
Tetrasporangia dimensions	ND	L = 51-130; D = 22-44	L = 47-79; D = 20-40	L = 29-113; D = 5-69	L = 54-98; D = 29-44	L = 44-81; D = 20-49	L = 74-152; D = 42-61	L = 49-76; D = 27-59	L = 42-69; D = 20-39
Tetrasporangia arrangement	Peripheral	Peripheral, may appear distributed across chamber floor	Peripheral	Peripheral	Peripheral	Peripheral, may appear distributed across chamber floor	Peripheral, may appear distributed across chamber floor	Peripheral, may appear distributed across chamber floor	Peripheral, may appear distributed across chamber floor

		as columella disintegrates				as columella disintegrates	as columella disintegrates	as columella disintegrates	as columella disintegrates
Central columella	Prominent; disintegrates to form a low mound with maturity	Prominent; disintegrates to form a low mound with maturity	Prominent; disintegrates to form a low mound with maturity	Prominent; disintegrates to low mound with maturity	Prominent; persists to maturity	Prominent; disintegrates to form a low mound with maturity	Prominent; disintegrates to form a low mound with maturity	Prominent; disintegrates to form a low mound with maturity	Prominent; disintegrates to form a low mound with maturity
Conceptacles buried or shed	Shed	Shed	Shed	Shed	Shed	Conceptacles mostly shed; occasionally tetrasporangia and spermatangia may be found buried	Shed	Shed	Conceptacles of all kinds found buried

[1] Data for *C. agulhense* have been taken from the description and Table S2 from van der Merwe *et al.* (2015).

[2] van der Merwe *et al*. (2015: 477) states that carpogonial conceptacles were not observed in *C. agulhense*. However, their Table S2 contains measurements for carpogonial conceptacles. The Table S2 column appears to have been incorrectly labelled as those measurements are more consistent with the carposporangial conceptacle measurements reported for the species (G.W. Maneveldt *pers. com*.).

[3] See van der Merwe *et al*. (2015: 482, Fig. 20).

[4] van der Merwe *et al.* (2015: 477, Fig. 23) did not describe the tapering of the pore canal, but it is evident in that publication.

TABLE 5. Characters found to be informative among South African species that would previously have been assigned to *Spongites*.

Character	*Chamberlainium agulhense*[1]	*Chamberlainium capense*	*Chamberlainium cochleare*	*Chamberlainium glebosum*	*Chamberlainium impar*	*Chamberlainium natalense*	*Chamberlainium occidentale*	*Chamberlainium tenue*	*Pneophyllum neodiscoidium*
Endemic	Yes	Yes	Yes	Yes	Yes	Yes	No (Namibia and South Africa)	Yes	Yes
Geographical distribution	Restricted distribution (± 10 km) along the southern west coast	Restricted distribution (± 43 km) along the southern west coast	Widely distributed (± 1,700 km) along the southern and eastern coasts	Disjunct distribution (± 220 and ± 200 km) along the west coast	Distributed (± 170 km) along the southern west coast	Widely distributed (± 1,720 km) along the southern west to eastern coasts	Widely distributed (± 1,200 km) along the west coast and southern west coasts	Widely distributed (± 1,200 km) along the south and east coasts	Distributed (± 220 km) along the southern west coast
Substrate	Epilithic	Epilithic on bedrock and boulders; epizoic on *S. cochlear* shells	Eplithic on bedrock, epizoic on limpet shells, especially *S. cochlear*	Epilithic on bedrock	Epilithic on primary bedrock	Largely epilithic on boulders and pebbles; occasionally epilithic on bedrock; epizoic on winkle shells	Epilithic on bedrock; epizoic on *S. cochlear* shells	Epilithic on bedrock	Epilithic on bedrock, boulders and pebbles, epizoic on winkle shells
Habitat	High (mostly) to mid-intertidal	Mid-intertidal (rock pools mostly) to low intertidal.	Mid- to low intertidal.	High to mid-shore (mostly) to occasionally on the low shore.	Mid- to low intertidal.	Mid- to low intertidal rock pools.	Mid- to low (largely) intertidal	High (largely) intertidal and mid-shore rock pools	Mid- to low intertidal rock pools.
Growth form	Encrusting (smooth)	Encrusting (smooth), becoming variably lumpy and slightly protuberant	Encrusting (smooth)	Lumpy, becoming highly protuberant	Encrusting (smooth), orbicular becoming confluent	Encrusting (smooth)	Encrusting (smooth) to warty (mostly) to lumpy, becoming slightly protuberant	Encrusting (smooth)	Primary thallus encrusting (smooth). Secondary thallus, discoid with orbicular protrusions that often produce crowded, contiguous, swollen protuberances
Habit	Individual thalli discernible, not fusing	Individual thalli discernible, not fusing	Individual thalli not discernible, fusing to form large expanses	Individual thalli discernible, not fusing	Individual thalli discernible, not fusing	Individual thalli discernible, not fusing	Individual thalli discernible, not fusing	Individual thalli discernible, not fusing	Individual primary thalli not discernible, fusing. Secondary discoid protrusions discernible, not fusing

Tables

Thallus construction	Dimerous	Monomerous	Monomerous	Monomerous	Monomerous	Monomerous	Monomerous	Monomerous	Primary thallus dimerous, becoming secondarily monomerous
Colour of living thalli (in well-lit conditions)	Brownish-pink	Bright to dusky pink	Greyish	Brownish pink to grey	Yellowish to yellow brown	Blue-grey	Brownish beige	Yellowish to bright pink	Pink to light purple to yellow brown
Trichocyte arrangement	None observed	Common, solitary (mostly) to paired	Common, solitary (mostly) to clustered, up to 6 (separated by normal vegetative filaments)	None observed	Rare, solitary to paired	Rare, solitary (mostly) to clustered, up to 6 (separated by normal vegetative filaments)	Common, solitary (mostly) to clustered, up to 6 (separated by normal vegetative filaments)	Common, solitary (mostly) to paired	None observed
No. of epithallial cell layers	1-3 (mostly 1-2)	1	1	1	4-6 (9)	1	1	1	2-4
Tetrasporangial development	Type 1	Type 1	Type 1	Type 1	Type 1	Type 1	Type 1	Type 1	Type 2

[1]Data for *C. agulhense* have been taken from the description and Table S2 from van der Merwe *et al.* (2015).

TABLE 6. A comparison of the appearance and vegetative structure of *C. cochleare* and *C. natalense* against the type of *S. yendoi*, the type of *L. natalense*, and Chamberlain's (1993) concept of *S. yendoi* from South Africa. Data from Chamberlain (1993) have been taken from both the descriptions and the figures. Unless otherwise stated, all measurements are in micrometres. ND = no data provided. L and D = length and diameter respectively.

Character	*Goniolithon yendoi* (type) (Chamberlain 1993)	South African *Spongites yendoi* (Chamberlain 1993)	*Chamberlainium cochleare* (This study)	*Lithophyllum natalense* (type) (Chamberlain 1993)	*Chamberlainium natalense* (This study)
Growth form	Encrusting (flat) with irregularly bumpy surface	Encrusting (smooth) to lumpy to knobbly	Encrusting (smooth)	Encrusting (smooth)	Encrusting (smooth)
Thallus construction	Monomerous	Monomerous	Monomerous	Monomerous	Monomerous
Maximum thallus thickness	ND	1000	370	ND	800
Habit	-	Individual thalli not discernible, fusing to form large expanses	Individual thalli not discernible, fusing to form large expanses	-	Individual thalli discernible, not fusing
Trichocytes	Solitary to paired	Solitary to paired	Common, solitary (mostly) to clustered, up to 6 (separated by normal vegetative filaments)	ND	Rare, solitary (mostly) to clustered, up to 6 (separated by normal vegetative filaments)
Trichocyte shape	Elongate	Bottle-shaped	Bottle-shaped	-	Bottle-shaped

Trichocyte dimensions	L = 15; D = 8	L = 10-20; D = 6-13	L = 15-27; D = 7-12	-	L = 12-29; D = 7-10
Trichocytes buried	ND	Yes	No	-	No
No. of epithallial cell layers	1	1	1	ND	1
Epithallial cell shape	Elliptical	Elliptical	Elliptical to domed	-	Flattened to elliptical
Epithallial cell dimensions	ND	L = 2-5; D = 3-8	L = 2-7; D = 5-7	-	L = 5-7; D = 5-7
Subepithallial cell shape	ND	Irregular in appearance	Square to rectangular	ND	Square to rectangular
Subepithallial cell dimensions	ND	ND	L = 3-10; D = 4-7	-	L = 7-10; D = 5-7
Cortical cell shape	Squarish	Square to elongate	Square to rectangular	Elongate	Square to rectangular
Cortical cell dimensions	L = 3-10; D = 3-8	L = 5-10; D = 3-8	L = 5-12; D = 4-12	L = 4-11; D = 4-8	L = 7-25; D = 5-7
Medullary cell shape	Elongate	Rectangular to elongate	Rectangular to elongate	Mainly squarish	Rectangular to elongate
Medullary cell dimensions	L = 6-12; D = 3-8	L = 10-27; D = 3-7	L = 10-30; D = 3-16	L = 10-25; D = 7-10	L = 15-20 D = 5-7

TABLE 7. A comparison of the reproductive anatomy of *C. cochleare* and *C. natalense* against the type of *S. yendoi* and the type of *L. natalense* and Chamberlains' (1993) concept of *S. yendoi* from South Africa. Data from Chamberlain (1993) have been taken from both the descriptions and the figures. Unless otherwise stated, all measurements are in micrometres. ND = no data provided. L and D = length and diameter respectively.

Character	*Goniolithon yendoi* (type) (Chamberlain 1993)	*South African Spongites yendoi* (Chamberlain 1993)	*Chamberlainium cochleare* (This study)	*Lithophyllum natalense* (type) (Chamberlain 1993)	*Chamberlainium natalense* (This study)
Spermatangial conceptacle elevation	Flush to raised	Raised	Raised to occasionally flush	Flushed to somewhat sunken	Raised
Mature spermatangial conceptacle external diameter	85-110	250	123-306	ND	110-130
Mature spermatangial conceptacle chamber diameter	ND	117-169	103-162	70-80	64-120
Mature spermatangial conceptacle chamber height	ND	52-60	20-49	25-35	25-69
Mature spermatangial pore characteristics	-	-	Occluded by a mucilage plug	-	Occluded by mucilage plug
Carpogonial conceptacle elevation	Sunken	Sunken	None observed	None observed	Raised
Mature carpogonial conceptacle external diameter	ND	ND	-	-	208-225
Mature carpogonial conceptacle chamber diameter	ND	ND	-	-	56-76
Mature carpogonial conceptacle chamber height	ND	ND	-	-	17-22

Carposporangial conceptacle elevation	None observed	Raised	None observed	None observed	Slightly raised
Mature carposporangial conceptacle external diameter	-	to 430	-	-	172-270
Mature carposporangial conceptacle chamber diameter	-	138-234 (450)	-	-	137-169
Mature carposporangial conceptacle chamber height	-	52-109	-	-	34-74
Mature carposporangial pore characteristics	-	Pore opening not occluded	-	-	Pore occluded by corona; canal tapered towards surface; terminal initials near base of canal point downward
No. of cells in gonimoblast filament	-	7	-	-	5-7
Fusion cell shape	-	Continuous	-	-	Discontinuous
Tetrasporangial conceptacle elevation	Flush to raised	Raised	Raised to flush to slightly sunken	Flushed to somewhat sunken	Raised above to flush
Mature tetrasporangial conceptacle external diameter	220-340	to 430	191-466	ND	221-343
Mature tetrasporangial conceptacle chamber diameter	170	147-207	179-294	150-250[1]	147-196
Mature tetrasporangial conceptacle chamber height	80	62-117	59-110	60	44-96
Mature tetrasporangial pore characteristics/occlusions	-	-	Occluded by a mucilage plug	-	Pore occluded by corona

Thickness of mature tetrasporangial conceptacle roof	30	26-65	29-76	50	27-66
No. of cells (incl. epithallial cells) in mature tetrasporangial conceptacle roof filaments	6	ND	6-8	to 6	6-8
Depth (no. of cells) of mature tetrasporangial conceptacle floor	ND	ND	12-22	ND	12-21
Shape of pore canal	Pore canal tapered towards surface or straight in very mature conceptacles	Pore canal tapered towards surface or straight in very mature conceptacles	Tapered towards the surface or straight in very mature conceptacles; terminal initials near base of canal point downward	Pore canal tapered towards the surface[2]	Tapered towards the surface or straight in very mature conceptacles; terminal initials near base of canal point downward
Tetrasporangia dimensions (L = length; D = diameter)	ND	ND L = 43-78; D = 15-47	L = 47-79; D = 20-40	ND	L = 44-81; D = 20-49
Tetrasporangia arrangement	Peripheral	Peripheral	Peripheral	Peripheral	Peripheral, may appear distributed across chamber floor as columella disintegrates
Central columella	Present	Prominent; disintegrates to form a low mound with maturity	Present; disintegrates to low mound	Present	Present; disintegrates to low mound
Conceptacles buried or shed	ND	Conceptacles mostly shed; occasionally spermatangia may be found buried	Shed	Conceptacles mostly shed; occasionally spermatangia may be found buried	Conceptacles mostly shed; occasionally tetrasporangia and spermatangia may be found buried within the thallus

[1] Chamberlain (1993, pg. 111) makes reference to a "conceptacle roof diameter" of 150-250 µm, this is actually the conceptacle diameter consistent with this entity.

[2] Chamberlain (1993, pg. 112) did not describe the shape of the pore canal, but it is evident in figure 54 of that publication.

TABLE 8. A comparison of the appearance and vegetative structure of *C. impar* against the type of *L. impar* and Chamberlains' (1994b) concept of *S. impar* from South Africa. Data from Chamberlain (1994b) have been taken from both the descriptions and the figures. Unless otherwise stated, all measurements are in micrometres. ND = no data provided. L and D = length and diameter respectively.

Character	*Lithophyllum impar* (type) (Foslie 1909)	South African *Spongites impar* (Chamberlain 1994b)	*Chamberlainium impar* (This study)
Growth form	Encrusting, highly wavy to somewhat knotted	Encrusting, becoming crested or convoluted	Encrusting (smooth), orbicular becoming confluent
Thallus construction	Monomerous	Monomerous	Monomerous
Maximum thallus thickness	ND	750	1800
Habit	Individual thalli discernible, not fusing	Individual thalli discernible, not fusing	Individual thalli discernible, not fusing
Trichocytes	ND	Absent	Rare, solitary to paired
Trichocyte dimensions	ND	-	L = 22-39; D = 10-12
No. of epithallial cell layers	ND	Up to 6 cells	4-6 (9)
Epithallial cell shape	Square to elongate	Elongate	Elliptical to rounded
Epithallial cell dimensions	L = 6-9; D = 5-7	L = 2.5-4; D = 3-6	L = 5-7; D = 5-7
Subepithallial cell shape	ND	ND	Square to rectangular
Subepithallial cell dimensions	ND	-	L = 5-12; D = 5-7
Cortical cell shape	ND	ND	Square to beaded
Cortical cell dimensions	L = 6-9; D = 5-7	Squarish	L = 7-10; D = 2-5
Medullary cell shape	ND	L = 2.5-10; D = 3-5	Rectangular to elongate
Medullary cell dimensions	L = 11-25; D = 5-9	ND	L = 5-25; D = 7-14

TABLE 9. A comparison of the reproductive anatomy of *C. impar* against the type of *L. impar* and Chamberlains' (1994b) concept of *S. impar* from South Africa. Data from Chamberlain (1994b) have been taken from both the descriptions and the figures. Unless otherwise stated, all measurements are in micrometres. ND = no data provided. L and D = length and diameter respectively.

Character	*Lithophyllum impar* (type) (Foslie 1909)	*South African Spongites impar* (Chamberlain 1994b)	*Chamberlainium impar* (This study)
Spermatangial conceptacle elevation	ND	Slightly raised becoming flush with maturity	Slightly raised becoming flush with maturity
Mature spermatangial conceptacle external diameter	ND	ND	160-221
Mature spermatangial conceptacle chamber diameter	ND	150-200	170-213
Mature spermatangial conceptacle chamber height	ND	35-40	39-73
Mature spermatangial pore characteristics	ND	Pore opening occluded by a mucilage spout	Pore opening occluded by either a mucilage plug or more commonly a mucilage spout
Carpogonial conceptacle elevation	ND	None observed	Flush to sunken
Mature carpogonial conceptacle external diameter	ND	-	196-294
Mature carpogonial conceptacle chamber diameter	ND	-	110-135
Mature carpogonial conceptacle chamber height	ND	-	29-54
Carposporangial conceptacle elevation	ND	None observed	Raised to flush to sunken
Mature carposporangial conceptacle external diameter	ND	-	420-550
Mature carposporangial conceptacle chamber diameter	ND	-	225-233
Mature carposporangial conceptacle chamber height	ND	-	91-96
Mature carposporangial pore characteristics	ND	-	Pore opening occluded by mucilage plug; canal tapered towards surface
No. of cells in gonimoblast filament	ND	-	5-7
Fusion cell shape	ND	-	Discontinuous

Tetrasporangial conceptacle elevation	ND	Slightly raised becoming flush with maturity	Slightly raised becoming flush with maturity
Mature tetrasporangial conceptacle external diameter	ND	ND	294-490
Mature tetrasporangial conceptacle chamber diameter	180-300	180-247	270-352
Mature tetrasporangial conceptacle chamber height	60-100	70-104	98-103
Mature tetrasporangial pore characteristics	ND	Pore opening occluded by a mucilage plug[1]	Pore opening occluded by a mucilage plug
Thickness of mature tetrasporangial conceptacle roof	ND	39-50	47-61
No. of cells (incl. epithallial cells) in mature tetrasporangial conceptacle roof	ND	to 9	6-7
Depth (no. of cells) of mature tetrasporangial conceptacle floor	ND	ND	15-21
Shape of pore canal	ND	Pore canal not arching, tapered towards surface[2]	Pore canal not arching, tapered towards surface
Tetrasporangia dimensions	ND	L = 55-119; D = 36-38	L = 54-98; D = 29-44
Tetrasporangia arrangement	ND	Peripheral	Peripheral
Central columella	ND	Prominent; may project into pore canal; disintegrates to low mound with maturity	Prominent; persists to maturity
Conceptacles buried or shed	ND	Shed	Shed

[1] Chamberlain (1994b, pg. 115) did not describe an occluded pore, but it is evident in figure 62 of that publication.

[2] Chamberlain (1994b, pg. 115) did not describe the shape of the pore canal, but it is evident in figure 62 of that publication.

TABLE 10. A comparison of the appearance and vegetative structure of *P. neodiscoideum* against the type of *L. discoideum* (Penrose & Woelkerling 1988) and Chamberlains' (1994b) concept of *S. discoideus* from South Africa. Data from Chamberlain (1994b) have been taken from both the descriptions and the figures. Unless otherwise stated, all measurements are in micrometres. ND = no data provided. L and D = length and diameter respectively.

Character	*Lithophyllum discoideum* (type) (Penrose & Woelkerling 1988)	South African *Spongites discoideus* (Chamberlain 1994b)	*Pneophyllum neodiscoideum* (This study)
Growth form	More or less circular, smooth-surfaced thalli	Primary thallus encrusting (smooth). Secondary thallus, discoid, circular, rosette-like, crested and protuberant	Primary thallus encrusting (smooth). Secondary thallus, discoid with orbicular protrusions that often produce crowded, contiguous, swollen protuberances
Maximum protuberance height	-	-	10 mm
Thallus construction	Primary thallus dimerous, secondary thallus monomerous	Primary thallus dimerous, becoming secondarily monomerous	Primary thallus dimerous, becoming secondarily monomerous
Maximum thallus thickness	ND	550	Primary thallus 310; Secondary thallus 3000
Habit	ND	Individual primary crusts not discernible, fusing. Secondary crusts discernible, not fusing	Individual primary thalli not discernible, fusing. Secondary discoid protrusions discernible, not fusing
Trichocytes	Absent	Rare	None observed
Trichocyte dimensions	-	ND	-
No. of epithallial cell layers	ND	4	2-4
Epithallial cell shape	ND	Flattened	Rounded

Epithallial cell dimensions	L = 4; D = 7	L = 2-3; D = 4-6	L = 5-7; D = 5-7
Subepithallial cell shape	ND	Elongate	Elongate
Subepithallial cell dimensions	ND	ND	L = 5-10; D = 5-7
Cortical cell shape	ND	Elongate	Square to rectangular
Cortical cell dimensions	L = 3-12; D = 4-7	L = 4-17; D = 4-11	L = 5; D = 3-5
Medullary cell shape	ND	Squarish to shorter than wide	Rectangular to elongate
Medullary cell dimensions	ND	ND	L = 12-20; D = 5-7
Erect filament cell shape	-	Elongate	Square to rectangular to elongate with rounded corners
Erect filament cell dimensions	-	L = 4-17; D = 4-11	L = 4-17; H = 2-12
Basal filament cell shape (in radial view)		Squarish to shorter than wide	Non-palisade, irregularly square
Basal filament cell dimensions (in radial view)	-	L = 17-16; D = 15-16	L = 17-22; H = 10-15
Basal filament cell shape (in tangential view)	-	-	Rectangular to palisade-like
Basal filament cell dimensions (in tangential view)	-	-	L = 12 – 15; H = 5-7

TABLE 11. A comparison of the reproductive anatomy of *P. neodiscoideum* against the type *L. discoideum* (Penrose & Woelkerling 1988) and Chamberlains' (1994b) description of *S. discoideus* from South Africa. Data from Chamberlain (1994b) have been taken from both the descriptions and the figures. Unless otherwise stated, all measurements are in micrometres. ND = no data provided. L and D = length and diameter respectively.

Character	*Lithophyllum discoideum* (type) (Penrose and Woelkerling 1988)	South African *Spongites discoideus* (Chamberlain 1994b)	*Pneophyllum neodiscoideum* (This study)
Spermatangial conceptacle elevation	ND	Appears flush[1]	Slightly raised to flush
Mature spermatangial conceptacle external diameter	ND	ND	81-103
Mature spermatangial conceptacle chamber diameter	120	52-91	83-98
Mature spermatangial conceptacle chamber height	48	17-31	34-39
Mature spermatangial pore characteristics	ND	None	Pore opening occluded by a mucilage plug
Carpogonial conceptacle elevation	None observed	None observed	Only buried carpogonial conceptacles observed
Mature carpogonial conceptacle external diameter	-	-	-
Mature carpogonial conceptacle chamber diameter	-	-	-
Mature carpogonial conceptacle chamber height	-	-	-
Carposporangial conceptacle elevation	None observed	Appears flush[2]	Flushed to slightly raised
Mature carposporangial conceptacle external diameter	-	ND	345-588
Mature carposporangial conceptacle chamber diameter	-	146-200	127-157
Mature carposporangial conceptacle chamber height	-	52-65	29-71
Mature carposporangial pore characteristics	-	Pore opening and canal occluded by a prominent mucilage plug; canal straight-sided	Pore opening and canal occluded by a prominent mucilage plug; canal straight-sided
No. of cells in gonimoblast filament	-	7	6-7

Fusion cell shape	-	Wide and thin, appears discontinuous[3]	Discontinuous
Tetrasporangial development	Type 1	Type 1	Type 2
Tetrasporangial conceptacle elevation	None observed	Raised[4]	Flush to sunken to raised
Mature tetrasporangial conceptacle external diameter	-	ND	490-660
Mature tetrasporangial conceptacle chamber diameter	-	169-190	172-225
Mature tetrasporangial conceptacle chamber height	-	52-65	44-74
Mature tetrasporangial pore characteristics	-	Pore opening occluded by a mucilage plug	Pore opening and canal occluded by a prominent mucilage plug
Thickness of mature tetrasporangial conceptacle roof	-	35-100	39-44
No. of cells (incl. epithallial cells) in mature tetrasporangial conceptacle roof	-	ND	6-22
Depth (no. of cells) of mature tetrasporangial conceptacle floor	-	ND	15-30
Shape of pore canal	-	Pore canal remains straight-sided	Pore canal not arching, remains straight sided
Tetrasporangia dimensions	-	L = 35-50; D = 13-26	L = 42-69; D = 20-39
Tetrasporangia arrangement	-	Peripheral, may appear distributed across chamber floor as columella disintegrates[5]	Peripheral, may appear distributed across chamber floor as columella disintegrates
Central columella	-	Present	Prominent; disintegrates to form a low mound with maturity
Conceptacles buried or shed	-	Conceptacles of all kinds are found buried within the thallus	Conceptacles of all kinds found buried

[1] Chamberlain (1994b, pg. 115) did not describe the elevation of the spermatangial conceptacle, but it is evident in figure 40 of that publication.

[2] Chamberlain (1994b, pg. 115) did not describe the elevation of the carposporangial conceptacle, but it is evident in figures 37 and 38 of that publication.

[3] Chamberlain (1994b, pg. 115) did not describe a discontinuous fusion cell, but a discontinuous one is evident in figures 37and 38 of that publication.

[4] Chamberlain (1994b, pg. 115) did not describe the elevation of the tetrasporangial conceptacle, but it is evident in figures 43 and 48 of that publication.

[5] Chamberlain (1994b, 115) did not describe the tetrasporangia distribution, but it is evident in figure 39 of that publication.

Table 12. Characters considered by Caragnano *et al*. (2018) to be informative in distinguishing morpho-anatomically between *Chamberlainium*, *Pneophyllum* and *Spongites*, and the corresponding characters established for the taxa in the present study.

Character/Taxon	*Chamberlainium* (Caragnano *et al*. 2018)	*Chamberlainium* (this study)	*Pneophyllum* (Caragnano *et al*. 2018)	*Pneophyllum* (*P. neodiscoideum*, this study)	*Spongites* (Caragnano *et al*. 2018)
Thallus thickness	< 1 mm	≤ 2 mm	Generally < 200 µm, or filaments up 20 cells	< 1 mm (primary thalli), ≤ 3 mm (secondary thalli)	Up to several mm
Thallus construction	Dimerous or monomerous, but not both	Dimerous or monomerous, but not both	Dimerous	Primarily dimerous, but may become secondarily monomerous	Dimerous or monomerous
No. of epithallial cells	1-4	1-6 (9)	1	2-4	1-3
Trichocyte arrangement (when present)	Solitary, paired	Solitary, paired, clustered in horizontal fields	Solitary, paired	None observed	Solitary, horizontal fields, vertical rows
Separation within trichocyte fields (where appropriate)	ND	Separated by normal vegetative filaments	ND	-	ND
Development of tetra/bisporangial conceptacle roof	Type 1	Type 1	Type 2	Type 2	Type 1
Diameter of tetra/bisporangial conceptacle chambers	< 300 µm	Up to 365 µm	< 350 µm	< 350 µm	> 300 µm
No. of tetra/bisporangial conceptacle roof cells	≤ 8	≤ 8 (9)	< 8	Up to 22	> 8
Central columella present/absent in tetra/bisporangial conceptacle chambers	Absent or present	Present, but may disintegrate with maturity	Absent or present	Present	Present, poorly developed
Distribution of tetra/bisporangial in tetra/bisporangial conceptacle chambers	Peripheral or across chamber floor	Peripheral, but may appear across the chamber floor as central columella disintegrates	Peripheral	Peripheral	Peripheral

Figure captions

Fig. 1. Neighbour-Joining tree based on *psb*A sequences. Species with sequenced type/'topotype' material are highlighted in bold. Species names are followed (in brackets) by their specimen herbarium voucher number. Newly established South African species names are followed (in brackets) by their collection number as they are yet to be assigned official herbarium (L = Naturalis, Netherlands, Leiden) numbers. Bootstrap support (BS) values are provided at branch nodes; BS values < 75 % are not shown. The asterisk (*) indicates the molecular reference for the generitype of *Spongites*, *Spongites fruticulosus*.

Fig. 2. Neighbour-Joining tree based on *rbc*L sequences. Species with sequenced type/'topotype' material are highlighted in bold. Species names are followed (in brackets) by their specimen herbarium voucher number. Newly established South African species names are followed (in brackets) by their collection number as they are yet to be assigned official herbarium (L = Naturalis, Netherlands, Leiden) numbers. Bootstrap support (BS) values are provided at branch nodes; BS values < 75 % are not shown.

Fig. 3. Maximum Likelihood tree based on *psb*A sequences. Species with sequenced type/'topotype' material are highlighted in bold. The first set of vertical lines indicates the Primary Species Hypothesis as determined by ABGD and identify individual species. Species names are followed (in brackets) by their specimen herbarium voucher number. Newly established South African species (identified as boxed clades A-H) names are followed (in brackets) by their collection number as they are yet to be assigned official herbarium (L = Naturalis, Netherlands, Leiden) numbers. Bootstrap support (BS) values are provided at branch

nodes; BS values < 75 % are not shown. The asterisk (*) indicates the molecular reference for the generitype of *Spongites, Spongites fruticulosus*.

Fig. 4. Maximum Likelihood tree based on *rbc*L sequences. Species with sequenced type/'topotype' material are highlighted in bold. The first set of vertical lines indicate the Primary Species Hypothesis as determined by ABGD and identify individual species. Species names are followed (in brackets) by their specimen herbarium voucher number. Newly established South African species (identified as boxed clades A-H) names are followed (in brackets) by their collection number as they are yet to be assigned official herbarium (L = Naturalis, Netherlands, Leiden) numbers. Bootstrap support (BS) values are provided at branch nodes; BS values < 75 % are not shown.

Fig. 5. Maximum Likelihood tree based on concatenated *psb*A and *rbc*L sequences. Species with sequenced type/'topotype' material are highlighted in bold. The first set of vertical lines indicate the Primary Species Hypothesis as determined by ABGD and identify individual species. Species names are followed (in brackets) by their specimen herbarium voucher number. Newly established South African species (identified as boxed clades A-H) names are followed (in brackets) by their collection number as they are yet to be assigned official herbarium (L = Naturalis, Netherlands, Leiden) numbers. Bootstrap support (BS) values are provided at branch nodes; BS values < 75 % are not shown.

Fig. 6. Gene tree topologies estimated in *BEAST for *C. occidentale* (clade F), *C. capense* (clade G) and *C. glebosum* (clade H) based on *psb*A (A) and *rbc*L (B) gene sequences (*psb*A, 851 bp; *rbc*L, 1365 bp), and the concatenated dataset (C). Posterior probabilities from the

*BEAST analysis are provided at the branch nodes. Scale bar indicates estimated mean evolutionary rate (0.0004 substitutions per site per year).

Fig. 7. Species tree topology estimated in *BEAST for *C. occidentale* (clade F), *C. capense* (clade G) and *C. glebosum* (clade H) based on the *psb*A and *rbc*L gene sequences, and the concatenated dataset. Posterior probabilities from the *BEAST analysis are provided at the branch nodes. Scale bar indicates estimated mean evolutionary rate (0.0004 substitutions per site per year).

Fig. 8. DensiTree representation of the consensus tree for *C. occidentale* (clade F), *C. capense* (clade G) and *C. glebosum* (clade H) with population sizes indicated as variably shaded (each shade representing a single sequence) line widths.

Fig. 9. Individual, thin, encrusting, epilithic thalli of *Chamberlainium agulhense* found in their common high intertidal habitat. Scale = 10 mm

Figures 10-22: *Chamberlainium capense*

Fig. 10. Encrusting to variably lumpy and slightly protuberant, epilithic thalli of *Chamberlainium capense* found in a mid-intertidal zone.

Figs 11-15. Habit and vegetative anatomy of *Chamberlainium capense*.

Fig. 11. Rock fragment showing holotype specimen (arrow) (L ???????, tetrasporangial). Scale bar = 20 mm.

Fig. 12. Encrusting to variably lumpy and slightly protuberant, epilithic thalli showing crusts abutting and easily discernible. Scale bar = 30 mm.

Fig. 13. Vertical section through the margin (arrow) showing the monomerous thallus construction with plumose medulla (M) giving rise to cortical filaments (C) that terminate in a single layer of epithallial cells (arrowhead) (UWC 16/17). Scale bar = 50 μm.

Fig. 14. Vertical section of the inner thallus showing cell fusions (f) between adjacent medullary filaments (UWC 16/17). Scale bar = 20 μm.

Fig. 15. Vertical section of the outer thallus showing a single layer of epithallial cells (e) subtended by a layer of subepithallial initials (i). Note the paired, bottle-shaped trichocytes (t) (UWC 16/24). Scale bar = 20 μm.

Figs 16-18. Spermatangial anatomy of *Chamberlainium capense* (UWC 16/21).

Fig. 16. Vertical section through the outer thallus showing a spermatangial conceptacle primordium with peripheral roof development (black arrows) and simple, spermatangial systems (arrowheads) confined to the conceptacle floor. Note the protective layer of epithallial cells (white arrow). Scale bar = 50 μm.

Fig. 17. Vertical section through a mature, raised spermatangial conceptacle showing the mucilage plug (white arrowhead) that occludes the pore opening and simple, spermatangial systems (black arrowheads) confined to the conceptacle floor. Scale bar = 50 μm.

Fig 18. Magnified view through a mature spermatangial conceptacle showing the mucilage plug (white arrowhead) that occludes the pore opening and simple, spermatangial systems (black arrowheads) confined to the conceptacle floor. Note that the pore canal is lined with terminal, elongate initials (black arrows) that project into the pore canal as papillae. Scale bar = 20 μm.

Figs 19-22. Tetrasporangial conceptacle anatomy of *Chamberlainium capense.*

Fig. 19. Vertical section through the outer thallus showing a later stage tetrasporangial conceptacle primordium with peripheral roof development (arrowheads) and tetrasporangial initials (t) arranged peripherally around a central columella (c). Note the persisting layer of protective epithallial cells (arrow) (L ???????). Scale bar = 50 μm.

Fig. 20. Vertical section through a mature, raised tetrasporangial conceptacle showing tetrasporangia (t) with a stalk cell (black arrowhead), peripherally arranged around a well-defined central columella (C). Note the remains of a corona (white arrow) that surrounds the pore opening (L ???????). Scale bar = 50 μm.

Fig. 21. Vertical section through a mature, raised tetrasporangial conceptacle showing tetrasporangia (t) with stalk cells (black arrowheads), appearing to be arranged across the chamber floor as the columella (c) has disintegrated. Note the absence of the corona (white arrow) (UWC 16/09). Scale bar = 50 μm.

Fig. 22. Magnified view of the pore canal of a mature tetrasporangial conceptacle showing the base of the pore canal sunken (arrowheads) into the chamber with terminal, elongate initials near the base pointing downward (black arrows) and the remains of a corona (white arrow) that surrounds and occludes the pore opening. (L ???????). Scale bar = 20 μm.

Figures 23-37: *Chamberlainium cochleare*

Fig. 23. Encrusting, thin epilithic thalli of *Chamberlainium cochleare*, which is commonly associated with the territorial, gardening limpet *Scutellastra cochlear* within the Cochlear zone on the low shore. Scale bar = 30 mm

Figs 24-28. Habit and vegetative anatomy of *Chamberlainium cochleare*.

Fig. 24. Rock fragment showing holotype specimen (L ???????, tetrasporangial). Scale bar = 20 mm.

Fig. 25. Encrusting, thin epilithic thalli showing coalescing crusts forming a large indistinguishable expanse. Scale bar = 30 mm.

Fig. 26. Vertical section through the margin (arrow) showing the monomerous thallus construction with plumose medulla (M) giving rise to cortical filaments (C) that terminate in a single layer of epithallial cells (arrowhead) (L ???????). Scale bar = 50 μm.

Fig. 27. Vertical section of the inner thallus showing a plumose medulla (M) giving rise to cortical filaments (C) and cell fusions (f) between adjacent medullary filaments (L ???????). Scale bar = 20 μm.

Fig. 28. Vertical section of the outer thallus showing a single layer of epithallial cells (e) subtended by a layer of subepithallial initials (i). Note the solitary, bottle-shaped trichocytes (t) that are separated by normal vegetative filaments and the cell fusions (f) between adjacent cortical filaments (L ???????). Scale bar = 20 μm.

Figs 29-31. Spermatangial anatomy of *Chamberlainium cochleare* (UWC 10/104).

Fig. 29. Vertical section through the outer thallus showing a spermatangial conceptacle primordium with peripheral roof development (black arrows) and simple spermatangial systems (black arrowheads) confined to the conceptacle floor. Note the protective layer of epithallial cells (white arrow) and the pattern of secondary growth (white arrowheads) suggesting successive production of this male conceptacle in the same area of a previous reproductive event. Scale bar = 50 μm.

Fig. 30. Vertical section through a mature, raised spermatangial conceptacle showing the mucilage plug (white arrowhead) that occludes the pore opening and simple, spermatangial systems (black arrowheads) confined to the conceptacle floor. Scale bar = 50 μm.

Fig. 31. Magnified view through a mature spermatangial conceptacle showing the mucilage plug (white arrowhead) that occludes the pore opening and simple, spermatangial systems (black arrowheads) confined to the conceptacle floor. Note that the pore canal is lined with terminal, elongate initials (black arrow) that project into the pore canal as papillae. Scale bar = 20 μm.

Figs 32-37. Tetrasporangial conceptacle anatomy of *Chamberlainium cochleare.*

Fig. 32. Vertical section through the outer thallus showing a slightly raised mature tetrasporangial conceptacle. Note the pattern of secondary growth (white arrowheads) suggesting successive production of this tetrasporangial conceptacle in the same area of a previous reproductive event (UWC 08/20). Scale bar = 100 μm.

Fig. 33. Vertical section through the outer thallus showing an early stage tetrasporangial conceptacle primordium with tetrasporangial initials (arrowheads) and a protective layer of epithallial cells (arrow) (L ???????). Scale bar = 50 μm.

Fig. 34. Vertical section through the outer thallus showing a later stage tetrasporangial conceptacle primordium with peripheral roof development (black arrowheads) and a developing central columella (white arrowhead). Note the persisting layer of protective epithallial cells (e) (L ???????). Scale bar = 50 μm.

Fig. 35. Vertical section through a maturing tetrasporangial conceptacle showing peripheral roof development (black arrowheads) and tetrasporangial initials (t) arranged peripherally around a central columella (between white arrowheads). Note the layer of protective epithallial cells (e) being shed (L ???????). Scale bar = 50 μm.

Fig. 36. Vertical section through a mature, raised tetrasporangial conceptacle showing tetrasporangia (t) with stalk cells (white arrowheads), peripherally arranged around a low mounded remnant of the central columella (C). Note the pore canal is lined with terminal, elongate initials (black arrowheads) that project into the pore canal as papillae and the mucilage plug (white arrow) that occludes the pore opening (UWC 08/20). Scale bar = 50 μm.

Fig. 37. Magnified view of the pore canal of a mature tetrasporangial conceptacle showing the base of the pore canal sunken (arrowheads) into the chamber with terminal, elongate initials near the base pointing downward (black arrows) and the mucilage plug (white arrow) that occludes the pore opening (UWC 08/20). Scale bar = 20 μm.

Figures 38-50: *Chamberlainium glebosum*

Fig. 38. Thick and lumpy to highly protuberant epilithic thalli of *Chamberlainium glebosum* found in the mid-intertidal zone. Scale bar = 20 mm

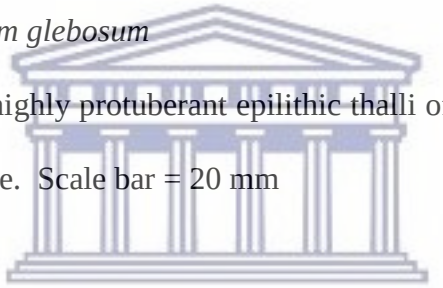

Figs 39-43. Habit and vegetative anatomy of *Chamberlainium glebosum*.

Fig. 39. Rock fragment with holotype specimen showing the region (arrow) of the holotype from which all analyses were done (L ???????, tetrasporangial). Scale bar = 20 mm.

Fig. 40. Magnified view showing highly protuberant nature of *C. glebosum* holotype specimen (L ???????). Scale bar = 2 mm.

Fig. 41. Vertical section through the margin (arrow) showing the monomerous thallus construction with plumose medulla (M) giving rise to cortical filaments (C) that terminate in a single layer of epithallial cells (arrowhead) (UWC 15/34). Scale bar = 100 μm.

Fig. 42. Vertical section of the inner thallus showing cell fusions (f) between adjacent medullary filaments (UWC 15/34). Scale bar = 10 μm.

Fig. 43. Vertical section of the outer thallus showing a single layer of epithallial cells (e) subtended by a layer of subepithallial initials (i). Note the cell fusions (f) between adjacent cortical filaments (UWC 15/34). Scale bar = 20 μm.

Figs 44-45. Spermatangial anatomy of *Chamberlainium glebosum* (UWC 15/34).

Fig. 44. Vertical section through the outer thallus showing spermatangial conceptacle primordium with peripheral roof development (black arrows) and simple spermatangial systems (arrowheads) confined to the conceptacle floor. Note the protective layer of epithallial cells (white arrow). Scale bar = 50 μm.

Fig. 45. Vertical section through the outer thallus showing a mature, raised spermatangial conceptacle with the mucilage plug (arrow) that occludes the pore opening and simple, spermatangial systems (white arrowheads) confined to the conceptacle floor. Note that the pore canal is lined with terminal, elongate initials (black arrowheads) that project into the pore canal as papillae. Scale bar = 50 μm.

Figs 46-50. Tetrasporangial conceptacle anatomy of *Chamberlainium glebosum.*

Fig. 46. Vertical section through the outer thallus showing an early stage tetrasporangial conceptacle primordium with peripherally arranged tetrasporangial initials (arrowheads) and a protective layer of epithallial cells (arrow) (UWC 15/17). Scale bar = 50 μm.

Fig. 47. Vertical section through the outer thallus showing a later stage tetrasporangial conceptacle primordium with peripheral roof development (black arrowheads) with a developing central columella (white arrowhead). Note the persisting layer of protective epithallial cells (arrow) (UWC 15/17). Scale bar = 50 μm.

Fig. 48. Vertical section through a maturing tetrasporangial conceptacle showing tetrasporangial initials (t) arranged peripherally around a central columella (between white

arrowheads). Note the layer of protective epithallial cells (arrow) being shed (L ???????). Scale bar = 50 μm.

Fig. 49. Vertical section through a mature, raised tetrasporangial conceptacle showing tetrasporangia (t) with stalk cells (white arrowheads), peripherally arranged around a well-defined central columella (C). Note the base of the pore canal sunken into the chamber with terminal, elongate initials near the base pointing downward (black arrowheads) (UWC 15/55). Scale bar = 100 μm.

Fig. 50. Magnified view of the pore canal of a mature tetrasporangial conceptacle showing terminal, elongate initials (arrows) that project into the pore canal as papillae and the base of the pore canal sunken (arrowheads) into the chamber with terminal, elongate initials near the base pointing downward. (UWC 15/55). Scale bar = 20 μm.

Figures 51-71: *Chamberlainium impar*

Fig. 51. Thick, encrusting and orbicular epilithic thalli of *Chamberlainium impar* that are characteristically pachydermatous like an elephant's skin, found in the low intertidal zone. Scale bar = 30 mm

Figs. 52-57. Habit and vegetative anatomy of *Chamberlainium impar*.

Fig. 52. Thick, encrusting and orbicular epilithic thalli showing crusts easily discernible. Scale bar = 20 mm.

Fig. 53. Thick, encrusting and seemingly confluent epilithic thalli showing raised margins that still make plants easily discernible. Scale bar = 20 mm.

Fig. 54. Vertical section through the margin (arrow) showing the monomerous thallus construction with plumose medulla (M) giving rise to cortical filaments (C) that terminate in multiple layers of epithallial cells (arrowhead) (UWC 13/22). Scale bar = 100 μm.

Fig. 55. Vertical section of the inner thallus showing cell fusions (f) between adjacent medullary filaments (UWC 13/22). Scale bar = 20 μm.

Fig. 56. Vertical section of the outer thallus showing a multi-layered epithallus (e) subtended by a layer of subepithallial initials (i). Note the solitary, bottle-shaped trichocyte (t) and cell fusions (arrowheads) between adjacent cortical filaments (UWC 13/22). Scale bar = 20 μm.

Fig. 57. Vertical section of the outer thallus showing a multi-layered epithallus (e) subtended by a layer of subepithallial initials (i) and a cell fusion (arrowhead) between adjacent cortical filaments. Note the solitary, bottle-shaped trichocyte (t) with intact trichome (arrow) (UWC 13/22). Scale bar = 20 μm

Figs 58-61. Spermatangial anatomy of *Chamberlainium impar*.

Fig. 58. Vertical section through the outer thallus showing a spermatangial conceptacle primordium with peripheral roof development (black arrows) and developing spermatangial systems (arrowheads) confined to the conceptacle floor. Note the protective layer of epithallial cells (white arrow) (UWC 13/22). Scale bar = 50 μm.

Fig. 59. Vertical section through the outer thallus showing a later stage spermatangial conceptacle primordium with developing mucilage spout (black arrow) and simple, spermatangial systems (arrowheads) confined to the conceptacle floor. Note the shedding of the protective layer of epithallial cells (white arrows) (UWC 13/22). Scale bar = 50 μm.

Fig. 60. Vertical section through a mature, sunken spermatangial conceptacle with its pore opening occluded by a mucilage spout (white arrow) and simple, spermatangial systems (black arrowheads) confined to the conceptacle floor (UWC 13/20). Scale bar = 50 μm.

Fig. 61. Magnified view through a mature spermatangial conceptacle showing the pore opening occluded by a mucilage spout (white arrow) and simple, spermatangial systems (black arrowheads) confined to the conceptacle floor. Note that the pore canal is lined with terminal,

elongate initials (black arrows) that project into the pore canal as papillae (UWC 13/20). Scale bar = 20 μm.

Figs 62-66. Female anatomy of *Chamberlainium impar*.

Fig. 62. Vertical section through a mature, flush carpogonial conceptacle (UWC 15/64). Scale bar = 20 μm.

Fig. 63. Magnified view of a mature carpogonial conceptacle with carpogonial branches comprised of a single support cell (s), a hypogynous cell (h), with sterile cell (arrowhead) attached, bearing a carpogonium (c) extended into a trichogyne (black arrows) that may projects out of the pore. Note that the pore canal is lined with terminal, elongate initials (white arrows) that project into the canal as papillae (UWC 15/64). Scale bar = 20 μm.

Fig. 64. Vertical section through a mature carposporangial conceptacle with a discontinuous central fusion cell (white arrowhead) and peripherally arranged gonimoblast filaments each terminating in a carposporangium (C). A mucilage plug (arrow) occludes the pore opening. Note, the base of the pore canal sunken into the conceptacle chamber with terminal, elongate initials near the base pointing downward (black arrowheads) (UWC 13/22). Scale bar = 50 μm.

Fig. 65. Magnified view of the pore canal of a mature carposporangial conceptacle showing the base of the pore canal sunken (arrowheads) into the conceptacle chamber with terminal, elongate initials near the base pointing downward (black arrows) (UWC 13/22). Scale bar = 20 μm.

Fig. 66. Magnified view of the floor of a carposporangial conceptacle showing a discontinuous central fusion cell (arrowheads) bearing a peripherally arranged gonimoblast filament (1-4) terminating in a carposporangium (C). The remains of unfertilised carpogonial branches

(arrow) persist across the dorsal surface of the central fusion cell (UWC 13/22). Scale bar = 20 μm.

Figs. 67-71. Tetrasporangial conceptacle anatomy of *Chamberlainium impar*.

Fig. 67. Vertical section of the outer thallus showing an early stage tetrasporangial conceptacle primordium with peripherally arranged tetrasporangial initials (arrowheads) and a protective layer of epithallial cells (arrow) (UWC 13/22). Scale bar = 50 μm.

Fig. 68. Vertical section through the outer thallus showing an early stage tetrasporangial conceptacle primordium with a peripherally arranged tetrasporangial initial (arrowhead) (UWC 15/64). Scale bar = 50 μm.

Fig. 69. Vertical section through a maturing tetrasporangial conceptacle showing the pore canal lined with terminal, elongate initials (arrowheads) that project into the pore canal as papillae. Note the well-defined central columella (C) and the layer of protective epithallial cells (arrow) being shed (UWC 13/21). Scale bar = 50 μm.

Fig. 70. Vertical section through a mature, raised tetrasporangial conceptacle showing tetrasporangia (t) with stalk cells (arrowheads), peripherally arranged around a well-defined central columella (C). Note the mucilage plug (arrow) that occludes the pore opening (UWC 13/22). Scale bar = 50 μm

Fig. 71. Magnified view of the pore canal of a mature tetrasporangial conceptacle showing the base of the pore canal sunken (black arrowheads) into the conceptacle chamber with terminal, elongate initials near the base of the pore canal pointing downward (black arrows) and a mucilage plug (white arrow) that occludes the pore opening (UWC 13/20). Scale bar = 20 μm.

Figures 72-88: *Chamberlainium natalense*

Fig. 72. Encrusting, thin epilithic (on a boulder) thalli of *Chamberlainium natalense* found in a mid-intertidal rock pool. Scale bar = 30 mm.

Figs 73-76. Habit and vegetative anatomy of *Chamberlainium natalense*.

Fig. 73. Encrusting, thin epilithic thalli showing crusts abutting and easily discernible. Scale bar = 10 mm.

Fig. 74. Vertical section through the margin (arrow) showing the monomerous thallus construction with plumose medulla (M) giving rise to cortical filaments (C) that terminate in a single layer of epithallial cells (arrowhead) (UWC 10/209). Scale bar = 30 μm.

Fig. 75. Vertical section of the inner thallus showing a plumose medulla (M) giving rise to cortical filaments (C). Note the cell fusions (arrowheads) between adjacent medullary filaments (UWC 08/04). Scale bar = 20 μm.

Fig. 76. Vertical section of the outer thallus showing a single layer of epithallial cells (e) subtended by a layer of subepithallial initials (i). Note the solitary, bottle-shaped trichocytes (t) that are separated by normal vegetative filaments and the cell fusions (arrowheads) between adjacent cortical filaments (UWC 10/209). Scale bar = 20 μm.

Figs. 77-82. Gametangial anatomy of *Chamberlainium natalense*.

Fig. 77. Vertical section through the outer thallus showing a spermatangial conceptacle primordium with peripheral roof development (black arrows) and simple spermatangial systems (arrowheads) confined to the conceptacle floor. Note the protective layer of epithallial cells (white arrow) (UWC 09/125). Scale bar = 20 μm.

Fig. 78. Vertical section through a mature, raised spermatangial conceptacle showing the mucilage plug (arrow) that occludes the pore opening and simple, spermatangial systems (arrowheads) confined to the conceptacle floor (UWC 08/04). Scale bar = 20 μm.

Fig. 79. Vertical section through a mature, raised carpogonial conceptacle with carpogonial branches comprised of a single support cell (white arrow) bearing a carpogonium (white arrowheads) extended into a trichogyne (black arrowheads) projecting out of the pore (black arrows) (UWC 11/26). Scale bar = 20 μm.

Fig. 80. Vertical section through a mature carposporangial conceptacle showing a discontinuous central fusion cell (arrowheads) bearing peripherally arranged gonimoblast filaments each terminating in a carposporangium (c). Note the downward-pointing ring of initials (white arrowhead) near the base of the pore canal and the pore opening occluded by a corona (black arrow) that surrounds the pore opening (UWC 09/125). Scale bar = 50 μm.

Fig. 81. Magnified view of the pore canal of a mature carposporangial conceptacle showing terminal, elongate initials near the base of the pore canal pointing downward (arrowheads). Note the corona (arrows) that surrounds the pore opening (UWC 09/125). Scale bar = 20 μm.

Fig. 82. Magnified view of the floor of a carposporangial conceptacle showing a discontinuous central fusion cell (arrowheads) bearing a peripherally arranged gonimoblast filament (1-5) terminating in a carposporangium (C). The remains of unfertilised carpogonial branches (arrow) persist across the dorsal surface of the central fusion cell (UWC 09/125). Scale bar = 20 μm.

Figs. 83-88. Tetrasporangial conceptacle anatomy of *Chamberlainium natalense.*

Fig. 83. Vertical section through the outer thallus showing an early stage tetrasporangial conceptacle primordium with peripherally arranged tetrasporangial initials (arrowheads) and a protective layer of epithallial cells (e) (UWC 11/26). Scale bar = 50 μm.

Fig. 84. Vertical section through the outer thallus showing a later stage tetrasporangial conceptacle primordium with peripheral roof development (black arrowheads) with a developing central columella (white arrowhead). Note the persisting layer of protective epithallial cells (e) (UWC 11/26). Scale bar = 50 μm.

Fig. 85. Vertical section through the outer thallus showing a maturing tetrasporangial conceptacle with peripheral roof development (black arrowheads) and tetrasporangial initials (t) peripherally arranged around a central columella (between white arrowheads). Note the layer of protective epithallial cells (e) being shed (UWC 11/26). Scale bar = 50 μm.

Fig. 86. Vertical section through a mature, raised tetrasporangial conceptacle showing tetrasporangia (t) with stalk cells (white arrowheads), peripherally arranged around a well-defined central columella (C). Note the pore canal lined with , terminal, elongate initials that project into the pore canal as papillae, those near the base of the pore canal pointing downward (black arrowheads) and the corona (arrow) that surrounds the pore opening (UWC 10/133). Scale bar = 50 μm.

Fig. 87. Magnified view of the pore canal of a mature tetrasporangial conceptacle showing the base of the pore canal sunken (arrowheads) into the conceptacle chamber with terminal, elongate initials (black arrows) that project into the pore canal as papillae and a corona (white arrow) that surrounds and occludes the pore opening Note, the top portion of a peripherally arranged tetrasporangium (UWC 08/04). Scale bar = 20 μm.

Fig. 88. Vertical section through the outer thallus showing mature raised tetrasporangial conceptacles with diminished central columellas (arrowheads). Note, the corona (right arrow) and the remains of a corona (left arrow) that surrounds and occludes the pore openings. (UWC 09/125). Scale bar = 50 μm.

Figures 89-104: *Chamberlainium occidentale*

Fig. 89. Encrusting to variably warty to lumpy epilithic thalli of *Chamberlainium occidentale* found in the mid-intertidal zone. Scale bar = 30 mm

Figs 90-94. Habit and vegetative anatomy of *Chamberlainium occidentale*.

Fig. 90. Rock fragment with holotype specimen showing the region (arrow) of the holotype from which all analyses were done (L ???????, tetrasporangial). Scale bar = 10 mm.

Fig. 91. Vertical section through the margin (arrow) showing the monomerous thallus construction with plumose medulla (M) giving rise to cortical filaments (C) that terminate in a single layer of epithallial cells (arrowhead) (UWC 15/59). Scale bar = 50 μm.

Fig. 92. Vertical section of the inner thallus showing cell fusions (f) between adjacent medullary filaments (UWC 15/56). Scale bar = 20 μm.

Fig. 93. Vertical section of the outer thallus showing a single layer of epithallial cells (e) subtended by a layer of subepithallial initials (i). Note the cell fusions (f) between adjacent cortical filaments (UWC 15/59). Scale bar = 20 μm.

Fig. 94. Vertical section of the outer thallus showing a single layer of epithallial cells (e) subtended by a layer of subepithallial initials (i). Note a cluster of bottle-shaped trichocytes (t) each separated by vegetative filaments (UWC 15/59). Scale bar = 20 μm.

Figs 95-100. Gametangial anatomy of *Chamberlainium occidentale*.

Fig. 95. Vertical section through the outer thallus showing a spermatangial conceptacle primordium with peripheral roof development (black arrows) and simple spermatangial systems (arrowheads) confined to the conceptacle floor. Note the protective layer of epithallial cells (white arrow) (L ???????). Scale bar = 50 μm.

Fig. 96. Vertical section through a mature, raised spermatangial conceptacle showing the mucilage plug (white arrowhead) that occludes the pore opening and simple, spermatangial systems (black arrowheads) confined to the conceptacle floor (UWC 15/56). Scale bar = 50 μm.

Fig 97. Magnified view through a mature spermatangial conceptacle showing the pore canal lined with terminal, elongate initials (arrowheads) that project into the pore canal as papillae (UWC 15/56). Scale bar = 20 μm.

Fig. 98. Magnified view of a mature carpogonial conceptacle with carpogonial branches comprised of a single support cell (s), a hypogynous cell (h) with sterile cell (arrowhead), and a carpogonium (c) extended into a trichogyne (black arrows) that may project out of the pore. Note that the pore canal is lined with terminal, elongate initials (white arrows) that project into the pore canal as papillae (L ???????). Scale bar = 20 μm.

Fig. 99. Vertical section through a mature carposporangial conceptacle showing a discontinuous central fusion cell (arrowhead) with peripherally arranged gonimoblast filaments each terminating in a carposporangium (C). (L ???????). Scale bar = 50 μm.

Fig. 100. Magnified view of the floor of a carposporangial conceptacle showing a discontinuous central fusion cell (arrowheads) bearing a peripherally arranged gonimoblast filament (1-6) terminating in a carposporangium (C). The remains of unfertilised carpogonial branches (arrow) persist across the dorsal surface of the central fusion cell (L ???????). Scale bar = 20 μm.

Figs 101-105. Tetrasporangial conceptacle anatomy of *Chamberlainium occidentale.*

Fig. 101. Vertical section through the outer thallus showing an early stage tetrasporangial conceptacle primordium with peripheral roof development (arrowheads) and a protective layer of epithallial cells (e) (L ???????). Scale bar = 50 μm.

Fig. 102. Vertical section through the outer thallus showing a later stage tetrasporangial conceptacle primordium with peripheral roof development (arrowheads) and tetrasporangial (t) initials arranged peripherally around a central columella (c). Note the persisting layer of protective epithallial cells (e) (UWC 93/220). Scale bar = 50 μm.

Fig. 103. Vertical section through the outer thallus showing a maturing tetrasporangial conceptacle with peripheral roof development (arrowheads) and tetrasporangial (t) initials, peripherally arranged around a central columella (c). Note the layer of protective epithallial cells (e) (UWC 93/220). Scale bar = 50 μm.

Fig. 104. Vertical section through a mature, raised tetrasporangial conceptacle showing tetrasporangia (t) with stalk cells (arrowhead), peripherally arranged around a well-defined central columella (C). Note, the sunken and unoccluded pore opening (arrow) (UWC 93/220). Scale bar = 100 μm.

Fig. 105. Magnified view of the pore canal of a mature tetrasporangial conceptacle showing terminal, elongate initials (arrows) that project into the pore canal as papillae and the base of the pore canal sunken (arrowheads) into the chamber with terminal, elongate initials near the base pointing downward. Note, the sunken and unoccluded pore opening (white arrow) (UWC 93/220). Scale bar = 20 μm.

Figures 106-117: *Chamberlainium tenue*

Fig. 106. Encrusting, thin epilithic thalli of *Chamberlainium tenue* found in the high intertidal zone. Scale bar = 20 mm

Figs 107-110. Habit and vegetative anatomy of *Chamberlainium tenue*.

Fig. 107. Rock fragment with holotype specimen showing the region (arrow) of the holotype from which all analyses were done (L ???????, tetrasporangial). Scale bar = 20 mm.

Fig. 108. Vertical section through the margin (arrow) showing the monomerous thallus construction with plumose medulla (M) giving rise to cortical filaments (C) that terminate in a single layer of epithallial cells (arrowhead) (UWC 15/23). Scale bar = 20 μm.

Fig. 109. Vertical section of the inner thallus showing a plumose medulla (M) giving rise to cortical filaments (C) and cell fusions (f) between adjacent filaments (UWC 15/23). Scale bar = 20 μm.

Fig. 110. Vertical section of the outer thallus showing a single layer of epithallial cells (arrowhead) subtended by a layer of subepithallial initials (i). Note the cell fusions (f) between adjacent cortical filaments and the paired, bottle-shaped trichocytes (t) that are not separated by normal vegetative filaments (UWC 15/23). Scale bar = 20 μm.

Figs 111-112. Spermatangial anatomy of *Chamberlainium tenue* (UWC 10/202).

Fig. 111. Vertical section through a mature, slightly raised spermatangial conceptacle showing the simple, spermatangial systems (arrowheads) confined to the conceptacle floor. Scale bar = 50 μm.

Fig 112. Magnified view through a mature spermatangial conceptacle showing the mucilage plug (arrow) that occludes the pore opening. Note that the pore canal is lined with terminal, elongate initials (arrowheads) that project into the pore canal as papillae. Scale bar = 20 μm.

Figs 113-117. Tetrasporangial conceptacle anatomy of *Chamberlainium tenue.*

Fig. 113. Vertical section through the outer thallus showing an early stage tetrasporangial conceptacle primordium with peripheral roof development (arrowheads). Note the layer of protective epithallial cells (arrow) (UWC 08/07). Scale bar = 50 μm.

Fig. 114. Vertical section through the outer thallus showing a later stage tetrasporangial conceptacle primordium with terminal, elongate initials (arrowheads) that project into the pore

as papillae and developing tetrasporangia (t) that are peripherally arranged. (L ???????). Scale bar = 50 μm.

Fig. 115. Vertical section through a mature, raised tetrasporangial conceptacle showing tetrasporangia (t) peripherally arranged around a well-defined central columella (C). Note the mucilage plug (arrow) that occludes the pore opening (L ???????). Scale bar = 50 μm.

Fig. 116. Vertical section though a mature, raised tetrasporangial conceptacle showing tetrasporangia (t) with a stalk cell (arrowhead), appearing to be distributed across the chamber floor as the columella (c) disintegrates. Note the mucilage plug (arrow) that occludes the pore opening (L ???????). Scale bar = 50 μm.

Fig. 117. Magnified view of the pore canal of a mature tetrasporangial conceptacle showing the base of the pore canal (arrowheads) sunken into the conceptacle chamber and terminal, elongate initials (black arrows) that project into the pore as papillae. Note the mucilage plug (white arrow) that occludes the pore opening (L ???????). Scale bar = 20 μm.

Figures 118-136: *Pneophyllum neodiscoideum*

Fig. 118. Encrusting, thin epilithic primary thalli (*) giving rise to thick, discoid secondary thalli (arrows) of *Pneophyllum neodiscoideum* in a mid- shore rock pool. Scale bar = 20 mm

Fig. 118 insert: Magnified view of an encrusting, thin primary thallus (*) giving rise to secondarily thick and discoid thalli (black arrows) with laterally fused protuberances (white arrow). Scale bar = 5 mm

Fig. 119. Magnified view of an encrusting, thin primary thallus (*) giving rise to a secondarily thick, discoid thallus (black arrows) bearing laterally fused protuberances. Scale bar = 2 mm

Figs 1120-125. Habit and vegetative anatomy of *Pneophyllum neodiscoideum*.

Fig. 120. Rock fragment with holotype specimen showing the region (X) of the holotype from which all analyses were done (L ???????, tetrasporangial). Scale bar = 10 mm.

Fig. 121. Vertical section through the margin (arrowhead) showing the primarily dimerous thallus construction becoming secondarily monomerous (arrow). Note the irregularly square basal (B) cells and cell fusions (f) between adjacent filaments (UWC 09/131). Scale bar = 20 μm.

Fig. 122. Vertical section of the inner thallus showing the primarily dimerous thallus construction in radial view. Note the irregularly square basal (B) cells and cell fusions (f) between adjacent erect filaments (UWC 09/131). Scale bar = 20 μm.

Fig. 123. Vertical section of inner thallus showing the primarily dimerous thallus construction in tangential view. Basal cells (B) appear palisade-like in this view. Note the cell fusions (f) between adjacent erect filaments (UWC 09/131). Scale bar = 20 μm.

Fig. 124. Vertical section of the inner thallus showing the secondarily monomerous thallus construction with cell fusions (f) between adjacent filaments (L ???????). Scale bar = 20 μm.

Fig. 125. Vertical section of the outer thallus showing a multi-layered epithallus (e) subtended by a layer of subepithallial initials (i). Note the newly divided, lighter staining, epithallial cells (arrowheads) and cell fusions (f) between adjacent filaments (L ???????). Scale bar = 20 μm.

Figs 126-131. Gametangial anatomy of *Pneophyllum neodiscoideum*.

Fig. 126. Magnified view through a mature, slightly raised spermatangial conceptacle showing the mucilage plug (white arrowhead) that occludes the pore opening and simple, spermatangial systems (black arrowheads) confined to the conceptacle floor. Note that the pore canal is lined with terminal, elongate initials (black arrows) that project into the pore canal as papillae (UWC 11/22). Scale bar = 20 μm.

Fig. 127. Vertical section through the outer thallus showing a carpogonial conceptacle primordium with peripheral roof development (black arrowheads) and developing carpogonial branches (white arrowhead). Note a protective layer of epithallial cells (e) (L ???????). Scale bar = 50 μm

Fig. 128. Magnified view through a mature, buried carpogonial conceptacle (UWC 09/131). Scale bar = 50 μm

Fig. 129. Vertical section through the outer thallus showing a mature carposporangial conceptacle with peripherally arranged gonimoblast filaments each terminating in a carposporangium (C). The remains of unfertilised carpogonial branches (arrowhead) persist across the dorsal surface of the discontinuous central fusion cell. Note the extensive mucilage plug (arrow) that occludes the pore opening (L ??????). Scale bar = 50 μm.

Fig. 130. Magnified view of the floor of a carposporangial conceptacle showing a discontinuous central fusion cell (white arrowheads) bearing a peripherally arranged gonimoblast filament (1-5) terminating in a carposporangium (C). Note that the base of the pore canal (black arrowhead) is sunken into the conceptacle chamber (L ??????). Scale bar = 20 μm.

Fig. 131. Magnified view of the pore canal of a mature carposporangial conceptacle showing terminal, elongate initials (arrowheads) that project into the pore canal as papillae. Note the extensive mucilage plug that occludes the pore opening (white arrow) (L ??????). Scale bar = 20 μm.

Figs 132-136. Tetrasporangial conceptacle anatomy of *Pneophyllum neodiscoideum.*

Fig. 132. Vertical section through the outer thallus showing an early stage tetrasporangial conceptacle primordium showing roof development from filaments peripheral (arrowheads) to

the developing central columella (c). Note the protective layer of epithallial cells (arrow) (L ???????). Scale bar = 50 μm.

Fig. 133. Vertical section through the outer thallus showing a later stage tetrasporangial conceptacle primordium showing roof development (black arrowheads) from filaments both peripheral to the fertile area as well as from filaments interspersed (white arrowheads) amongst the developing tetrasporangial initials (t), all of which are peripheral to a central columella (c). Note the persisting layer of protective epithallial cells (black arrow) (L ???????). Scale bar = 50 μm.

Fig. 134. Vertical section through a senescent tetrasporangial conceptacle showing the remains of interspersed filaments (arrowheads) that contributed to the conceptacle roof (UWC 11/22). Scale bar = 50 μm.

Fig. 135. Vertical section through a mature, sunken tetrasporangial conceptacle showing tetrasporangia (t) peripherally arranged around a disintegrating central columella (c). Note the extensive mucilage plug that occludes the pore canal and opening (white arrow). (L ???????). Scale bar = 20 μm.

Fig. 136. Magnified view of the pore canal of a mature tetrasporangial conceptacle showing the base of the pore canal sunken (arrowheads) into the conceptacle chamber with terminal, elongate, balloon-like initials (black arrows) projecting into the pore canal as papillae, those near the base of the pore canal pointing downward. Note the extensive mucilage plug that occludes the pore opening (white arrow) (UWC 09/131). Scale bar = 50 μm.

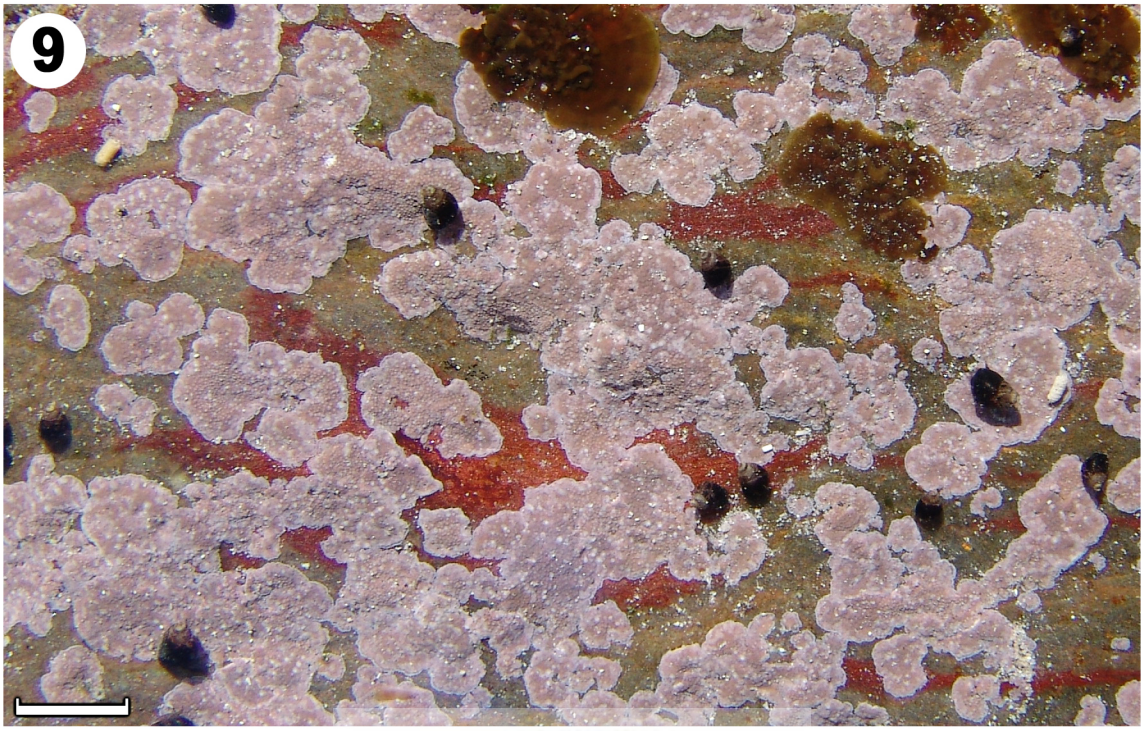

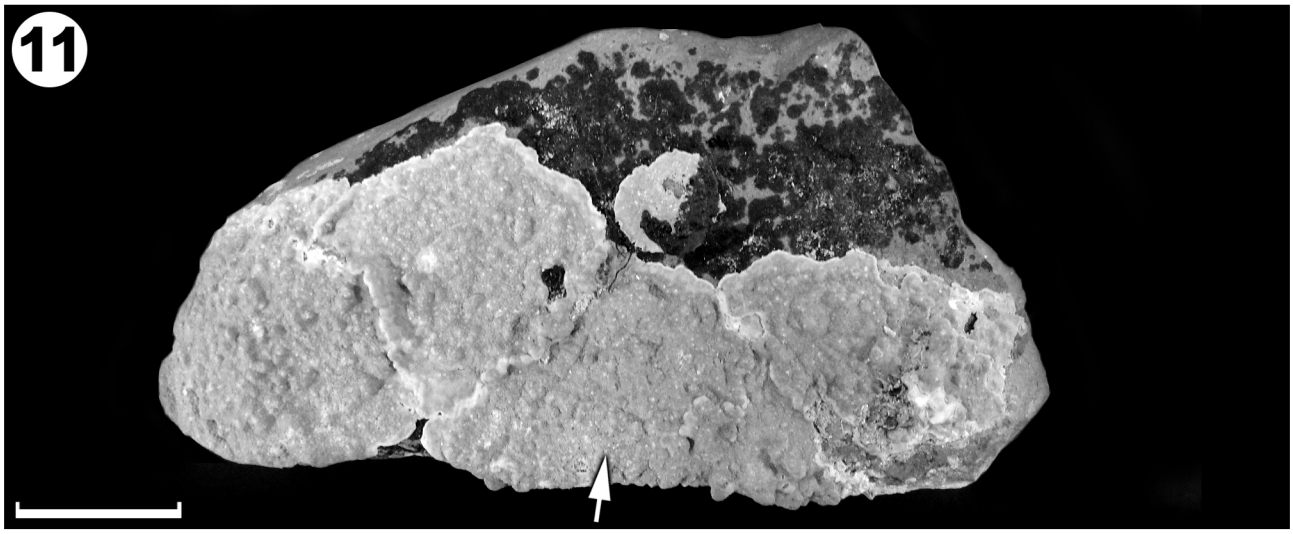

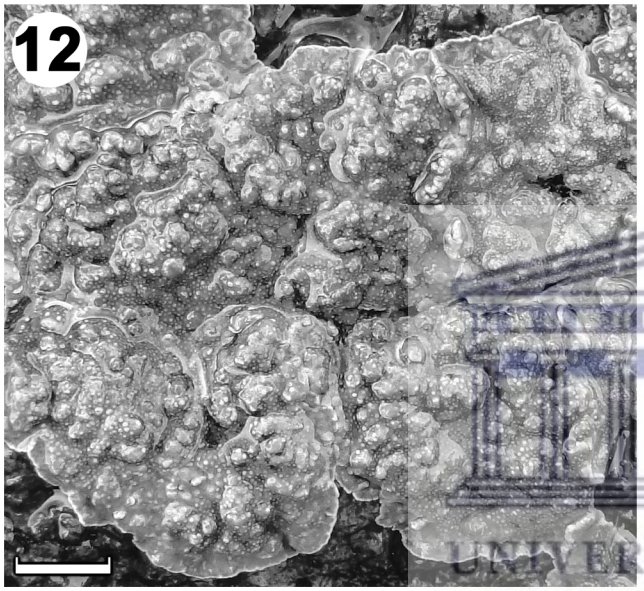

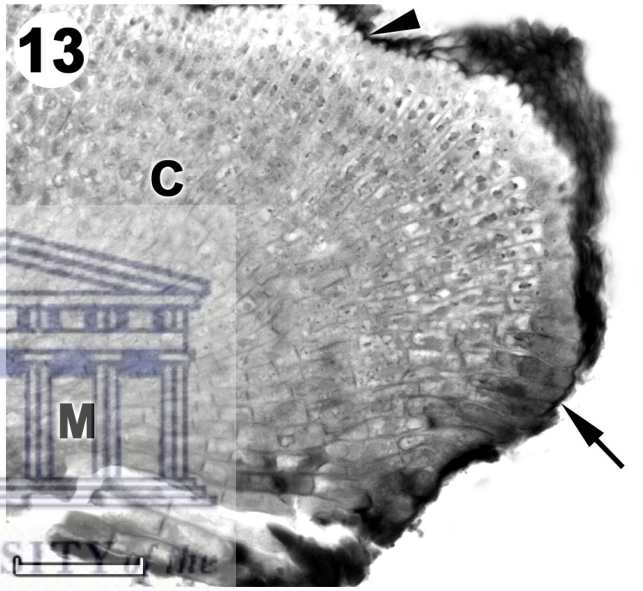

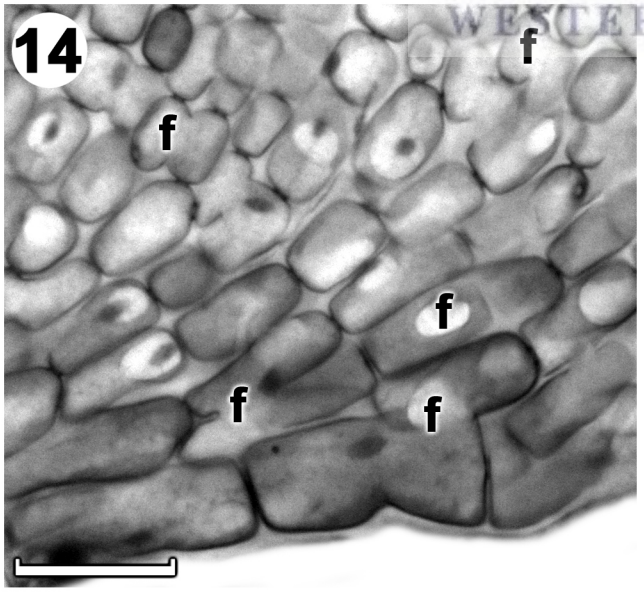

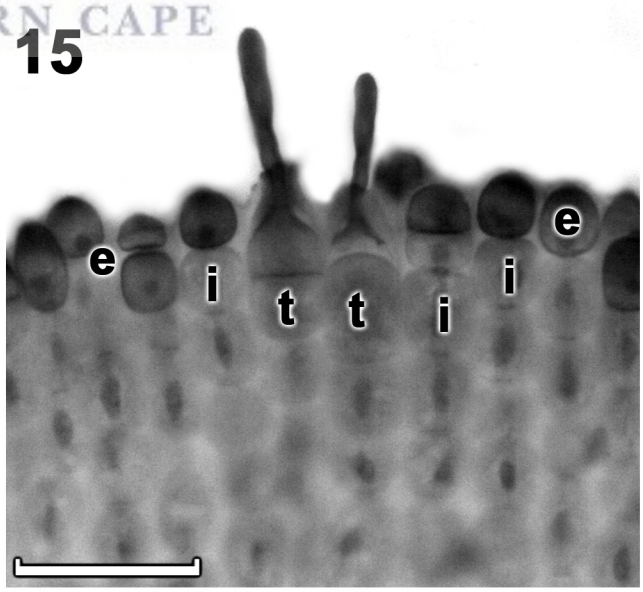

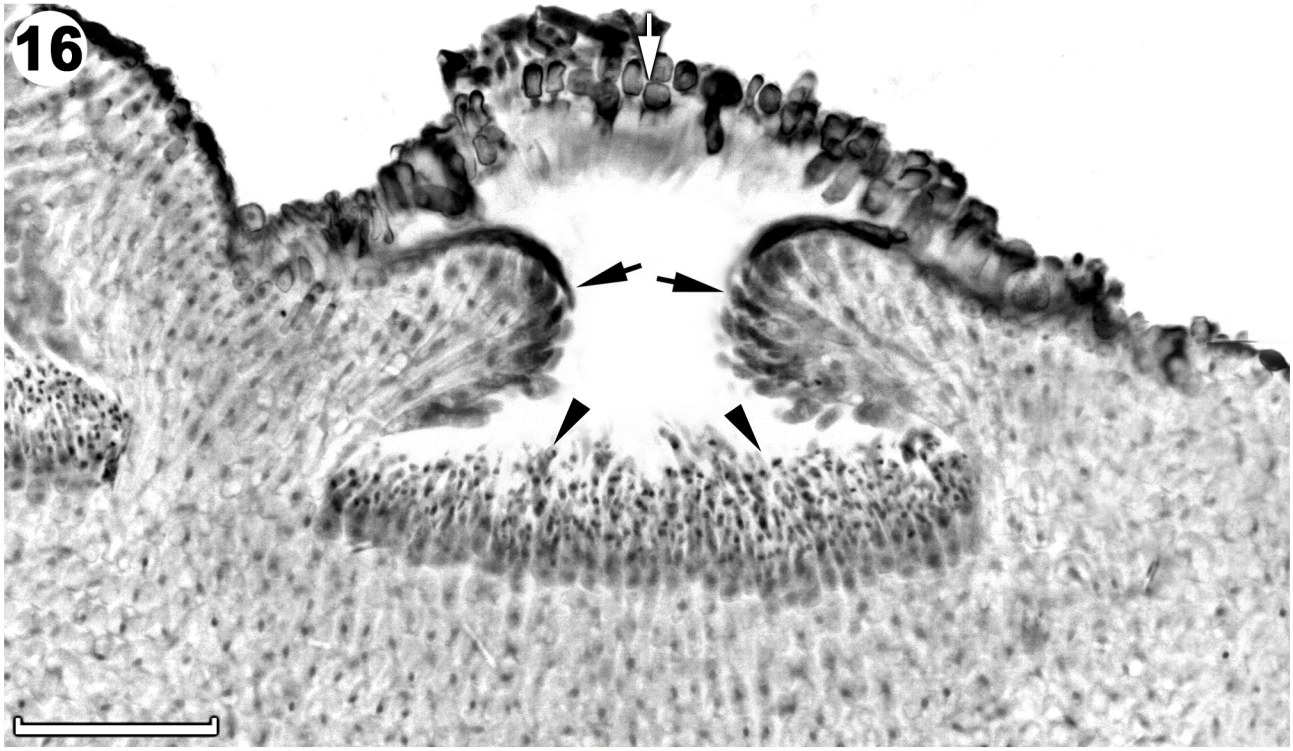

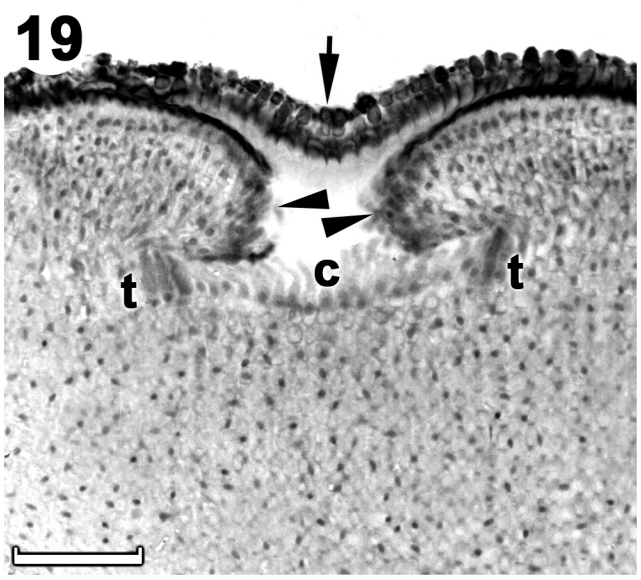

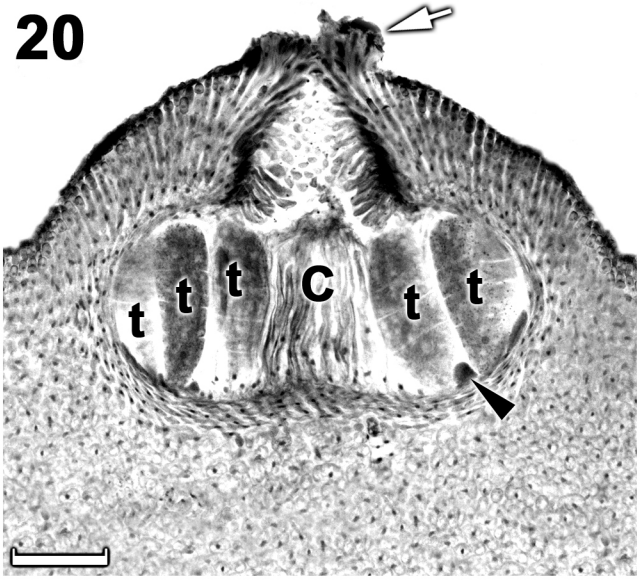

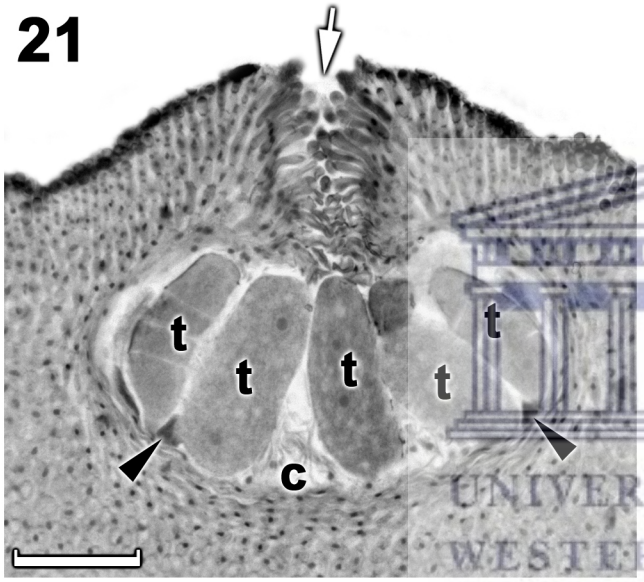

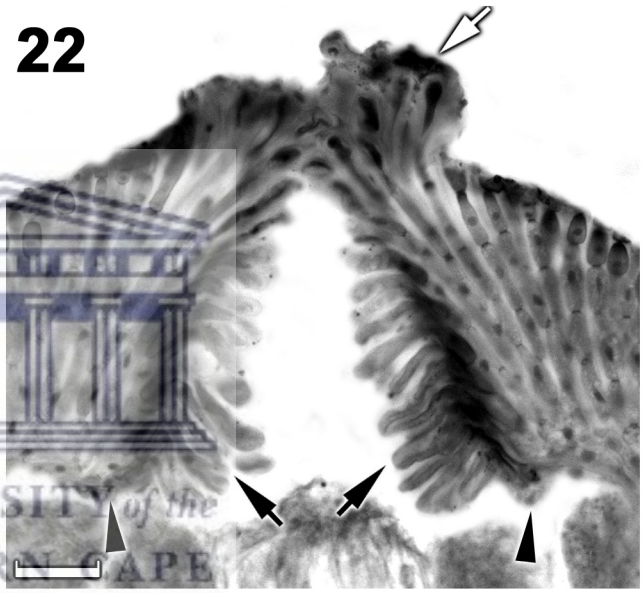

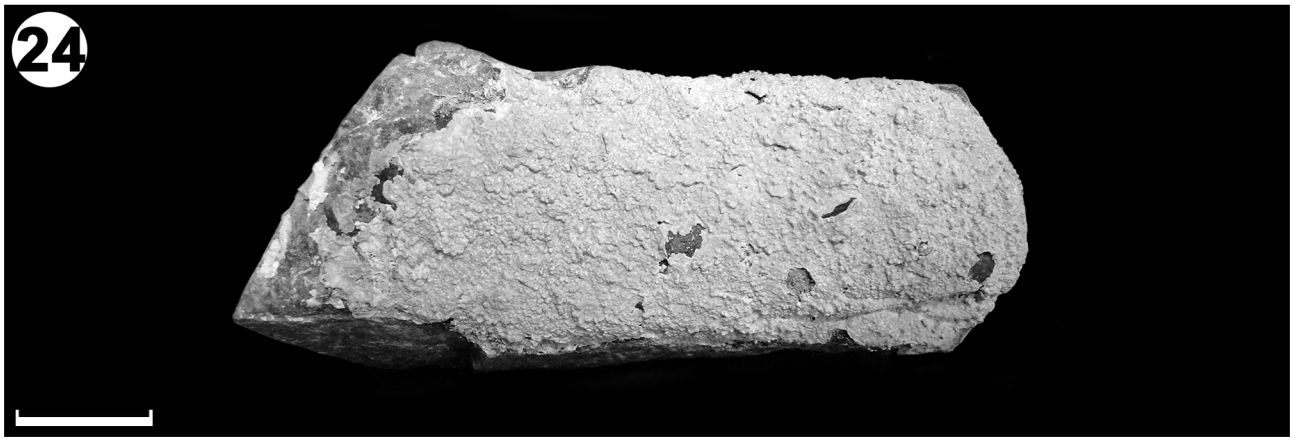

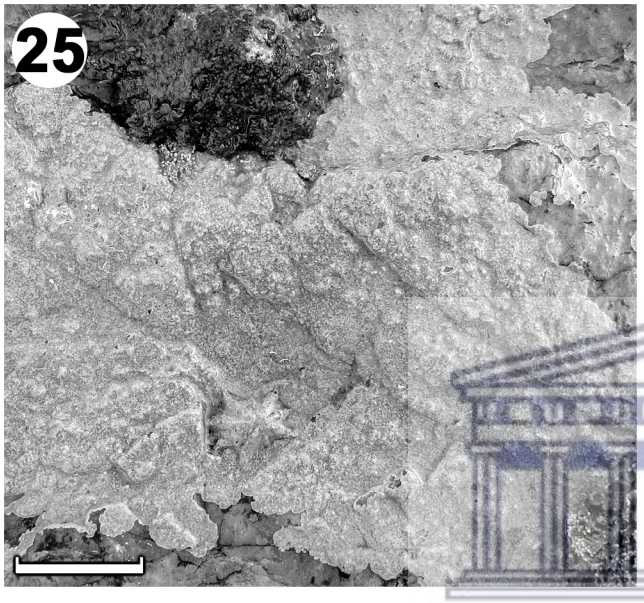

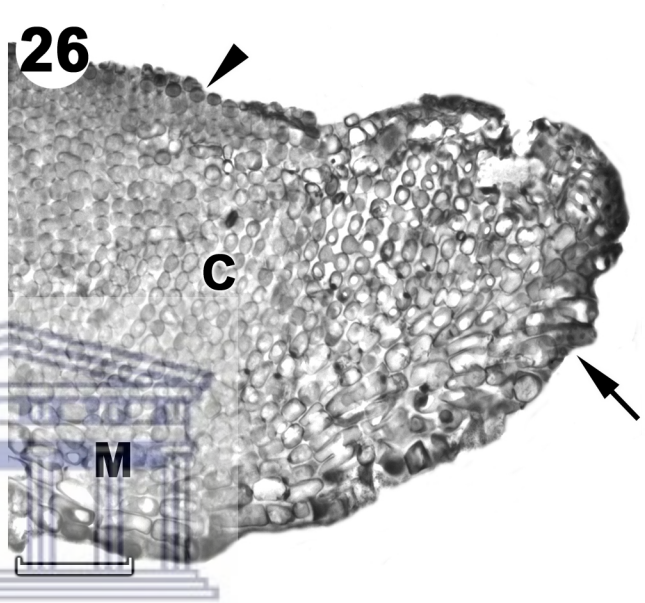

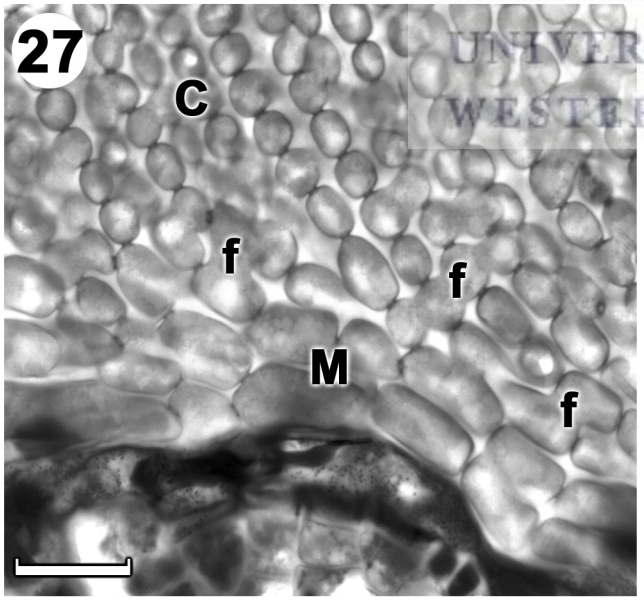

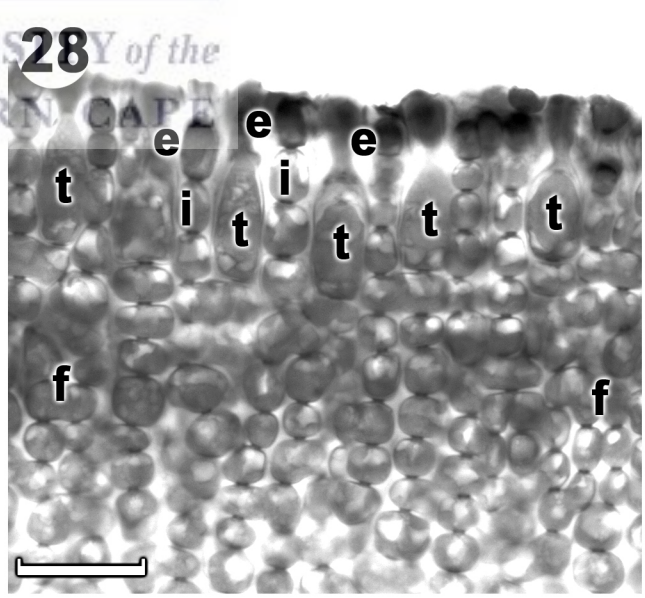

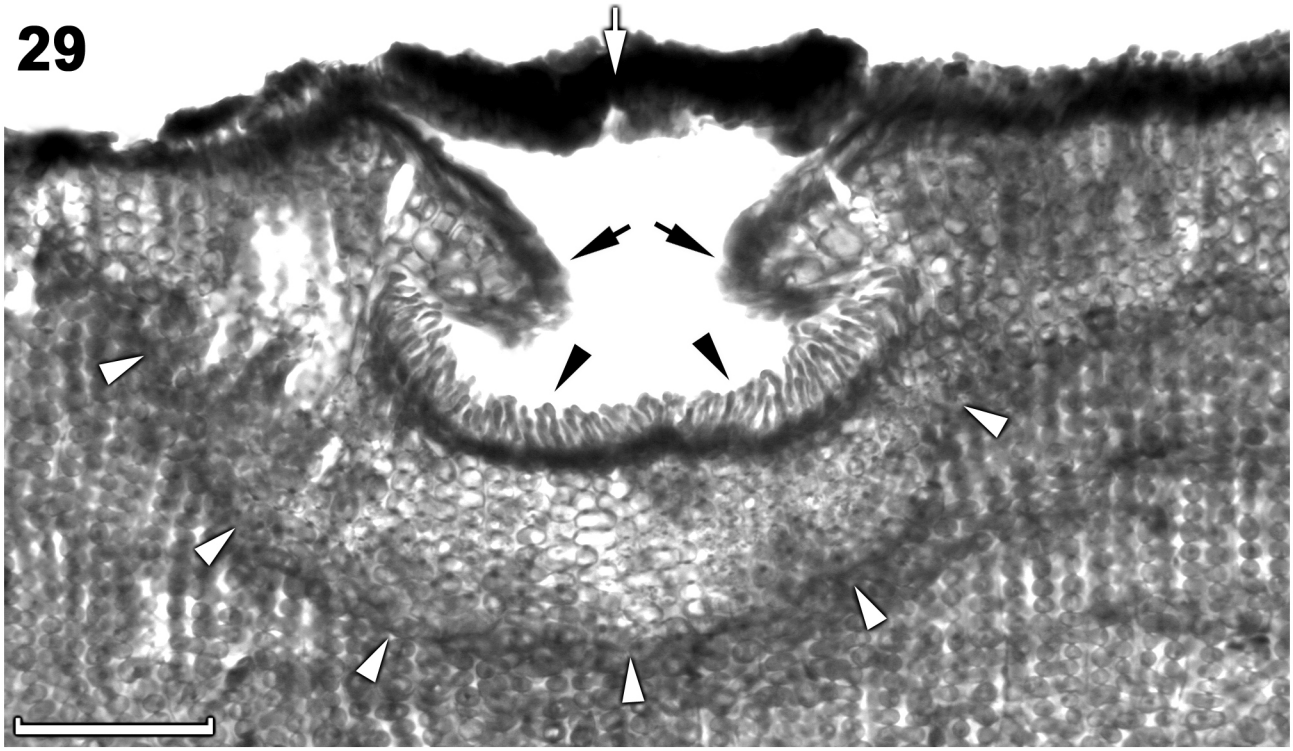

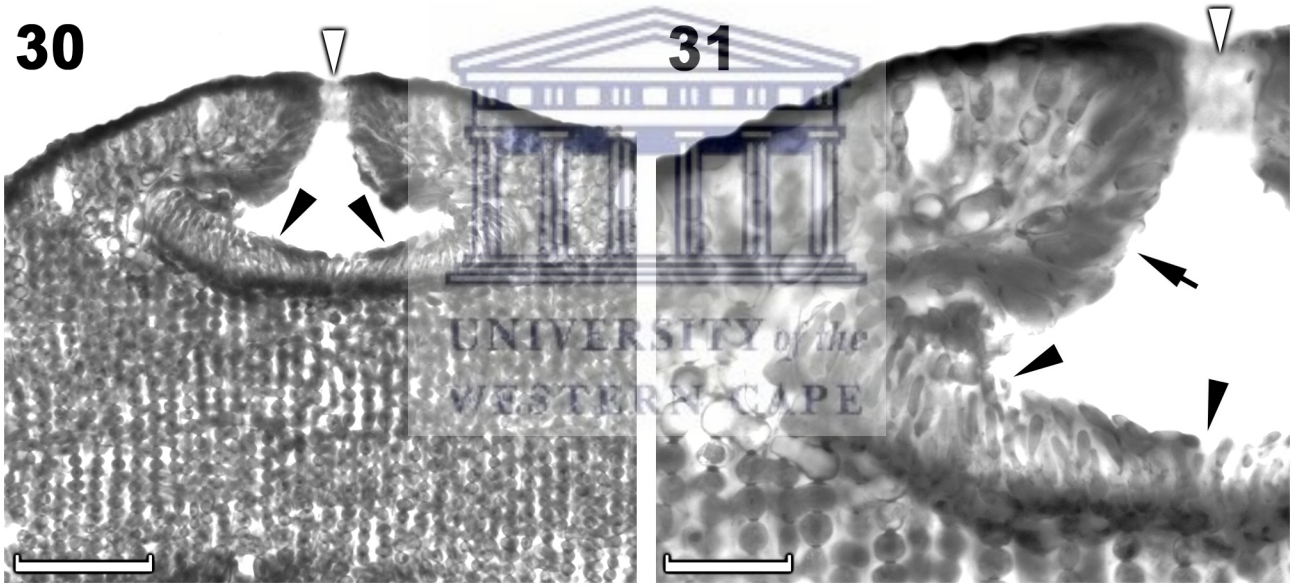

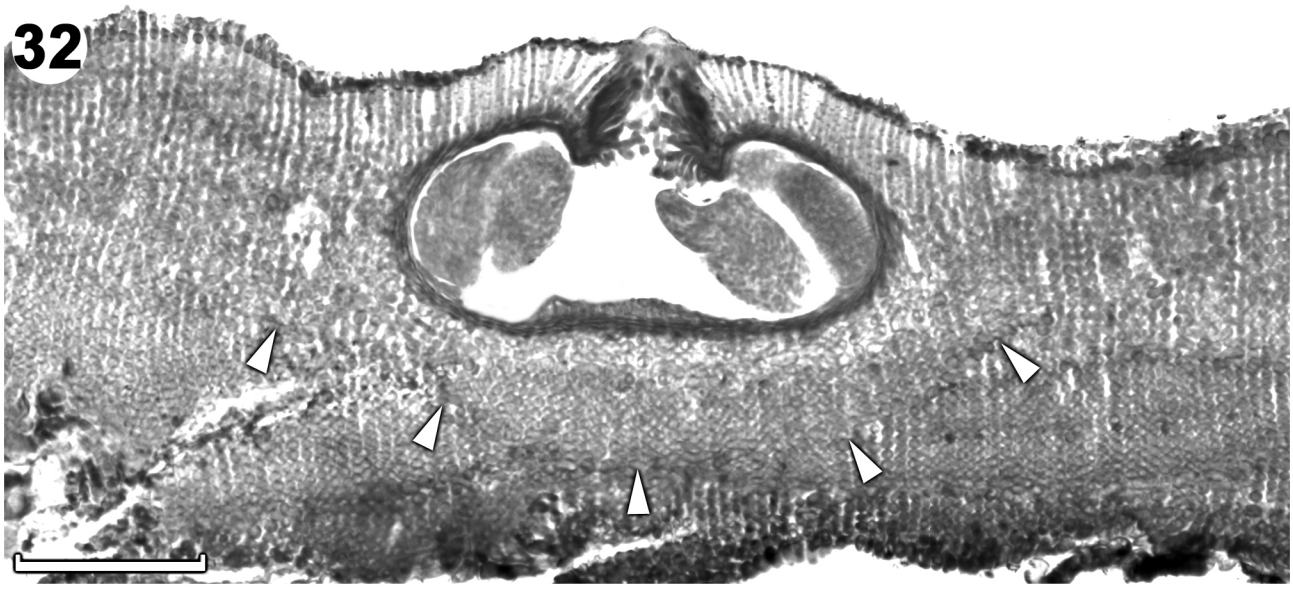

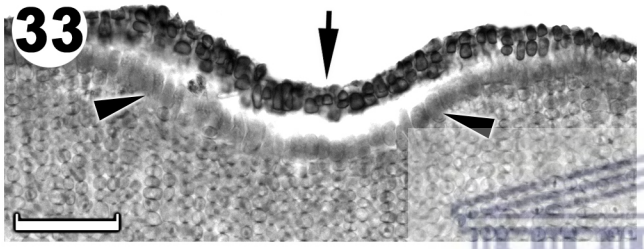

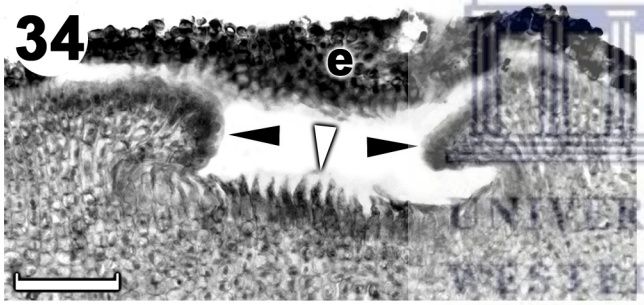

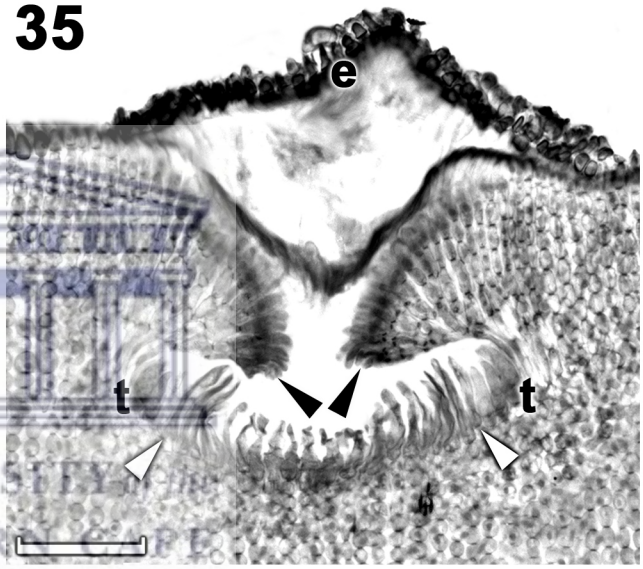

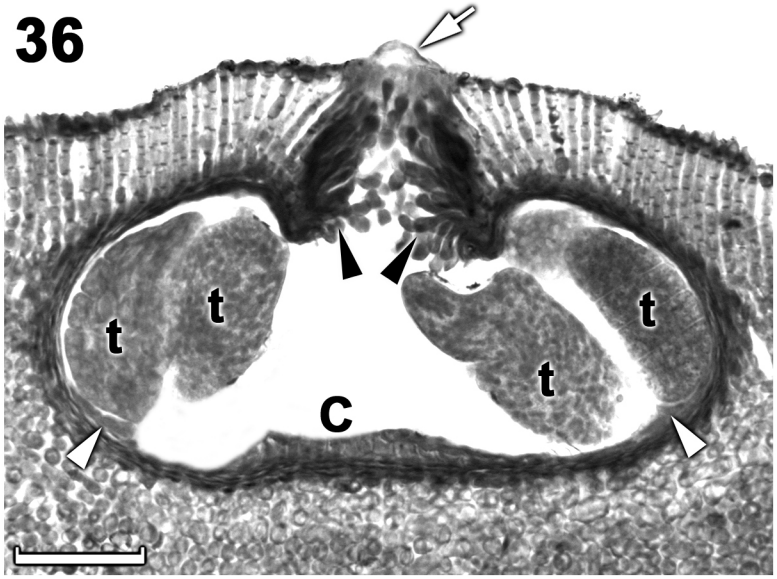

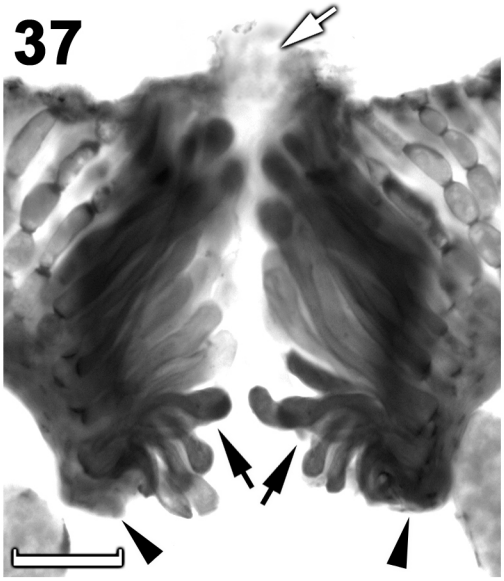

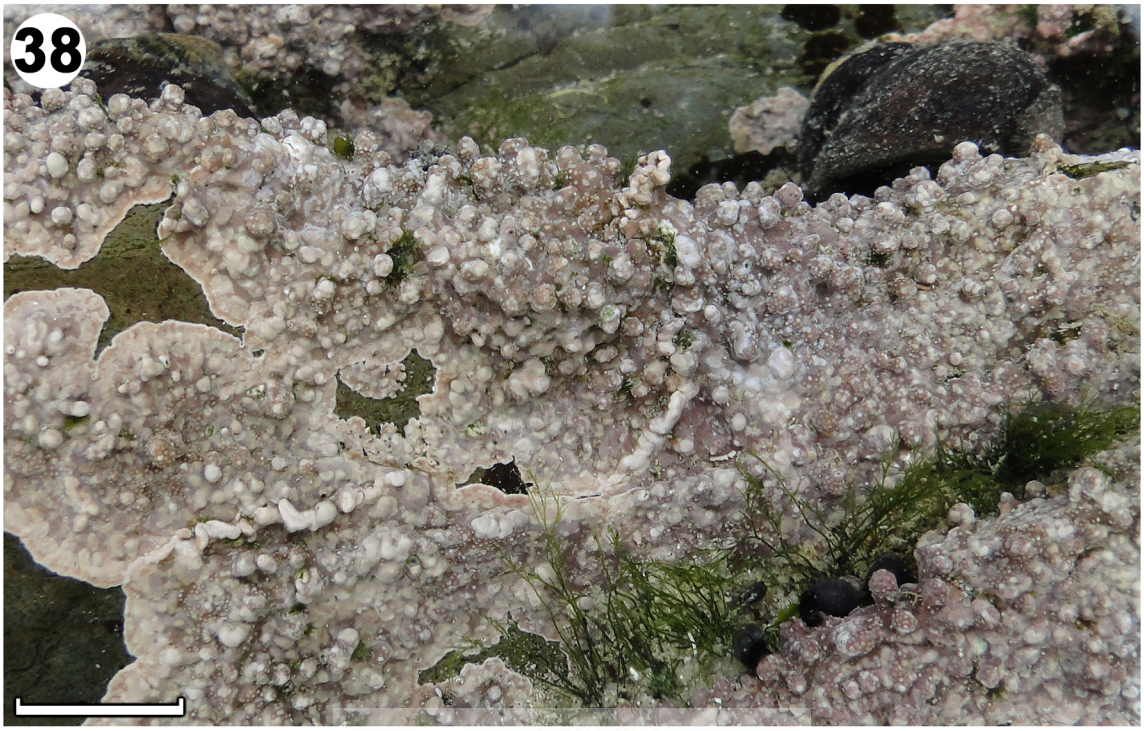

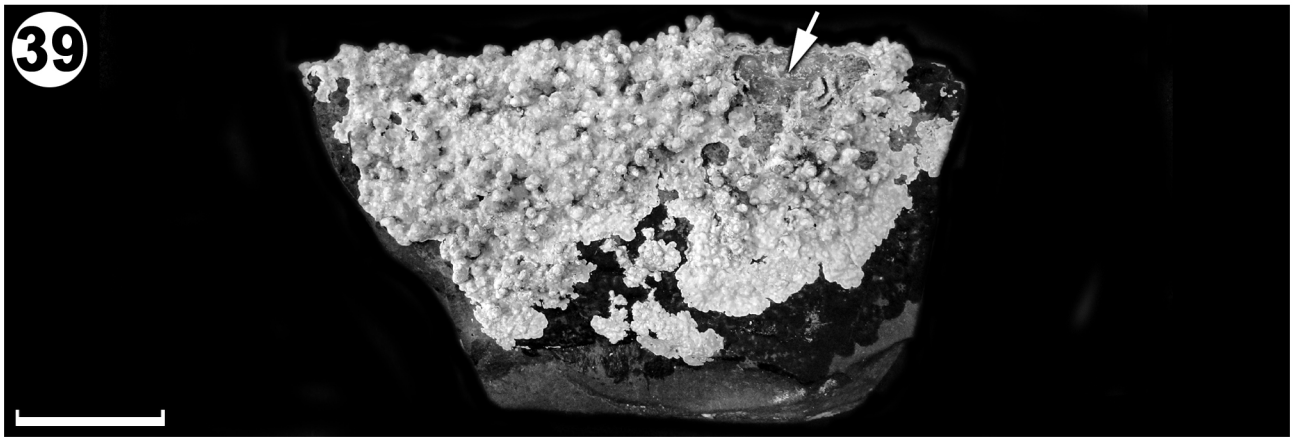

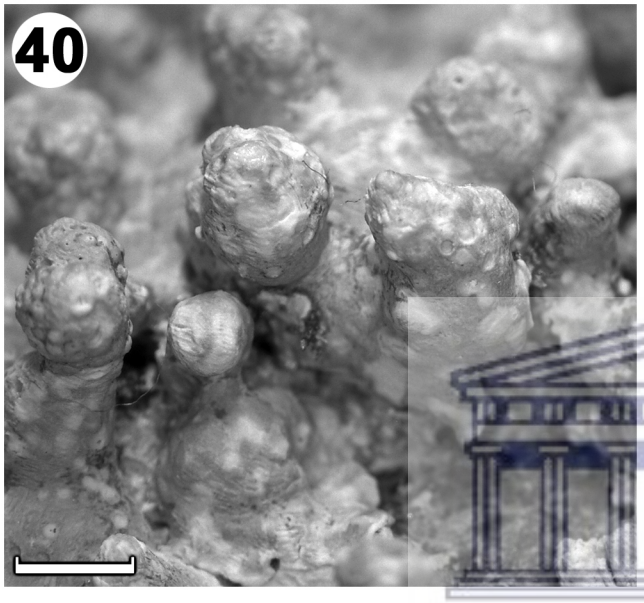

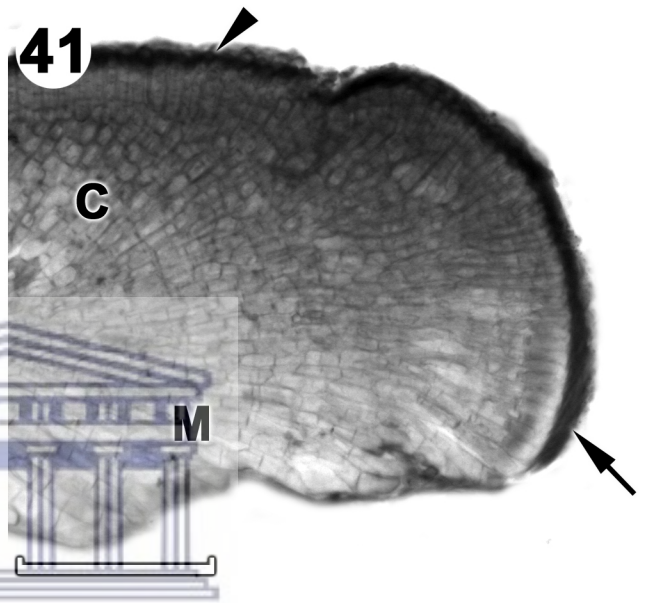

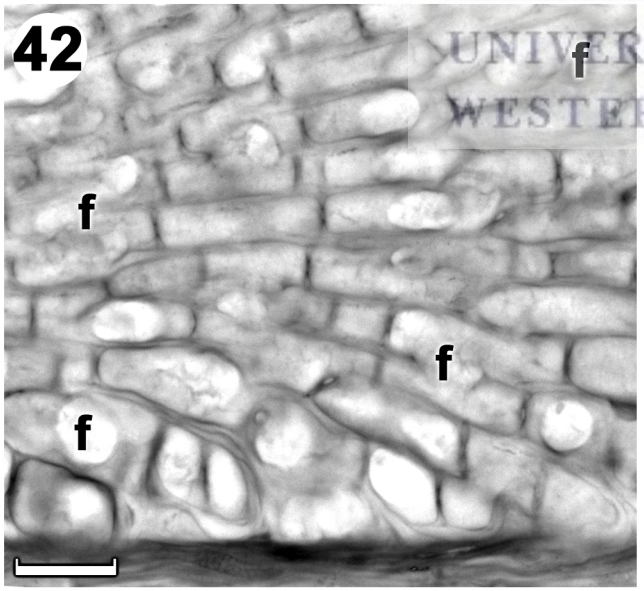

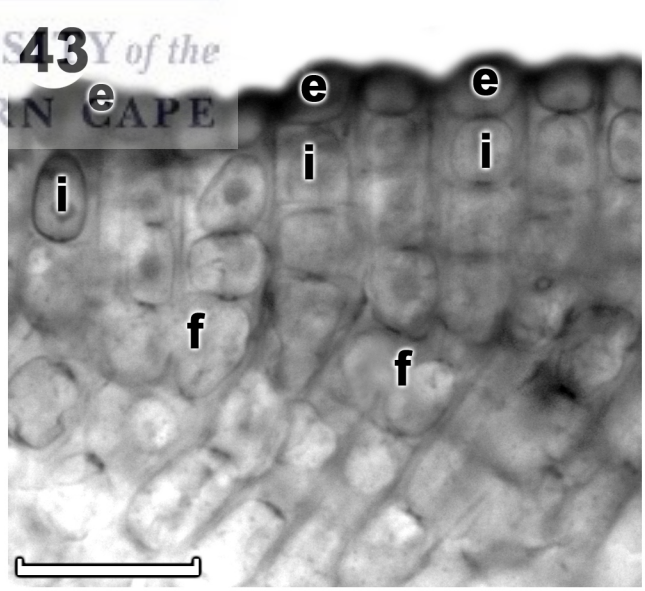

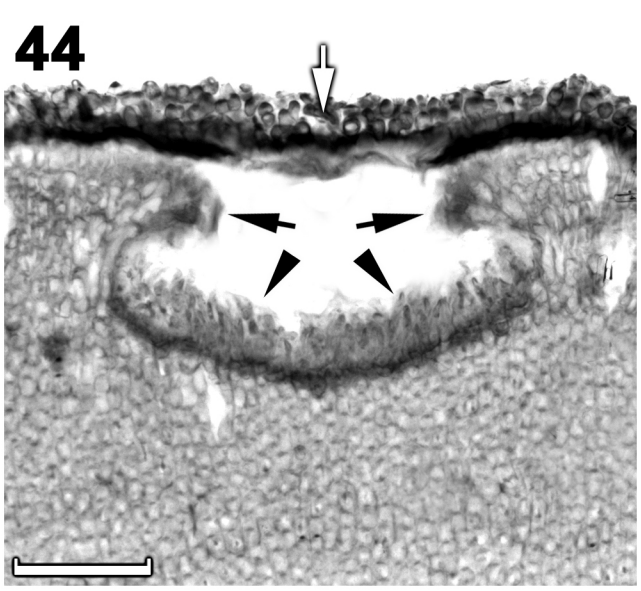

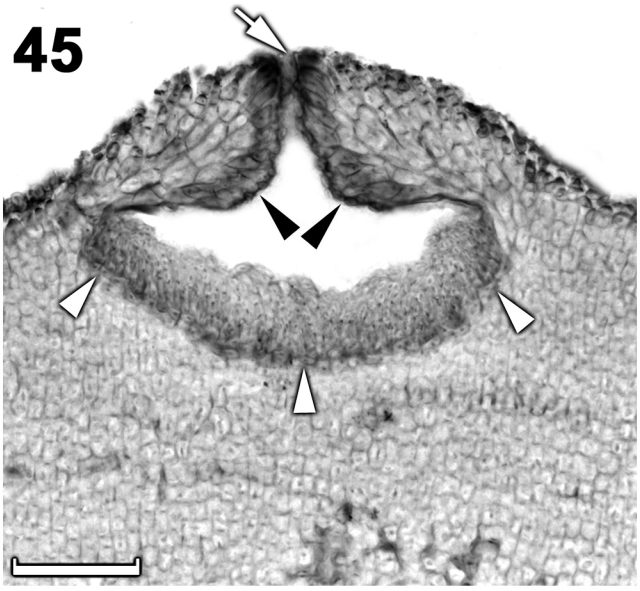

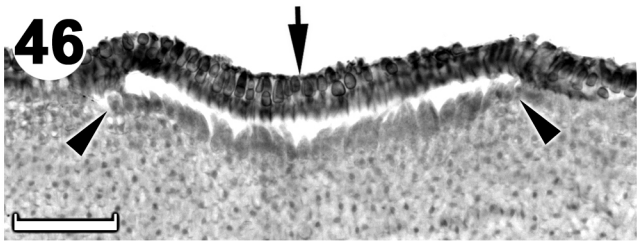

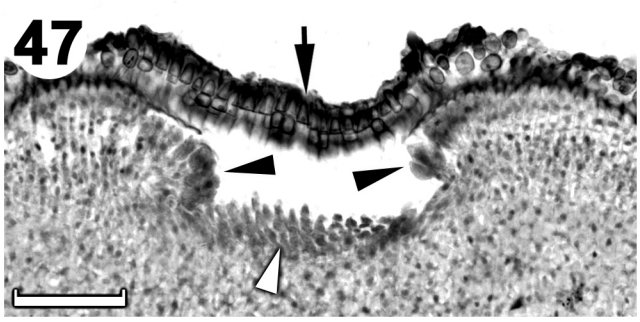

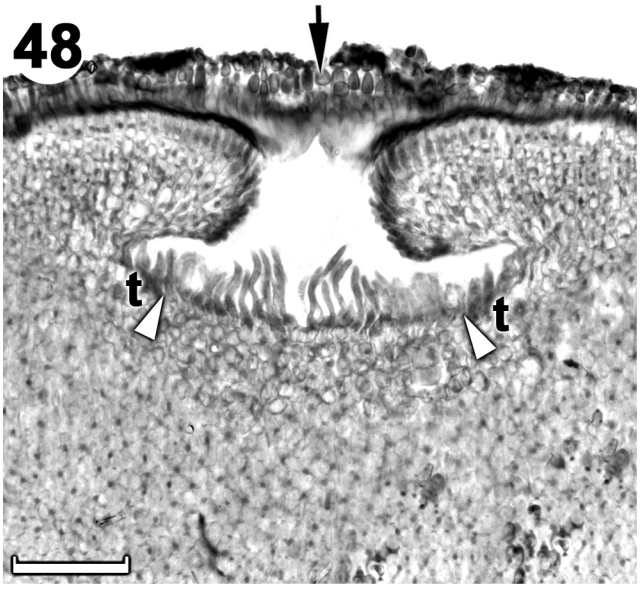

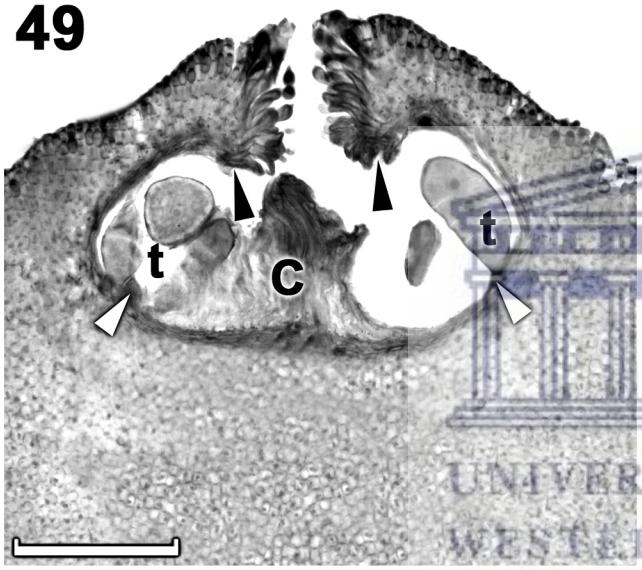

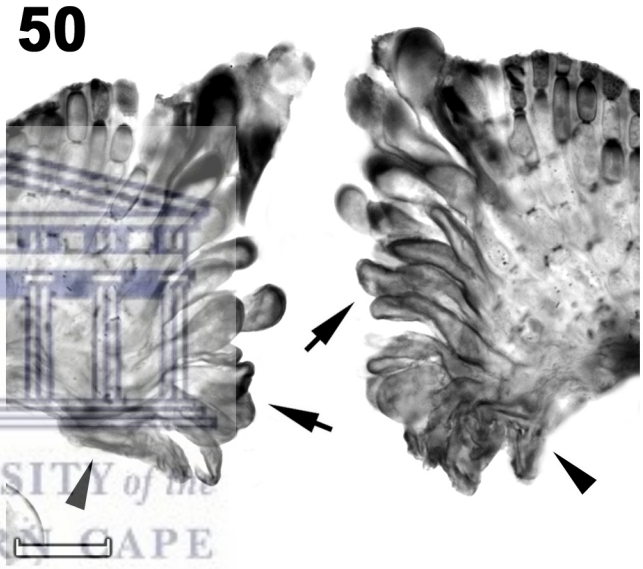

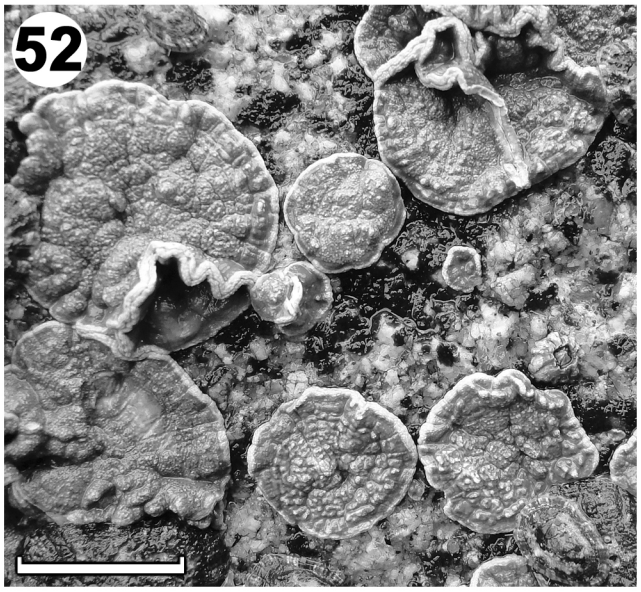

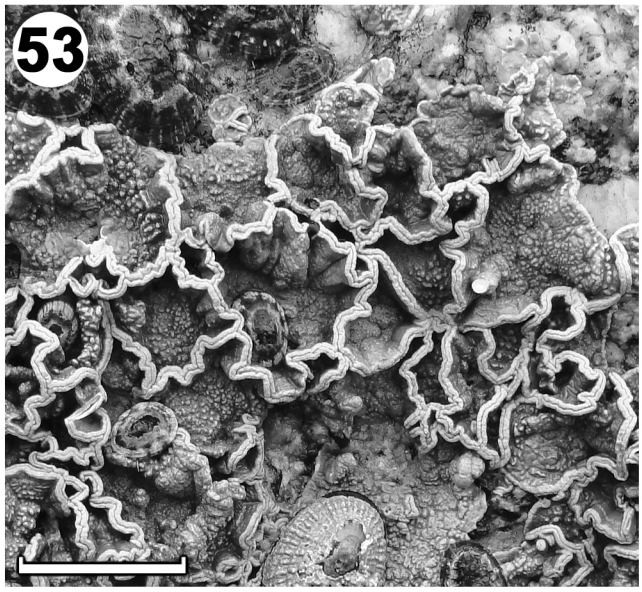

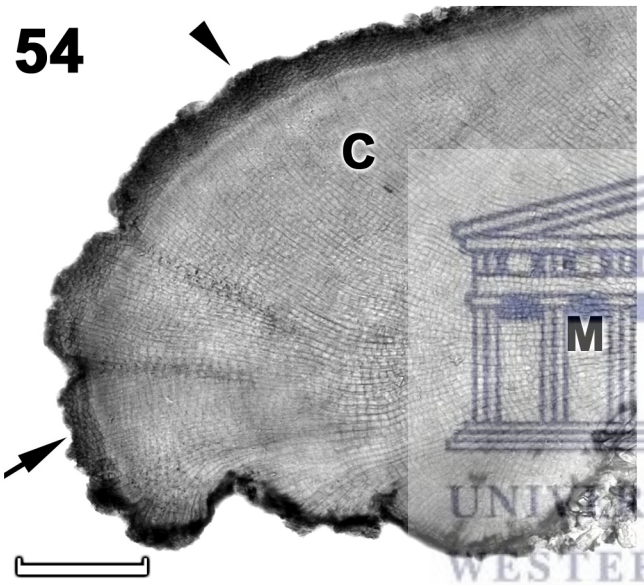

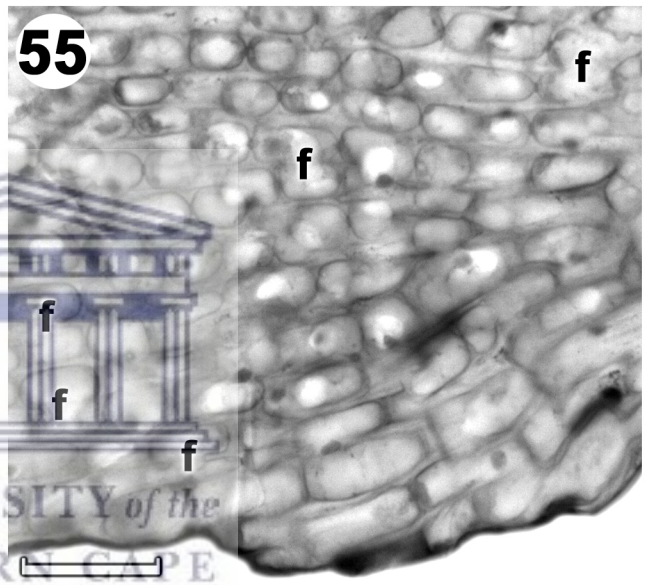

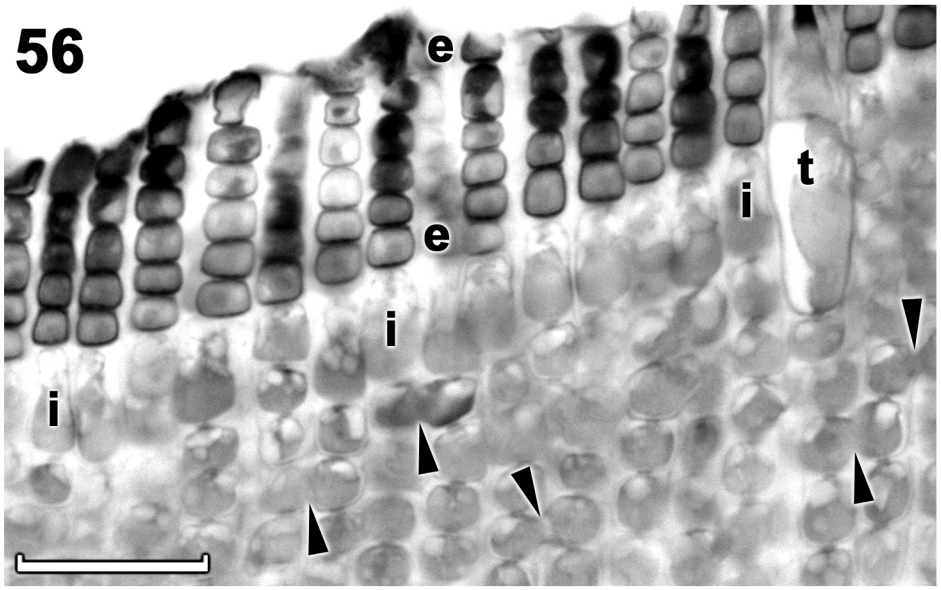

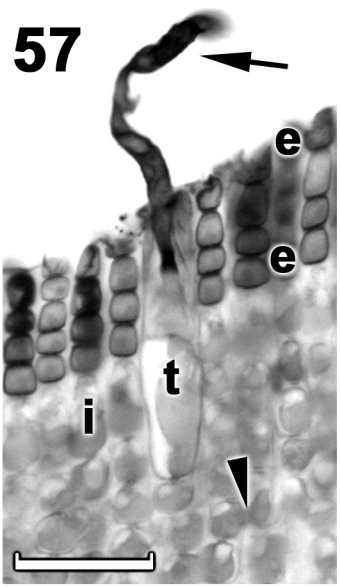

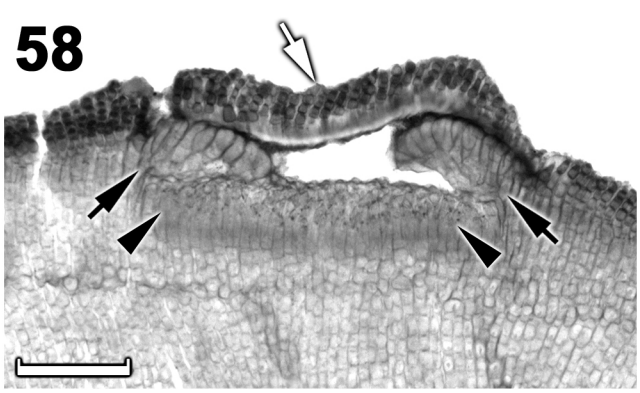

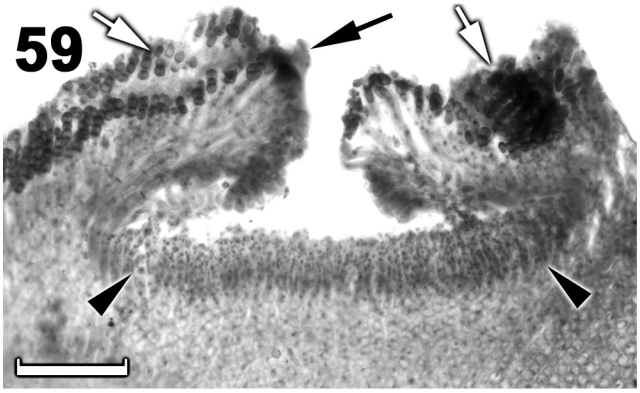

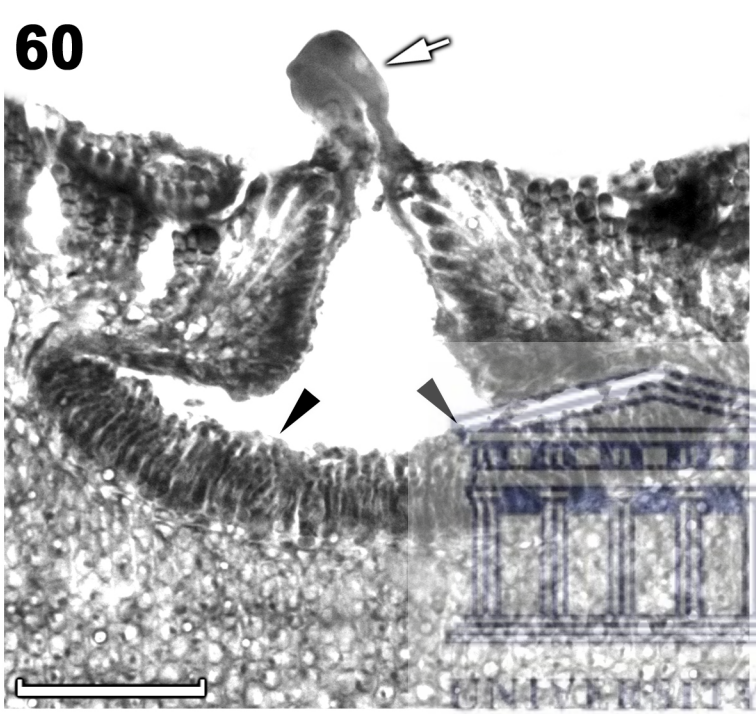

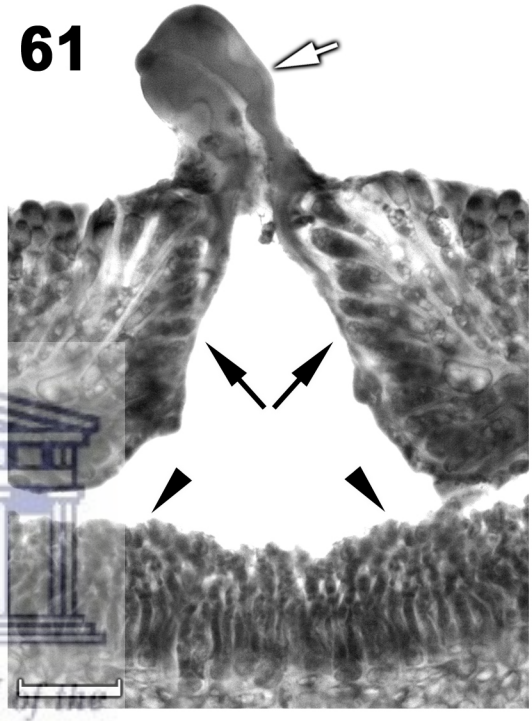

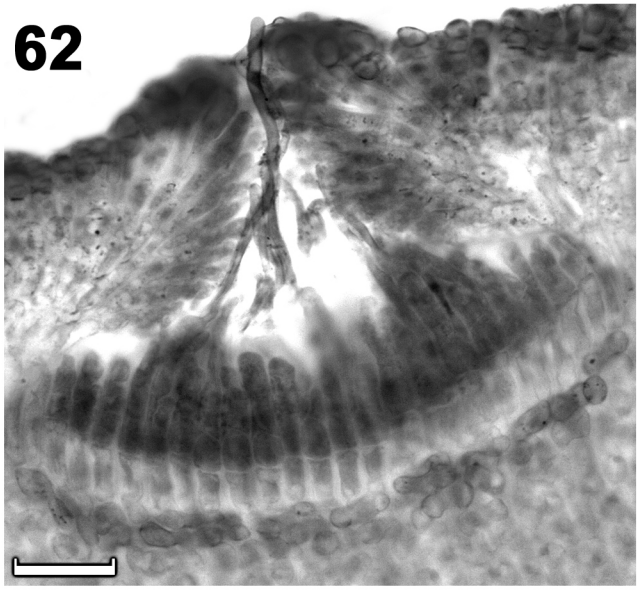

62

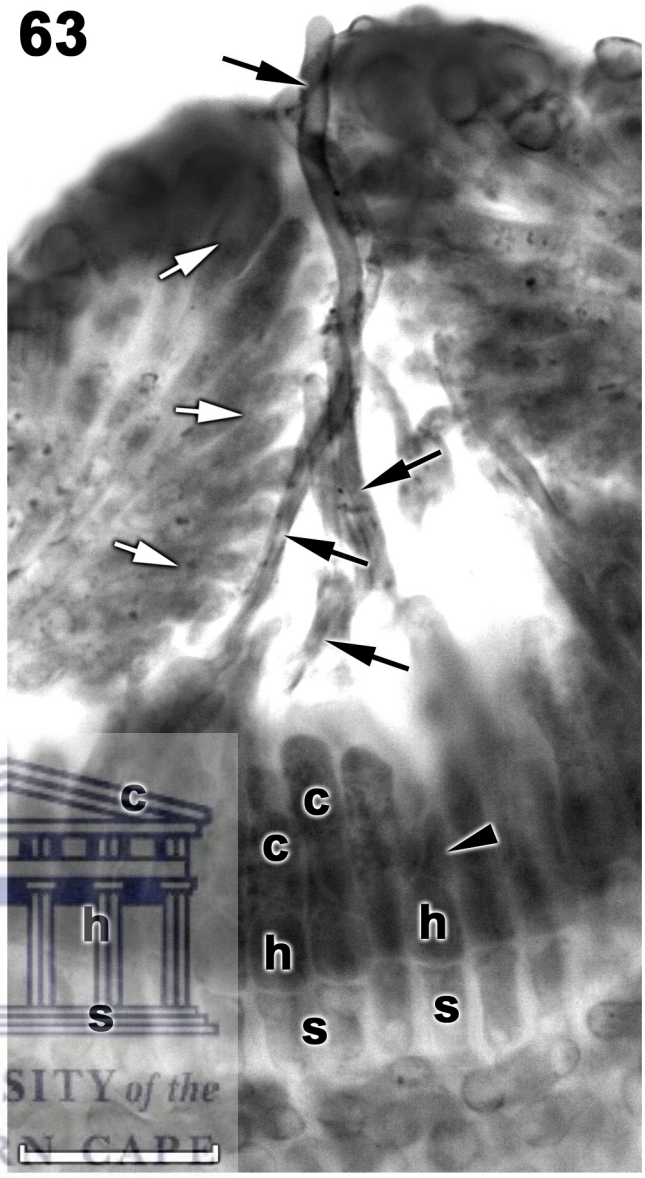

63

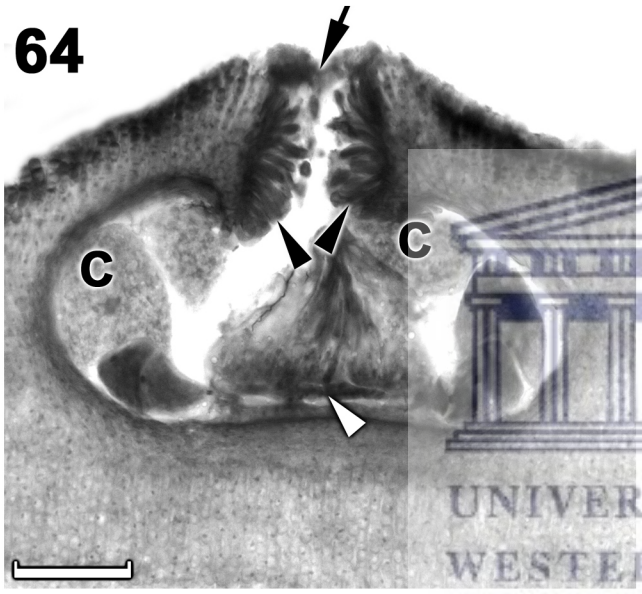

64

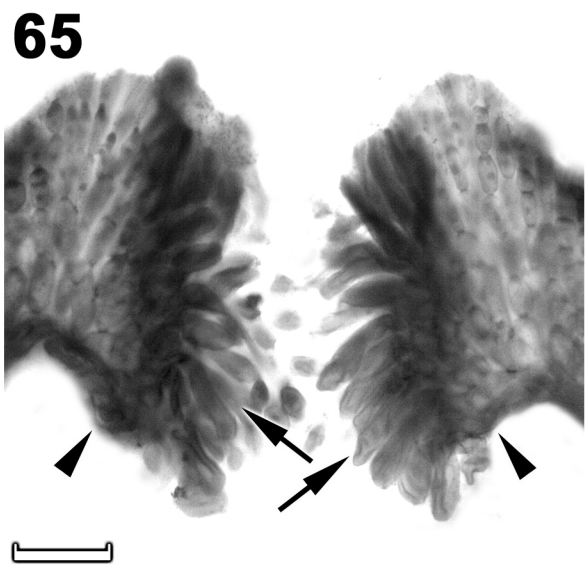

65

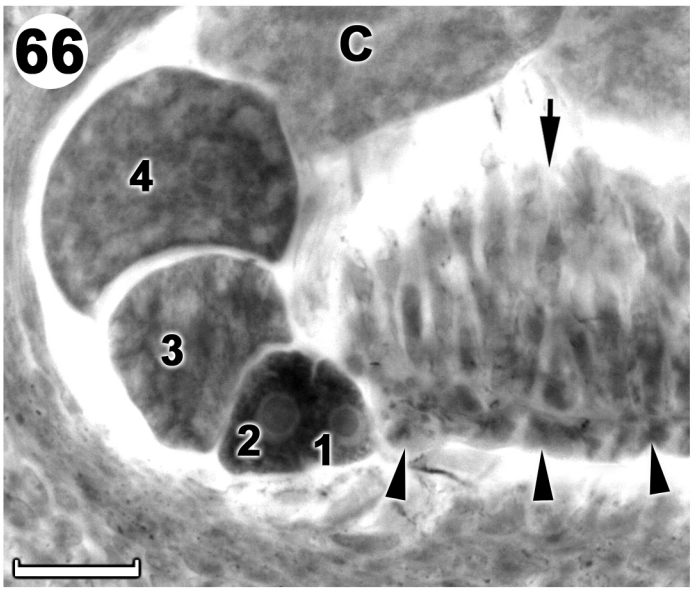

66

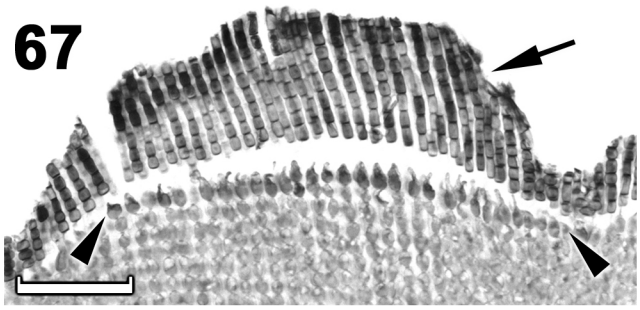

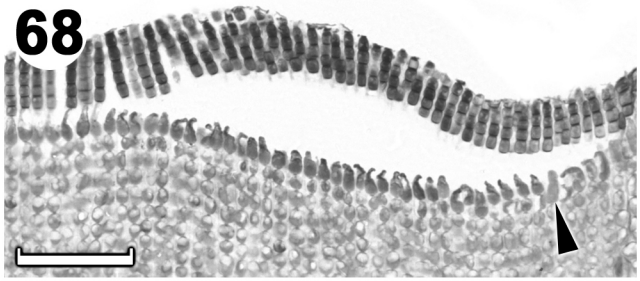

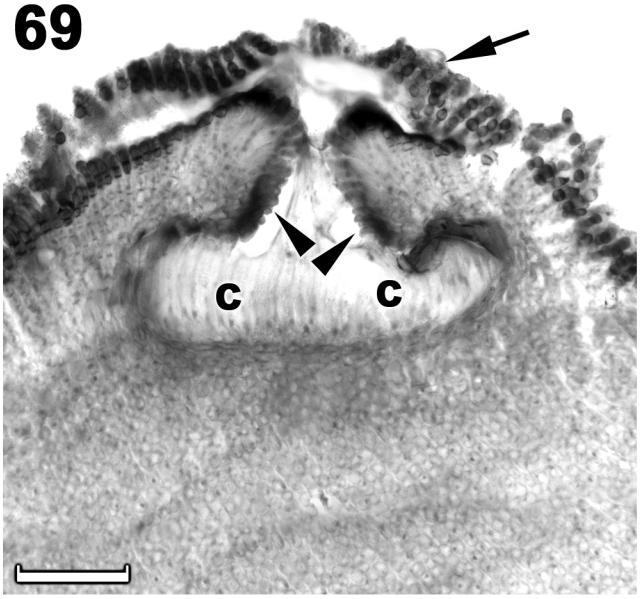

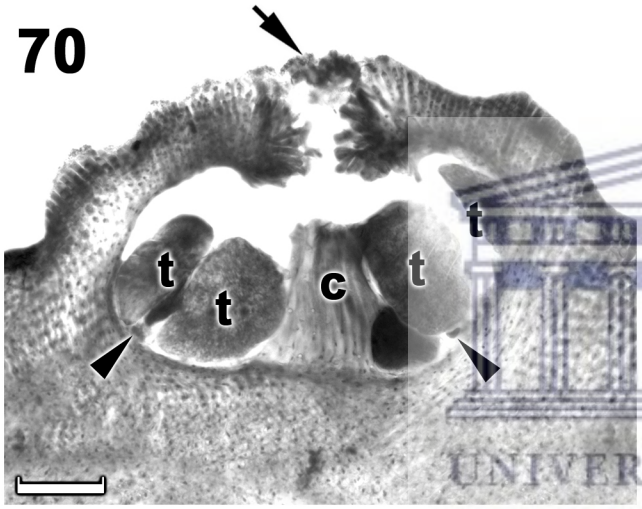

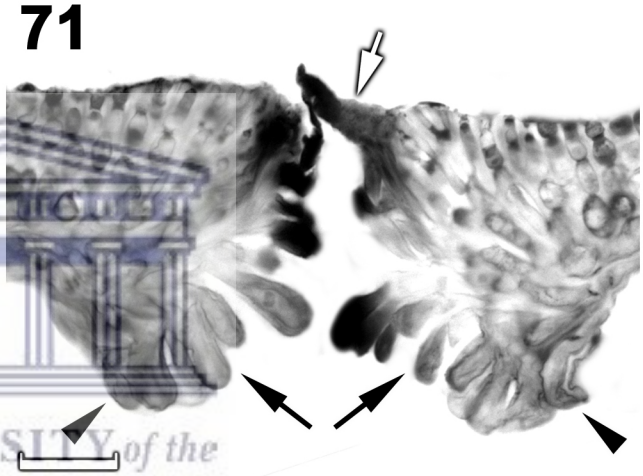

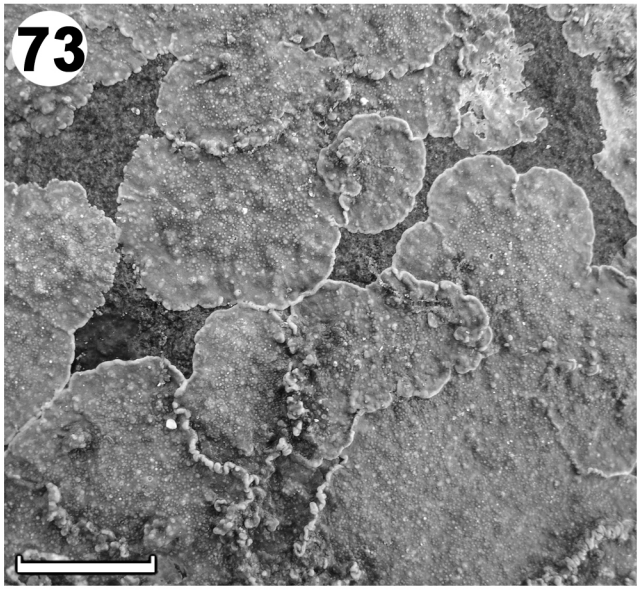

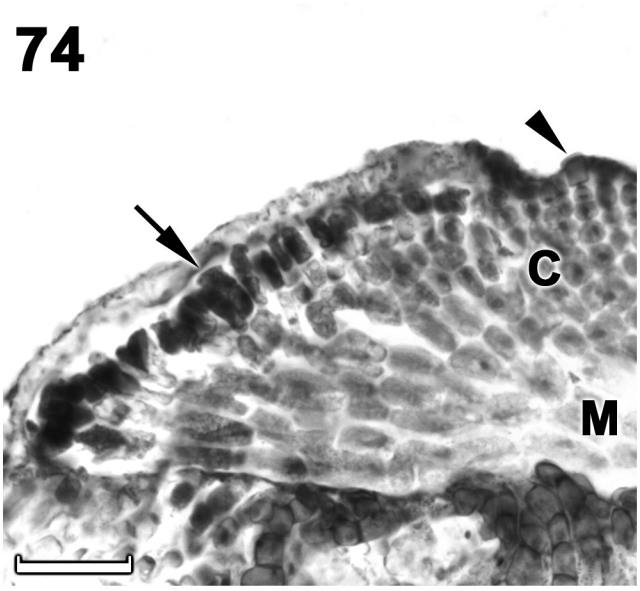

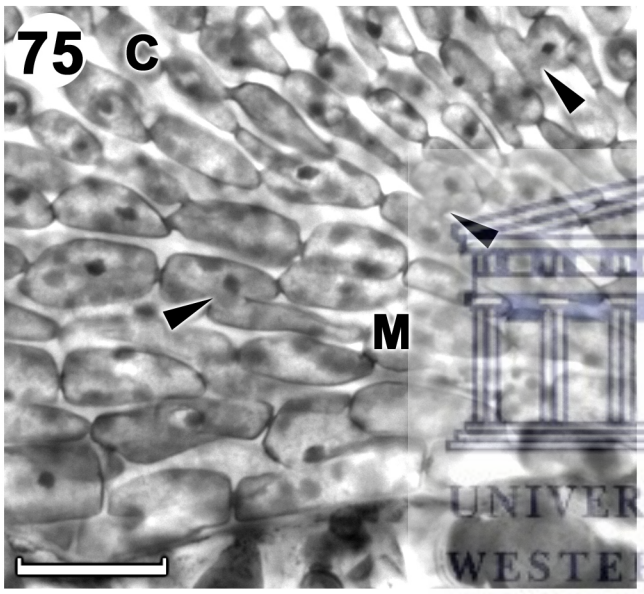

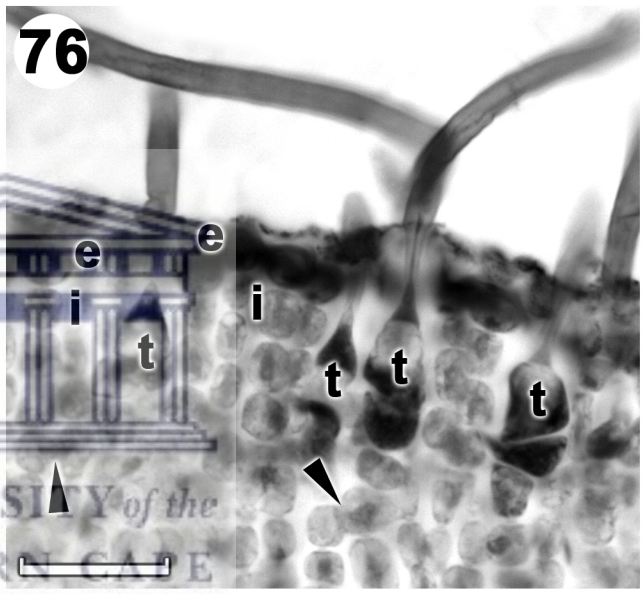

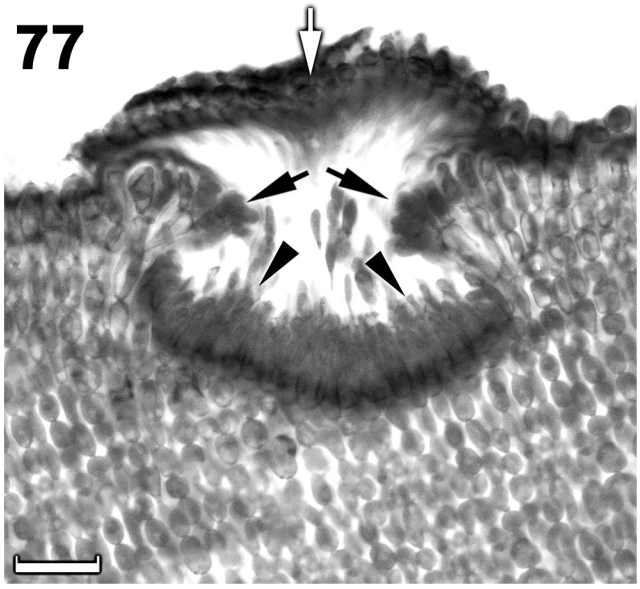

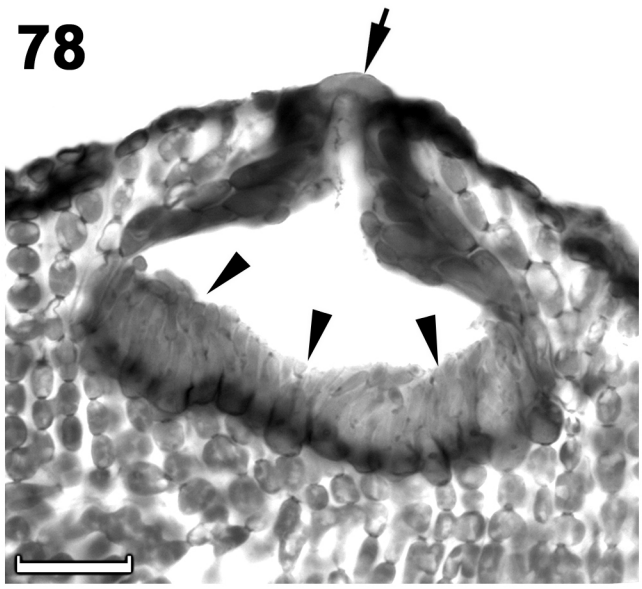

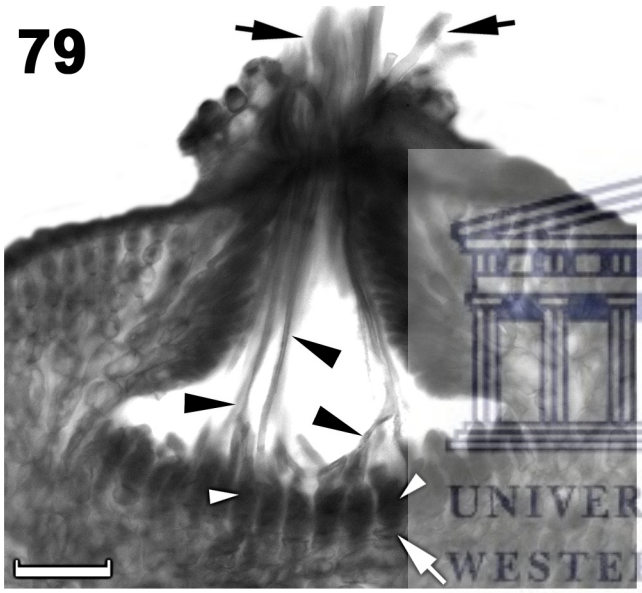

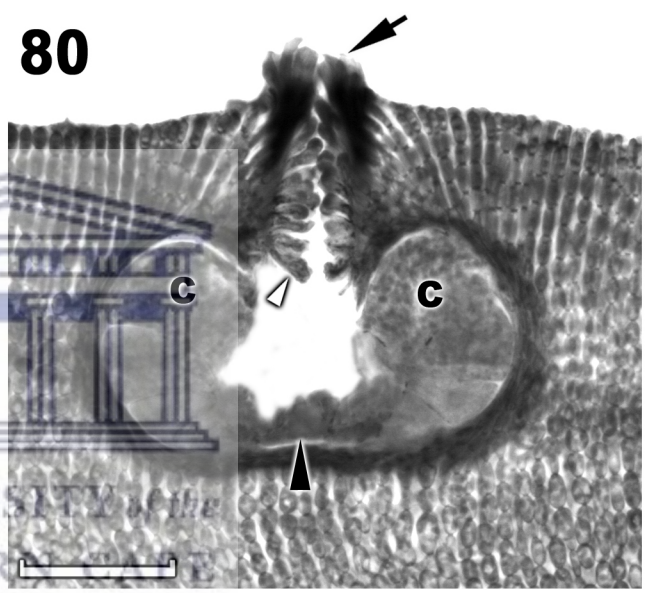

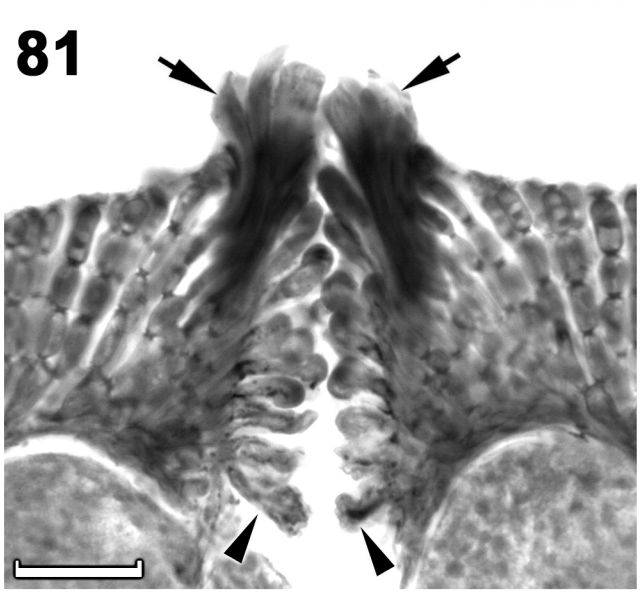

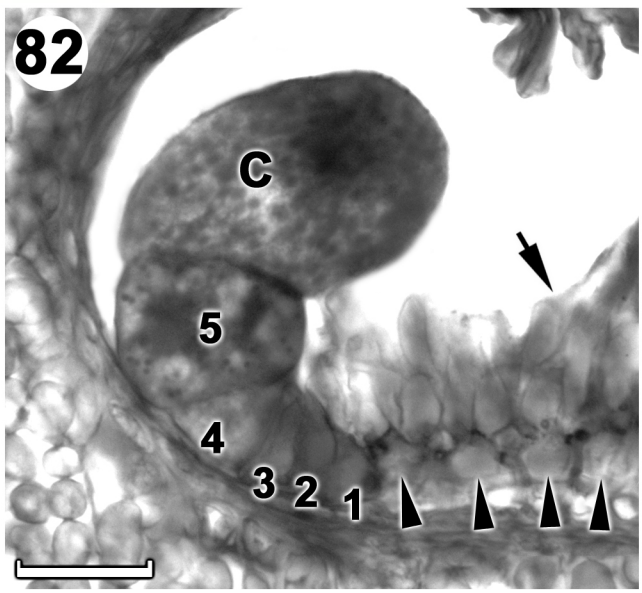

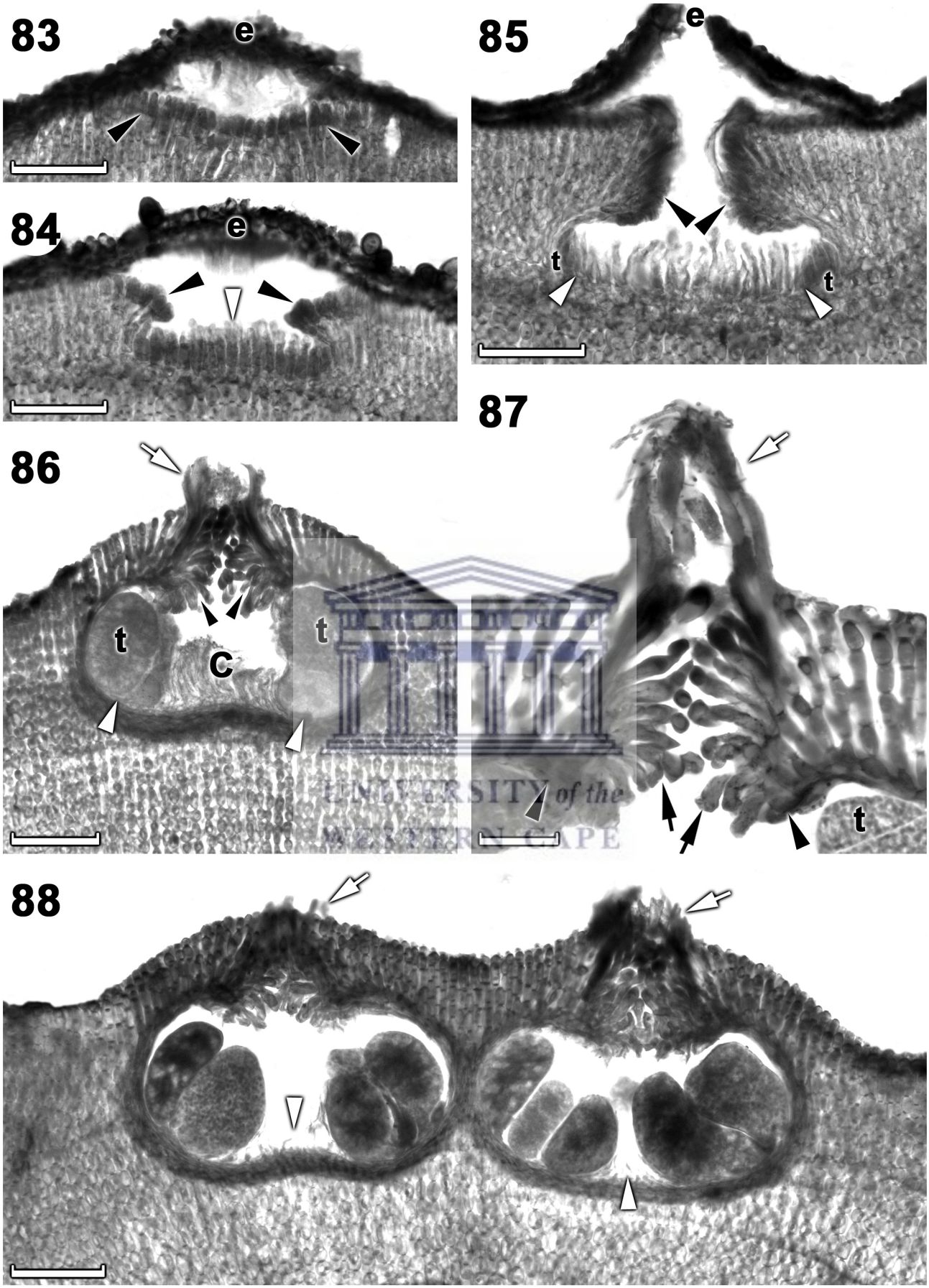

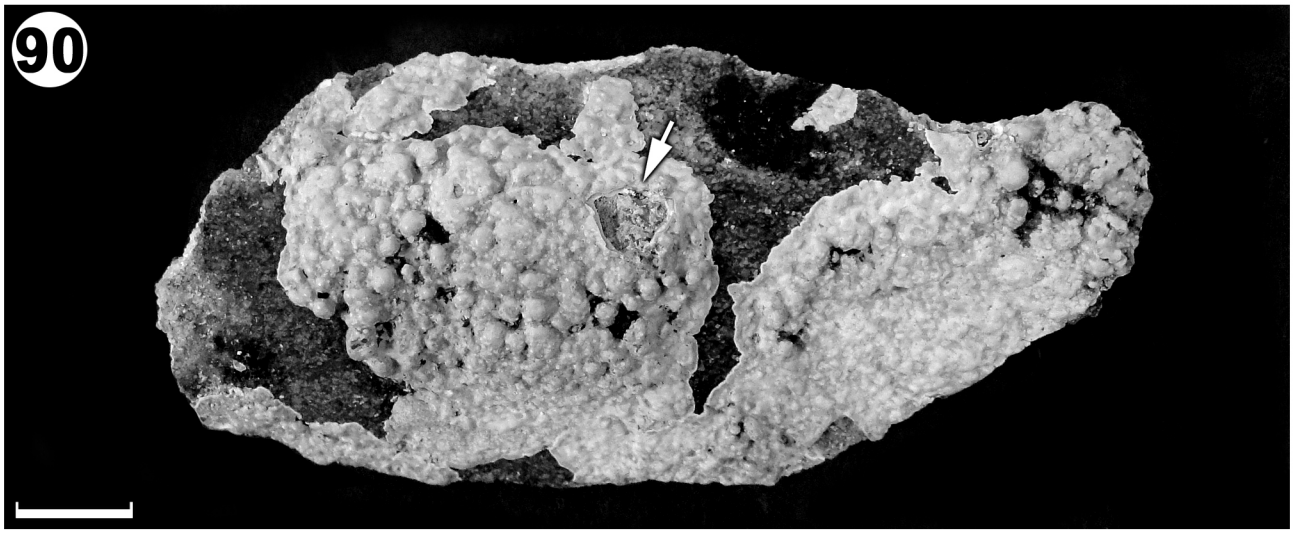

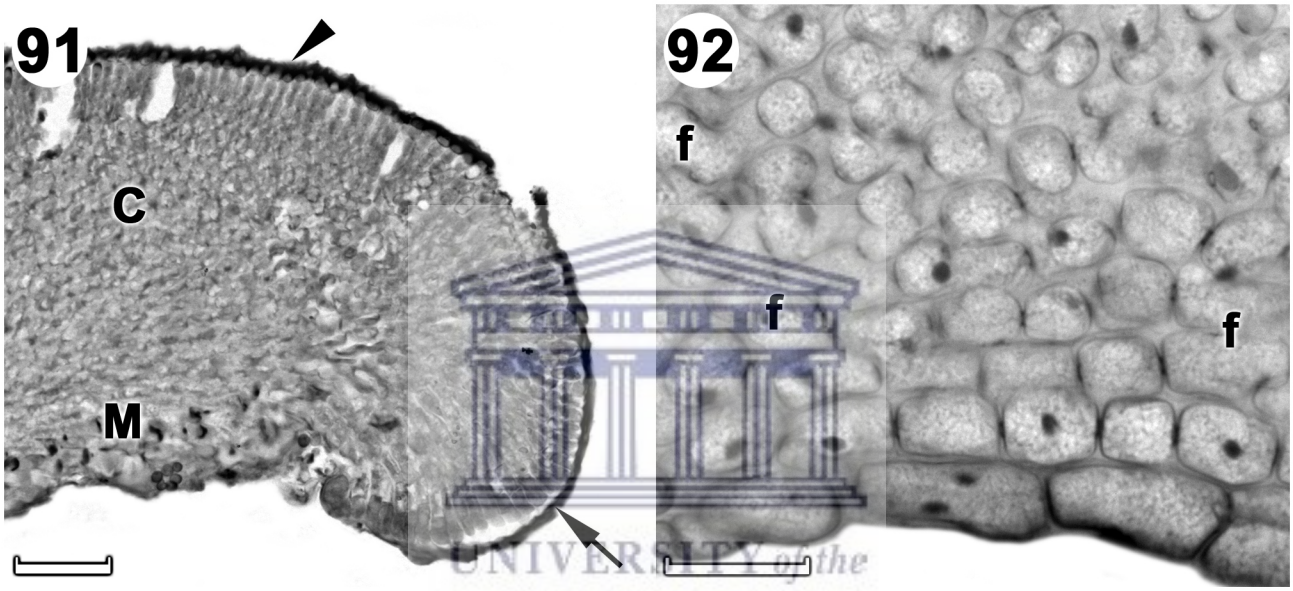

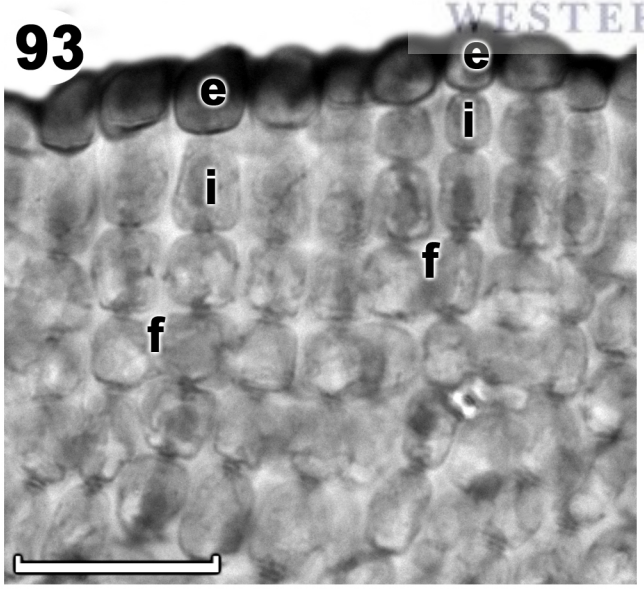

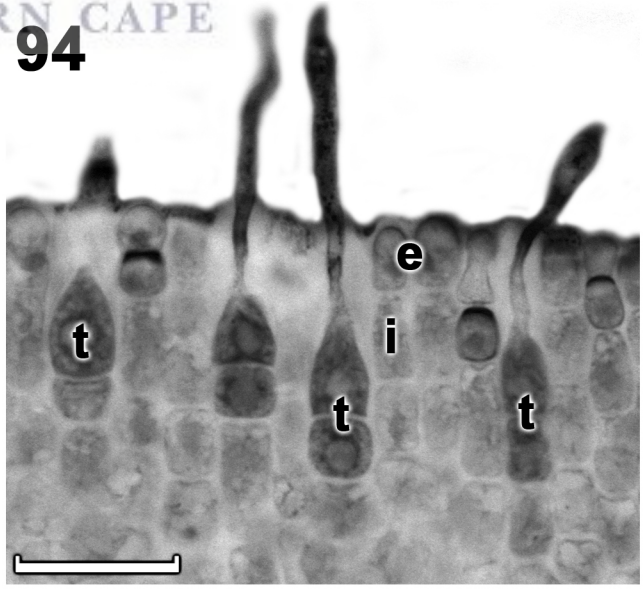

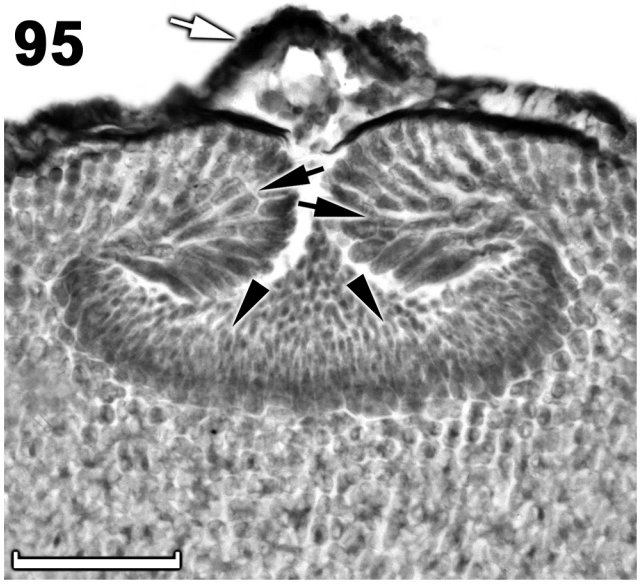

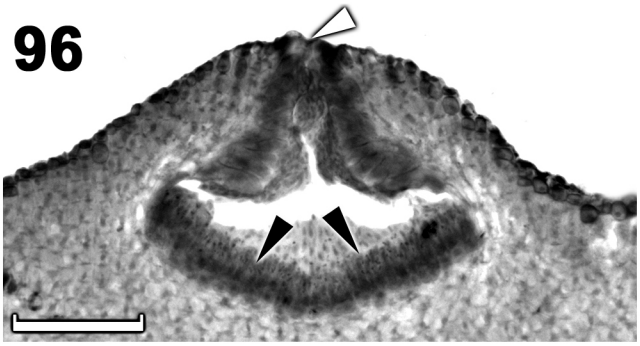

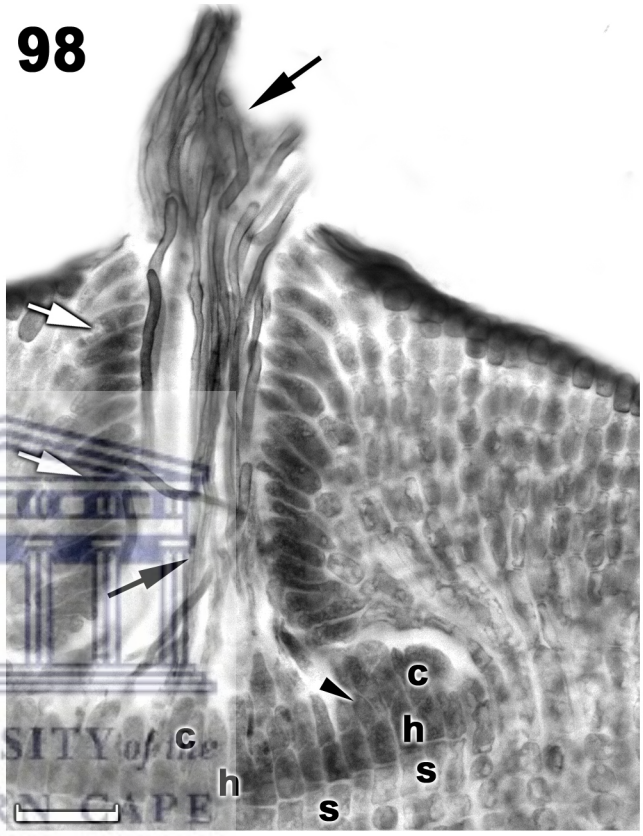

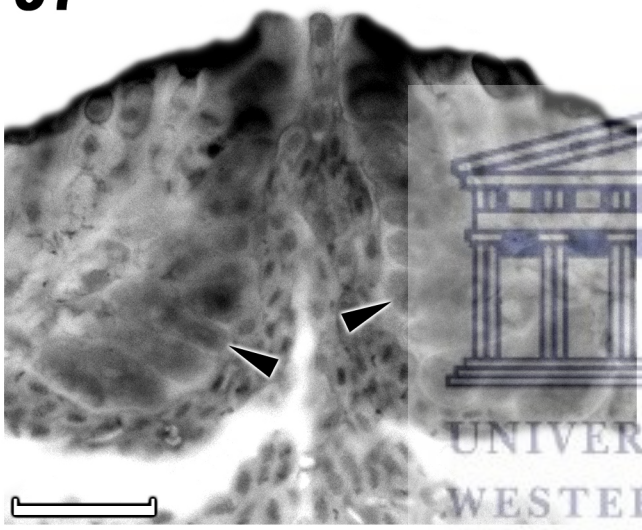

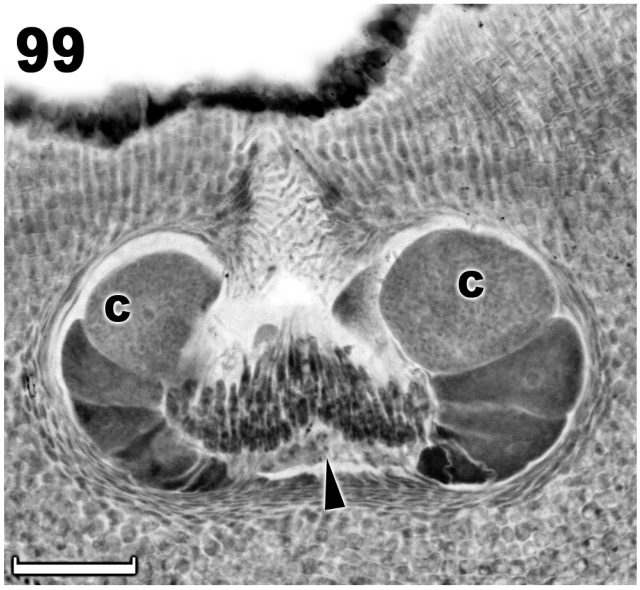

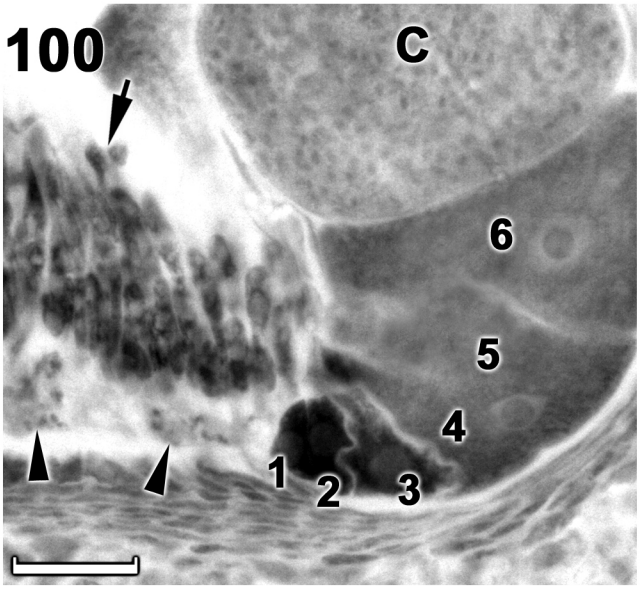

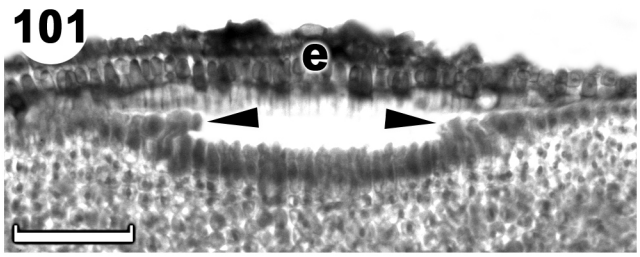

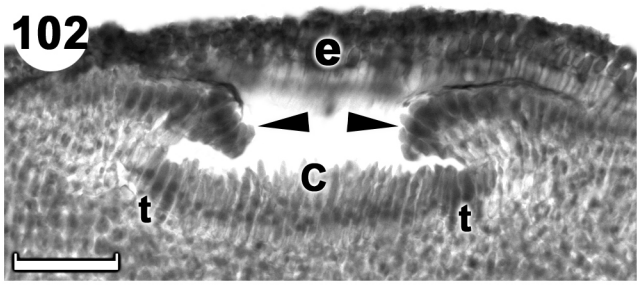

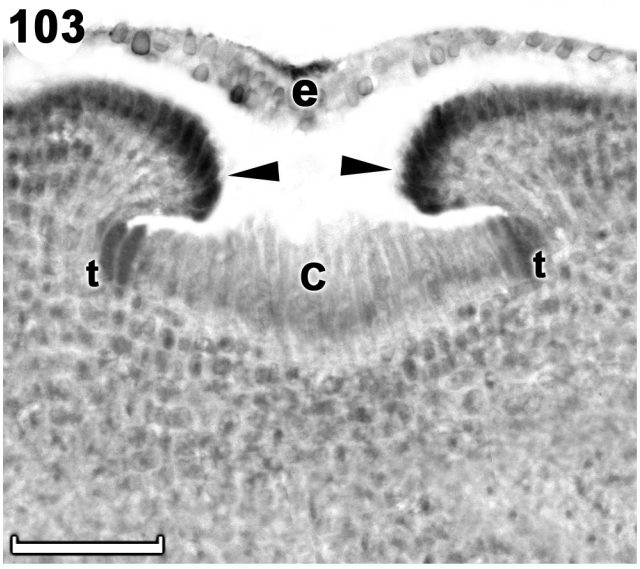

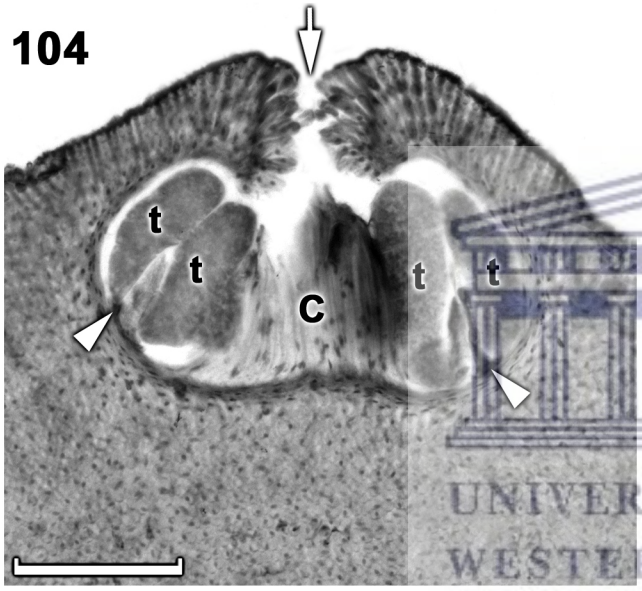

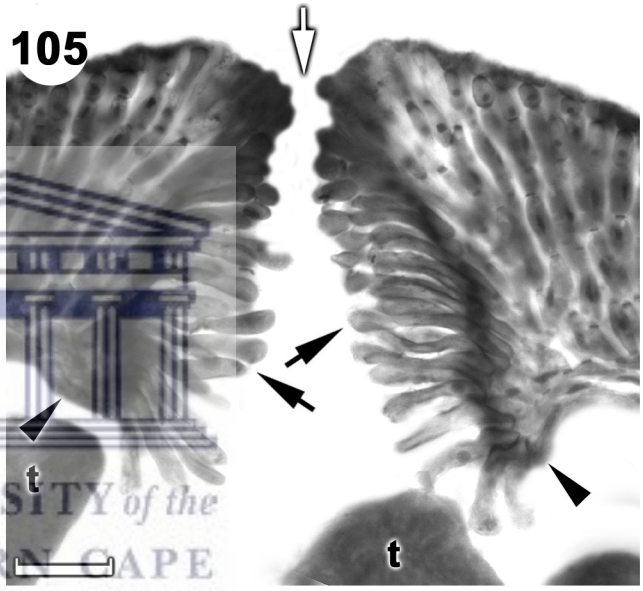

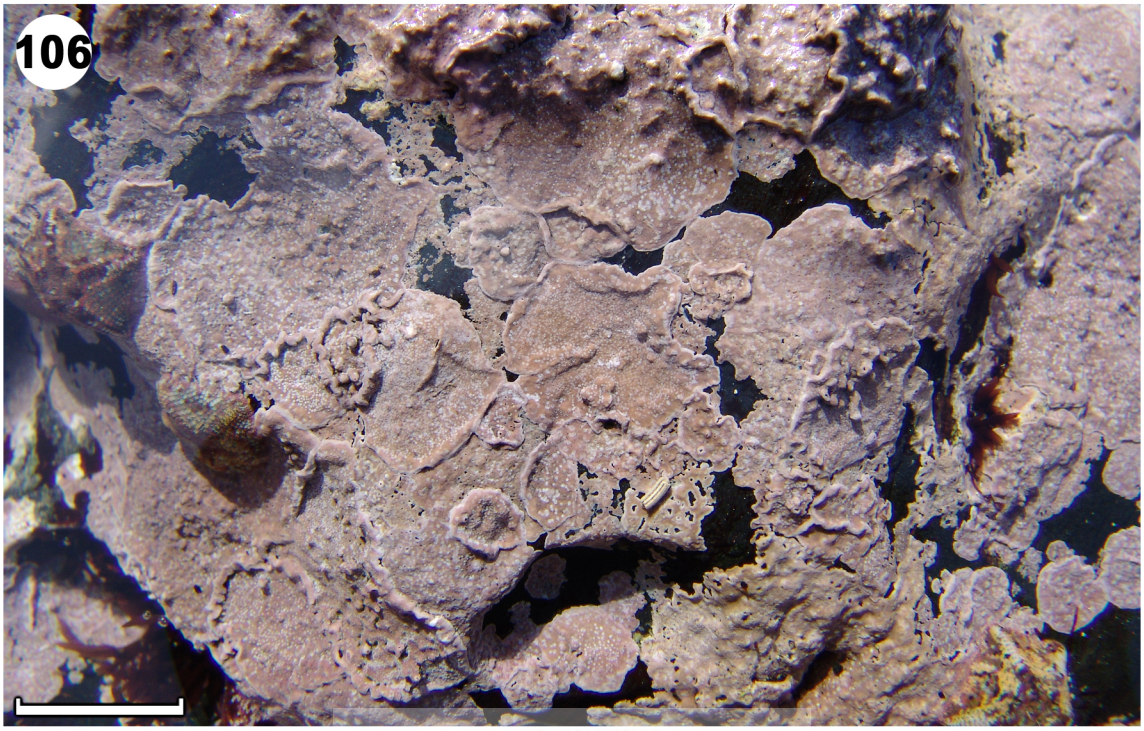

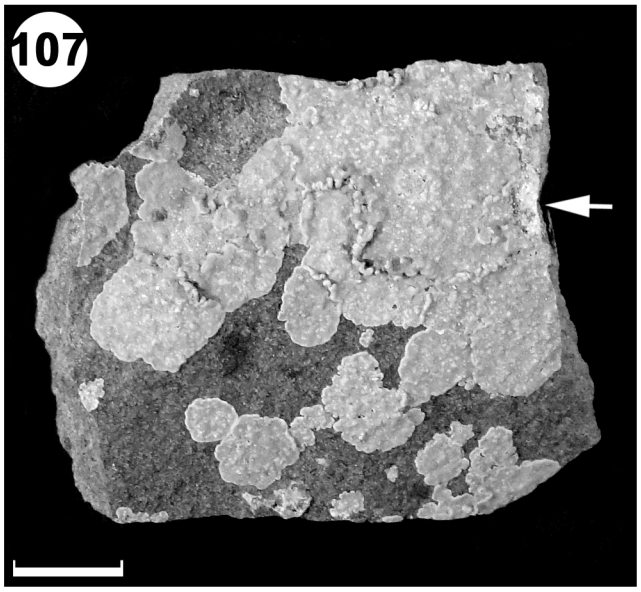

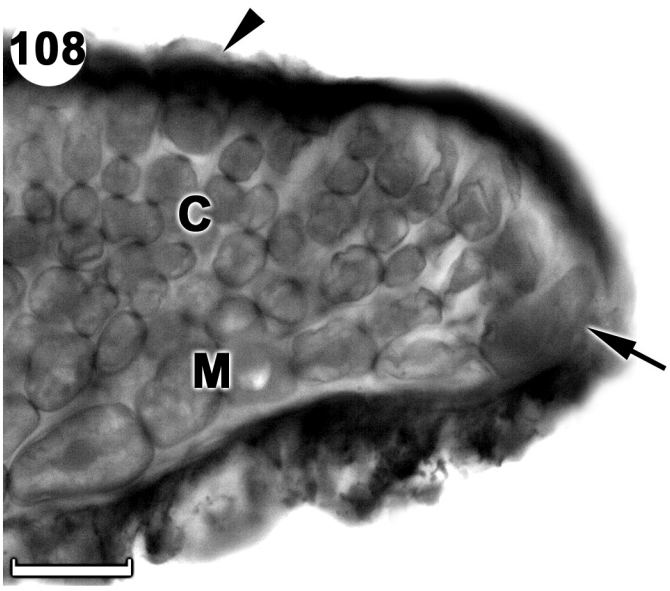

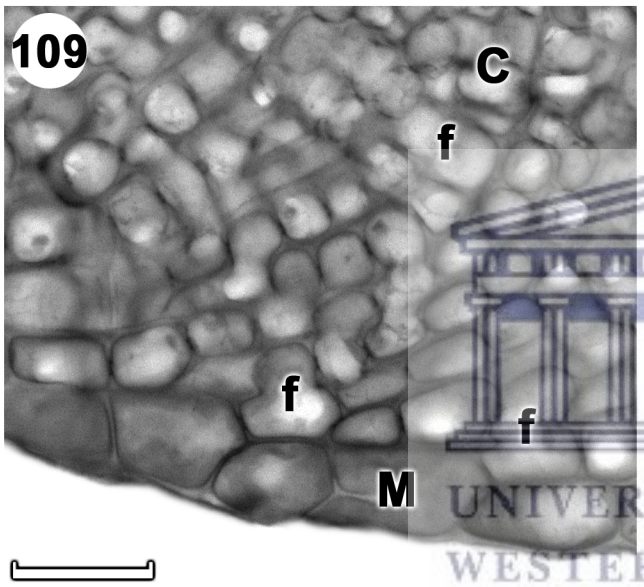

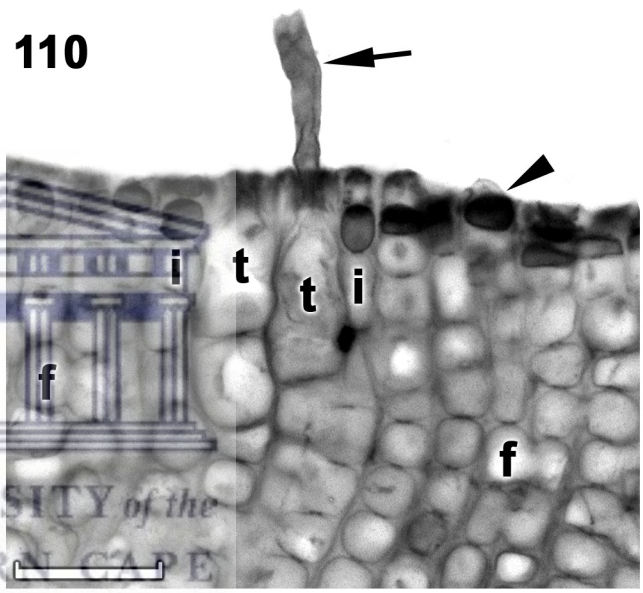

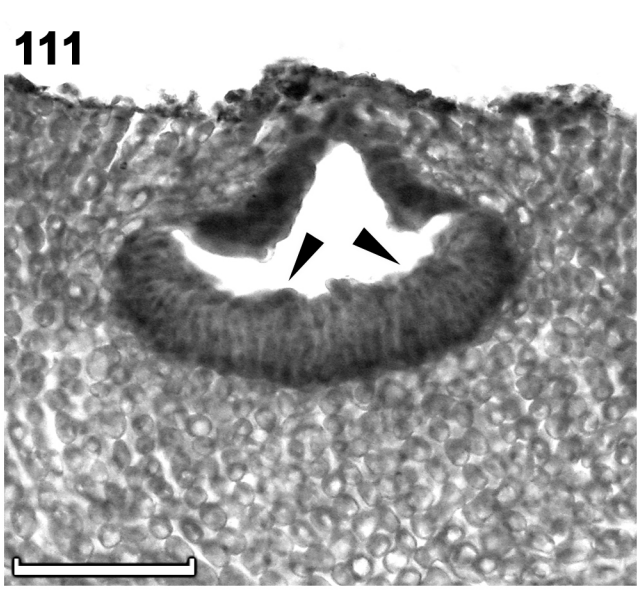

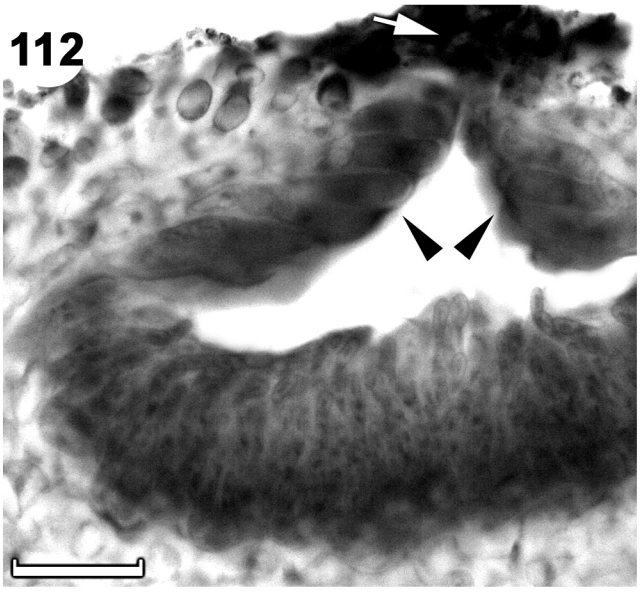

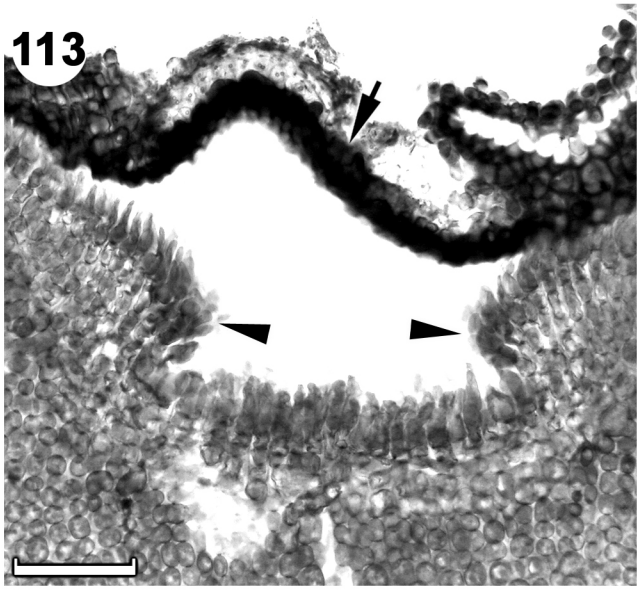

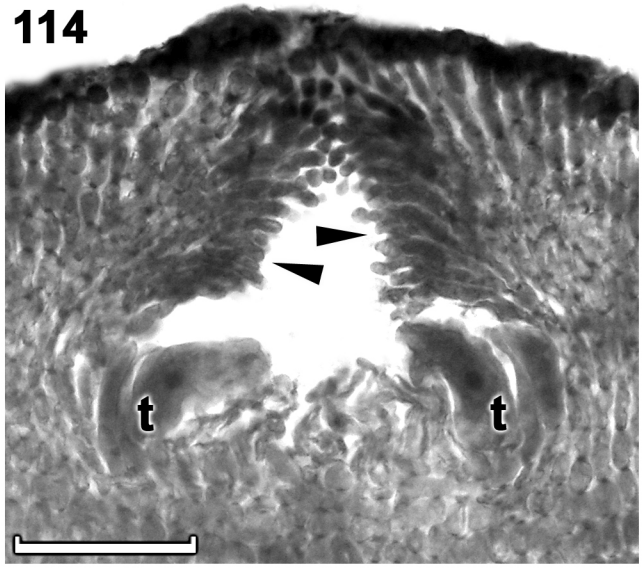

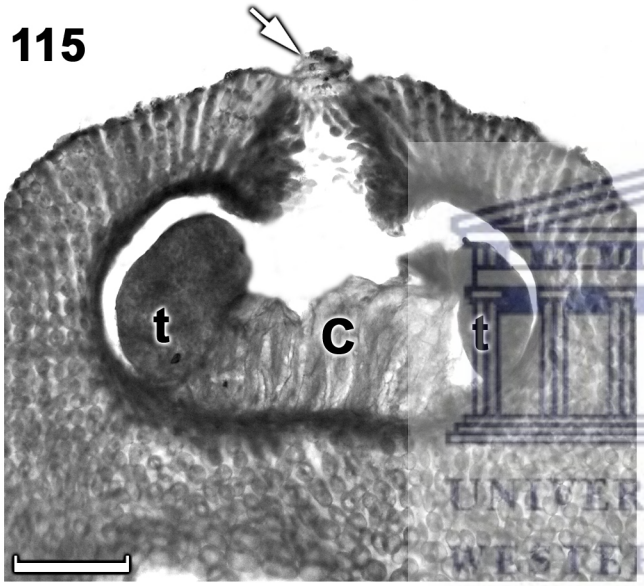

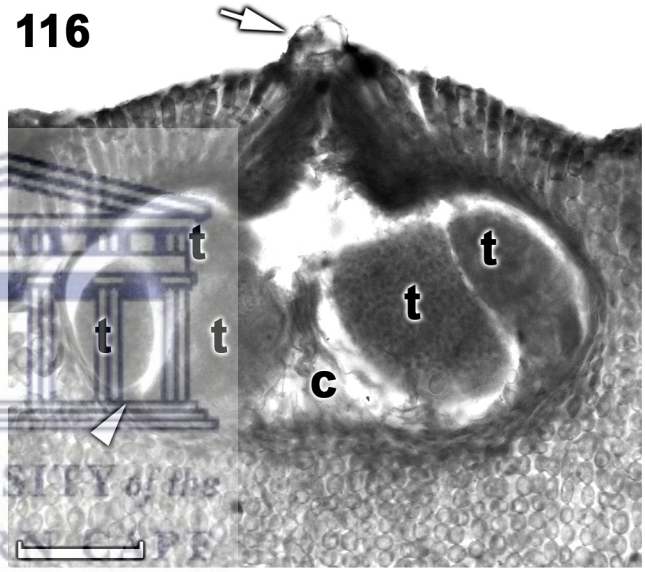

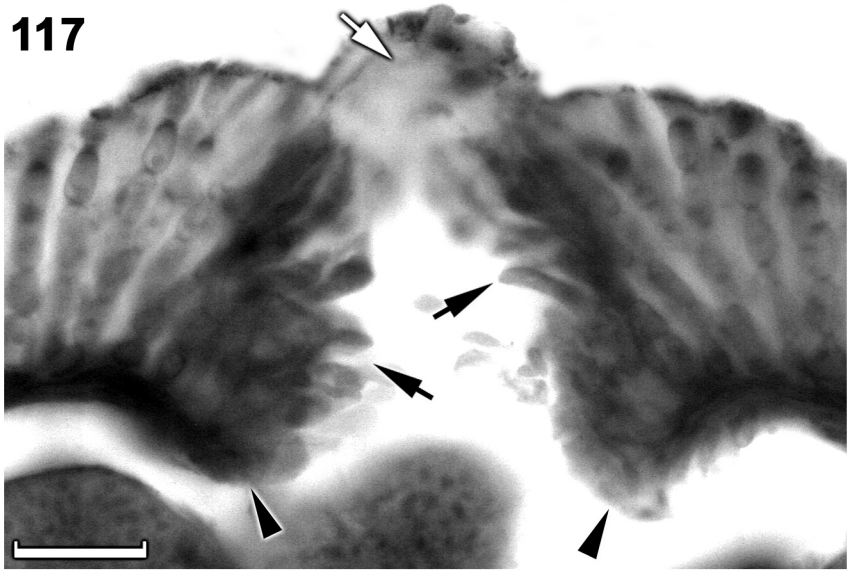

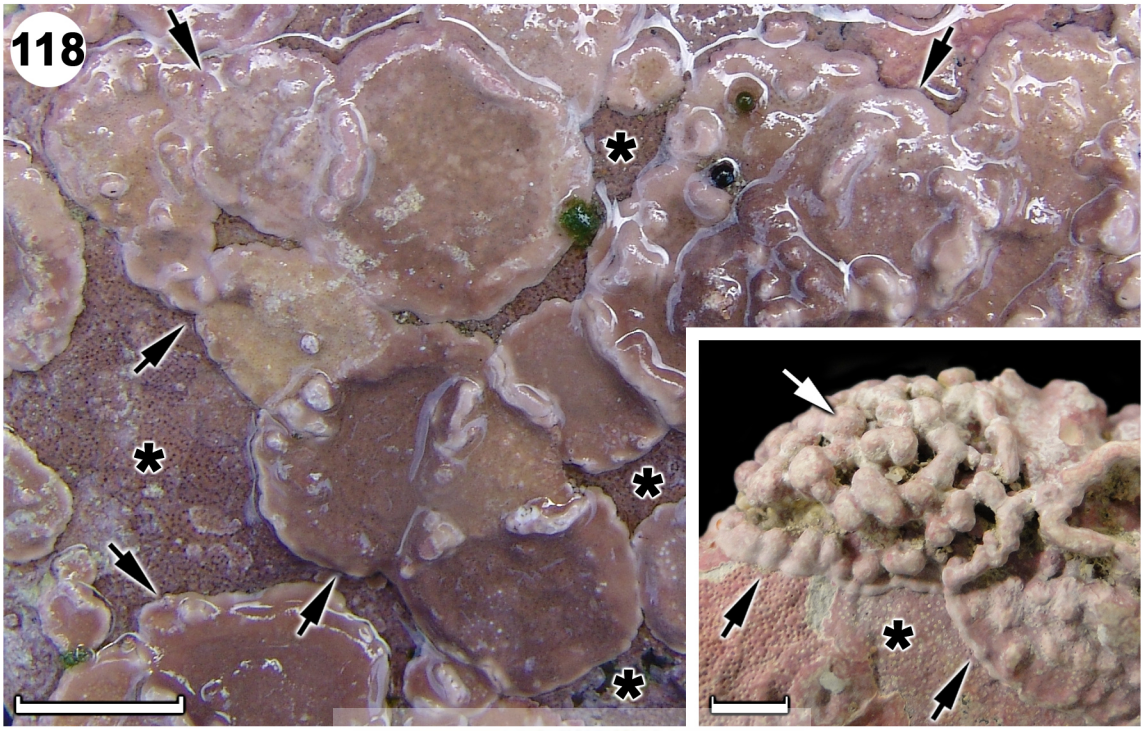

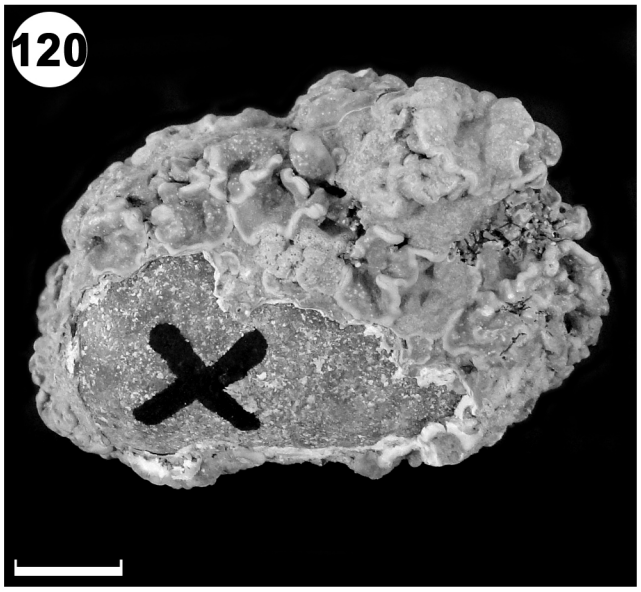

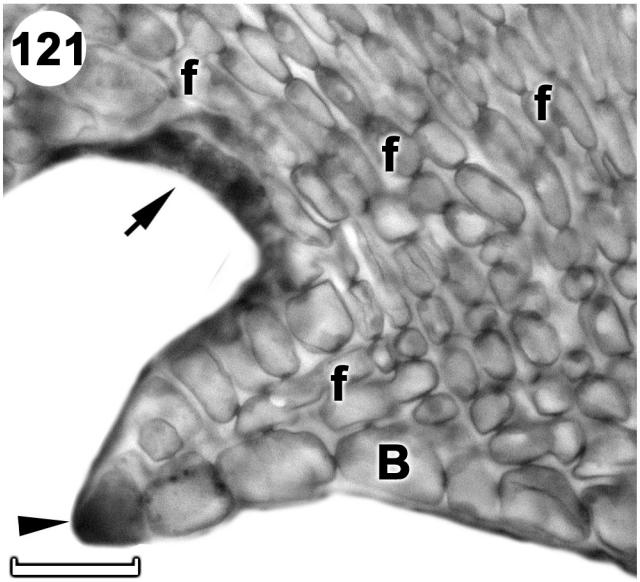

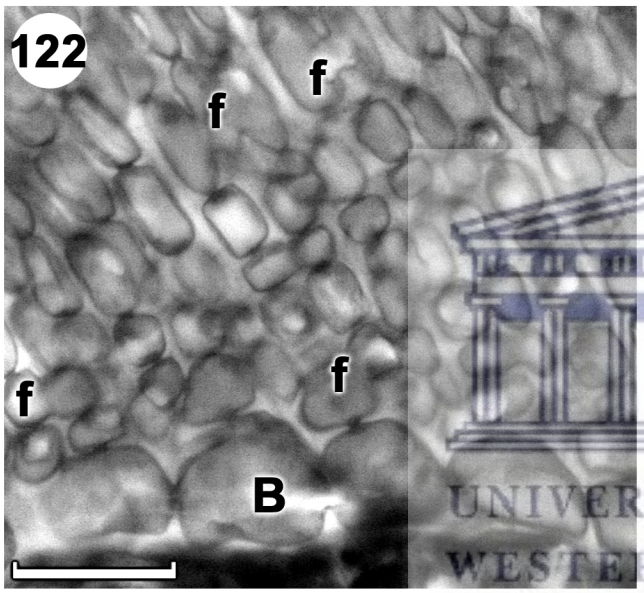

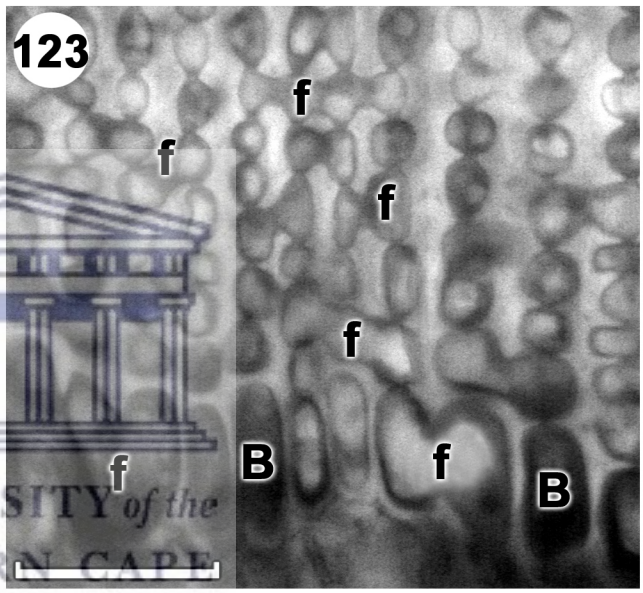

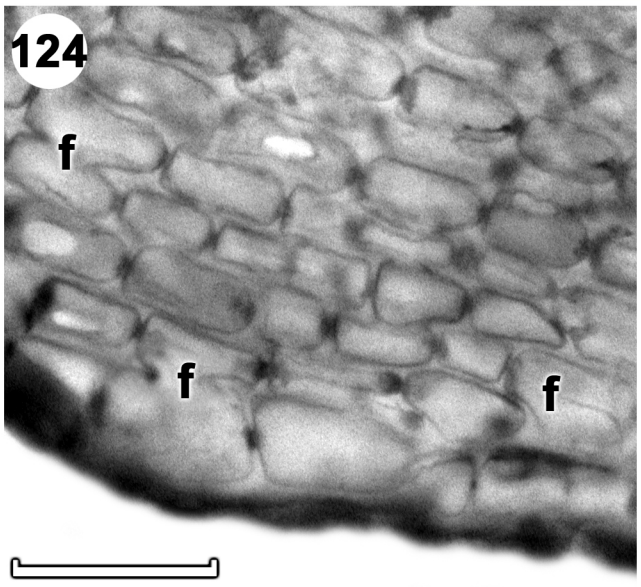

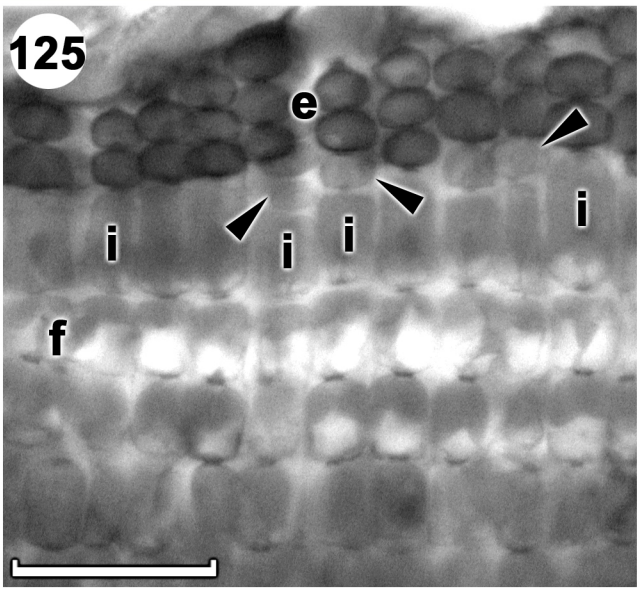

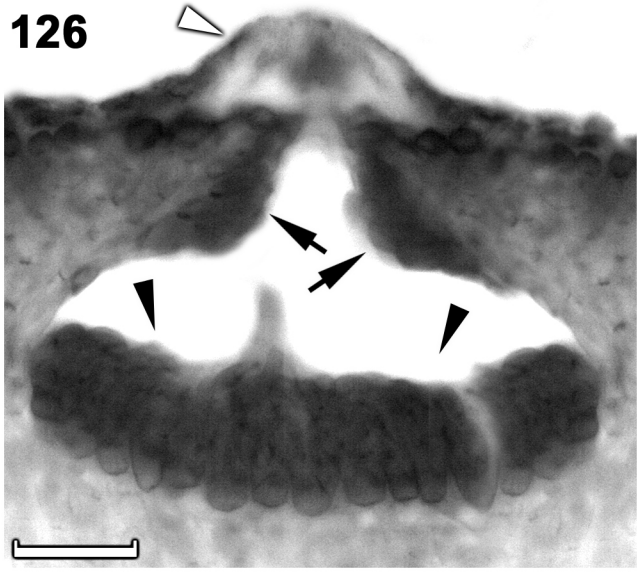

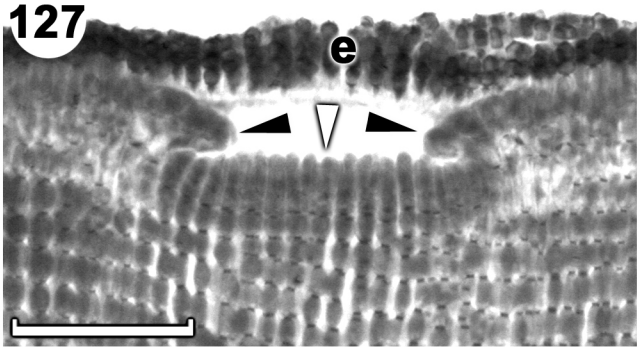

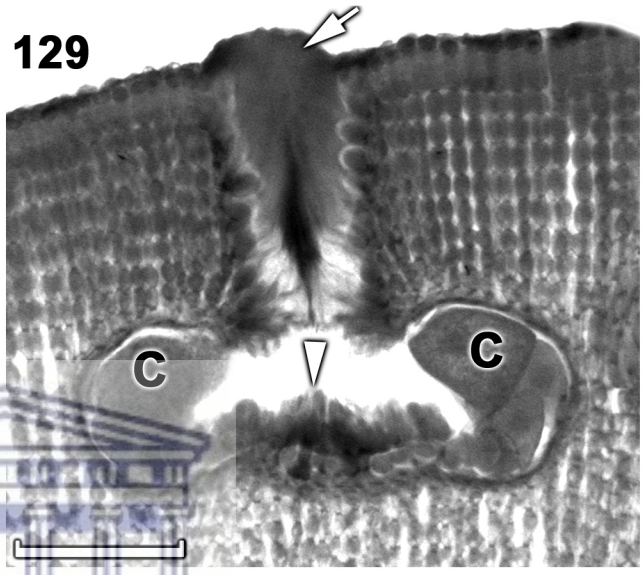

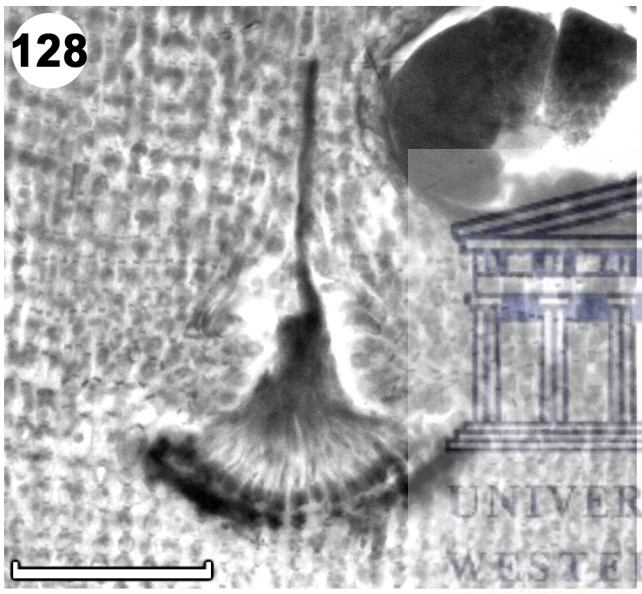

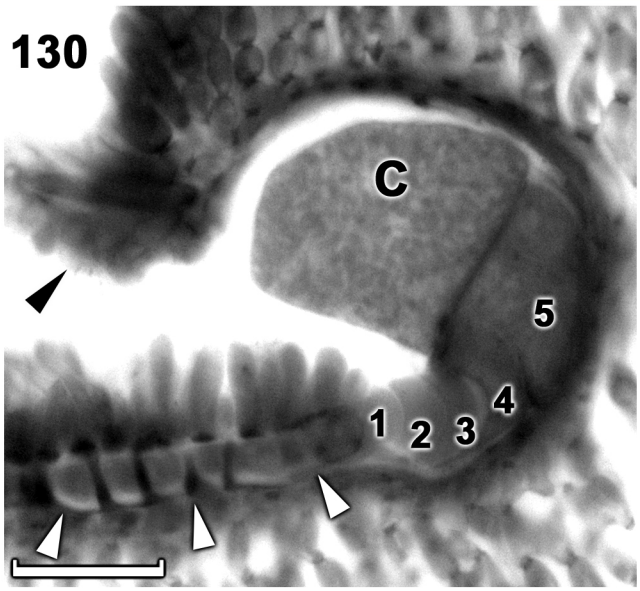

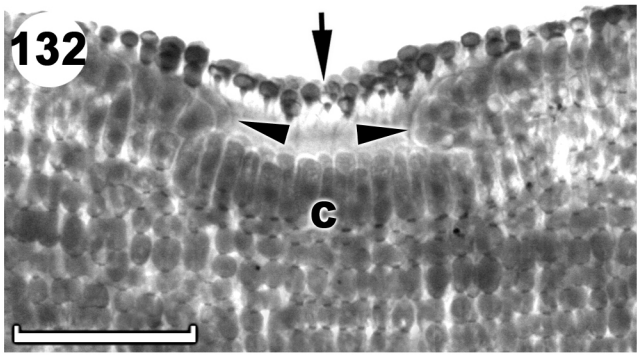

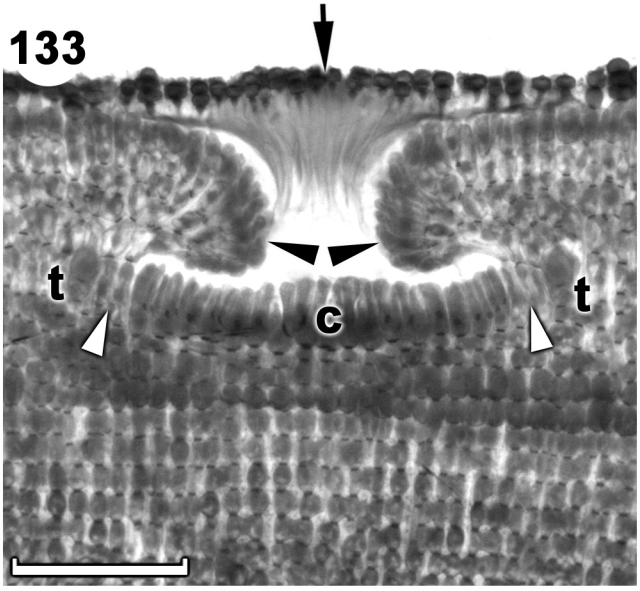

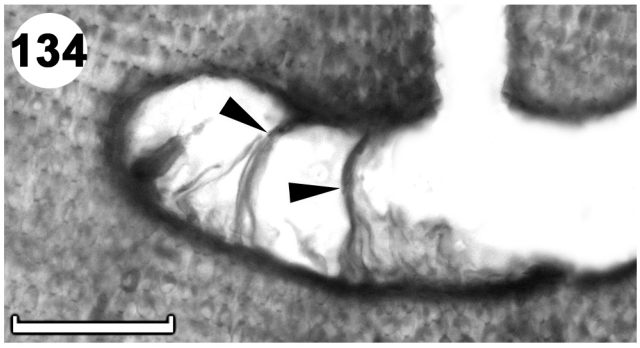

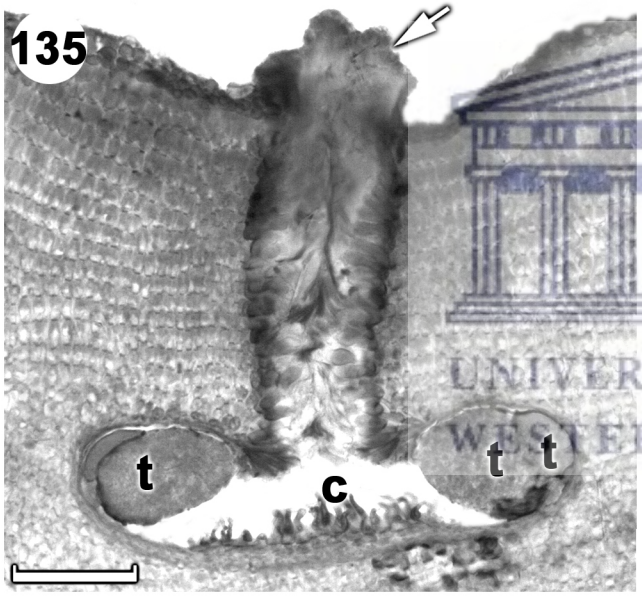

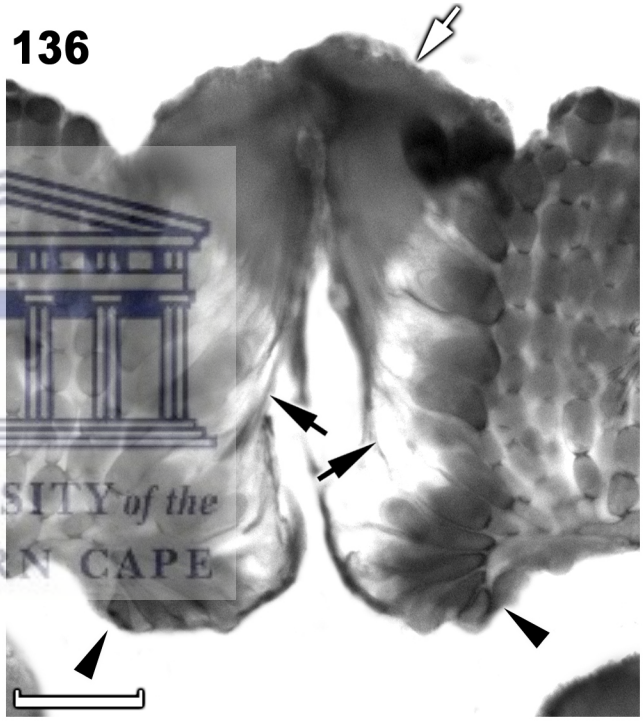

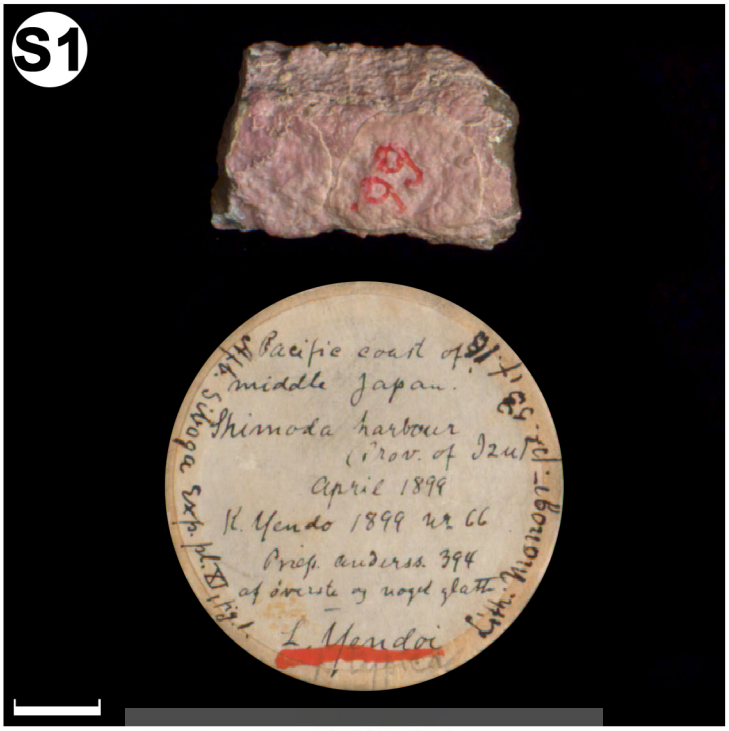

Supplementary table

Table S1: List of taxa, the reason for their inclusion in the phylogenetic analyses, their reference information and GenBank accession numbers. Sequences generated for this study are in bold; GenBank accession numbers (denoted by GBxxxxxx) are still to be obtained. Newly established South African species are identified by their collection number as they are yet to be assigned official herbarium (L = Naturalis, Netherlands, Leiden) numbers.

Taxon	Reason of inclusion	Voucher/Collection No.	Location	Reference	GenBank Accession No.	
					*psb*A	*rbc*L
Bossiella plumosa	'Topotype'	UC 1966627	USA, California	(Hind *et a*l. 2014a)	JQ917409	-
				(Gabrielson *et al*. 2011)	-	HQ322280
***Chamberlainium* sp.**	Phylogeny distribution	ANT2-16.15viii16	Antarctica, Litchfield Island	This study	GBxxxxxx	GBxxxxxx
***Chamberlainium* sp.**	Phylogeny distribution	AMC13.9x17	Chile, Bahia Mansa	This study	GBxxxxxx	GBxxxxxx
***Chamberlainium* sp.**	Phylogeny distribution	C174.2xii08	Chile, Puerto Montt	This study	GBxxxxxx	GBxxxxxx
***Chamberlainium* sp.**	Phylogeny distribution	AMC17.2x17	Chile, Bahia Mansa	This study	GBxxxxxx	GBxxxxxx
***Chamberlainium* sp.**	Phylogeny distribution	C18.17ii09	Chile, Viña del Ma	This study	GBxxxxxx	GBxxxxxx
Chamberlainium agulhense	'Topotype'	UWC 11/23	South Africa, Cape Agulhas	van der Merwe *et al.* 2015	JQ917419	KT184833

Supplementary table

Chamberlainium agulhense	Paratype	UWC 11/24	South Africa, Struisbaai	van der Merwe *et al.* 2015	KT184812	KT184834
Chamberlainium agulhense	Phylogeny distribution	UWC 11/50	South Africa, Cape Agulhas	This study	GBxxxxxx	GBxxxxxx
Chamberlainium capense	Holotype	16/05	South Africa, Mouille Point	This study	GBxxxxxx	GBxxxxxx
Chamberlainium capense	Phylogeny distribution	UWC 16/09	South Africa, Sea Point	This study	GBxxxxxx	-
Chamberlainium capense	Phylogeny distribution	UWC 16/10	South Africa, Sea Point	This study	GBxxxxxx	-
Chamberlainium capense	Phylogeny distribution	UWC 16/17	South Africa, Kommetjie	This study	GBxxxxxx	-
Chamberlainium capense	Phylogeny distribution	UWC 16/18	South Africa, Kommetjie	This study	GBxxxxxx	-
Chamberlainium capense	Phylogeny distribution	UWC 16/21	South Africa, Kommetjie	This study	GBxxxxxx	GBxxxxxx
Chamberlainium capense	Phylogeny distribution	UWC 16/23	South Africa, Slangkop	This study	GBxxxxxx	GBxxxxxx
Chamberlainium capense	Phylogeny distribution	UWC 16/24	South Africa, Slangkop	This study	GBxxxxxx	-
Chamberlainium capense	Phylogeny distribution	UWC 16/27	South Africa, Slangkop	This study	GBxxxxxx	-
Chamberlainium cochleare	Phylogeny distribution	UWC 09/157	South Africa, Kalk Bay	This study	GBxxxxxx	GBxxxxxx

Supplementary table

Chamberlainium cochleare	Phylogeny distribution	UWC 11/38	South Africa, Kalk Bay	This study	GBxxxxxx	GBxxxxxx
Chamberlainium cochleare	Phylogeny distribution	UWC 12/02A	South Africa, Kalk Bay	This study	GBxxxxxx	GBxxxxxx
Chamberlainium cochleare	Phylogeny distribution	UWC 93/299	South Africa, Holbaaipunt	This study	GBxxxxxx	-
Chamberlainium cochleare	Holotype	14/12	South Africa, Stinkbaai	This study	GBxxxxxx	-
Chamberlainium cochleare	Isotype	UWC 14/13	South Africa, Stinkbaai	This study	GBxxxxxx	-
Chamberlainium cochleare	Isotype	UWC 14/14	South Africa, Stinkbaai	This study	GBxxxxxx	-
Chamberlainium cochleare	Phylogeny distribution	UWC 09/104	South Africa, Struisbaai	This study	GBxxxxxx	GBxxxxxx
Chamberlainium cochleare	Phylogeny distribution	UWC 15/11	South Africa, Struisbaai	This study	GBxxxxxx	-
Chamberlainium cochleare	Phylogeny distribution	UWC 15/14	South Africa, Struisbaai	This study	GBxxxxxx	-
Chamberlainium cochleare	Phylogeny distribution	UWC 15/15	South Africa, Struisbaai	This study	GBxxxxxx	-
Chamberlainium cochleare	Phylogeny distribution	UWC 10/104	South Africa, Stilbaai	This study	GBxxxxxx	-
Chamberlainium cochleare	Phylogeny distribution	UWC 08/20	South Africa, Tsitsikamma	This study	GBxxxxxx	GBxxxxxx

Supplementary table

Chamberlainium cochleare	Phylogeny distribution	NCU 659868	South Africa, Kidds Beach	This study	-	GBxxxxxx
Chamberlainium cochleare	Phylogeny distribution	UWC 15/24	South Africa, Ballito Bay	This study	GBxxxxxx	-
Chamberlainium decipiens	Holotype	NCU 622324	USA, California	van der Merwe *et al.* 2015	JQ917420	KT184835
Chamberlainium glebose	Phylogeny distribution	UWC 93/27	South Africa, Port Nolloth	This study	GBxxxxxx	-
Chamberlainium glebose	Phylogeny distribution	UWC 93/304	South Africa, Port Nolloth	This study	GBxxxxxx	-
Chamberlainium glebose	Phylogeny distribution	UWC 93/306	South Africa, Port Nolloth	This study	GBxxxxxx	-
Chamberlainium glebose	Phylogeny distribution	UWC 15/50	South Africa, Port Nolloth	This study	GBxxxxxx	-
Chamberlainium glebose	Phylogeny distribution	UWC 15/51	South Africa, Port Nolloth	This study	GBxxxxxx	GBxxxxxx
Chamberlainium glebose	Phylogeny distribution	UWC 15/55	South Africa, Groenriviermond	This study	GBxxxxxx	GBxxxxxx
Chamberlainium glebose	Phylogeny distribution	UWC 15/63B	South Africa, Cape St. Martin	This study	GBxxxxxx	GBxxxxxx
Chamberlainium glebose	Phylogeny distribution	UWC 15/16	South Africa, Jacobsbaai	This study	GBxxxxxx	GBxxxxxx
Chamberlainium glebose	Phylogeny distribution	UWC 15/17	South Africa, Jacobsbaai	This study	GBxxxxxx	GBxxxxxx

Supplementary table

Chamberlainium glebose	Phylogeny distribution	UWC 15/20	South Africa, Jacobsbaai	This study	GBxxxxxx	GBxxxxxx
Chamberlainium glebose	Phylogeny distribution	UWC 15/21	South Africa, Jacobsbaai	This study	GBxxxxxx	-
Chamberlainium glebose	Phylogeny distribution	UWC 15/33	South Africa, Grotto Bay	This study	-	GBxxxxxx
Chamberlainium glebose	Phylogeny distribution	UWC 15/34	South Africa, Grotto Bay	This study	-	GBxxxxxx
Chamberlainium glebose	Phylogeny distribution	UWC 15/35	South Africa, Grotto Bay	This study	-	GBxxxxxx
Chamberlainium glebose	Phylogeny distribution	UWC 16/07	South Africa, Mouille Point	This study	-	GBxxxxxx
Chamberlainium glebose	Phylogeny distribution	UWC 16/12	South Africa, Mouille Point	This study	-	GBxxxxxx
Chamberlainium glebose	Phylogeny distribution	UWC 16/14	South Africa, Sea Point	This study	-	GBxxxxxx
Chamberlainium glebose	Phylogeny distribution	UWC 16/25	South Africa, Slangkop	This study	-	GBxxxxxx
Chamberlainium glebose	Phylogeny distribution	UWC 16/26	South Africa, Slangkop	This study	-	GBxxxxxx
Chamberlainium glebose	Phylogeny distribution	UWC 16/27	South Africa, Slangkop	This study	-	GBxxxxxx
Chamberlainium glebose	Holotype	18/05		This study	GBxxxxxx	GBxxxxxx

Supplementary table

Chamberlainium impar	Phylogeny distribution	UWC 12/01	South Africa, Sea Point	This study	GBxxxxxx	GBxxxxxx
Chamberlainium impar	Phylogeny distribution	UWC 13/20	South Africa, Sea Point	This study	GBxxxxxx	-
Chamberlainium impar	Phylogeny distribution	UWC 13/21	South Africa, Sea Point	This study	GBxxxxxx	-
Chamberlainium impar	Phylogeny distribution	UWC 13/22	South Africa, Sea Point	This study	GBxxxxxx	-
Chamberlainium impar	Phylogeny distribution	UWC 15/64	South Africa, Cape St. Martin	This study	GBxxxxxx	-
Chamberlainium natalense	Phylogeny distribution	UWC 16/20	South Africa, Kommetjie	This study	GBxxxxxx	-
Chamberlainium natalense	Phylogeny distribution	UWC 11/41	South Africa, Kalk Bay	This study	GBxxxxxx	GBxxxxxx
Chamberlainium natalense	Phylogeny distribution	UWC 12/02B	South Africa, Kalk Bay	This study	GBxxxxxx	GBxxxxxx
Chamberlainium natalense	Phylogeny distribution	UWC 12/03	South Africa, Kalk Bay	This study	GBxxxxxx	-
Chamberlainium natalense	Phylogeny distribution	UWC 13/24	South Africa, Kalk Bay	This study	GBxxxxxx	-
Chamberlainium natalense	Phylogeny distribution	UWC 13/25	South Africa, Kalk Bay	This study	GBxxxxxx	-
Chamberlainium natalense	Phylogeny distribution	UWC 09/103	South Africa, Struisbaai	This study	GBxxxxxx	GBxxxxxx

Supplementary table

Chamberlainium natalense	Phylogeny distribution	UWC 09/125	South Africa, Struisbaai	This study	-	GBxxxxxx
Chamberlainium natalense	Phylogeny distribution	UWC 11/26	South Africa, Struisbaai	This study	GBxxxxxx	GBxxxxxx
Chamberlainium natalense	Phylogeny distribution	UWC 14/18	South Africa, Shark Bay	This study	GBxxxxxx	GBxxxxxx
Chamberlainium natalense	Phylogeny distribution	UWC 15/10	South Africa, Shark Bay	This study	GBxxxxxx	GBxxxxxx
Chamberlainium natalense	Phylogeny distribution	UWC 15/13	South Africa, Shark Bay	This study	GBxxxxxx	-
Chamberlainium natalense	Phylogeny distribution	UWC 10/133	South Africa, Cape Agulhas	This study	GBxxxxxx	GBxxxxxx
Chamberlainium natalense	Phylogeny distribution	UWC 08/04	South Africa, Tsitsikamma	This study	GBxxxxxx	GBxxxxxx
Chamberlainium natalense	Phylogeny distribution	UWC 08/06	South Africa, Tsitsikamma	This study	GBxxxxxx	GBxxxxxx
Chamberlainium natalense	Phylogeny distribution	UWC 08/13	South Africa, Tsitsikamma	This study	GBxxxxxx	GBxxxxxx
Chamberlainium natalense	Phylogeny distribution	UWC 10/209	South Africa, Kei Mouth	This study	GBxxxxxx	GBxxxxxx
Chamberlainium natalense	Phylogeny distribution	UWC 15/26	South Africa, Ballito Bay	This study	GBxxxxxx	-
Chamberlainium occidentalum	Phylogeny distribution	UWC 92/302	Namibia, Lüderitz	This study	GBxxxxxx	-

Supplementary table

Chamberlainium occidentalum	Phylogeny distribution	UWC 93/37	South Africa, Groenriviermond	This study	GBxxxxxx	-
Chamberlainium occidentalum	Phylogeny distribution	UWC 15/56	South Africa, Groenriviermond	This study	GBxxxxxx	GBxxxxxx
Chamberlainium occidentalum	Phylogeny distribution	UWC 15/57	South Africa, Groenriviermond	This study	GBxxxxxx	GBxxxxxx
Chamberlainium occidentalum	Isotype	UWC 15/59	South Africa, Lamberts Bay	This study	GBxxxxxx	-
Chamberlainium occidentalum	Isotype	UWC 15/58	South Africa, Lamberts Bay	This study	GBxxxxxx	GBxxxxxx
Chamberlainium occidentalum	Isotype	UWC 15/61A	South Africa, Lamberts Bay	This study	GBxxxxxx	-
Chamberlainium occidentalum	Holotype	15/61B	South Africa, Lamberts Bay	This study	GBxxxxxx	GBxxxxxx
Chamberlainium occidentalum	Phylogeny distribution	UWC 15/63A	South Africa, Cape St. Martin	This study	GBxxxxxx	GBxxxxxx
Chamberlainium occidentalum	Phylogeny distribution	UWC 93/220	South Africa, Holbaai Punt	This study	GBxxxxxx	-
Corallina officinalis	'Topotype'	NCU 593281	USA, Alaska	Hind *et al.* 2014b	-	KJ591669
Corallina officinalis	Linked to type specimen	NCU 586656	USA, Alaska	Hind *et al.* 2014b	KJ637655	KJ591678
Chamberlainium tenue	Phylogeny distribution	UWC 08/25	South Africa, Knysna Heads	This study	GBxxxxxx	GBxxxxxx

Supplementary table

Chamberlainium tenue	Phylogeny distribution	UWC 08/07	South Africa, Tsitsikamma	This study	-	GBxxxxxx
Chamberlainium tenue	Phylogeny distribution	NCU 659867	South Africa, Kidds Beach	This study	-	GBxxxxxx
Chamberlainium tenue	Phylogeny distribution	NCU 659869	South Africa, Kidds Beach	This study	GBxxxxxx	GBxxxxxx
Chamberlainium tenue	Isotype	UWC 10/202	South Africa, Kei Mouth	This study	-	GBxxxxxx
Chamberlainium tenue	Holotype	UWC 10/205	South Africa, Kei Mouth	This study	GBxxxxxx	GBxxxxxx
Chamberlainium tenue	Phylogeny distribution	UWC 15/23	South Africa, Ballito Bay	This study	GBxxxxxx	-
Chamberlainium tumidum	Linked to type specimen	NCU 600394	USA, California	van der Merwe *et al*. 2015	KT184830	KT184844
Clathroporphum compactum	Linked to type specimen	US 170929	Canada, Labrador	Adey *et al.* 2015	KP142730	KP142774
Gelidium corneum	Holotype	CNU000127	Korea, Youngjin	Boo *et al.* 2016	KT920333.1	-
				Kim *et al.* 2012	-	JQ340391
Heydrichia cerasina	Isotype	NCU617165	South Africa, Cape Agulhas	Richards *et al.* 2017	MF034551	KY994128
Heydrichia woelkerlingii	'Topotype'	NCU 597127	South Africa, Oudekraal,	van der Merwe *et al*. 2015	JQ917415	-
				Adey *et al*. 2015	-	KP142788
Leptophytum laeve	"Representative DNA Barcode"	US170934	Canada, Labrador	Adey *et al*. 2015	KP142754	KP142789

Supplementary table

Lithophyllum discoideum	Lectotype	TRH! A9-449	Argentina, Tierra del Fuego	This study	-	GBxxxxxx
Lithophyllum impar	Holotype	TRH! A3-146	South Africa, Cape Point	This study	-	GBxxxxxx
Lithophyllum natalense	Holotype	TRH! A2-107	South Africa, Kwa-Zulu Natal	This study	GBxxxxxx	-
Mesophyllum lichenoides	Liked to holotype specimen	NCU 590286	England, South Devon	Richards *et al*. 2017	MF034552	KY994129.2
Neopolyporolithon reclinatum	Holotype	TRH B17-2590	Canada, British Columbia	Adey *et al*. 2015	-	KP142803
Neopolyporolithon reclinatum	Linked to type specimen	UBC A88609	Canada, British Columbia	Adey *et al*. 2015	KP142762	KP142806
Phymatolithon calcareum	Neotype	BM000712373	England, Falmouth	Hernández-Kantún *et al.* 2015	JQ896231	KX020487.1
Pneophyllum cetinaensis	Holotype	AZ-2016	Croatia, Otok Ljubavi	Žuljevic *et al*. 2016	KT783425	-
Pneophyllum fragile	'Topotype' - molecular reference	BM001033381	Spain, Almadra	Žuljevic *et al*. 2016	KT783426.1	-
Pneophyllum fragile (New Zealand)	Phylogeny distribution	NZC0737	New Zealand	Hart *et al.* unpublished	DQ167969.1	-
Pneophyllum neodiscoideum	Phylogeny distribution	UWC 09/160	South Africa, Kalk Bay	This study	GBxxxxxx	GBxxxxxx
Pneophyllum neodiscoideum	Phylogeny distribution	UWC 09/158	South Africa, Kalk Bay	This study	GBxxxxxx	GBxxxxxx

Supplementary table

Pneophyllum neodiscoideum	Phylogeny distribution	UWC 11/39	South Africa, Kalk Bay	This study	GBxxxxxx	GBxxxxxx
Pneophyllum neodiscoideum	Holotype	09/132	South Africa, L'Agulhas	This study	GBxxxxxx	GBxxxxxx
Pneophyllum neodiscoideum	Isotype	UWC 09/131	South Africa, L'Agulhas	This study	GBxxxxxx	GBxxxxxx
Pneophyllum neodiscoideum	Isotype	UWC 09/133	South Africa, L'Agulhas	This study	GBxxxxxx	GBxxxxxx
Pneophyllum neodiscoideum	Phylogeny distribution	UWC 11/22	South Africa, L'Agulhas	This study	GBxxxxxx	GBxxxxxx
Pneophyllum neodiscoideum	Phylogeny distribution	UWC 09/119	South Africa, Struisbaai	This study	GBxxxxxx	GBxxxxxx
Spongites fruticulosus	'Topotype' - molecular reference	LLG4146	Spain, Cala Chumba	Peña *et al*. 2014	KJ710351	-
***Spongites* sp.**	Phylogeny distribution	C40.2xii08	Chile Valparaiso	This study	GBxxxxxx	GBxxxxxx
Spongites yendoi	Phylogeny distribution	NZC0488	New Zealand	Hart *et al*. unpublished	DQ167896	-
Spongites yendoi	Phylogeny distribution	NZC0482	New Zealand, Golden Bay	Hart *et al*. unpublished	DQ167905	-
Spongites yendoi	Phylogeny distribution	NZC0516	New Zealand	Hart *et al*. unpublished	DQ167902	-
Spongites yendoi	Phylogeny distribution	ND126	New Zealand, Kaikoura	Farr *et al*. 2009	FJ361459	-

Supplementary table

Spongites yendoi	Phylogeny distribution	NZC0096	New Zealand	Hart *et al*. unpublished	DQ167878	-
Spongites yendoi	Phylogeny distribution	NZC0076	New Zealand, Kaikoura,	Hart *et al*. unpublished	DQ167988	-
Spongites yendoi	Phylogeny distribution	NZC0777	New Zealand,Te One Creek	Hart *et al*. unpublished	DQ167944	-
Spongites yendoi	Phylogeny distribution	NZC0778	New Zealand	Hart *et al*. unpublished	DQ167952	-
Spongites yendoi	Phylogeny distribution	NZC0781	New Zealand, Heaphy	Hart *et al*. unpublished	DQ167979	-
Spongites yendoi	Phylogeny distribution	NZC0749	New Zealand	Hart *et al*. unpublished	DQ168003	-
Spongites yendoi	Phylogeny distribution	ND88	New Zealand	Farr *et al*. 2009	FJ361440	-
Spongites yendoi	Phylogeny distribution	ND110	New Zealand	Hart *et al*. unpublished	FJ361448	-
Spongites yendoi	Phylogeny distribution	NZC0507	New Zealand	Hart *et al*. unpublished	DQ167903	-
Spongites yendoi	Phylogeny distribution	NZC0623	New Zealand	Hart *et al*. unpublished	DQ167916	-
Spongites yendoi	Phylogeny distribution	NZC0645	New Zealand	Hart *et al*. unpublished	DQ167901	-
Spongites yendoi	Phylogeny distribution	NZC0627	New Zealand	Hart *et al*. unpublished	DQ167907	-

Supplementary table

Sporolithon ptychoides	'Topotype'	NCU606660	Egypt, El Tor	Richards *et al.* 2017	MF034541	KY994117